

A COMPUTER SIMULATION OF THE
TURBOCHARGED TURBOCOMPOUNDED DIESEL ENGINE SYSTEM
FOR STUDIES OF LOW HEAT REJECTION ENGINE PERFORMANCE

by

DIONISSIOS NIKOLAOU ASSANIS

B.Sc., Marine Engineering
University of Newcastle Upon Tyne
(1980)

S.M., Naval Architecture and Marine Engineering
S.M., Mechanical Engineering
Massachusetts Institute of Technology
(1983)

SUBMITTED IN PARTIAL FULFILLMENT
OF THE REQUIREMENTS FOR THE
DEGREE OF

DOCTOR OF PHILOSOPHY
IN
POWER AND PROPULSION

at the

MASSACHUSETTS INSTITUTE OF TECHNOLOGY

September 1985

VOLUME I

Signature of Author: Dennis Assanis
Department of Ocean Engineering
September 1985

Certified by: John B. Heywood
Thesis Supervisor
Prof. John B. Heywood
Dept. of Mechanical Engineering

Accepted by: A. Douglas Carmichael
Prof. Douglas A. Carmichael, Chairman
Departmental Graduate Committee
Department of Ocean Engineering

MASSACHUSETTS INSTITUTE
OF TECHNOLOGY

MAR 27 1986

LIBRARIES

A COMPUTER SIMULATION OF THE
TURBOCHARGED TURBOCOMPOUNDED DIESEL ENGINE SYSTEM
FOR STUDIES OF LOW HEAT REJECTION ENGINE PERFORMANCE

by

DIONISSIOS NIKOLAOU ASSANIS

B.Sc., Marine Engineering
University of Newcastle Upon Tyne
(1980)

S.M., Naval Architecture and Marine Engineering
S.M., Mechanical Engineering
Massachusetts Institute of Technology
(1983)

SUBMITTED IN PARTIAL FULFILLMENT
OF THE REQUIREMENTS FOR THE
DEGREE OF

DOCTOR OF PHILOSOPHY
IN
POWER AND PROPULSION

at the

MASSACHUSETTS INSTITUTE OF TECHNOLOGY

September 1985

VOLUME I

Signature redacted

Signature of Author:

Department of Ocean Engineering
September 1985

Signature redacted

Certified by:

Thesis Supervisor
Prof. John B. Heywood
Dept. of Mechanical Engineering

Signature redacted

Accepted by:

Prof. Douglas A. Carmichael, Chairman
Departmental Graduate Committee
Department of Ocean Engineering

MASSACHUSETTS INSTITUTE
OF TECHNOLOGY

MAR 27 1986

LIBRARIES

A COMPUTER SIMULATION OF
THE TURBOCHARGED TURBOCOMPOUNDED DIESEL ENGINE SYSTEM
FOR STUDIES OF LOW HEAT REJECTION ENGINE PERFORMANCE

by

DIONISSIOS NIKOLAOU ASSANIS

Submitted to the Department of Ocean Engineering
on September 10, 1985 in partial fulfillment of the
requirements of the Degree of Doctor of Philosophy
in Power and Propulsion

ABSTRACT

A computer simulation of the turbocharged turbocompounded direct-injection diesel engine system has been developed in order to study the performance characteristics of the total system as major design parameters and materials are varied. Quasi-steady flow models of the compressor, turbines, manifolds, intercooler, and ducting are coupled with a multi-cylinder reciprocator diesel model, where each cylinder undergoes the same thermodynamic cycle. The master cylinder model describes the reciprocator intake, compression, combustion and exhaust processes in sufficient detail to define the mass and energy transfers in each sub-system of the total engine system. Appropriate thermal loading models relate the heat flow through critical system components to material properties and design details. From this information, the simulation predicts the performance gains, and assesses the system design trade-offs which would result from the introduction of selected heat transfer reduction materials in key system components, over a range of operating conditions. Results of the simulation are compared against test data from the Cummins Adiabatic Diesel Program and show reasonable agreement.

Thesis Supervisor: Prof. John B. Heywood

Title: Professor of Mechanical Engineering,
Director of Sloan Automotive Laboratory

ACKNOWLEDGEMENTS

I am most grateful to my thesis supervisor, Professor John Heywood, for all the expert guidance, superb insight and valuable professional advice he has given me throughout my thesis. It has been a challenge, a unique learning experience and a pleasure to work with him.

I would like to express my thanks and appreciation to Professor A. Douglas Carmichael, who supervised my Master's Thesis and participated in my Ph.D. thesis committee, for his invaluable help, personal advice and concern throughout my studies at M.I.T.

I would like to thank Dr. Jack Ekchian, who acted as my advisor during the early parts of this work, for his enthusiasm and support in the project, and his good sense of humor. I would also like to thank Professor Warren Rohsenow for his encouragement and his participation in my doctoral thesis committee.

I would like to thank my colleagues in the project, Rick Frank and Kriss Replogle, for their contributions and excellent cooperation. I would particularly like to thank Rick for all his help and for being a good friend. I wish to thank Karla Stryker for her time and efforts in putting this thesis in a really nice final form. Also, my thanks to Duane Page for his continuous efforts to keep our computer running. And many words of thanks to all my friends in the Sloan Lab and M.I.T. at large who made my five year stay there an enjoyable one.

I would like to express my deepest and everlasting gratitude to my parents, Nikolaos and Kyriaki, for their love, support and encouragement throughout my life.

I would like to dedicate this thesis to my wife, Helen, for her love and devotion. Her contribution is a very real one.

This work was supported by the DOE Heavy Duty Transport Technology Program under NASA Grant NAG 3-394 and by the M.I.T. Consortium on the Use of Ceramic Materials in IC Engines. The contributions of the technical grant monitors and the members of the Ceramics Consortium are gratefully appreciated.

TABLE OF CONTENTS

	<u>Page</u>
TITLE PAGE	1
ABSTRACT	2
ACKNOWLEDGEMENTS	3
TABLE OF CONTENTS	4
LIST OF TABLES	9
LIST OF FIGURES	11
CHAPTER	
1. INTRODUCTION	17
2. BASIC ASSUMPTIONS OF SYSTEM MODELS	23
2.1 Reciprocator Engine Model	23
2.2 Other Component Models	25
3. CONSERVATION EQUATIONS	27
3.1 Conservation of Mass	27
3.1.1 Conservation of total mass	27
3.1.2 Conservation of fuel mass	27
3.2 Conservation of Energy	29
3.3 Application of Conservation Equations to Reciprocator Cycle	32
4. MODELLING OF RECIPROCATOR ENGINE PROCESSES	34
4.1 Gas Exchange	34
4.2 Combustion Model	35
4.3 Ignition Delay Model	40
4.4 Heat Transfer	42
4.4.1 Convective heat transfer	43
4.4.2 Radiative heat transfer	45
4.5 Turbulent Flow Model	49

	<u>Page</u>
4.6 Engine Friction Model	53
5. MODELLING OF OTHER SYSTEM COMPONENTS	56
5.1 Turbomachinery Modeling	56
5.2 Turbocharger Dynamics	59
5.3 Turbocharger Matching Procedure	60
5.3.1 Single-stage turbocharged case	60
5.3.2 Turbocharged turbocompounded case	61
5.4 Intercooler Model	62
5.5 Exhaust Manifold Model	63
5.6 Manifold Conservation Equations	65
5.7 Manifold Heat Transfer	67
5.7.1 Reciprocator exhaust port	68
5.7.2 Exhaust manifold	70
5.7.3 Connecting pipe between the turbines	72
5.8 Pressure Losses	72
5.8.1 General	72
5.8.2 Exhaust manifold and turbine connecting pipe	73
6. WALL CONDUCTION MODELS	74
6.1 Introduction	74
6.2 Steady-State Problem	76
6.2.1 Flat composite wall	76
6.2.2 Cylindrical composite wall	77
6.2.3 Determination of steady-state inside wall surface temperature	78
6.3 Time-Periodic Problem	80
6.3.1 Formulation of finite difference scheme	80
6.3.2 Application of finite difference scheme	83

	<u>Page</u>
6.4 Combined Solution	85
7. METHOD OF SOLUTION AND PROGRAM INPUTS AND OUTPUTS	86
7.1 Basic Method of Solution	86
7.2 Program Inputs and Outputs	88
7.2.1 Inputs	88
7.2.2 Outputs	92
8. MODEL CALIBRATION AND VALIDATION	95
8.1 Introduction	95
8.2 Calibration	95
8.3 Model Validation	97
8.3.1 Constant load comparison	97
8.3.2 Constant-speed comparison	98
8.3.3 Pressure and temperature comparison across the system ..	99
9. BEHAVIOR OF SIMULATION SUB-MODELS	101
9.1 Gas Exchange Process Model	101
9.2 Combustion Model	102
9.3 Heat Transfer Model	103
9.4 Turbulent Flow Model	107
9.5 Exhaust Manifold Model	109
10. SYSTEM PERFORMANCE RESULTS	110
10.1 Study Methodology	110
10.1.1 Sensitivity of radiative heat transfer to degree of insulation	111
10.1.2 Sensitivity of optimum injection timing to degree of insulation	112
10.1.3 Sensitivity of optimum gear ratio to degree of insulation	113
10.2 Effect of Insulation on System Performance	114

	<u>Page</u>
10.2.1 Assumptions	114
10.2.2 Effect of variation of combustion chamber surface temperature	115
10.2.3 Effect of variation of liner temperature on system performance	119
10.2.4 Effect of higher turbomachinery component efficiencies on system performance	120
11. WALL CONDUCTION MODEL RESULTS	121
11.1 Effects of Wall Surface Temperature Variations on System Performance	121
11.2 Effects of Wall Surface Temperature Variations on Component Thermal Loading	123
11.3 Use of Alternative Ceramic Materials to Achieve a Desired Degree of Insulation	124
11.4 Effects of Speed and Load on Degree of Insulation	127
11.4.1 Effect of speed	127
11.4.2 Effect of load	128
11.5 Effect of Material Thickness on Degree of Insulation	128
11.6 Effect of Air Gap on Degree of Insulation	130
12. SUMMARY & CONCLUSIONS	132
REFERENCES	135
TABLES	141
FIGURES	160
APPENDIX	
A. THERMODYNAMIC PROPERTIES	200
B. THERMODYNAMIC DATA FOR FUEL VAPOR	203
C. TRANSPORT PROPERTIES	204
D. LINEARIZATION OF TOTAL HEAT TRANSFER RATE AT THE GAS/WALL INTERFACE .	206
E. DERIVATION OF EXACT SOLUTION FOR A TWO-PARALLEL LAYER COMPOSITE SLAB SUBJECT TO A TIME-PERIODIC BOUNDARY CONDITION	207

	<u>Page</u>
F. TURBOCHARGED TURBOCOMPOUNDED DIESEL ENGINE CYCLE SIMULATION CODE	211
G. DEFINITIONS OF INPUT VARIABLES FOR COMPUTER CODE	367
H. SAMPLE INPUT FILES FOR COMPUTER CODE	374
I. SAMPLE OUTPUT FILES FROM COMPUTER CODE	382

LIST OF TABLES

	<u>Page</u>
Table 1. Appropriate heat release profile constants for different engine designs	141
Table 2. Constants for Arrhenius equation for ignition delay	142
Table 3. Relative importance of radiant heat flux	143
Table 4. Engine Parameters	144
Table 5. Calibration of diffusion-burning shape factor k_3	145
Table 6. Comparison of predictions with data	146
Table 7. Effect of variation of combustion chamber surface temperature on system performance	147
Table 8. Effect of variation of liner temperature on system performance	148
Table 9. Effect of 5% higher turbomachinery component efficiencies on the performance of a partially-insulated system configuration	149
Table 10. Sensitivity of performance gains due to more efficient turbomachinery to degree of insulation	150
Table 11. Effect of wall surface temperature cyclic variations on system performance	151
Table 12. Properties of selected materials for engine applications	152
Table 13. Thermal loading of selected materials for engine applications	153
Table 14. Effect of insulating thickness of zirconia on degree of insulation	154

	<u>Page</u>
Table 15. Effect of various thicknesses of air-gap on degree of insulation	155
Table A-1. Burned gas composition under 1000 K	156
Table A-2. Coefficients for polynomial fit to thermodynamic properties	157
Table B-1. Coefficients for polynomial fit to fuel vapor data from 300 to 1500 K	158
Table B-2. Fuel analysis of No. 2 Diesel Fuel	159

LIST OF FIGURES

	<u>Page</u>
Figure 1. Turbocompounded diesel system configuration	160
Figure 2. Typical rate of heat release diagram for a direct injection diesel engine	161
Figure 3. Turbulent energy cascade model. K: mean kinetic energy; k: turbulent kinetic energy	162
Figure 4. Single-stage turbocharged system configuration	163
Figure 5. Generalized manifold open system	164
Figure 6. Typical temperature distribution within a ceramic/metal composite wall structure in the engine combustion chamber .	165
Figure 7. Comparison of exact and numerical solutions for the temperature profile in a 4 mm ceramic coating (with $k = 1 \text{ W/m-k}$ and $\alpha = 0.5 \times 10^{-5} \text{ m}^2/\text{s}$) exposed to a specified harmonically-varying gas temperature	166
Figure 8. Flowchart of simulation program	167
Figure 9. Comparison between cylinder pressure diagrams calculated for different values of the constant k_3 (used in the calculation of the diffusion burning shape factor C_{d2}) against experimental pressure trace obtained from Cummins	168
Figure 10. Measured and predicted reciprocator brake power, power turbine brake power and overall brake specific fuel consumption as a function of reciprocator speed for constant load operation	169
Figure 11. Measured and predicted turbocharger rotor speed, boost pressure ratio and mass flow through the compressor as a	

	<u>Page</u>
function of reciprocator speed for constant load operation .	170
Figure 12. Measured and predicted reciprocator brake power, power turbine brake power and overall brake specific fuel consumption as a function of fueling rate (i.e., reciprocator load) for operation at a constant speed of 1900 RPM	171
Figure 13. Measured and predicted turbocharger rotor speed, boost pressure ratio and mass flow through the compressor as a function of fueling rate (i.e., reciprocator load) for operation at a constant speed of 1900 RPM	172
Figure 14. Mass flow rates through the intake (bottom) and exhaust (top) valves corresponding to the filling and emptying processes of the master cylinder	173
Figure 15. Velocity profiles of the conical jet flows through the intake and the exhaust valve opening, non-dimensionalized with respect to the mean piston speed. (i.e., two times the piston stroke times the rotational speed of the crankshaft) .	174
Figure 16. Predicted fuel burning rate profile normalized with respect to the total fuel injected per cycle per cylinder at rated speed and load	175
Figure 17. Pressure trace predicted by the simulation at rated speed and load	176
Figure 18. Bulk gas temperature (top), gas to wall heat transfer rate (middle) and convective heat transfer coefficient (bottom) as a function of crank-angle over the engine cycle	177

	<u>Page</u>
Figure 19. Simulation predictions of the radiative, convective, and total heat transfer rates over the duration of the expansion process in a cooled diesel engine. Results presented are based on the flame radiation model (continuous curves), and the Annand's radiation model with calibrating constants equal to 2.0 (dashed curves) and 1.0 (dotted-dashed curves)	178
Figure 20. Temperature of air zones, temperature of bulk gas, characteristic radiant temperature and adiabatic flame temperature as a function of crank angle during the expansion process of a cooled metal engine	179
Figure 21. Breakdown of the convective (top) and radiative (bottom) heat transfer rates among cylinder head, piston, and liner over the duration of the expansion process	180
Figure 22. Variation of mean flow velocity, turbulent intensity, and resultant effective heat transfer velocity, defined by Eq. (4-18), with crank-angle. All velocity scales are normalized with respect to the mean piston speed	181
Figure 23. Predictions of the variation of non-dimensional turbulent intensity over the duration of the compression and expansion processes based on the Poulos and Heywood model and the extended model which includes the effects of rapid distortion	182
Figure 24. Predicted macroscale of turbulence, non-dimensionalized with respect to the cylinder bore, plotted against crank-angle throughout the engine cycle	183

	<u>Page</u>
Figure 25. Exhaust manifold temperature and pressure crank-angle histories for a six cylinder turbocharged diesel engine . . .	184
Figure 26. Comparison of the convective, radiative, and total heat transfer rates over the duration of the expansion process for the partially insulated (solid curves) and the baseline (dashed curves) system configurations	185
Figure 27. Comparison of mean bulk gas and characteristic radiant temperature profiles over the duration of the expansion process for the partially insulated (solid curves) and the baseline (dashed curves) engines	186
Figure 28. Predictions of radiative heat transfer rate against crank-angle based on the flame model and the Annand model (with $C_r = 2.0$) for the partially-insulated (solid curves) and the baseline (dashed curves) engines	187
Figure 29. Variation of brake mean effective pressure with injection timing in a cooled (dashed curves) and a partially-insulated (solid curves) engine based on a specified ignition delay (top) and predicted ignition delay (bottom)	188
Figure 30. Variation of reciprocator brake power, power turbine brake power, and total brake power with power turbine gear ratio in a cooled and a partially-insulated engine	189
Figure 31. Simulation predictions of the radiative (solid curves), convective (dashed curves), and total (dashed-dotted curves) heat transfer rates throughout the cycle in a fully-insulated engine	190

- Figure 32. Temperature profiles of the mean bulk gas and the piston surface throughout the engine cycle for two system configurations. The dashed curves refer to a baseline engine with cooled, cast iron combustion chamber walls. The solid curves refer to a partially-insulated engine having 1.5 mm plasma-sprayed zirconia coating applied to the cylinder head and the piston, and a cooled, cast iron liner 191
- Figure 33. Penetration depth of the cyclic transients in a plasma-sprayed zirconia coated piston (top) and a cast-iron baseline piston (bottom) at a reciprocator speed of 1900 RPM 192
- Figure 34. Perturbations from the quasi-steady temperature profiles at three instants (300 deg., 350 deg., and 400 deg. crank-angle) during the engine cycle for a cast-iron piston coated with a 1.5 mm layer of plasma sprayed zirconia (top) and an all cast-iron baseline piston (bottom) 193
- Figure 35. Cyclic variations from the mean temperature (800 K) at the surface of (i) a piston coated with a 1.5 mm layer of plasma-sprayed zirconia ($k = 0.6 \text{ W/m-K}$); (ii) a piston coated with a 3.0 mm layer of sprayed zirconia ($k = 1.2 \text{ W/m-K}$); (iii) a monolithic reaction-bonded silicon nitride piston ($k = 5 \text{ W/m-K}$) with an overall thickness of 13.4 mm. All designs achieve the same degree of insulation (55% reduction in heat loss) 194
- Figure 36. Cyclic variations from the mean surface temperature of a cast-iron piston coated with a 1.5 mm layer of plasma-sprayed zirconia at two reciprocator speeds: 1900 RPM (rated speed)

	<u>Page</u>
and 1500 RPM (a medium speed)	195
Figure 37. Cyclic variations from the mean surface temperature of a cast-iron piston coated with a 1.5 mm layer of plasma-sprayed zirconia at two reciprocator loads: full load and 75% of full load (light load)	196
Figure 38. Instantaneous surface temperature (top) and cyclic variations from the mean surface temperatures (bottom) for various thicknesses of zirconia coatings applied to the piston and the cylinder head	197
Figure 39. Reduction in total heat loss to the coolant as a function of the thickness of zirconia coating applied to the piston and the cylinder head. Results shown are for a non-insulated, cooled, cast-iron liner	198
Figure 40. Predicted surface temperature profiles in a composite piston (ceramic/air-gap/metal) as a function of the thickness of air-gap separating the 2.5 mm zirconia crown from the cast- iron base	199

CHAPTER 1

INTRODUCTION

During the past few years, ceramic components have undergone successful feasibility demonstrations in a variety of heat engines. The potential for use of ceramics in heavy duty diesel engine applications is especially promising [1]. For example, the highest temperatures likely to be attained in ceramics in diesels are lower than in gas turbines. Furthermore, while the use of insulation in a spark-ignition gasoline engine is likely to result in the onset of combustion knock [2], it is ideal for the diesel engine where the promotion of ignition is desirable. Also, because the environment is relatively less demanding than in other heat engines, a wider range of ceramics is likely to be available for use in diesel engines.

The Propulsion Systems Division of the U.S. Army Tank-Automotive Command (TACOM) in conjunction with Cummins Engine Company began the development of an "Adiabatic Diesel Engine" ten years ago. This engine concept insulates parts of the diesel combustion chamber, such as the piston, cylinder head, valves, cylinder liner and exhaust ports, using high temperature ceramic materials. It should be noted that "adiabatic" engine operation, in the true thermodynamic sense of the word, implies that no heat flux crosses the gas system boundary at any instant during the engine cycle. In practice, the insulated engine strives to minimize the interchange of heat between the cylinder gases and the combustion chamber walls. For this reason, this concept is more correctly described as a "low-heat-rejection" engine, a term first used by Siegl and Amann [3].

The TACOM/Cummins program has demonstrated that the insulated engine concept has two types of advantages over a conventional cooled diesel engine

system [4]. First, the potential for elimination of the engine cooling system, including cooling fans, pumps, radiators, hoses, shrouds, etc. can result in greatly reduced parasitic losses, increased reliability, reduced maintenance, and reduced weight and cost. Second, and equally important, reductions in cooling system and exhaust heat losses at appropriate points in the diesel system result in substantially increased exhaust enthalpy. Since an adverse effect of hot component walls is a reduction in volumetric efficiency due to the heating of the incoming charge of air [3], [4], combustion chamber insulation is mainly considered for turbocharged diesels. In these engines, part of the available exhaust energy is used to increase the boost pressure so as to maintain approximately constant airflow. Conversion of the remaining available energy into useful work can be achieved by means of exhaust heat recovery systems. Several such systems have been investigated in the context of heavy duty diesel engines, including turbocompounding [5], and steam and organic-based Rankine compounding systems [6],[7].

In Rankine cycle compounding, more of the exhaust energy is usable, since the top temperature of the vapor cycle can be near the exhaust temperature of the engine and the outlet gas temperature can be as low as 422 K (sulfuric acid condensation limit). However, possible damage to system components due to freezing (primarily in water-based Rankine cycles), tube degradation problems associated with decomposition of organic fluids, and the added complication, cost, maintenance, reliability problems, and packaging difficulties pose engineering challenges that have yet to be resolved. In the meantime, turbocompounding has emerged as the most attractive means of extracting the available energy in the exhaust of a low-heat-rejection turbocharged diesel engine.

This engine concept consists of several sub-systems: compressor, intercooler, reciprocator, turbocharger turbine, turbine connected with the drive shaft, and ducting. Opportunities for use of ceramic materials, ranging from sprayed and partially stabilized zirconia oxides to silicon nitrides and carbides, have widely different degrees of difficulty and benefits. Suitable insulated engine analysis tools, both for predictions of system performance and structural modeling, need to be developed in order to examine the full potential and limitations of ceramic containing diesel systems.

In the past, several investigators have published predictions of the efficiency benefits that result from combustion chamber insulation [8]-[14]. However, there is a considerable variation in the level of sophistication and assumptions of the various theoretical studies, and thus the capabilities of the models and the range of efficiency benefits that they claim. Among the earliest studies, Griffiths [8] and Zapf [9] have predicted that very little (about 1% or less) can be gained in terms of improved engine efficiency by insulation. Their studies have been based on single-stage turbocharged diesel engines without turbocompounding. On the other hand, Kamo and Bryzik [4], [5], [10] have claimed that the efficiency improvement of a turbocharged turbocompounded diesel system (over a cooled baseline case) would be about 10%, while an additional 6-7% could be realized from the elimination of parasitic losses. Then, Wallace et al [11] predicted that the overall gain in efficiency of a turbocharged turbocompounded system would be rather small (of order of 2%) with 50% reduction in heat loss to coolant. Among the most recent studies, Watson et al [12], Sudhakar [13], and Hoag et al [14] seem to reach a consensus that about 4% improvement in overall efficiency can be gained with 60% reduction in heat losses. The limited experimental data published to date by Cummins [13] and Komatsu [15] seem to indicate that the

performance gains can be anywhere between zero and ten percent, depending on the system configuration, the insulation strategy, the ceramic materials used in the application, the efficiencies of the turbomachinery components, etc.

At this stage, it is premature to draw any conclusions regarding the validity of any of these theoretical or experimental predictions. It is clear, though, that some of these studies have not considered the turbocompounding approach towards improving the overall system performance. Furthermore, some models do not balance the complexity in the treatment of the various system components (reciprocator, turbomachinery, manifolds, etc.), or the various system processes (thermodynamic, convective and radiative heat transfer, and heat conduction through the component walls). In comparing insulated versus cooled system configurations, assumptions and constraints (such as fixed mass flows through the system, fixed turbomachinery component efficiencies, constant wall surface temperatures over the engine cycle) are introduced, but not always clearly stated or justified. Finally, most of these studies do not give a clear indication of the relationship between the dimensions of combustion chamber insulation and the resulting degree of insulation and component thermal loading for different candidate materials. Therefore, there is a need for a complete analytical model of this engine concept, at the appropriate level of detail, to enable engineers to define the trade-offs associated with introducing ceramic materials in various parts of the total engine system, and to carry out system performance and optimization studies.

The scope of the present thesis is to develop a computer simulation of the complete turbocharged turbocompounded diesel engine system, and to use the simulation to examine the operating characteristics of low-heat-rejection system configurations as major design parameters and materials are varied.

The approach that we follow is to couple thermodynamic and heat transfer models for the various system components and processes to develop a quasi-steady simulation of the complete system. The focus of this simulation is to define the mass flows and energy transfers (heat transfers, heat release, work transfers) in each sub-system and the relationships between the sub-systems. Since the complete system model must function as a single-unit, a deliberate effort is made to maintain a balance in the complexity of the various sub-system descriptions.

Figure 1 illustrates the overall model structure. The air flow is followed through an air filter, ducting, turbocharger compressor, ducting, cooler and engine intake system to the diesel reciprocator. The reciprocator simulation is a mathematical model of the processes occurring in the direct-injection four-stroke diesel-engine. Engine friction sub-models are then used to obtain brake quantities from the computed reciprocator indicated performance quantities. The exhaust gas flow is followed through the engine exhaust ports, manifold runners and plenum, to the turbocharger turbine; it is then followed through additional ducting to the compounded turbine; the flow then passes through the exhaust system and muffler to the atmosphere.

The thesis is arranged as follows. The basic assumptions of the reciprocator and the other component models are summarized in Chapter 2. Then, the mathematical relationships for mass and energy conservation for an open system, such as the reciprocator and the manifolds are developed in Chapter 3. The sub-models which represent the thermodynamic and heat transfer processes in the various components of the total system are described in Chapter 4 (reciprocator) and Chapter 5 (other components). Appropriate thermal loading models, steady and transient, that relate heat flow through critical system components to design and material details are presented in

Chapter 6. Then, Chapter 7 summarizes the method of solution of the complete model that results from the integration of the various sub-models, and briefly describes the inputs and outputs for the system computer simulation. The calibration and subsequent validation of the simulation against data from a cooled Cummins engine is summarized in Chapter 8. Further, the behavior of the key individual system sub-models is illustrated in Chapter 9. Next, the simulation is applied to the study of the low-heat-rejection turbocompounded diesel system. Chapter 10 presents simulation predictions for the performance of the complete system for various degrees of reduction of heat loss to coolant, and under a certain set of underlying assumptions. Chapter 11 illustrates the behavior of the thermal models and assesses the trade-offs between increasing degree of component insulation and component stress loading (gas-side wall surface temperature swings, penetration of transient temperature waves within wall structure, etc.). Finally, Chapter 12 summarizes the major conclusions of this thesis.

CHAPTER 2

BASIC ASSUMPTIONS OF SYSTEM MODELS

2.1 Reciprocator Engine Model

The diesel four-stroke cycle is treated as a sequence of continuous processes: intake, compression, combustion (including expansion), and exhaust. The durations of the individual processes are as follows. The intake process begins when the intake valve opens (IVO) and ends when the intake valve closes (IVC). The compression process begins at IVC and ends at the time of ignition (IGN). The combustion process begins when ignition occurs and ends when the exhaust valve opens (EVO). The exhaust process begins at EVO and ends at IVO (and not when the exhaust valve closes).

In the reciprocator simulation, the system of interest is the instantaneous contents of a cylinder, i.e. air, fuel and combustion products. In general, this system is open to the transfer of mass, enthalpy, and energy in the form of work and heat. Throughout the cycle, the cylinder is treated as a variable volume plenum, spatially uniform in pressure. Furthermore, the cylinder contents are represented as one continuous medium by defining an average equivalence ratio and temperature in the cylinder at all times.

Gas properties are calculated assuming ideal gas behavior. At low temperatures (below 1000 K), the cylinder contents are treated as a homogeneous mixture of non-reacting ideal gases. At high temperatures (above 1000 K), the properties of the cylinder contents are calculated with allowance for chemical dissociation by assuming that the burned gases are in equilibrium, using an approximate calculation method based on hydrocarbon-air combustion.

Quasi-steady, adiabatic, one-dimensional flow equations are used to predict mass flows past the intake and exhaust valves. The intake manifold and

the exhaust port are treated as plenums whose pressure and temperature history is determined by solution of the manifold state equations. When reverse flow past the intake valve occurs, rapid mixing of the back flow gases within the intake manifold is assumed.

The compression process is defined so as to include the ignition delay period, i.e. the time interval between the start of the injection process (the point at which the injector needle starts to lift) and the ignition point (the start of positive heat release due to combustion). The total length of the ignition delay is related to the mean cylinder gas temperature and pressure during the delay period by an empirical Arrhenius expression.

Combustion is modelled as a uniformly distributed heat release process. The rate of heat release is assumed to be proportional to the rate of fuel burning which is modelled empirically. Since the diesel combustion process is comprised of a pre-mixed and a diffusion-controlled combustion mechanism, Watson's fuel burning rate correlation [16], consisting of the sum of two algebraic functions, one for each combustion mechanism, is used. The fraction of the total fuel injected that is burnt by either mechanism depends on the length of the ignition delay period and the engine load and speed.

Heat transfer is included in all the engine processes. Convective heat transfer is modelled using available engine correlations based on turbulent flow in pipes. The characteristic velocity and length scales required to evaluate these correlations are obtained from a mean and turbulent kinetic energy model. Radiative heat transfer is added during combustion. The steady-state inside wall surface temperatures of the piston, cylinder head, and liner can be either specified or calculated from a specification of the component wall structure. Additionally, the time-dependent temperature distribution in the piston and cylinder head can be computed using a one-dimensional finite difference model.

Finally, an empirical friction model is used to convert the indicated engine performance quantities to brake performance quantities.

2.2 Other Component Models

The reciprocator engine model calculates the state variables in one master cylinder of a multi-cylinder engine, while the manifolds and the other component models have inherent multi-cylinder capability. The interaction between the master cylinder model and the other components is accounted for in the manifolds. To simulate the effect of additional cylinders on the manifold conditions, and hence on the entire system behavior, the conditions in the other cylinders are assumed to vary as echoes of the master cylinder, shifted by the appropriate phase angles. The following additional assumptions are made in order to develop models for the various components of the complete turbocharged turbocompounded diesel engine system:

Intake air and exhaust gas can be modelled as ideal gases. There is perfect and instantaneous mixing of all mass flows that enter each manifold (or section of the manifold) with the gases in the manifold. This implies that there is no spatial variation in properties within a manifold (or manifold section) at any instant of time, and all flows leaving a manifold have the properties of the manifold (or manifold section) contents. The connecting pipes to and from the intake manifold are included as parts of the intake manifold. The exhaust manifold is modeled as a series of connected open systems: exhaust port, manifold runner and manifold plenum.

There is instantaneous mixing of all mass flows that enter the intake manifold with the gases in the manifold; thus there is no variation in properties within the intake manifold at any instant of time. All flows leaving the intake manifold have the properties of the manifold contents.

Similarly, the gas properties are assumed to be uniform within each individual section of the exhaust manifold at any instant of time and the flow out of any section has the properties of that section.

There are no mass transfers except along the routes indicated; i.e., there are no losses or leakages from any component of the system. The flow through the wastegate can be specified as a fraction of the exhaust gas stream. The two exhaust gas streams, through and bypassing the turbocharger turbine, reunite with no loss of thermal energy, at the turbocharger turbine exit pressure. An open-system duct model connects the turbocharger turbine and compounded turbine.

The steady-state inside wall surface temperatures of the manifold sections and ducting can be specified or calculated from wall design information. Empirical correlations are used to calculate instantaneous heat transfer rates from the gas to the walls and pressure losses. Conduction through the walls is modeled as axisymmetric. The boundary conditions on the outside wall surface of each component are specified. From these, the steady-state temperature distribution within the walls of each component can be calculated.

The turbomachinery performance is defined by maps that interrelate efficiency, pressure ratio, mass flow rate and shaft speed for each component. The compressor, turbine, and power turbine are assumed to be adiabatic, i.e., there is no heat transfer from these components to the environment. The turbocharger dynamics are controlled by the rotor inertia and damping. The turbocharger turbine and compressor speeds are equal. Finally, the power turbine shaft is connected to the engine crankshaft via a specified gear ratio transmission. Hence, the power turbine speed can be determined directly from the reciprocator engine speed.

CHAPTER 3
CONSERVATION EQUATIONS

In this chapter, equations for the conservation of mass and energy are developed for the contents of an open thermodynamic system. The conservation equation for the fuel mass is used to develop a differential equation for the change in fuel-air equivalence ratio of the system. The energy conservation equation is developed to obtain a differential equation for the change in temperature of the thermodynamic system.

3.1 Conservation of Mass

3.1.1 Conservation of total mass

The rate of change of the total mass in any open system is equal to the sum of the mass flow rates into and out of the system:

$$\dot{m} = \sum_j \dot{m}_j \quad (3-1)$$

Note that the convention used in our model assumes that mass flow rates into the open system are taken as positive, while mass flow rates out of the system are negative.

3.1.2 Conservation of fuel mass

In particular, conservation of the fuel species can be expressed as

$$\dot{m}_f = \sum_j \dot{m}_{f,j} \quad (3-2)$$

where m_f denotes the fuel content in the open system (includes fuel added by injection and fuel in the form of combustion products).

Defining the fuel fraction, F , in the system as

$$F = m_f/m$$

where m is the total mass in the system, equation (3-2) can be re-written as

$$\frac{d}{dt}(mF) = \sum_j \dot{m}_j F_j \quad (3-3)$$

where F_j denotes the fuel fraction of the mass flow entering or leaving the open system through the j port.

Differentiating the left-hand side of equation (3-3) gives

$$m\dot{F} = \sum_j \dot{m}_j F_j - \dot{m}F \quad (3-4)$$

or substituting for \dot{m} from equation (3-1) results in a differential equation for the change in the fuel fraction of the open system, i.e.

$$\dot{F} = \sum_j (\dot{m}_j/m)(F_j - F) \quad (3-5)$$

An average fuel-air equivalence ratio, ϕ , for the contents of the open system can be defined as

$$\phi = \frac{m_f/m}{\text{FASTO}} \quad (3-6)$$

where m_a is the mass of air in the open system and FASTO denotes the stoichiometric fuel to air ratio.

Expressing the equivalence ratio, ϕ , in terms of the fuel fraction, F , i.e.

$$\phi = \frac{1}{\text{FASTO}} \frac{F}{1-F} \quad (3-7)$$

and differentiating (3-7) with respect to time we obtain an equation for the rate of change of the equivalence ratio of the open system, i.e.

$$\dot{\phi} = \frac{1}{\text{FASTO}} \frac{\dot{F}}{(1-F)^2} \quad (3-8)$$

with \dot{F} given from equation (3-5).

3.2 Conservation of Energy

The general energy equation for an open thermodynamic system may be written as

$$\dot{E} = \sum_j \dot{m}_j h_j - \dot{Q}_W - \dot{W} \quad (3-9)$$

with the rate of change of the energy of the system being given by

$$\dot{E} = \frac{d}{dt}(mh) - \frac{d}{dt}(pV) \quad (3-10)$$

where

$\sum_j \dot{m}_j h_j$ is the net rate of influx of enthalpy

$\dot{Q}_W = \sum_i \dot{Q}_i$ is the total heat transfer to the walls, i.e. the sum of the

heat transfer rates to the different surfaces of the control volume of interest

$\dot{W} = p\dot{V}$ is the rate at which the system does work by boundary displacement.

The dots denote differentiation with respect to time. Note that the convention used is that heat loss from the system and work done by the system are taken as positive.

Differentiating the left-hand side of equation (3-9) gives

$$\dot{mh} = \sum_j \dot{m}_j h_j - \dot{Q}_W + p\dot{V} - \dot{mh} \quad (3-11)$$

The contents of any open system, i.e. air and combustion products, can be represented as one continuous medium by defining an average equivalence ratio at each point in time. Gas properties are obtained assuming ideal gas behavior and thermodynamic equilibrium (see Appendix A). With these assumptions, we can express the enthalpy, h , and the density, ρ , of the mixture of air and combustion products as

$$h = h(T, p, \phi) \quad (3-12)$$

$$\rho = \rho(T, p, \phi) \quad (3-13)$$

Hence, the rate of change of the above fluid properties with respect to time, or crank-angle, can be written as

$$\dot{h} = c_p \dot{T} + c_T \dot{p} + c_\phi \dot{\phi} \quad (3-14)$$

where

$$c_p = \left(\frac{\partial h}{\partial T} \right)_{p, \phi}$$

$$c_T = \left(\frac{\partial h}{\partial p} \right)_{T, \phi}$$

$$c_\phi = \left(\frac{\partial h}{\partial \phi} \right)_{T, p}$$

and

$$\dot{\rho} = \left(\frac{\partial \rho}{\partial T} \right)_{p, \phi} \dot{T} + \left(\frac{\partial \rho}{\partial p} \right)_{T, \phi} \dot{p} + \left(\frac{\partial \rho}{\partial \phi} \right)_{T, p} \dot{\phi} \quad (3-15)$$

The equation of state for ideal gases

$$p = R\rho T \quad (3-16)$$

can be expressed in differential form as

$$\frac{\dot{p}}{p} = \frac{\dot{R}}{R} + \frac{\dot{p}}{\rho} + \frac{\dot{T}}{T} \quad (3-17)$$

Re-arranging equation (3-17) and using (3-16), we can write

$$\dot{R} = \frac{1}{\rho T} \dot{p} - \frac{p}{\rho^2 T} \dot{\rho} - \frac{p}{\rho T^2} \dot{T} \quad (3-18)$$

Substituting for $\dot{\rho}$ from equation (3-15) into the above equation, we can express \dot{R} in terms of \dot{p} , \dot{T} and $\dot{\phi}$, i.e.

$$\dot{R} = \left(\frac{1}{\rho T} - \frac{p}{\rho^2 T} \frac{\partial \rho}{\partial p} \right) \dot{p} - \left(\frac{p}{\rho T^2} + \frac{p}{\rho^2 T} \frac{\partial \rho}{\partial T} \right) \dot{T} - \frac{p}{\rho T} \frac{\partial \rho}{\partial \phi} \dot{\phi} \quad (3-19)$$

From the differential form of the equation of state, we can express the time rate of change of pressure as

$$\dot{p} = p \left(\frac{\dot{R}}{R} + \frac{\dot{m}}{m} + \frac{\dot{T}}{T} - \frac{\dot{V}}{V} \right) \quad (3-20)$$

or substituting for \dot{R} from equation (3-19), and with some manipulation, we obtain the time rate of change of pressure:

$$\dot{p} = \frac{p}{\partial \rho / \partial p} \left(-\frac{\dot{V}}{V} - \frac{1}{\rho} \frac{\partial \rho}{\partial T} \dot{T} - \frac{1}{\rho} \frac{\partial \rho}{\partial \phi} \dot{\phi} + \frac{\dot{m}}{m} \right) \quad (3-21)$$

Returning to the energy equation (3-11), and expressing \dot{h} in terms of its partial derivatives with respect to T , p and ϕ , we obtain

$$m c_p \dot{T} = \sum_j \dot{m}_j h_j - \dot{Q}_w + (V - m c_T) \dot{p} - m c_\phi \dot{\phi} - \dot{h} m \quad (3-22)$$

Finally, substituting for \dot{p} from equation (3-21), we obtain an equation for the rate of change of temperature that does not explicitly depend on the rate of change of pressure of the system, i.e.

$$m c_p \dot{T} = \left(\sum_j \dot{m}_j h_j - \dot{Q}_w \right) - m c_\phi \dot{\phi} - \dot{h} m + m B \left(-\frac{\dot{V}}{V} - \frac{1}{\rho} \frac{\partial \rho}{\partial T} \dot{T} - \frac{1}{\rho} \frac{\partial \rho}{\partial \phi} \dot{\phi} + \frac{\dot{m}}{m} \right) \quad (3-23)$$

$$\text{where } B = \frac{1}{(\partial\rho/\partial p)} (1 - \rho c_T) \quad (3-24)$$

Dividing (3-23) by m , and collecting terms in \dot{T} , $\dot{\phi}$ and \dot{m} , we get

$$(c_p + \frac{B}{\rho} \frac{\partial\rho}{\partial T}) \dot{T} = \frac{1}{m} (\sum_j \dot{m}_j h_j - \dot{Q}_w) - (c_\phi + \frac{B}{\rho} \frac{\partial\rho}{\partial\phi}) \dot{\phi} + B \frac{\dot{m}}{m} (1 - \frac{h}{B}) - B \frac{\dot{V}}{V} \quad (3-25)$$

leading to

$$\dot{T} = \frac{B}{A} [\frac{\dot{m}}{m} (1 - \frac{h}{B}) - \frac{\dot{V}}{V} - \frac{C}{B} \dot{\phi} + \frac{1}{Bm} (\sum_j \dot{m}_j h_j - \dot{Q}_w)] \quad (3-26)$$

where

$$A = c_p + \frac{B}{\rho} \frac{\partial\rho}{\partial T} = c_p + \frac{(\partial\rho/\partial T)}{(\partial\rho/\partial p)} (1 - c_T) \quad (3-27)$$

$$C = c_\phi + \frac{B}{\rho} \frac{\partial\rho}{\partial\phi} = c_\phi + \frac{(\partial\rho/\partial\phi)}{(\partial\rho/\partial p)} (1 - c_T) \quad (3-28)$$

3.3 Application of Conservation Equations to Reciprocator Cycle

The above conservation equations can be applied to the thermodynamic processes of the four-stroke diesel cycle as follows:

i) Intake

$$\dot{m} = \dot{m}_{in} - \dot{m}_{ex} \quad (3-29)$$

$$\dot{F} = -\frac{\dot{m}_{in}}{m} (F_{in} - F) - \frac{\dot{m}_{ex}}{m} (F_{ex} - F) \quad (3-30)$$

$$\dot{T} = \frac{B}{A} [\frac{\dot{m}}{m} (1 - \frac{h}{B}) - \frac{\dot{V}}{V} - \frac{C}{B} \dot{\phi} + \frac{1}{Bm} (\dot{m}_{in} h_{in} - \dot{m}_{ex} h_{ex} - \dot{Q}_w)] \quad (3-31)$$

ii) Compression

$$\dot{m} = 0 \quad (3-32)$$

$$\dot{F} = 0 \quad (3-33)$$

$$\dot{T} = \frac{B}{A} \left[-\frac{\dot{V}}{V} - \frac{\dot{Q}_w}{Bm} \right] \quad (3-34)$$

(iii) Combustion

$$\dot{m} = \dot{m}_f \quad (3-35)$$

$$F = \frac{\dot{m}_f}{\dot{m}} (1 - F) \quad (3-36)$$

$$\dot{T} = \frac{B}{A} \left[\frac{\dot{m}_f}{m} \left(1 - \frac{h}{b} \right) - \frac{\dot{V}}{V} - \frac{C}{B} \dot{\phi} + \frac{1}{Bm} (\dot{m}_f h_f - \dot{Q}_w) \right] \quad (3-37)$$

where h_f is the absolute fuel enthalpy, given by (B-1).

(iv) Exhaust

$$\dot{m} = -\dot{m}_{ex} \quad (3-38)$$

$$F = -\frac{\dot{m}_{ex}}{\dot{m}} (F_{ex} - F) \quad (3-39)$$

$$\dot{T} = \frac{B}{A} \left[-\frac{\dot{m}_{ex}}{m} \left(1 - \frac{h}{B} \right) - \frac{\dot{V}}{V} - \frac{C}{B} \dot{\phi} + \frac{1}{Bm} (-\dot{m}_{ex} h_{ex} - \dot{Q}_w) \right] \quad (3-40)$$

Note that the fuel fraction of the mass flow rate through the exhaust port, F_{ex} , could be different from the cylinder fuel fraction, F , in reverse flow situations.

CHAPTER 4

MODELING OF RECIPROCATOR ENGINE PROCESSES

4.1 Gas Exchange

A one-dimensional quasi-steady compressible flow model is used to calculate the mass flow rates through the intake and the exhaust valves during the gas exchange process. The intake manifold and the exhaust port are treated as plenums with known pressures. Furthermore, the temperature and average equivalence ratio of the intake charge (fresh air at intake manifold conditions) and the exhaust charge (mixture of air and combustion products at cylinder conditions) are known. When reverse flow into the intake manifold occurs, a rapid-mixing model is used, i.e., instantaneous mixing between the back-flowing charge and the intake charge is assumed.

At each step of the gas exchange process, values for the valve open areas and discharge coefficients are obtained from tabulated data. Given the open area, the discharge coefficient, and the pressure ratio across a particular valve, the mass flow rate across that valve is calculated from:

$$\dot{m} = c_d A \frac{p_o}{RT_o} \sqrt{\gamma RT_o} \left\{ \frac{2}{\gamma-1} \left[\left(\frac{p_s}{p_o} \right)^{2/\gamma} - \left(\frac{p_s}{p_o} \right)^{(\gamma+1)/\gamma} \right] \right\}^{1/2} \quad (4-1)$$

where

c_d = discharge coefficient

A = valve open area

p_o = stagnation pressure upstream of restriction

p_s = static pressure at restriction

T_o = stagnation temperature upstream of restriction

γ = ratio of specific heats

R = gas constant

When the kinetic energy in the cylinder is negligible, the stagnation pressure and temperature reduce to the static pressure and temperature, respectively. For the case of choked flow, equation (4-1) reduces to

$$\dot{m} = c_d A \frac{p_o}{RT_o} \sqrt{\gamma RT_o} \left(\frac{2}{\gamma+1}\right)^{(\gamma+1)/2(\gamma-1)} \quad (4-2)$$

The mass, $m(t)$, in the cylinder at any time t can be found from integration of the mass conservation equation (3-1), i.e.

$$m(t) = m_o + \int_{t_o}^t \dot{m}_{in} dt - \int_{t_o}^t \dot{m}_{ex} dt \quad (4-3)$$

where m_o is the mass in the cylinder at the start of the cycle calculation, inlet valve opening (IVO).

4.2 Combustion Model

The diesel combustion process is a complex, unsteady, heterogeneous, three-dimensional process. A complete mathematical combustion analysis would require accurate models of compressible viscous air motion, fuel spray penetration, droplet break-up and evaporation, air entrainment into the spray, combustion kinetics, turbulent diffusion and so on. The details of the combustion process would depend on the characteristics of the fuel, the design of the combustion chamber and the fuel injection system, and on the engine's operating conditions. Although an adequate conceptual understanding of diesel combustion has been developed to date, a comprehensive quantitative model of all the individual processes has yet to be proposed.

A useful approach to the problem of combustion simulation has been to model combustion as a heat release process, as originally proposed by Lyn [17]. The rate of heat release (or, equivalently, the rate of fuel burning) can be defined as the rate at which the chemical energy of the fuel is

released by combustion. Based on heat release analysis and high-speed photography, Lyn has provided an excellent description of the different stages of diesel combustion. These stages can be identified on the typical rate of heat release diagram for a DI engine shown in Fig. 2 as follows:

Ignition delay: The period between the start of injection (the point at which the injector needle starts to lift) and ignition (the start of positive heat release due to combustion).

Pre-mixed or rapid combustion phase: In this phase, combustion of the fuel which has mixed with air to within the flammability limits during the ignition delay period occurs rapidly in a few crank angle degrees. This results in the high initial rate of burning generally observed in direct-injection diesel engines.

Mixing controlled combustion phase: Once the fuel and air premixed during the ignition delay have been consumed, the heat release rate (or burning rate) is controlled by the rate at which mixture becomes available for burning. The heat release rate may or may not reach a second (usually lower) peak in this phase; it decreases as this phase progresses.

Late combustion phase: Heat release continues at a low rate well into the expansion stroke. Eventually, the burning rate asymptotically approaches zero. The nature of combustion during this phase is not well understood. Possible processes are that a small fraction of the fuel may not yet have burned, or energy present in soot and fuel-rich combustion products can still be released, etc. Given the somewhat arbitrary limits of this phase, combustion models usually focus on the main heat release periods, i.e. the pre-mixed and mixing controlled combustion phases.

Based on his observations, Lyn [17] proposed a method of predicting burning rates from the rate of fuel injection. The fuel injected is divided into elements according to the order in which they enter the combustion chamber. These fuel elements become "ready for burning" according to a certain law. Thus, a "ready for burning" diagram can be obtained from the rate of injection diagram. At the ignition point, which occurs after the lapse of the delay period, the part of the injected fuel which has already been made "ready for burning" is added onto the current "ready for burning" diagram, causing the initial sharp peak in the burning rate diagram. Subsequent burning is essentially governed by the rate of injection. Although this method gives a reasonable fit to data obtained over a wide range of speeds and loads, it requires further refinement and calibration before it can be used in computer simulation work.

An alternative approach to modelling combustion, in the context of computer simulations predicting engine performance, is to describe the apparent fuel burning rate by algebraic expressions. The constants in these expressions can be chosen suitably to reflect the dependence of the actual fuel burning rate on engine type and particular operating conditions.

Shipinski et al [18] attempted to correlate the apparent rate of fuel burning with the rate of fuel injection by fitting a Wiebe function to heat release diagrams obtained from tests on a high-speed swirl-type direct injection engine. Although Shipinski obtained a reasonable agreement with his engine data, the heat release shape defined by the Wiebe function alone has a notable difference from the two-part characteristic with the initial spike that is measured on most engine types.

To overcome this problem, Watson et al [19] proposed that the apparent fuel burning rate could be expressed as the sum of two components, one relating to pre-mixed and the other to diffusion-controlled burning, i.e.

$$\dot{m}_t = \dot{m}_p + \dot{m}_d \quad (4-4)$$

where \dot{m} is the fuel burning rate with respect to crank angle and subscripts t, p, d denote total, pre-mixed and diffusion burning, respectively.

In order to quantify the proportion of the fuel burnt by either mechanism, a phase proportionality factor, β , is introduced. This expresses the cumulative fuel burnt by pre-mixed burning as a fraction of the total fuel injected, i.e.

$$\beta = \frac{\dot{m}_p}{\dot{m}_t} \quad (4-5)$$

Consequently, a non-dimensional apparent fuel burning rate curve can be written as

$$\dot{M}_t(\tau) = \beta \dot{M}_p(\tau) + (1 - \beta) \dot{M}_d(\tau) \quad (4-6)$$

where $\dot{M}(\tau)$ is the non-dimensional burning rate distribution, and τ the normalized crank position.

The phase proportionality factor, β , is considered to be controlled by the length of the ignition delay period (since the fuel that is prepared for burning during this period governs the pre-mixed burning phase), and the overall cylinder equivalence ratio, ϕ_{ove} . This can be expressed by a relation of the form

$$\beta = 1 - a \frac{\phi_{ove}^b}{ID^c} \quad (4-7)$$

where ID is the ignition delay (see Section 4.3), and a, b, c are suitable constants to fit engine cylinder pressure data.

Furthermore, Watson concluded that the best representation of the experimental data was achieved using the following component burning rate distributions:

Premixed burning:

$$M_p(\tau) = 1 - (1 - \tau^{C_{p1}})^{C_{p2}} \quad (4-8a)$$

$$\text{or} \quad \dot{M}_p(\tau) = C_{p1} C_{p2} \tau^{(C_{p1}-1)} (1 - \tau^{C_{p1}})^{(C_{p2}-1)} \quad (4-8b)$$

Diffusion controlled burning (Wiebe function)

$$M_d(\tau) = 1 - \exp(-C_{d1} \tau^{C_{d2}}) \quad (4-9a)$$

$$\text{or} \quad \dot{M}_d(\tau) = C_{d1} C_{d2} \tau^{(C_{d2}-1)} \exp(-C_{d1} \tau^{C_{d2}}) \quad (4-9b)$$

where C_{p1} , C_{p2} , C_{d1} , C_{d2} are shape factors. The shape factors in equations (4-8) and (4-9) can be determined as a function of the engine operating conditions.

Using data from three typical turbocharged truck engines, (design details are summarized in Table 1), Watson established that the pre-mixed burning factors C_{p1} and C_{p2} were adequately modeled, for all three designs, by the following correlations:

$$C_{p1} = 2.0 + 1.25 \times 10^{-8} (ID \times N)^{2.4} \quad (4-10a)$$

$$C_{p2} = 5000 \quad (4-10b)$$

where ID = ignition delay, ms (see Section 4.3)

N = engine speed, RPM

The diffusion burning factors C_{d1} , controlling the rate and duration of diffusion burning, and C_{d2} , controlling the timing of the peak diffusion burning rate, were modeled by correlations of the form

$$C_{d1} = k_1 \phi_{ove}^{-k_2} \quad (4-11a)$$

$$C_{d2} = k_3 C_{d1}^{k_4} \quad (4-11b)$$

where ϕ_{ove} is the overall cylinder equivalence ratio, and k_1, k_2, k_3, k_4 are constants appropriate for each combustion chamber design. Table 1 summarizes the values for the diffusion-burning constants in equation (4-11) and the phase-proportionality constants in equation (4-7) that Watson established for the three engines used in his tests. In our engine simulation, we have followed Watson's approach to describe the heat release profile.

4.3 Ignition Delay Model

The ignition delay period in a diesel engine was defined in section 4.2 as the time (or crank angle) interval between the start of injection and the start of combustion. The start of injection is usually taken as the time when the injector needle lifts off its seat (determined from a needle lift indicator). The start of combustion is more difficult to determine. It is best identified from the change in slope of the heat release rate versus time curve which occurs at ignition.

Both physical and chemical processes must take place before the injected fuel can burn. The physical processes are: the atomization of the liquid fuel jet; the vaporization of the fuel droplets; the mixing of fuel vapor with air. The chemical processes are the precombustion reactions of the fuel, air, residual-gas mixture which lead to autoignition. These processes are affected by engine design and operating variables, and fuel characteristics.

Ignition delay data from fundamental experiments in combustion bombs and flow reactors have usually been correlated by equations of the form

$$ID = A p^{-n} \exp(E/RT) \quad (4-12)$$

where ID = ignition delay, ms

E = apparent activation energy for the fuel autoignition process

R = universal gas constant

p = gas pressure, atm

T = gas temperature, Kelvins

and A and n are constants dependent on the fuel and the injection and air-flow characteristics. Representative values for A, n and E are given in Table 2. Additional details can be found in [20]-[22].

These correlations have usually been derived from tests in uniform air environments where the pressure and temperature only changed due to the cooling effect of the fuel vaporization and fuel heating processes. However, in a diesel engine, pressure and temperature change considerably during the delay period due to the compression resulting from piston motion. Another problem is that the form of these simple correlations is not sufficiently flexible to allow all the influencing fuel and engine parameters to be included in the calculation of the ignition delay.

Hardenberg and Hase [23] have developed an empirical formula for predicting the ignition delay in DI engines as a function of fuel characteristics, engine parameters and ambient conditions. Dent [24] has shown that this formula can give reasonable agreement with experimental data over a wide range of engine conditions. However, the pressure and temperature used in this correlation are identified as the corresponding conditions at top dead centre, estimated using a polytropic model for the compression process.

It is felt that such a polytropic model is not appropriate in our simulation context, where pressures and temperatures can be accurately predicted over the duration of the ignition delay period.

We have included two approaches for ignition delay in this simulation:

- a. The crank angle at start of combustion can be specified: this often is useful when it is desired to suppress changes in combustion timing (which may shift the combustion process relative to its optimum location in the cycle).
- b. The ignition delay period is calculated as the difference between the time at which combustion occurs (t_{ign}) and the time at which injection starts (t_{inj}). The time t_{ign} is obtained by integrating over the duration of the ignition delay period the reciprocal of the predicted ignition delay at each time step until the following relationship is satisfied:

$$\int_{t_{inj}}^{t_{ign}} \frac{dt}{ID(t)} = 1 \quad (4-13)$$

where the instantaneous estimates of the ignition delay are calculated from an equation of the form of (4-12), with pressure and temperature taken at their instantaneous values.

4.4 Heat Transfer

The heat transfer mechanisms in a diesel engine include forced convection (\dot{Q}_c) from the turbulent flow in the cylinder to the combustion chamber walls, and radiation (\dot{Q}_r) from the flame and the burning soot particles. The total heat transfer rate (\dot{Q}_w) is therefore given by

$$\dot{Q}_w = \dot{Q}_c + \dot{Q}_r \quad (4-14)$$

4.4.1 Convective heat transfer

The convective heat transfer at the gas-to-cylinder wall interface will depend on the temperature gradient in the boundary layer at the surface. However, due to the inherent difficulties in calculating the details of turbulent fluid motion in the combustion chamber during the operating cycle of the engine, the convective heat transfer rate is usually expressed as

$$\dot{Q}_c = h A (T_g - T_w) \quad (4-15)$$

where

h = convective heat transfer coefficient

A = surface area

T_g = bulk mean gas temperature

T_w = inside wall surface temperature of cylinder head, piston, or liner, as appropriate.

The problem is then to devise a method to calculate the convective heat transfer coefficient that appears in (4-15). The approach usually taken is to calculate h from a Nusselt-Reynolds number correlation analogous to that used for steady turbulent flow in a pipe [25]-[29], i.e.,

$$Nu = a Re^d Pr^e \quad (4-16)$$

where

Nu = hL/λ : Nusselt number

Re = VL/ν : Reynolds number

Pr = $\mu c_p / \lambda$: Prandtl number

L = a characteristic length

- V = a characteristic velocity
- λ = thermal conductivity
- ν = kinematic viscosity
- μ = dynamic viscosity
- ρ = density
- c_p = specific heat at constant pressure

and a, d, e are constants adjusted to fit experimental data.

Fortunately, there is little variation in the Prandtl number for air and combustion products, which is usually close to unity. Consequently, we may drop the Prandtl number dependence in equation (4-16) with little loss in accuracy, so that

$$Nu = a Re^d \quad (4-17)$$

To calculate the convective heat transfer coefficient from correlation (4-17), instantaneous values for the characteristic length and velocity scales, and the gas transport properties (μ , ρ , and λ) are needed. Currently, it is not possible to predict these parameters and their spatial and temporal variation with any accuracy in an internal combustion engine. To overcome this difficulty, representative values of the characteristic length and velocity scales, and the gas temperature, pressure, and equivalence ratio at which the gas properties are to be evaluated are chosen.

For our heat transfer model, the characteristic length scale is taken to be the macroscale of turbulence, as defined by equation (4-36). The characteristic velocity V is postulated to be an effective velocity due to contributions from the mean kinetic energy, the turbulent kinetic energy and piston motion, i.e.

$$V = [U^2 + u'^2 + (v_p/2)^2]^{1/2} \quad (4-18)$$

where

U = mean flow velocity, defined by (4-28)

u' = turbulent intensity, defined by (4-29)

V_p = instantaneous piston speed

While this expression for V is speculative, it is constructed in such a way that increases in any of the three component velocities lead to increases in the heat transfer rate, while at the same time errors due to overestimating the contribution from any one component are minimized.

Many attempts have been reported to determine the constants a and d , through curve-fitting experimental results [25]-[29]. Suggested values are

$$a = 0.035 \text{ to } 0.13 \quad (4-19)$$

$$d = 0.7 \text{ to } 0.8$$

depending on intensity of charge motion. The gas density and the transport properties, μ and λ , that appear in correlation (4-17) are evaluated at the mean gas temperature, pressure, and equivalence ratio of the cylinder contents (see Appendix C).

4.4.2 Radiative heat transfer

The primary sources of radiative heat transfer in a diesel engine are the high temperature burned gases and the soot particles which are formed as an intermediate step in the turbulent diffusion-controlled diesel flame. Because the particle size distribution, number density, and temperature, and flame geometry are not well defined in a diesel engine, direct measurements of radiation on operating engines are required.

Estimates of the relative importance of radiation in cooled diesel engines have varied between a few and 50 percent of the total heat transfer [26],[27],[30]-[37]. The limited experimental engine radiation measurements to date are summarized in Table 3. In general, the radiant heat flux depends

on the location on the combustion chamber surface, crank angle in the operating cycle, engine load, engine size, and engine design. At high load, the measurements suggest that the radiant heat flux is between 25 and 45 percent of the total heat flux.

Due to the complexity of the problem, accepted prediction formulas for radiant heat flux in a diesel engine are not available. Annand [26] has proposed a radiation term based on the average bulk gas temperature of the form:

$$\dot{Q}_r = k_r A (T_g^4 - T_w^4) \quad (4-20)$$

where k_r = empirical radiation constant

A = surface area

T_g = average bulk gas temperature

T_w = inside wall surface temperature of cylinder head, piston or liner, as appropriate.

During the intake, compression and exhaust processes, the radiative heat flux is taken to be zero. During combustion, Annand and Ma [27] suggested that

$$k_r = C_r \sigma \quad (4-21)$$

where σ is the Stephan-Boltzmann constant ($56.7 \times 10^{-12} \text{ kW/m}^2 \text{K}^4$), and C_r is an adjustable calibrating constant with values in the range of 0.6-3.1, depending on the engine speed and load. Note that since the temperature used is the average bulk temperature and not the flame temperature, C_r is not an emissivity. Limited evaluation of this approach has shown that $C_r = 0.6$ gave approximately correct radiant flux magnitude for one engine but was too low for another [30], while $C_r = 1.6$ gave radiant heat fluxes higher than experimental data [31]. Flynn et al [37] have measured the instantaneous radiant heat transfer in a direct-injection diesel engine under a wide range

of engine operating conditions. A monochromator was used to measure intensity of radiation at seven wavelengths. By assuming a monochromatic emissivity law consistent with observed radiation from very small particles [38] and integrating over all wavelengths, Flynn et al. obtained an apparent radiant temperature, an apparent grey-body emissivity, and a total radiant heat transfer rate at each crank angle during the cycle. The results of Flynn's work indicate that the apparent radiant temperature is much higher than the average bulk gas temperature. In fact, during the time of peak heat release, the apparent radiant temperature was found to be very close to the flame temperature. Furthermore, during the period of maximum radiation, the apparent emissivity was 0.8 to 0.9, and it dropped almost linearly to zero by the end of the combustion process.

In the light of Flynn's results, and due to the absence of any real fundamental basis or experimental support for Annand's model, an alternative radiation model was developed for the present work. The instantaneous radiant heat flux is expressed as

$$\dot{Q}_r = \epsilon_a \sigma A (T_r^4 - T_w^4) \quad (4-22)$$

where ϵ_a = apparent grey-body emissivity

σ = Stephan-Boltzmann constant

A = surface area

T_r = apparent radiant temperature

Flynn's data suggest that the apparent radiant temperature is close to the adiabatic flame temperature during the period of peak heat release. The adiabatic flame temperature can be modeled as the temperature of slightly greater than stoichiometric zones of hydrocarbon-air combustion products, i.e., $T(\phi = 1.1)$. However, as combustion progresses and relatively fewer

close-to-stoichiometric fuel-air zones are found in the cylinder, this adiabatic flame temperature becomes considerably higher than Flynn's apparent radiant temperature [37]. A better estimate (in reasonable agreement with the data) of the apparent radiant temperature was found to be the mean of the adiabatic flame temperature and the average bulk gas temperature, i.e.

$$T_r = \frac{T_{ad} + T(\phi = 1.1)}{2} \quad (4-23)$$

The temperature of combustion products at an equivalence ratio of 1.1, $T(\phi = 1.1)$, is computed as a function of the instantaneous air temperature and pressure from a correlation obtained by applying a least-squares curve-fitting technique to results of the NASA equilibrium program [39], for constant pressure hydrocarbon-air combustion. Satisfactory accuracy (less than 1% error) was obtained by considering two adjacent air temperature ranges, i.e.:

$$T(\phi = 1.1) = [1 + 0.0002317(T_{air} - 950)] \times (2726.3 + 0.9306p - 0.003233p^2) \quad (4-24)$$

for $800 \text{ K} < T_{air} < 1200 \text{ K}$

$$T(\phi = 1.1) = [1 + 0.000249(T_{air} - 650)] \times (2497.3 + 4.7521p - 0.11065p^2 + 0.000898p^3) \quad (4-25)$$

for $450 \text{ K} < T_{air} < 800 \text{ K}$.

The instantaneous air temperature, T_{air} , is calculated assuming adiabatic compression of the air from the condition at the start of combustion (subscript ign), i.e.

$$T_{air} = T_{air,ign} (p/p_{ign})^{(\gamma-1)/\gamma} \quad (4-26)$$

where γ is the ratio of specific heats for air at the instantaneous temperature and pressure.

The apparent emissivity is assumed to vary linearly between its maximum value (taken as 0.9) and zero over the duration of the combustion process, i.e.

$$\epsilon_a(t) = 0.9 \left(1 - \frac{t - t_{ign}}{t - t_{evo}}\right) \quad (4-27)$$

where t_{evo} is the time when the exhaust valve opens.

4.5 Turbulent Flow Model

The heat transfer model of the cycle simulation requires estimates of the characteristic velocity and length scales. To estimate these scales in a way which incorporates the key physical mechanisms affecting charge motion in the cylinder, a turbulent flow model is used. This model is a variation of the models used by Mansouri et al [40], Poulos and Heywood [41] in previous engine simulation work.

The turbulence model consists of a zero-dimensional energy cascade. Mean flow kinetic energy, K , is supplied to the cylinder through the valves. Mean kinetic energy, K is converted to turbulent kinetic energy, k , through a turbulent dissipation process. Turbulent kinetic energy is converted to heat through viscous dissipation. When mass flows out of the cylinder, it carries with it both mean and turbulent kinetic energy. Figure 3 illustrates the energy cascade model.

At any time during the cycle, the mean flow velocity, U , and the turbulent intensity, u' , are found from knowledge of the mean and turbulent kinetic energies, K and k , respectively. Thus, the following equations apply:

$$K = \frac{1}{2} m U^2 \quad (4-28)$$

$$k = \frac{3}{2} m u'^2 \quad (4-29)$$

where the factor 3 in equation (4-29) comes from assuming that the small scale turbulence is isotropic (and accounting for all three orthogonal fluctuating velocity components).

The time rate of change of the mean kinetic energy, K is given by

$$\frac{dK}{dt} = \frac{1}{2} \dot{m}_i V_i^2 - P - K \frac{\dot{m}_e}{m} \quad (4-30)$$

Similarly, the rate of change of the turbulent kinetic energy, k, is

$$\frac{dk}{dt} = P - m\epsilon - k \frac{\dot{m}_e}{m} + A \quad (4-31)$$

with $\epsilon \approx \frac{u'^3}{l} = \frac{(2k/3m)^{3/2}}{l}$ (4-32)

where m = mass in the cylinder

\dot{m}_i = mass flow rate into the cylinder

\dot{m}_e = mass flow rate out of the cylinder

V_i = jet velocity into the cylinder

P = rate of turbulent kinetic energy production

ϵ = rate of turbulent kinetic energy dissipation per unit mass

A = rate of turbulent kinetic energy amplification due to rapid distortion

l = characteristic size of large-scale eddies

In equations (4-30) and (4-31), the production term P has to be defined in terms of flow and geometrical parameters of the chamber. However, since the above model does not predict spatially resolved flow parameters, P must be estimated from mean flow quantities only.

Assuming that turbulence production in the engine cylinder is similar to turbulence production in a boundary layer over a flat plate [42], we can express P as

$$P = \mu_t \left(\frac{\partial U}{\partial y} \right)^2 \quad (4-33)$$

where $\mu_t = C_\mu k^2 / (m\varepsilon)$ is turbulent viscosity, and $C_\mu = 0.09$ is a universal constant. Again, as the velocity field in the cylinder is not known, the velocity gradient $(\partial U / \partial y)$ is approximated as

$$\left(\frac{\partial U}{\partial y} \right)^2 = C_\beta \left(\frac{U}{L} \right)^2 \quad (4-34)$$

where C_β is an adjustable constant and L is a geometric length scale.

Using equations (4-33), (4-34), (4-28) and (4-32), we can express P as

$$P = 2 \left(\frac{3}{2} \right)^{3/2} C_\mu C_\beta \left(\frac{K\ell}{L^2} \right) \left(\frac{k}{m} \right)^{1/2} \quad (4-35)$$

Furthermore, the characteristic size of the large-scale eddies, ℓ , and the representative geometric length scale, L will be both identified with the macroscale of turbulence, assumed to be given by

$$\ell = L = V / (\pi B^2 / 4) \quad (4-36a)$$

where V is the instantaneous volume of the combustion chamber and B is the cylinder bore, subject to the restriction that

$$L \leq B/2 \quad (4-36b)$$

Hence, equation (4-35) can be re-written as

$$P = 0.3307 C_\beta \left(\frac{K}{L} \right) \left(\frac{k}{m} \right)^{1/2} \quad (4-37)$$

During the compression and the combustion processes, the turbulent kinetic energy decays due to viscous dissipation. At the same time the turbulent kinetic energy is amplified due to the rapid distortion that the cylinder charge undergoes with rising cylinder pressures. Consequently, an amplification term, A, was added to equation (4-31) to account for this effect. The amplification term will be larger during combustion when the unburned gas is assumed to be compressed by the flame at a sufficiently high rate. However, in the diesel engine context of high compression ratios, the amplification term is included during compression, too.

Using equation (4-29), the rate of turbulence amplification due to rapid distortion can be expressed as

$$A = 3 m u' \frac{du'}{dt} \quad (4-38)$$

where the rate of change of the turbulent intensity du'/dt can be estimated assuming that conservation of mass and angular momentum can be applied to the large scale eddies during the rapid distortion period.

Under these assumptions, conservation of mass for a single eddy of volume V_L requires that

$$\rho V_L = \rho_o V_{Lo} \quad (4-39)$$

where ρ is the mean gas density and subscript o refers to the conditions at the start of compression. Then, since

$$V_L \sim L^3 \quad (4-40)$$

where L is the macroscale of turbulence, we can re-write (4-39) as

$$\frac{L}{L_o} = \left(\frac{\rho_o}{\rho}\right)^{1/3} \quad (4-41)$$

Conservation of eddy angular momentum requires that

$$U_{\omega} L = U_{\omega 0} L_0 \quad (4-42)$$

where U_{ω} is the characteristic velocity due to eddy vorticity.

Combining (4-41) and (4-42) with the assumption that

$$U_{\omega} \sim u' \quad (4-43)$$

the following relation is obtained for the evolution of the turbulent intensity during the rapid compression period

$$\frac{u'}{u'_0} = \left(\frac{\rho}{\rho_0}\right)^{1/3} \quad (4-44)$$

Differentiating both sides of equation (4-44) and re-arranging we get

$$\frac{du'}{dt} = \frac{u'}{3\rho} \frac{d\rho}{dt} \quad (4-45)$$

Hence, combining equations (4-38) and (4-45), the rate of turbulence amplification is given by

$$A = \frac{mu'^2}{\rho} \frac{d\rho}{dt} \quad (4-46)$$

or, introducing (4-29),

$$A = \frac{2}{3} k \frac{\dot{\rho}}{\rho} \quad (4-47)$$

with $\dot{\rho}$ given from equation (3-15).

4.6 Engine Friction Model

To convert indicated engine performance quantities to brake engine performance quantities, engine friction estimates are required. However, the measurement and analysis of engine frictional losses are yet to be satisfactorily resolved. This is primarily due to the inherent problem of

direct, accurate measurement of these losses under actual running conditions. This problem occurs because the total loss is a summation of losses arising from the operation of the many components of the engine, and these components respond differently to changes in pressure, temperature and speed.

Direct motoring of an engine is the common method of measuring losses, but clearly the motoring losses are not the same as the losses under firing conditions. Some of the reasons are the lower pressure acting on piston rings and bearings, the lower temperatures of the piston and cylinder bore surfaces and thus the greater oil viscosity, the greater running clearance of the piston, and the missing exhaust blowdown period.

Nevertheless, a breakdown analysis of motoring losses supplemented by experiments on piston and ring friction rigs can be used to identify the relative importance of the many components of the total friction and their response to changes in design variables. In general, the components of the losses expressed in terms of mean effective pressure, mep, tend to fall into three groups:

- (i) Losses due to boundary lubrication, where the friction forces are approximately invariant with speed. These losses are undoubtedly influenced by the compression ratio.
- (ii) Losses associated with hydrodynamically lubricated surfaces in relative motion, which vary directly with speed. All major rotating parts fall into this group.
- (iii) Losses associated with fluid (air, water and oil) pumping, which vary as the square of the speed.

Therefore, the motoring losses can be expressed in the form

$$F = A + BN + CN^2 \quad (4-48)$$

where F are the losses in mep, N is engine speed, and A, B and C are constants.

Millington and Hartles [43] have measured motoring losses on a large variety of automotive diesel engines during the course of development of prototype engines. Their work suggests a readjustment of equation (4-48) coupled with suitable selection of the constants as follows:

$$F = A + 7.0 \frac{N}{1000} + 1.5 \left(\frac{V}{1000} \right)^2 \quad (4-49)$$

where F = motoring mep, psi

A = compression ratio minus 4 for a DI diesel

N = engine speed, RPM

V = mean piston speed, ft/min

Equation (4-49) represents a sound empirical correlation of the motoring loss data obtained from diesel engines. It is used to obtain brake quantities from the indicated quantities computed in the engine simulation.

CHAPTER 5

MODELING OF OTHER SYSTEM COMPONENTS

5.1 Turbomachinery Modeling

Steady-state performance maps give the interrelationships among mass flow rate, efficiency, pressure ratio and rotor speed for each of the three turbomachinery components: turbocharger compressor, turbocharger turbine and power turbine. The map variables of mass flow rate, \dot{m}_{map} , and rotor speed, ω_{map} , are corrected by factors relating actual inlet conditions to standard conditions. The speed correction factor involves inlet temperature, and the mass flow rate correction factor involves inlet temperature and pressure, so that

$$\omega_{map} = \omega_{actual} (T_{std} / T_{in})^{1/2} \quad (5-1)$$

$$\dot{m}_{map} = \dot{m}_{actual} (p_{std} / p_{in}) (T_{in} / T_{std})^{1/2} \quad (5-2)$$

where the subscripts in and std refer to actual inlet and map standard inlet conditions, respectively.

The turbomachinery maps, usually obtained in graphical form, are entered into the simulation in tabular form, i.e. as a one-dimensional array of rotor speeds, ranked in ascending order; and a three-dimensional array of the remaining map variables, arranged as follows: for each of the speeds stored in the speed array, a uniform number of data points is recorded, each consisting of the values of mass flow, efficiency and pressure ratio at that point. The data points for each speed curve for each map are ranked in ascending order of pressure ratio. Note that for the compressor map this implies entering data in descending order of mass flow.

At a particular step in the cycle simulation, the tables need to be interpolated to find the necessary information. Appropriate routines were developed to interpolate the performance maps of the various turbomachinery components. In general, these routines perform two-dimensional interpolation to calculate two unknown map variables from two known variables. Speed is always one of the two known variables and efficiency is one of the two unknown variables. Then, either mass flow rate is known and pressure ratio unknown, or vice-versa, depending on the turbomachinery component and the system configuration.

The method of map interpolation, as applied for example to the compressor map, is the following. Given a corrected speed, a search of the compressor speed array is performed, from the lowest value (i.e. the first array element) until a speed greater than the input speed is found. Using that greater speed and the speed just previous to that (the lesser speed), a speed interpolation parameter is calculated. This speed interpolation parameter is used to calculate values of pressure ratio at the input speed, until a pressure ratio greater than the input pressure ratio is found. This pressure ratio search, from low to high, will thus define a pressure ratio interpolation parameter. Then, using the speed and pressure ratio interpolation parameter, a two-dimensional linear interpolation is performed to calculate the mass flow and efficiency that correspond to the input values of speed and pressure ratio.

Certain important physical constraints must be considered in modeling turbomachinery component performance:

- (a) Compressor Surge Line: When the mass flow rate through a compressor is reduced while maintaining a constant pressure ratio, a point arises at which local flow reversal occurs in the boundary layers. This will relieve the adverse pressure gradient until a new flow regime at a lower

pressure ratio is established. Then, the flow will build up to the initial conditions, and thus flow instability will continue at a fixed frequency. This phenomenon is called surge. Clearly, a compressor should not operate in the low-efficiency, unstable region, to the left of the surge line.

(b) Turbine Choking Characteristics: The mass flow range of a radial turbine, such as the turbocharger and the turbocompounded turbines, is limited by choking at high pressure ratios. The choking characteristics of the turbine are speed dependent. This effect is caused due to the centrifugal field created by the speed of the rotor.

To avoid any potential problems associated with the above constraints, certain provisions have been incorporated in the logic of the turbomachinery interpolation routines:

(i) Since the pressure ratio versus turbocharger speed line is fairly flat close to the compressor surge limit, small changes in pressure ratio can result in disproportionately large changes in output mass flow rate values. In order to avoid any oscillations in the system convergence procedure which could result in a substantial increase in computational time, the pressure ratio versus mass flow rate curves are modeled as single-valued, with a small, non-zero, slope close to the surge line.

(ii) During the turbocharger matching calculation, the rotor speed at some instant could become too low for the required boost pressure ratio. This means that the mass flow would have to be to the left of the surge boundary. Under these circumstances, the speed of the rotor is increased until an acceptable mass flow solution at the given input pressure ratio is obtained.

(iii) During the course of the simulation iterations, certain engine operating conditions could correspond to points that lie beyond the normal operating regime of the turbomachinery maps. Then, linear extrapolation is performed to extend the range of the map characteristics. This extrapolation is subject to certain checks, so that the map regimes are not extended beyond the turbine choking characteristics or to the left of the compressor surge line. Furthermore, if the final converged solution for the engine-turbocharger matching is well beyond the normal map regimes, the turbomachinery used is not appropriate for the given engine design and operating conditions. The calculation should be repeated with more suitable turbomachinery components (different machine sizes, or higher component efficiencies).

5.2 Turbocharger Dynamics

The rate of change of the mechanical energy of the turbocharger rotor, $E_{t/c}$, depends on the difference between the power required to drive the compressor (negative), and the power delivered by the turbocharger turbine (positive):

$$\dot{E}_{t/c} = \dot{W}_{\text{compressor}} + \dot{W}_{\text{turbine}} \quad (5-3)$$

The change in mechanical energy relates to the change in rotor speed according to the turbocharger dynamics, i.e.,

$$\dot{E}_{t/c} = J\dot{\omega} + B\omega^2 \quad (5-4)$$

where

J = rotational inertia of turbocharger

B = rotational damping of turbocharger

ω = angular velocity

The compressor and the turbine powers can be expressed as:

$$\dot{W}_{\text{compressor}} = \dot{m}_c (h_1 - h_2) \quad (5-5)$$

$$\dot{W}_{\text{turbine}} = \dot{m}_t (h_8 - h_9) \quad (5-6)$$

Solving for the change in speed $\dot{\omega}$ gives:

$$\dot{\omega} = \{(\dot{m}_c (h_1 - h_2) + \dot{m}_t (h_8 - h_9) - B\omega^2)\} / J\omega \quad (5-7)$$

Note that the enthalpy changes across the compressor and turbine can be calculated assuming compressible flow across the two turbomachines, i.e.,

$$(h_1 - h_2) = -\frac{h_1}{\eta_c} \left[\left(\frac{p_2}{p_1} \right)^{R/c_p} - 1 \right] \quad (5-8)$$

$$(h_8 - h_9) = \eta_t h_8 \left[\left(\frac{p_8}{p_9} \right)^{R/c_p} - 1 \right] \quad (5-9)$$

5.3 Turbocharger Matching Procedure

The simulation code is set up to analyze two different system configurations: i) a single stage turbocharged diesel system and, ii) a turbocharged turbocompounded diesel system. Suitable turbocharger matching procedures have been developed for each case. These are summarized below.

5.3.1 Single-stage turbocharged case

The system configuration for this case is shown in Fig. 4. At a given instant, the values of the variables describing the state of the various system components are known (from the integration of the system governing equations over the previous time step). These include the intake and exhaust

manifold pressures and the turbocharger rotor speed. Additionally, the compressor inlet pressure and the turbine exhaust pressure are fixed, i.e., atmospheric pressure less intake air filter pressure drop and atmospheric pressure plus muffler pressure drop, respectively. By relating the compressor discharge pressure to the intake manifold pressure and the turbine inlet pressure to the exhaust manifold pressure, through suitable pressure drops, the pressure ratio across each turbomachine is determined. Hence, the compressor and turbine maps can be entered using the calculated pressure ratios and the rotor speed (same for both turbomachines) as inputs. The output of the map interpolation routines determines the mass flow rate and efficiency for each component for the next time step. From these, the power required to drive the compressor, and the power delivered by the turbine are determined. Any excess power will result in a change in the rotor speed according to the turbocharger dynamics, i.e., Eq. (5-4). Finally, the values of the other state variables for the next time step will be determined from solution of the mass and energy conservation equations, where the compressor and turbine mass fluxes are taken from the output of the turbomachinery interpolation routines.

5.3.2 Turbocharged turbocompounded case

This case is relatively more complicated. For this system configuration, shown in Figure 1, the intake side, and hence the compressor map treatment is identical to the single-stage turbocharged case. However, on the exhaust side, although the available pressure ratio can be defined as for the turbocharged case, the division of the pressure ratio between the two turbines is not known a priori. This calculation requires a special iterative procedure, based on continuity of mass flow through the exhaust system. At each time step, the calculation is started by assuming a mass flow going

through the first turbine (taken as the value at the previous time step). Then, the turbocharger turbine interpolation routine is entered with the mass flow rate and rotor speed as inputs. From the turbine pressure ratio returned by the routine, and the known exhaust manifold pressure, the first turbine exit pressure is determined. The latter, and the system exit pressure (atmospheric plus muffler pressure drop), specify the pressure ratio across the power turbine. Then, the power turbine map can be interpolated with the pressure ratio and shaft speed (gear ratio times reciprocator speed) as input, thus defining the mass flow through the power turbine. An updated estimate of the mass flow through the first turbine can be then calculated based on the previous estimate and the power turbine mass flow. The scheme used involves under-relaxation to increase the stability and efficiency of the matching procedure. For a converged solution, the mass flow through the turbocharger turbine (plus flow through the wastegate, if appropriate) must equal the flow through the power turbine. Once the turbocharger turbine flow and efficiency are established, the system state variables for the next time step can be determined following the same procedure as for the single-stage turbocharged case.

5.4 Intercooler Model

The intercooler, situated between the compressor discharge and the intake manifold, serves to increase the density of the charge air by lowering its temperature. The intercooler is modelled as a heat exchanger of fixed area, over-all heat-transfer coefficient and cooling flow rate. The change in charge air temperature is determined from the non-dimensional heat exchanger effectiveness, ϵ ,

$$\epsilon = \frac{(T_{h1} - T_{h2})}{(T_{h1} - T_{c1})} \quad (5-10)$$

where the subscripts h and c refer to the charge air flow (hot) and the coolant flow (cold) respectively; 1 and 2 refer to inlet and exit conditions; and

T_{h1} = compressor discharge temperature

T_{h2} = intercooler discharge temperature

T_{c1} = coolant inlet temperature (assumed to be fixed).

The heat exchanger effectiveness is either known as a design parameter, or can be derived from graphical correlations that are available for the various typical heat exchanger configurations [44]. From the latter, ϵ can be determined as a function of the capacity rate ratio, C_{\min}/C_{\max} , and the number of heat transfer units, N_A , where C_{\min} and C_{\max} are respectively the smaller and larger of the products of charge air and coolant flow rates with their respective specific heats, and

$$N_A = AU/C_{\min}$$

where A = heat exchange surface area (fixed)

U = over-all heat transfer coefficient based on A .

Assuming that C_{\max} is much larger than C_{\min} , the expression for effectiveness reduces to the following simple form:

$$\epsilon = 1 - \exp(-N_A) \quad (5-11)$$

5.5 Exhaust Manifold Model

In most engine simulation programs of this type, the exhaust manifold is treated as a global open system [16]. A simple plenum is used with the exhaust gases from each cylinder flowing into the system and mixing with the

all of the gases in the manifold. This approach has three primary disadvantages. First, the exhaust gases from a given cylinder are diluted by the gases in the manifold in a manner that is not representative of a real manifold, where individual runners keep the gases from different cylinders separated during much of the flow path between the exhaust valve and the turbine. This dilution decreases substantially the gas temperature oscillations that occur in the manifold and at the turbine inlet.

The second disadvantage of a common plenum model is that it is not possible to follow the change in gas temperature as the gases flow through the exhaust manifold, mix with the gases in each section, and lose heat to the surroundings. With a common control volume, only one temperature is used to represent the temperature of the gases in the exhaust manifold. Again, this is not a good representation of a real exhaust manifold where the gas temperature varies along the length of the path between the exhaust valve and the turbine inlet.

The third disadvantage with a single control volume is that it is impossible to match the approximate volume, the inside surface area, and the cross-sectional area of a real manifold with only one set of dimensions for the model. The approximate volume is important for the accurate determination for the exhaust manifold pressure which in turn is an important factor in determining the turbocharger performance. The cross-sectional area and inside surface area are important for determining the temperature of the gases at the inlet to the turbocharger. With the single control volume approach, one is forced to compromise one or more of these geometric factors when specifying the dimensions of the manifold to be used for the simulation.

To avoid these disadvantages with a single plenum model, the exhaust manifold is divided into a series of connected open systems. The manifold is

considered to be a composite of ports, runners, and a common plenum section. The port section is taken to be the volume contained within the head of the engine. The runner represents the section of the manifold outside the head where the gases from one cylinder flow without mixing with the gases from any other cylinder. The plenum is defined as the volume where the gases from each of the engine cylinders, ports and runners are mixed before entering the turbine. A fourth system is also followed during the simulation that is composed of the runner from each cylinder and the plenum. This system has the properties that represent the average properties of the separate sub-systems, and it is used to determine the change in pressure in the manifold based on the overall mass balance.

As is done with the engine cylinders, the simulation only calculates the properties of the ports and runners for one master port and one representative master runner. The master port and runner information necessary to include the other cylinders in the engine calculation is stored in high-speed memory and is retrieved with the appropriate phase shift to determine what was occurring in other ports and runners at any given time during the cycle.

5.6 Manifold Conservation Equations

The general manifold open system model is shown in Figure 5. The differential equations for the change in total mass and fuel fraction for the manifold come directly from the continuity relations derived earlier in Section 3.1, i.e.,

$$\dot{m}_m = \sum_j \dot{m}_j, \quad (5-12)$$

$$\dot{F}_m = \sum_j \frac{\dot{m}_j}{m_m} (F_j - F_m) \quad (5-13)$$

where the subscript m refers to the intake manifold, or exhaust manifold section, and the subscript j refers to the j-th mass flow that enters or leaves the system of interest.

The mass flows entering and leaving the intake manifold include the compressor mass flow (entering) which is found from the compressor map; and the engine intake mass flow (leaving or entering) which is found from the reciprocator model. The mass flows entering and leaving the exhaust manifold as a whole include the turbine mass flow (leaving) which is found from the turbocharger turbine map; the engine exhaust mass flow (entering or leaving) which is found from the reciprocator model; and the wastegate mass flow (leaving).

The differential equation for the change in intake manifold temperature is derived from the generalized temperature equation applied to an open system, i.e.,

$$\dot{T}_m = \frac{1}{A} \left[\left(\frac{\dot{m}}{m} \right) (B - h_m) - C \dot{\phi}_m + \frac{1}{m} \left(\sum_j \dot{m}_j h_j - \dot{Q} \right) \right] \quad (5-14)$$

where A, B, and C are defined in Eqs. (3-27), (3-24) and (3-28), and are calculated by the thermodynamic property routines; \dot{Q} is heat transfer rate to the manifold walls; and $\dot{\phi}$ is related to \dot{F} and F by Eq. (3-8).

The differential equation for the change in intake manifold pressure is derived from the generalized pressure equation applied to an open system, i.e:

$$\dot{p}_m = \frac{\rho}{\partial \rho / \partial p} \left[- \frac{1}{\rho} \frac{\partial \rho}{\partial T} \dot{T}_m + \left(\frac{\dot{m}}{m} \right) \frac{1}{m \rho} \frac{\partial \rho}{\partial \phi} \dot{\phi}_m \right] \quad (5-15)$$

where the density derivatives are calculated by the thermodynamic property routines.

The exhaust manifold is broken down into a series of connected open systems that are contained within the overall manifold system (see section 5.5). For these sub-systems, the pressure derivative is determined by applying the conservation equations (5-12) to (5-15) to the exhaust manifold as a whole. The exhaust ports are considered outside of the overall exhaust manifold control volume. However, the pressure derivative for the exhaust ports is set equal to that for the exhaust manifold as a whole.

The rate of change of mass within each of these sub-systems can be obtained by rearranging equation (5-15) as follows:

$$\dot{m}_i = V_i \left(\frac{\partial \rho}{\partial p} \dot{p}_i + \frac{\partial \rho}{\partial T} \dot{T}_i + \frac{\partial \rho}{\partial \phi} \dot{\phi}_i \right) \quad (5-16)$$

where the subscript i refers to the different sub-systems of the exhaust manifold. The rate of change of temperature and composition of each section are calculated from equations (5-14) and (5-13), respectively.

The mass flow between sections of the exhaust manifold is determined by the mass flow through the exhaust valve (see section 4.1) and the rate of mass storage within any sections upstream of the section in question due to changes in the properties of those sections. For instance, the mass flow out of the port section and into the runner section is found by subtracting the change in mass in the port as found by equation (5-16) from the mass flow through the exhaust valve.

5.7 Manifold Heat Transfer

With the incorporation of an intercooler, heat transfer from the intake manifold to the environment becomes small enough to be neglected. Heat transfer from the exhaust manifold, however, is significant. Heat transfer from the gas in the exhaust manifold to the environment involves a combination

of forced convective heat transfer from the gas to the inside walls, conduction from the inside walls to the outside walls and to the water jacket, and natural (and probably forced) convection from the outer surfaces to the environment.

To determine the heat transfer in the exhaust manifold, each section is considered separately. Within each section, the gas temperature, the heat transfer coefficient, and the inside wall surface temperature are assumed to be uniform. Both the gas temperature and heat transfer coefficient are allowed to vary with time while the inside wall surface temperature is taken as constant with time. The inside wall surface temperature can be either specified as an input, or calculated from a specification of the component wall structure, in the manner described in sections 6.2.2 and 6.2.3.

5.7.1 Port heat transfer

The heat transfer in the exhaust port is highly unsteady. As the exhaust valve first comes open, a high velocity jet of high temperature gases sets up recirculation zones in the port [45] that result in a high heat transfer coefficient. When the exhaust valve is fully open, the flow resembles turbulent pipe flow and the heat transfer coefficient is diminished. Then, as the exhaust valve is going closed, there is another period when a narrow jet of gases enhances the heat transfer by setting up a recirculation zone. The valve open period is followed by a much longer period with very low mass flow and a correspondingly low heat transfer coefficient.

In order to quantify the heat transfer in the exhaust port, the results of Caton [46] are applied. Based on fine wire temperature measurements of the port gas temperature in a spark ignition engine, Caton arrived at the following correlations for the heat transfer during different phases of the exhaust valve opening:

Valve opening phase ($l/D < 0.2$):

$$Nu = 0.4 Re_j^{0.6} \quad (5-17)$$

Valve open phase ($l/D > 0.2$):

$$Nu = 0.023 C_R C_{EE} Re^{0.8} Pr^{0.4} \quad (5-18)$$

Valve closing phase ($l/D < 0.2$):

$$Nu = 0.5 Re_j^{0.5} \quad (5-19)$$

Valve closed:

$$Nu = 0.023 Re^{0.8} Pr^{0.4} \quad (5-20)$$

where Nu = Nusselt number

Pr = Prandtl number

$Re_j = \frac{V_j l}{\nu}$: Jet Reynolds number

$Re = \frac{VD}{\nu}$: Pipe Reynolds number, based on cycle-averaged mass flow

V_j = Velocity of flow through exhaust valve

V = Pipe flow velocity

l = Valve lift

D = Valve diameter

ν = Dynamic viscosity for flow

C_R = Correction factor for surface roughness

C_{EE} = Correction factor for entrance effects

Some modifications were made to these results for the present study. A correction factor was added to the correlation for the valve open phase to account for the sharp bend for an exhaust port. This factor is the correction

for bent pipes discussed in section 5.7.2. Also, during the period when the valve is closed, the mass flow is based on the instantaneous mass flow between sections instead of on the average flow over the complete cycle, as was done by Caton. For a turbocharged engine, this flow is not zero, in general, because gas flow is induced in inactive sections of the exhaust manifold by the pressure pulsations produced when other cylinders exhaust.

5.7.2 Exhaust manifold

Turbulent pipe flow correlations are usually applied to the exhaust manifold heat transfer. For fully developed pipe flow in a straight pipe with large temperature gradients, the heat transfer coefficient can be derived from the following experimental correlation that relates Nusselt, Reynolds and Prandtl numbers [44]:

$$Nu = 0.023 Re^{0.8} Pr^{0.3} \quad (5-21)$$

In the exhaust manifold of an engine, not all of the qualifying conditions for this equation apply. Most significantly, the flow is not fully developed, due to the short length of the pipe, and the pipe is not straight. To correct for these differences, two correction factors are introduced, based on empirical results of studies of the effects of entrance length and pipe bends on pipes.

The correction factor for entrance effects is based on the work of Boelter, Young, and Iversen [47]. They conducted experimental work on the variation of the heat transfer coefficient along the length of a tube starting at the inlet of the tube. Fitting a curve to the experimental results for a tube with an elbow at the entrance, yields the following equation for the local heat transfer coefficient:

$$C_{EE} = \frac{Nu_x}{Nu_\infty} = 2.2 \left(\frac{x}{D}\right)^{-0.3} \quad (5-22)$$

valid for $3 < x/D < 14$

where x = entrance length

Nu_x = local Nusselt number

Nu_∞ = Nusselt number for fully developed flow.

In order to find the average correction factor for a section, equation (5-22) is integrated over the section and divided by the length of the section, leading to

$$C_{EE} = 3.1 D^{0.3} \frac{(L_2)^{0.7} - (L_1)^{0.7}}{L_2 - L_1} \quad (5-23)$$

where D = diameter of the section

L_1 = distance from the exhaust valve to the inlet of the section

L_2 = distance from the exhaust valve to the outlet of the section

The correction factor for bent pipe is based on the work of Seban and McLaughlin [48] and Rogers and Mayhew [49]. They found that the appropriate correction factor for bent pipe is:

$$C_{BP} = \frac{Nu_S}{Nu_{BP}} = \left(\frac{r}{R}\right)^{0.1} Re^{0.05} \quad (5-24)$$

where r = Pipe radius

R = Bend radius

Nu_{BP} = Nusselt number for the bent pipe

Nu_S = Nusselt number for a straight pipe.

The Nusselt number for the bent pipe is the average of the heat transfer coefficient around the circumference of the pipe.

Combining the formula for fully developed straight pipe flow with the correction factors for entrance effects and for pipe bends gives the

correlation used for the heat transfer coefficient for sections of the pipe downstream of the port section, and for the exhaust port during the periods when the exhaust valve is fully open or closed:

$$Nu = 0.023 C_{EE} C_{BP} Re^{0.8} Pr^{0.3} \quad (5-25)$$

5.7.3 Connecting pipe between the turbines

The heat transfer for the connecting pipe between the turbocharger and the power turbines is treated in the same way as for the exhaust manifold. The heat transfer coefficient is based on turbulent pipe flow using equation (5-25). The overall heat transfer coefficient and the inside wall surface temperature are calculated in the manner described in sections 6.2.2 and 6.2.3.

5.8 Pressure Losses

5.8.1 General

Pressure loss terms have been included at five locations in the overall system model. These are:

- between compressor discharge and intercooler inlet,
- across intercooler,
- between exhaust manifold and turbine inlet,
- between turbine outlet and power turbine inlet,
- between power turbine outlet and atmosphere.

Each of these pressure drops is calculated using the corresponding friction factors and friction coefficients for the geometry of each passage. For straight-sections:

$$\Delta P = 4f(L/D)(\rho V^2/2) \quad (5-26)$$

where L = length of passage

D = diameter of passage

ρ = bulk density

V = average velocity

f = friction factor, which is correlated by (5-17) for the surface roughness and range of Reynolds numbers to be encountered.

Note that

$$f = 0.046/(\text{Re})^{0.2} \quad (5-27)$$

with $\text{Re} = \rho V D / \mu$

For bends, enlargements, contractions, etc:

$$\Delta P = K_f \rho V^2 / 2 \quad (5-28)$$

where K_f = friction coefficient for a particular passage geometry. Values of K_f for typical geometries are commonly available [44].

5.8.2 Exhaust manifold and turbine connecting pipe

The pressure drop for the exhaust manifold of a 6 cylinder diesel engine was found by Primus [50] to be a factor of 10 to 15 times higher than the pressure drop calculated based on equations (5-26) and (5-27) alone. This increase in flow losses is apparently due to the complex shape of the manifold and the interaction of the flow with the open passageways from other cylinders. For this reason, equation (5-28) is used for the calculation of the exhaust manifold pressure drop with K_f left as an input parameter for the user to specify. Primus found that values of 2 to 3.5 were appropriate for his test manifold. Different values may be used for manifolds of different designs. A similar user option to input K_f for the connecting pipe between the turbine is also included in the code.

CHAPTER 6

WALL CONDUCTION MODELS

6.1 Introduction

As described in sections 4.4 and 5.7, the heat transfer rates from the gas to the walls of the various system components depend on the instantaneous difference between the gas and the wall temperature. Estimates of these engine wall temperatures have been calculated in the past [51], [16] based on the following assumptions:

- (i) each heat transfer surface of interest is at a uniform surface temperature; i.e. surface temperature variations across a particular area are neglected.
- (ii) The heat transfer surface temperatures are constant with time; i.e. cycle-periodic surface temperature variations are not considered.
- (iii) Heat transfer by conduction through the walls is treated on a one-dimensional basis.

The one-dimensional, uniform surface temperature model is certainly a simplification for surfaces with large temperature variations, such as piston bowls, or for surfaces with complicated heat transfer path lengths, such as the cylinder liner. Also, uniform surface temperatures are not adequate for detailed thermal stress calculations. For most surfaces, however, temperature varies much more rapidly in directions perpendicular to the surface, so that the above one-dimensional treatment is justified.

The assumption of constant wall temperatures over the engine operating cycle is reasonable for engines with high conductivity metal walls and forced convection jacket cooling. Measurements by LeFeuvre [36] and Whitehouse [52] on conventional engines have suggested that cyclic surface temperature swings

are fairly small, ranging from 5 to 15 Kelvins. However, for engine surfaces insulated with low-conductivity materials, such as ceramics, surface temperature swings are expected to be more critical [53].

Figure 6 shows a typical ceramic/metal composite wall structure. The heat transfer rate from the gas to the wall is a harmonic function of time, with a period of one engine cycle. This time-dependent boundary condition will set up periodic temperature waves that will propagate into the wall structure. Because of the relatively low thermal diffusivities of ceramics, these disturbances will only penetrate a small distance from the surface of the material, beyond which the temperature distribution is steady-state.

These cyclic transients, should not be confused with engine start-up wall transients which die-away once steady-state engine operation is established. Cyclic transients are superposed on the steady-state conduction temperature profiles. Thus, their effect should be taken into account for the accurate prediction of maximum wall surface temperatures (important for lubrication considerations) and temperature distribution in the wall structures (important for material stress considerations).

Assuming uniform material properties which do not vary with temperature, the total temperature (steady plus time-periodic) $T(x,t)$, at any point x within the wall, and at any time t , will satisfy the heat conduction equation, i.e.

$$\nabla^2 T = \frac{1}{\alpha} \frac{\partial T}{\partial t} \quad (6-1)$$

where α is the thermal diffusivity of the material. The solution to eq. (6-1) is developed in the following sections by decomposing the problem into its steady-state and time-periodic components.

6.2 Steady-State Problem

The steady-state heat transfer rate per unit inside surface area, \dot{Q}_s , through a composite wall structure is given by

$$\dot{Q}_s = U(\bar{T}_w - T_c) \quad (6-2)$$

where U = over-all coefficient of heat transfer based on inside surface area

\bar{T}_w = steady-state inside wall surface temperature

T_c = outside wall surface temperature, coolant temperature, or ambient temperature

The cylinder head and the piston crown of the insulated engine are modelled as flat composite walls, while the cylinder liner, manifolds, and connecting ducting are modelled as cylindrical composite walls. The appropriate expressions for the over-all heat transfer coefficient and steady-state temperature distribution for these two types of wall structure are summarized in sections 6.2.1 and 6.2.2. The inside wall steady-state surface temperature is determined through a heat balance between the cycle-averaged heat transfer rate from the gas to the walls and the steady-state wall heat conduction. This involves an iterative procedure which is described in section 6.2.3.

6.2.1 Flat composite wall

The overall coefficient of heat transfer, U_p , for a flat composite wall is defined as

$$\frac{1}{U_p} = \sum_{i=1}^n \frac{L_i}{k_i} \quad (6-3)$$

where n = number of flat layers

L_i = thickness of i^{th} layer

k_i = thermal conductivity of i^{th} layer

If the boundary condition on the outside wall surface is specified in terms of an outside heat transfer coefficient and a coolant or ambient temperature (versus a specified outside wall temperature), a modified overall heat transfer coefficient is defined as

$$\frac{1}{U_p} = \sum_{i=1}^n \frac{L_i}{k_i} + \frac{1}{h_c} \quad (6-4)$$

where h_c is the heat transfer coefficient to the outside.

The steady-state temperature distribution for the i^{th} layer is obtained from the solution of Eq. (6-1) in its steady form, i.e.

$$\frac{\partial^2 T_s}{\partial x^2} = 0 \quad (6-5)$$

The boundary conditions are

$$T_s = T_s(\dot{Q}_s, x_i), \text{ at } x = x_i \quad (6-6a)$$

$$T_s = T_s(\dot{Q}_s, x_{i+1}), \text{ at } x = x_{i+1} \quad (6-6b)$$

leading to the following temperature distribution within the i^{th} layer

$$T_s(x) = [T_s(x_{i+1}) - T_s(x_i)] \frac{(x-x_i)}{L_i} + T_s(x_i) \quad (6-7)$$

6.2.2 Cylindrical composite wall

The overall coefficient of heat transfer, U_c , based on the inside surface area of a cylindrical wall structure is defined as

$$\frac{1}{r_1 U_c} = \sum_{i=1}^m \frac{\ln(r_{i+1}/r_i)}{k_i} \quad (6-8)$$

where m = number of cylindrical layers

r_i = inside radius of i^{th} layer

r_{i+1} = outside radius of i^{th} layer

k_i = thermal conductivity of i^{th} layer

Again, if the outside boundary condition involves the heat transfer coefficient to the outside, the overall heat transfer coefficient is modified as follows:

$$\frac{1}{r_1 U_c} = \sum_{i=1}^m \frac{\ln(r_{i+1}/r_i)}{k_i} + \frac{1}{r_{m+1} h_c} \quad (6-9)$$

where r_{m+1} = outside radius of m^{th} layer

h_c = heat transfer coefficient to the outside

The steady-state temperature distribution for the i^{th} layer is obtained from solution of equation (6-1) in its steady form, i.e.

$$\frac{1}{r} \frac{\partial}{\partial r} \left(r \frac{\partial T}{\partial r} \right) = 0 \quad (6-10)$$

The boundary conditions are

$$T_s = T_s(\dot{Q}_s, r_i) , \text{ at } r = r_i \quad (6-11a)$$

$$T_s = T_s(\dot{Q}_s, r_{i+1}) , \text{ at } r = r_{i+1} \quad (6-11b)$$

leading to the following temperature distribution within the i^{th} layer

$$T_s(r) = (T_s(r_i) - T_s(r_{i+1})) \frac{\ln(r/r_{i+1})}{\ln(r_i/r_{i+1})} + T_s(r_{i+1}) \quad (6-12)$$

6.2.3 Determination of steady-state inside wall surface temperature

The steady-state inside wall surface temperatures of each of the engine components is not known a priori. At the start of the cycle simulation,

approximate estimates of these temperatures are assumed. Based on these estimates, the instantaneous heat transfer rates, convective and radiative, to the combustion chamber walls are calculated throughout the cycle. At the end of the cycle, a heat balance is performed between the cycle-averaged gas/wall heat transfer rate and the heat conducted through the walls of each component to compute a new surface temperature. These new temperatures are used in the next cycle iteration, until the calculation converges. Details of the heat balance follow.

The instantaneous heat transfer rate to the combustion chamber walls is calculated from

$$\dot{Q}_w(t) = h(t)(T_g(t) - \bar{T}_w) \quad (6-13)$$

where \bar{T}_w = inside wall temperature at cycle start

$T_g(t)$ = instantaneous gas temperature

$h(t)$ = instantaneous heat transfer coefficient

During combustion, $h(t)$ is replaced by an effective linearized heat transfer coefficient $h_{eff}(t)$, given by Eq. (D-7), to take into account the effects of radiation on the total heat transfer rate.

The cycle-averaged gas/wall heat transfer rate is given by

$$\dot{Q}_w = \frac{\int h(t)(T_g(t) - \bar{T}_w) dt}{\int dt} \quad (6-14)$$

where \int denotes integration over the complete cycle. Equation (6-14) can be rewritten as

$$\dot{Q}_w = \overline{h T_g} - \bar{T}_w \bar{h} \quad (6-15)$$

where the bar denotes cycle-averaged.

The steady-state heat transfer rate conducted through a composite wall structure was expressed by equation (6-2), involving an over all wall heat transfer coefficient. Combining equations (6-2) and (6-15), an updated wall temperature can be computed according to

$$\bar{T}'_w = \frac{\bar{h} \bar{T} + UT}{\bar{h} + U} \quad (6-16)$$

where the prime denotes the temperature to be used in the next cycle iteration. The calculation is repeated until the new wall temperature is within a certain percentage of its value at the end of the previous cycle.

6.3 Time-Periodic Problem

6.3.1 Formulation of finite difference scheme

The time-periodic part, $T_p(x,t)$, of the temperature distribution within any parallel slab will satisfy the unsteady conduction equation, i.e.,

$$\frac{\partial^2 T}{\partial x^2} = \frac{1}{\alpha} \frac{\partial T}{\partial t} \quad (6-17)$$

In order to solve this continuous partial differential equation, a finite difference technique will be used. The slab is modeled by a number of N discrete nodal points, x_i . At each node, the finite-difference approximation to the governing equation provides an algebraic equation connecting the instantaneous nodal temperature to those at the surrounding nodes.

The finite difference schemes which have been used to solve partial differential equations of the form of Eq. (6-17), can be grouped into two general categories: explicit and implicit [54]. In explicit schemes, the instantaneous value of the variable at any node is given by the values of the

variable at the node and its neighboring nodes calculated from the previous time step. These schemes are fairly simple, and computationally very efficient. However, they are stable only under certain conditions and are limited to uniformly-spaced discrete nodes. On the other hand, implicit schemes are unconditionally stable, and some can handle arbitrarily spaced discrete nodes. From the computational point of view, though, implicit schemes are very intensive. Since the instantaneous value of a nodal variable depends on the neighboring values of the variable at the current and previous time steps, these schemes, unfortunately, involve large matrix inversions.

For the purposes of the current work, it is desired to calculate the temperature distribution within the walls of the engine combustion chamber in parallel with the engine simulation calculation. Thus, special effort was made to develop a numerical scheme that would be:

- (i) least demanding in computer time
- (ii) able to handle arbitrarily-spaced discrete nodes, so as to maximize the accuracy of the solution within the relatively thin penetration depth of the cyclic engine transients
- (iii) stable.

To satisfy all the above requirements, an Euler explicit scheme was suitably modified, by mapping the arbitrarily-spaced discrete nodes x_i of the desired solution domain into corresponding uniformly-spaced nodes y_i , according to the following transformation:

$$y = \frac{a + bx}{1 + cx} \quad (6-18)$$

This transformation was selected because of its following merits [55]:

- (i) three of the nodes x_i can be mapped into three specified nodes y_i .
- (ii) all other nodes x_i are then mapped smoothly in between the three specified nodes y_i .

(iii) the transformation is differentiable up to any order.

Using (6-18), Eq. (6-17) can take the following form for each node x_i :

$$\left(\frac{\partial y}{\partial x}\right)_i \left[\frac{\partial}{\partial y} \left(\frac{\partial T}{\partial x}\right)_i\right] = \frac{1}{\alpha} \left(\frac{\partial T}{\partial t}\right)_i \quad (6-19)$$

By approximating the derivative with respect to y through finite differences, and recalling (6-18), Eq. (6-19) can be re-written as

$$\left(\frac{1}{\Delta y}\right) \left(\frac{\partial y}{\partial x}\right)_i \left[\left(\frac{\partial y}{\partial x}\right)_{i+1/2} \left(\frac{\partial T}{\partial y}\right)_{i+1/2} - \left(\frac{\partial y}{\partial x}\right)_{i-1/2} \left(\frac{\partial T}{\partial y}\right)_{i-1/2}\right] = \frac{1}{\alpha} \left(\frac{\partial T}{\partial t}\right)_i \quad (6-20)$$

where Δy is the uniform spacing between two adjacent nodes in the transformed coordinate system.

Once again, by taking finite difference expressions for the derivatives with respect to y , and after some rearrangement, we get

$$T_i = T_i^{\circ} + \frac{DYDXM}{CN} [DYDXR(T_{i+1}^{\circ} - T_i^{\circ}) - DYDXL(T_i^{\circ} - T_{i-1}^{\circ})] \quad (6-21)$$

$$\text{where } DYDXM = \left(\frac{\partial y}{\partial x}\right)_i \quad (6-22a)$$

$$DYDXR = \left(\frac{\partial y}{\partial x}\right)_{i+1/2} \quad (6-22b)$$

$$DYDXL = \left(\frac{\partial y}{\partial x}\right)_{i-1/2} \quad (6-22c)$$

$$CN = \frac{\Delta y^2}{\alpha \Delta t} : \text{Courant number} \quad (6-23)$$

and the superscript \circ denotes temperature values at the previous time step.

Note that the method is stable provided that [56]

$$CN \geq 2 \quad (6-24)$$

For time-step sizes of the order of one engine crank angle, and material diffusivities in the range of 10^{-5} to 10^{-6} m^2/s (most materials of interest), this condition will be satisfied for nodal spacings as small as 1/10 to 1/100 of a mm.

6.3.2 Application of finite difference scheme

The finite difference scheme was applied to calculate the periodic temperature distribution in the two parallel layer wall structure (piston or head), shown in Fig. 6. In general, under typical engine operating conditions, the cyclic transients do not penetrate into the wall structure for a distance greater than a few mm (and thus will not extend into the second layer). However, to maximize the flexibility of the code to analyze even thin coatings (of order of a mm), the code is set-up with a capability to calculate transients over the entire wall region. Obviously, more nodes should be placed in the first layer than in the second one.

For the first layer, the transformation (6-18) is introduced, so that

$$x = -L_1 \quad \text{maps into } y = 0$$

$$x = 0 \quad \text{maps into } y = 1$$

$$x = -L_1 + \delta \quad \text{maps into } y = F$$

with $F = 0.4$ to 0.7 , meaning that 40 to 70 percent of the nodes x_i are placed within a distance of the order of the penetration depth δ in the first layer. These three conditions determine a, b, c in Eq. (6-18). Then, the temperature $T_{1,i}$ at any node i of the first layer, can be calculated from Eq. (6-21).

For the second layer, a relatively small number of uniformly-spaced nodes is sufficient. Then, with $y = x$, Eq. (6-21) for the temperature $T_{2,j}$ at any node j of the second layer, simplifies to the following standard form [56]:

$$T_{2,j} = \frac{T_{2,j-1}^{\circ} + (CN-2)T_{2,j}^{\circ} + T_{2,j+1}^{\circ}}{CN} \quad (6-25)$$

Note again that for stability, $CN \geq 2$. (The limit $CN = 2$ would imply that the local node temperature has no effect on its future value).

At the interface between the two layers ($x=0$), continuity of temperature and heat flux leads to the following boundary conditions:

$$T_{1,N} = T_{2,1} \quad (6-26)$$

where N is number of nodes in first layer, and

$$k_1 \left(\frac{\partial T}{\partial x} \right)_{x=0^-} = k_2 \left(\frac{\partial T}{\partial x} \right)_{x=0^+}$$

or, introducing transformation (6-18) in the first layer, and approximating the derivatives through finite differences, we get

$$k_1 \left(\frac{\partial T}{\partial x} \right)_{x=0} = \frac{3T_{1,N} - 4T_{1,N-1} + T_{1,N-2}}{\Delta y} = k_2 \frac{-3T_{2,1} + 4T_{2,2} - T_{2,3}}{\Delta x_2} \quad (6-27)$$

where Δy was defined in Eq. (6-20) and Δx_2 is the uniform spacing between two adjacent nodes in the second layer.

To validate the numerical scheme and to optimize the number and spacing of the nodal points, the method was applied to calculate the temperature distribution in a series of flat composite slabs subject to a given, harmonically varying gas temperature at $x = -L_1$, and a constant ambient temperature at $x = L_2$. The exact solution was also obtained analytically for each case (see Appendix E). Figure 7 shows a comparison of temperature profiles, exact and numerical, in a 4 mm ceramic layer of conductivity 1 W/m-K and thermal diffusivity $0.5 \times 10^{-5} \text{ m}^2/\text{s}$, coated on a 10 mm cast-iron component. The results, which are representative of all the cases that we studied, show that the numerical solution is in excellent agreement with the exact solution. Furthermore, we concluded that, for a range of different materials and layer thicknesses, 99% accuracy (or better) can be obtained by introducing 15 nodes in the insulating layer, of which 60% are placed within the penetration depth of the cyclic transients.

6.4 Combined Solution

The total temperature distribution in each layer can be obtained by superposing the steady-state solution given by Eq. (6-7), and the time-periodic solution, given by Eqns. (6-21) and (6-25). The total temperature $T(x,t)$ must satisfy the full boundary conditions at the inside and outside wall surfaces.

At the hot gas side ($x = -L_1$),

$$-k_1 \left(\frac{\partial T}{\partial x} \right)_{x=-L_1} + \dot{Q}_s = h_g (T_g - T_w) \quad (6-28)$$

where \dot{Q}_s is the steady-state heat flux given by (6-2), h_g is an effective linearized coefficient (convective and radiative) defined by (D-7), and

$$T_w = \bar{T}_w + T_{1,1} \quad (6-29)$$

Introducing finite-difference approximations, (6-28) can be rewritten as

$$-k_1 \left(\frac{\partial T}{\partial x} \right)_{-L_1} \frac{3T_{1,1} - 4T_{1,2} + T_{1,3}}{2\Delta y} + \dot{Q}_s = h_g (T_g - T_w) \quad (6-30)$$

Similar equations apply for the boundary condition at the ambient or coolant side ($x = L_2$), where either the total heat flux or the total wall temperature can be prescribed.

The calculation is staged as follows. First, the steady-state solution for the temperature distribution within each component wall and the average heat flux conducted through each wall are obtained by following the iteration procedure described in section 6.2.3, i.e. assuming no cyclic transients. Once the steady-state heat flux is obtained, the transient calculation is performed by applying the finite difference scheme and the total boundary conditions (6-28) and (6-30).

CHAPTER 7

METHOD OF SOLUTION AND PROGRAM INPUTS AND OUTPUTS

7.1 Basic Method of Solution

The conservation equations of mass and energy for the contents of an open thermodynamic system are applied in turn to the master reciprocator cylinder, the intake manifold, and the series of exhaust manifold sections. Further, the individual submodels of the various system components and their thermodynamic and heat transfer processes are brought together to form a complete system model. The result is a set of simultaneous first-order ordinary differential equations. To perform predictive calculations with the cycle simulation, these equations must be integrated simultaneously over the full operating cycle. Note, however, that some of the governing equations like the mass flow rate through the intake or the exhaust valve, the non-dimensional fuel burning rate, etc. apply only during parts of the cycle.

Integration of the governing equations is performed numerically using a standardized code developed by Shampine and Gordon [57]. The method is based on a predictor-corrector technique that uses a modified divided difference form of the Adams Pece formulas. The code adjusts its order and step size internally to maximize efficiency and control the local error per unit step in a generalized sense. Detailed documentation of the integration routine is provided in the listing of the code.

A flow chart showing the overall structure of the entire system simulation is shown in Figure 8. After the initialization of the state variables, the program proceeds with the simultaneous integration of the governing system equations. The latter can be grouped into two major subsets: equations describing the thermodynamic processes in the master cylinder

of the reciprocator; and equations associated with other components in the system (manifolds, turbocharger, etc.) that have inherent multi-cylinder capability. The main program determines which equations in each sub-set will be passed to the integrator, couples the two sub-sets and transfers information across them, and prints out results as the cycle proceeds.

On the reciprocator model side, the main program passes to the integrator different subroutines corresponding to the intake, compression, combustion and exhaust processes of the master cylinder, as the engine cycle proceeds. On the other components side, the main program supplies the integrator with the same set of governing equations for the manifolds, turbocharger, etc. throughout the cycle. Appropriate utility routines, are called by the major routines to help in the evaluation of the necessary derivatives at each step. These include routines to calculate the steady-state and cyclic periodic temperature profiles within the various component wall structures, routines to calculate mass flow rates through valves and interpolate valve area tables (called by the intake and exhaust routines), routines to interpolate turbomachinery maps and predict the heat transfer and pressure losses in the ducting (called by the other components routine), and thermodynamic and transport property routines (called by all major routines).

The mass flow rate and enthalpy flux profiles of the master cylinder, generated by the simulation during the intake and the exhaust processes, are stored in the main program. Using this information, the main program calls a subroutine that:

- i) generates the profiles of all the other cylinders as echoes of the master cylinder profiles;
- ii) sums the intake and exhaust profiles contributed by each cylinder at every instant to give total reciprocator mass and enthalpy flows, etc. The

resultant profiles are communicated from the main program to the other components routine throughout the engine cycle.

Approximate estimates of all state variables are assumed, initially. More than one iteration is generally required to model system operation under steady conditions. The integration continues until the system reaches a quasi-steady condition, defined as the condition in which the value of each state variable at a particular crank-angle is within a specified interval of its value at that crank-angle in the previous engine cycle.

7.2 Program Inputs and Outputs

The input parameters which must be specified for each cycle simulation calculation include the following groups: system operating mode, system operating conditions, system dimensions and design parameters, parameters for the wall conduction models, empirical parameters for the various simulation sub-models, initial conditions of the system and certain computational parameters.

From this information, the simulation program can predict the performance of the total engine system under a wide range of operating conditions. The output includes mean engine performance parameters, such as power, specific fuel consumption, mean effective pressure, thermal efficiency, etc., as well as detailed information about the state of the total system as a function of crank-angle throughout each engine cycle.

7.2.1 Inputs

I. System operating mode

In order to maximize the flexibility of the code to handle different system configurations, and assess the effect of different modeling assumptions on system performance, the user is provided with a choice of several options:

- a. The system can be turbocharged and turbocompounded, or turbocharged only.
- b. The steady-state inside wall surface temperatures of the piston, cylinder head, cylinder liner, manifolds, and turbine connecting pipe can be specified as an input, or calculated from a specification of the component wall structure.
- c. Additionally, the time-dependent temperature distribution in the piston and cylinder head can be computed using a one-dimensional unsteady finite difference model for the component wall.
- d. The ignition delay period can be predicted based on our ignition delay model, or can be specified based on experimental data.
- e. Either the commonly used Annand's radiation model, or the flame radiation model developed here can be used to predict instantaneous radiative heat transfer rates.

II. System operating conditions

- a. Reciprocator speed (RPM)
- b. Mass of fuel injected per cycle
- c. Injection timing
- d. Fuel parameters
- e. Steady-state inside wall surface temperatures of piston, cylinder head, cylinder liner, manifold walls, and turbine connecting pipe (for specified wall temperature option only)
- f. Power turbine gear ratio

III. System dimensions and design parameters

- i. Reciprocator Parameters
 - a. Number of cylinders
 - b. Cylinder bore

- c. Cylinder stroke
 - d. Connecting rod length
 - e. Clearance volume
 - f. Valve timings (crank angles at which the intake and exhaust valves open and close)
 - g. Tabulated values for the effective valve open areas (including discharge coefficient effects)
- ii. Other Component Dimensions
- a. Intake and exhaust manifold dimensions
 - b. Turbine connecting pipe dimensions
- iii. Intercooler Characteristics
- a. Coolant flow heat capacity
 - b. Heat exchange surface area
 - c. Over-all heat transfer coefficient
- iv. Turbomachinery Parameters
- a. Compressor, turbocharger turbine and power turbine maps
 - b. Turbocharger rotational inertia
 - c. Turbocharger rotational damping
 - d. Power turbine transmission efficiency

IV. Wall conduction model parameters

These parameters need to be specified when it is desired to predict the steady-state and transient (for piston and cylinder head only) temperature distribution within the various system component walls. For each material layer of the piston, cylinder head, liner, manifold sections and turbine connecting pipe, the wall structure specifications include:

- a. Thickness
- b. Inside wall radius (cylindrical components only)

- c. Thermal conductivity
- d. Thermal diffusivity (piston and head only)

For each component, the boundary conditions on the outside wall surface must be specified, i.e.:

- a. Ambient (or coolant) temperature, and heat transfer coefficient from the outside wall surface to the ambient (or coolant), or
- b. specified wall temperature on outside surface.

Finally, for the finite difference scheme applied to the unsteady conduction through the piston and cylinder wall, the following are required

- a. Number of nodes placed within each layer of a given component
- b. Fraction of nodes of first layer placed within the penetration depth of cyclic engine transients.

V. Other sub-model empirical parameters

- a. Ignition delay correlation constants; e.g., (4-12)
- b. Burning rate distribution constants; e.g., (4-7), (4-8), (4-9)
- c. Nu-Re number correlation constants, appropriate for the reciprocator cylinder, exhaust port, manifolds, and turbine connecting pipe; Equations (4-17), and (5-17) up to (5-21)
- d. Turbulent dissipation constant; Eq. (4-34)
- e. Annand's radiation model calibrating constant
- f. Friction model constants; e.g., (4-48).

VI. Initial conditions

- a. Cylinder pressure, temperature, and composition
- b. Intake manifold pressure, temperature, and composition
- c. Exhaust manifold pressure, temperature, and composition

- d. Turbocharger speed

VII. Ambient conditions

- a. Intake temperature
- b. Intake pressure
- c. Final exhaust pressure

VIII. Computational parameters

- a. Convergence margins for each state variable
- b. Error tolerances for integration of the differential equations
- c. Other parameters used in the integration algorithm "ODERT"

(For a detailed description of these parameters, see the engine simulation code.)

7.2.2 Outputs

Four types of outputs are generated by the cycle simulation:

I. Input echo

A listing of all the input parameters, including some quantities derived directly from the given inputs (e.g. engine displacement and compression ratio).

II. Major crank-angle by crank angle results

At specified crank-angle intervals, the values of the following state variables are returned:

- a. Cylinder pressure, temperature, and average equivalence ratio
- b. Intake manifold pressure, temperature and average equivalence ratio
- c. Exhaust manifold pressure, temperature and average equivalence ratio

In addition, the following other quantities are reported at the same intervals:

- a. Heat transfer model results (such as heat transfer rates from gas to various component wall surfaces, instantaneous convective heat transfer coefficient, temperature profiles within various component wall structures)
- b. Turbulent flow model results (such as mean flow velocity, turbulent intensity, macroscale of turbulence)
- c. Code which monitors the performance of the integration routine.

Integrating through the different processes for the master cylinder, the following quantities are reported during the corresponding process:

- i. Intake
 - a. Mass flow through intake valve
 - b. Mass flow through exhaust valve
 - c. Velocity through intake valve
 - d. Velocity through exhaust valve
- ii. Combustion
 - a. Non-dimensional fuel burning rate
 - b. Fuel burnt as a function of total fuel injected
 - c. Flame radiation model results (such as radiant heat transfer, radiant temperature, adiabatic flame temperature, emissivity)
- iii. Exhaust
 - a. Mass flow rate through exhaust valve
 - b. Velocity through exhaust valve

III. Integrated results and cycle performance

After completion of an engine cycle, a summary of results obtained by integrating some of the governing equations over the cycle is given.

Integrated results include the following:

- a. Reciprocator thermal efficiency (gross indicated and brake)
- b. Overall system brake thermal efficiency
- c. Specific fuel consumption (reciprocator and overall)
- d. Volumetric efficiency (based on manifold and ambient conditions)
- e. Gross indicated, pumping, friction, and mean brake effective pressures
- f. Total heat loss (as a fraction of the fuel energy input)
- g. Mean exhaust temperature
- h. Mass of air inducted per cycle
- i. Ignition delay period
- j. Total heat and work transferred during each process
- k. Results of an overall energy balance

IV. Sub-model results

After the overall cycle results are listed, detailed results for the main sub-models of the cycle simulation are given at specified crank angle intervals. These quantities include the following:

- a. Total engine intake and exhaust mass flow rates
- b. Compressor, turbocharger turbine and power turbine speed, mass flow rate, pressure ratio and efficiency
- c. Power turbine work transfer
- d. Pressures and temperatures at various system locations
- e. Intake manifold, exhaust manifold, and turbine connecting pipe heat transfer data
- f. Intercooler performance data

CHAPTER 8

MODEL CALIBRATION AND VALIDATION

8.1 Introduction

Our modelling of the various processes which occur during the engine cycle necessarily involves a number of assumptions. In particular, some of the critical process sub-models contain empirical constants which require calibration against experimental data. Some examples are: constants in the heat release profile distributions and the ignition delay model; constants in the heat transfer correlations for the reciprocator and the manifolds; constants in the reciprocator friction model, etc. Thus, the development of a reliable simulation to study engine performance under a wide range of operating conditions necessitates an effective validation procedure. This section summarizes the calibration and subsequent validation of the simulation against data obtained from Cummins for a cooled turbocompounded diesel engine. Table 4 gives details of the engine geometry and operating conditions.

8.2 Calibration

The rated speed and load point of the engine was selected for model calibration, since a fairly complete test data set, including a pressure trace, was available for that point. The reference conditions were 1900 RPM, 141.8 lb/hr fueling rate, and 14 deg. BTC injection timing. Since the cylinder pressure trace primarily depends on the timing and shape of the heat release profile, the rate of gas-to-wall heat transfer, and the interaction of the two, it was used to establish the shape factors of the heat release profile for our combustion chamber, and the constant for the convective heat transfer correlation.

Our calibration strategy was the following: As a starting point, Watson's constants for ENGINE A (see Table 1) were used to describe our engine combustion profile. Then, a series of cycle-simulation calculations at standard conditions was performed for a range of values of the convective heat transfer correlation constant "a" (see Eq. 4-17) between 0.04 and 0.07. The predicted pressure traces were compared against the experimental Cummins pressure trace. Furthermore, by converting indicated to brake quantities, using Millington and Hartles correlation (4-49), simulation predictions and Cummins experimental brake performance measures were compared, as well. For the best case, i.e. for $c = 0.055$, the calculated peak cylinder pressure and the brake mean effective pressure were found to be 26% and 6.6% higher than the Cummins data, respectively. This suggests that the timing of the peak diffusion burning rate occurred too early, thus resulting in too rapid a pressure rise.

In order to bring the calculated cylinder pressure diagram into better agreement with the data, a new series of runs was performed for different values of the diffusion burning factor C_{d2} (which controls the timing of the peak diffusion rate). Figure 9 shows the pressure profiles corresponding to different values of the constant k_3 (used in the calculation of C_{d2} , see section 4.2). The values of k_3 range from 0.79 (suggested by Watson) to 1.10. Also, shown in Figure 9 is the Cummins pressure trace. It is apparent that k_3 would have to be between 1.0 and 1.10.

Table 5 shows a comparison of several system performance quantities obtained using $k_3 = 1.05$ against Cummins data. Again, for completeness, data obtained for $k_3 = 0.79$ (Watson's value) are tabulated. We concluded that for $c = 0.055$ and $k_3 = 1.05$, and for the other shape factors same as for ENGINE A, a very satisfactory agreement (within 1% error) between the model predictions

and the experimental performance data can be obtained. Then, to validate the model, performance predictions were compared with experimental values over the full load and speed range of the data. Additionally, predicted temperatures and pressures at various points in the total system were compared against data for base case operating conditions.

8.3 Model Validation

8.3.1 Constant Load Comparison

Figure 10 shows reciprocator brake power, power turbine brake power and overall brake specific fuel consumption plotted as a function of reciprocator speed for constant load operation. The expected almost linear relationship between reciprocator brake power and speed is predicted. Increases in engine speed affect the mass flow rates through the reciprocator and the turbomachinery components, and hence affect the power turbine power. The variation of bsfc with speed indicates that matching the turbocharger turbine for a given application involves a trade-off between improving low speed boost and not over-boosting at high speed.

The variation of all three predicted performance quantities with varying speed at constant load closely follows the data in both magnitude (within 2.5%) and trend. In summary, the correlation between predictions and data is best (within 1%) in the middle and high speed range, while the discrepancy increases (within 2.5%) at the extreme low speeds. This is primarily due to the increase in the relative importance of heat transfer with decreasing engine speed and errors in the assumed variation of friction with speed. Furthermore, the model predictions have been based on a fixed start of combustion over the entire speed range, while tests may have been carried out with injection timing optimized as a function of speed.

Figure 11 focuses on the variation of turbocharger rotor speed, boost pressure ratio and mass flow through the compressor with reciprocator speed, at constant load. Increases in reciprocator speed result in increased available energy at the engine exhaust. Owing to the higher turbocharger inlet temperature and expansion ratio, the speed of the turbocharger shaft increases with increasing reciprocator speed, thus leading to increasing boost pressure ratios. The latter cause an increase in airflow through the compressor as the reciprocator speed increases. Overall, the predictions of the turbomachinery performance are in excellent agreement with the measurements (error less than 1%), demonstrating the ability of the simulation to model coupled turbocharger-diesel engine systems. The small discrepancies (up to 2%) at the extreme low and high speeds are attributed to limitations associated with extrapolation of the turbomachinery maps to cover a range where data is not supplied by the turbocharger manufacturers.

8.3.2 Constant-Speed Comparison

Figure 12 shows reciprocator brake power, power turbine brake power and overall brake specific fuel consumption plotted as a function of fueling rate, (i.e., essentially reciprocator load) for operation at a constant speed of 1900 RPM. The expected almost linear relationship between reciprocator brake power and fuel rate is apparent. Further, the available energy, and hence the power turbine power, increase with load due to the influence of higher fuel/air ratio on exhaust gas temperature. Finally, increasing load decreases bsfc, since the mechanical efficiency of the cycle increases.

The trends in predicted performance quantities with varying load at constant speed are in good agreement with the data. In particular, for medium and high loads, the simulation predictions are within 1% of the Cummins experimental measurements. In the light load range, the discrepancy between

predictions and data is somewhat higher, but not more than 4%. These discrepancies may have resulted from inadequate modeling of the increased relative importance of engine heat transfer with decreasing load, errors in engine friction, and increased relative errors in measurement of system variables with reduction in load.

Figure 13 shows predictions and measured data for the representative set of turbomachinery variables described above as a function of reciprocator load, at a speed of 1900 RPM. Since higher loads result in higher exhaust gas temperatures and thus more available energy, the behavior of the system is qualitatively similar to the case of increasing reciprocator speed. The turbocharger rotor speed, the boost pressure ratio, and the intake airflow increase almost linearly with fueling rate. Once again, the simulation predictions follow closely the experimental turbomachinery performance data in both magnitude (within 1.5%) and trend.

8.3.3 Pressure and Temperature Comparison across the System

Table 6 compares pressure and temperature predictions at various points in the total system against corresponding data obtained from Cummins. The comparison is made at base case operating conditions of 1900 RPM and 141.8 lb/hr fuel rate. On the intake side, predictions of pressures and temperatures are in excellent agreement with the data (within 1%). On the exhaust side, the predicted temperature of the gas leaving the reciprocator exhaust ports is 40 K (i.e., 5%) higher than the corresponding experimental data. This is largely due to the fact that the experimental measurements, which were obtained using slow-response thermocouples, represent time-averaged quantities, and not mass-averaged quantities [58]. The measurements weight heavily the period when the exhaust valve is closed and relatively cool stagnant gases fill the exhaust port area resulting in a low estimate of the

true mean temperature. The computer simulation weights the instantaneous exhaust gas temperatures with the corresponding flow rates across the exhaust valves, and thus calculates the mass-averaged exhaust gas temperature. At the turbine inlet, where the fluctuations in exhaust gas temperature are dampened out, the time-averaged gas temperature is essentially the same as the corresponding mass-averaged quantity. This explains why the measured temperature at the turbine inlet is greater than the reported measurement at the exhaust port.

The predicted pressure at the exhaust port is about 9% higher than the pressure transducer measurement. This discrepancy is reduced to 4% at the turbine inlet. After the turbocharger turbine, predicted and measured values of pressure across the power turbine are in good agreement. Possible reasons for the discrepancy are the following:

(i) The model assumes that all sections of the exhaust manifold are at a uniform pressure.

(ii) The model does not include any exhaust pressure wave phenomena or pipe dynamics effects between the reciprocator exhaust ports and the turbine inlet.

With the above qualifications, the model gives sufficiently accurate predictions of trends and magnitudes to be useful for assessing the effect of changes in system design and operating variables on overall system performance.

CHAPTER 9

BEHAVIOR OF SIMULATION SUB-MODELS

The previous chapter has summarized the calibration and subsequent validation of the total system simulation over a range of speeds and loads. Before using the simulation for thermodynamic and heat transfer predictions, however, it is useful to examine the behavior of some key system sub-models, in detail. The purpose of this chapter is two-fold: first, to illustrate the behavior of the system sub-models for the base case operating conditions described in Chapter 8; second, to relate some of the predictions to experimental data or other published work.

9.1 Gas Exchange Process Model

The mass flow rates through the intake and the exhaust valve of each cylinder depend on the relative pressures upstream and downstream of the valves. Figure 14 shows the mass flow versus crank angle profiles corresponding to the filling and emptying events of the master cylinder. The intake valve flow rate essentially follows the piston motion, and exhibits a more gradual rate of acceleration and deceleration compared to the exhaust valve flow rate. The intake flow rate shows a fairly flat maximum, while the exhaust flow rate is peaked twice: the first peak, corresponding to the blowdown process of the cylinder, is caused by the high cylinder pressures and relatively low exhaust pressures when the exhaust valve opens; the second peak, lower in magnitude, is due to the upward piston motion during the exhaust stroke.

During the valve overlap period and before the intake valve closing, there is backflow (shown as a negative mass flow rate), when the cylinder

pressure exceeds the intake manifold pressure. Backflow also occurs through the exhaust valve during the valve overlap period. This is clearly an undesirable scavenging effect, since it reduces the amount of fresh air that is trapped in the cylinder.

Figure 15 shows the velocity profiles of the conical jet flows through the intake and the exhaust valve opening, non-dimensionalized with respect to the mean piston speed.* Since the intake valve is the minimum area for the flow, these jet velocities are the highest velocities in the intake system. The simulation predicts that the intake jet velocities are about ten times the mean piston speed, which is in good agreement with the data [59]. These high gas velocities are responsible for many of the subsequent features of the in-cylinder thermodynamic and heat transfer processes. Jet velocities through the exhaust valve reach very high values during the gas blowdown process, around forty times the mean piston speed, and subsequently drop to around twenty times the piston speed. The negative velocities at the valves correspond to the backflow conditions described above.

9.2 Combustion Model

Figures 16 and 17 show the normalized heat release profile (i.e., fuel burning rate divided by total fuel injected per cycle per cylinder) and the corresponding pressure trace predicted by the simulation at rated speed and load. Injection of the fuel starts at 14 degrees BTC. Following the four degree delay period, the part of the injected fuel which has been made ready for burning burns rapidly in a premixed flame. This causes the initial sharp peak in the burning rate diagram, and the kink in the pressure trace that is

*The latter is defined as twice the product of the piston stroke and the rotational speed of the crankshaft.

observed at 10 deg. BTC. Subsequent burning is controlled by the rate at which mixture becomes available for burning and occurs in a diffusion controlled turbulent flame. The heat release profile reaches a second, lower peak in this phase. Eventually, the burning rate asymptotically approaches zero. As already described in Chapter 8, our heat release profile has satisfactorily described the combustion process for a Cummins engine.

9.3 Heat Transfer Model

The effects of the fluid flow and combustion processes occurring inside the cylinder are clearly reflected on the bulk gas temperature and gas to wall heat transfer distributions over the engine cycle. In particular, the bulk gas temperature profile, shown in Fig. 18 (top), exhibits a rapid increase in slope at the point where combustion starts, i.e., at 10 deg. BTC. Subsequently, the temperature profile reaches its peak at approximately 30 deg. ATC, a point corresponding to the peak of the diffusion-controlled combustion phase (see Fig. 16).

Figure 18 also shows the total heat transfer rate (convective and radiative) plotted against crank-angle. Again the kink in the profile at the start of combustion is apparent. The total heat transfer rate peaks a little after TC, i.e., earlier than the bulk gas temperature. This is because the convective heat transfer rate depends on the product of the difference between the gas and the wall temperature times the convective heat transfer coefficient; the latter, based on the turbulent flow model, is sharply peaked close to TC, as shown in Fig. 18 (bottom). The strong variation of the convective heat transfer coefficient over a cycle underlines its importance in determining the correct magnitude of the time-varying boundary condition at the gas to wall interface, which is critical to the component wall conduction

models. Another feature of the heat transfer rate is that it becomes negative during parts of the intake process, when the wall surface temperatures are higher than the bulk gas temperature. This heating-up of the intake charge, and the resulting deterioration of volumetric efficiency play an important role in the study of low-heat-rejection engine configurations.

Figure 19 shows the importance of radiant heat transfer in a cooled diesel engine relative to the convective and the total heat transfer rates. Three different models for radiant heat transfer are presented. The continuous curve shows the results obtained from the flame radiation model developed for this thesis. The dashed curve and the dashed-dotted curves are generated from Annand's radiation model, using calibrating constants, C_r , equal to 2.0 and 1.0, respectively. For clarity, the relatively minor impact of different radiation assumptions on the distribution of convective heat transfer is neglected, so that a single convective heat transfer curve is plotted for all three cases. The total heat transfer profiles corresponding to the three radiant cases mentioned above are plotted on Fig. 19, as well.

Several important conclusions can be drawn from Fig. 19. On a time-average basis, the ratio of mean radiant to total heat transfer obtained from the flame model (19.5%) compares closely with the ratio (21%) calculated based on Annand's model with a calibrating constant of 2.0. On the other hand, the original Annand model (calibrating constant equals 1.0) predicts that the mean radiant heat transfer is only 12% of the total heat transfer. This estimate is relatively low compared to the engine radiation measurements reported in Table 3. It is a consequence of the fact that the bulk mean gas temperature can be appreciably below the temperature of the radiating soot particles.

A more detailed comparison between the results of the flame radiation model and Annand's model (with $C_r = 2.0$), reveals the following differences.

The radiant profile based on the flame model peaks earlier and focuses more over the primary heat release period compared to the profile based on Annand's model. Additionally, the radiant heat transfer rate based on the flame model decays to zero by the end of the combustion process (in agreement with Flynn's data), due to the time-varying emissivity of the radiating particles included in the model. On the other hand, since the calibrating constant in Annand's model does not change with crank angle (it is not an emissivity), the radiant heat transfer rate calculated by Annand's model must be abruptly set to zero at the end of combustion.

Figure 20 illustrates the behavior of the flame radiation model, in detail. The temperature of the air zones, calculated assuming adiabatic compression from the start of ignition, reaches a peak of about 800 K shortly after TC, and then drops smoothly down to 260 K by the end of expansion, following the piston motion. The adiabatic flame temperature calculation is performed by means of correlations (4-24) and (4-25), based on the instantaneous air temperature and pressure; it reaches a maximum of 2700 K corresponding to the maximum air temperature and then decays smoothly to 2300 K. The bulk gas temperature, as already described in Fig. 18, reflects the turbulent diffusion processes that occur in the cylinder during combustion. Following the lapse of the delay period, the gas temperature increases rapidly, reaches a peak close to 1670 K at about 30 deg. after TC, and then decays at a rate faster than the air temperature (or the adiabatic flame temperature), down to about 1000 K by the end of expansion. Flynn's measurements suggest that the bulk gas temperature is appreciably below the temperature of the radiating soot particles. On the other hand, use of the adiabatic flame temperature would overestimate the contribution of radiant heat transfer late in the combustion process. Our estimate of the

characteristic radiant temperature as the average of the adiabatic flame temperature and the bulk gas temperature is plotted in Fig. 20. Starting from a level of 1800 K, the radiant temperature reaches a peak of 2140 K at 20 deg. after TC (corresponding to the peak heat release) and then decays to 1650 K. These estimates were found to be in reasonable agreement with Flynn's data [37].

Figure 21 shows the breakdown of the convective and radiative heat transfer rates among cylinder head, piston, and liner, over the duration of the combustion process. The most important feature is the relation of the heat transfer rate to the liner compared to the rates to the other two surfaces. The liner heat transfer rate goes to zero at TC, when the piston covers the entire liner surface. As the piston moves downward, and the liner surface area exposed to the gases increases, the heat transfer rate to the liner reaches a peak at approximately 70 deg. after TC, and then remains the dominant influence until the end of expansion. However, the surface areas of the cylinder and piston are constant. Hence, the convective heat transfer rates to these surfaces reach their peaks when the gas temperature peaks (at 30 deg. after TC) while their radiative counterparts peak when the characteristic radiant temperature peaks (at 20 deg. after TC). It is interesting to note that the peak convective heat transfer rate to the liner is about 25% of the peak rate to the piston, while the peak radiative rate to the liner is 50% of the peak rate to the piston. This is due to the following two effects: i) the radiant temperature falls off, relatively, more slowly than the mean gas temperature, ii) the emissivity drops at a much slower rate compared to the rapid drop of the convective heat transfer coefficient, shown in Fig. 18.

9.4 Turbulent Flow Model

The heat transfer processes in the engine cylinder are driven by the mean gas motion and turbulence. The turbulent flow model developed for this simulation provides estimates of the characteristic velocity and length scales for the convective heat transfer calculations by taking into account these governing in-cylinder fluid mechanisms. Figure 22 shows the variation of the mean flow velocity, the turbulent intensity and the resultant effective heat transfer velocity, defined by Eq. (4-18), with crank angle. All the velocity scales are normalized with respect to the mean piston speed.

The mean flow velocity is very high during the intake process, rising to a maximum (about 8 times the mean piston speed) and then decreasing in response to the piston motion. During compression, the mean velocity decreases at a slower rate. During the exhaust process, a velocity term due to the blowdown process is superposed on the mean flow velocity characteristic, which reaches a second peak, of the order of two to three times the mean piston speed. Measurements of ensemble-averaged mean velocities within the cylinder through the application of laser doppler anemometry techniques, [60]-[62], suggest that the simulation predictions follow the general trends of the data.

The variation of turbulent intensity with crank-angle shows that very high turbulence levels are created by the intake flow. Subsequently, turbulence decays, since the rate of turbulence dissipation due to viscous shear stresses is larger than the rate of turbulence generation from shear in the mean flow. Most of the in-cylinder velocity measurements show that the turbulent intensity at top center, with open combustion chambers in the absence of swirl, has a value of about half the mean piston speed, while the simulation predicts that it is approximately equal to the mean piston speed [61].

Figure 23 focuses on the variation of the non-dimensional turbulent intensity with crank-angle over the duration of the compression and combustion processes. The turbulent intensity predicted by the turbulence model developed for this simulation is compared to that predicted by the Poulos and Heywood model [41]. The new model predicts an increase in turbulent intensity due to the rapid distortion resulting from gas compression due to piston motion and rising cylinder pressures during the end of compression and during combustion. In-cylinder velocity measurements provide some evidence for this behavior. Wong and Hault [63] have shown that the requirement for conservation of large-scale eddy angular momentum in the presence of these distortions leads to this increase in vorticity and turbulent intensity.

The characteristic velocity for convective heat transfer calculations is calculated from Eq. (4-18), by taking into account contributions from the mean flow velocity, the turbulent intensity, and the instantaneous piston speed. It is shown in Fig. 22 plotted against crank-angle. It is important to note the wide range of values that the effective heat transfer velocity assumes over a cycle, i.e., from one to nine times the mean piston speed. This is in agreement with predictions from other computer simulation work [64], and indicates the limitations of heat transfer correlations that are based on the mean piston speed.

Both large-scale and small-scale turbulent motions are important factors governing the overall behavior of the in-cylinder flow [65]. During the intake process, the eddies responsible for most of the turbulence production are the large-scale eddies in the inlet jet flow. In our turbulent flow model, we are focusing on the characteristic length of the large scale eddies, i.e., the macroscale of turbulence. These eddies are limited in size by the system boundaries. Fig. 24 shows the predicted macroscale of turbulence,

non-dimensionalized with respect to the cylinder bore, plotted against engine crank-angle. The model predicts that the turbulence macroscale will be given by the instantaneous distance between the cylinder head and the piston. When this distance becomes greater than half the bore, the scale is taken as half the bore. These predictions are in reasonable agreement with the available data [66]-[68], which suggest that the macroscale at the TC is of order 2-5 mm.

9.5 Exhaust Manifold Model

Figure 25 shows the exhaust manifold temperature and pressure time histories. Both exhibit the same behavior, i.e., a series of six identical repeating pulses, each produced by the emptying process of the individual cylinders of our six cylinder engine. Note that the temperature profile shown corresponds to an overall manifold system model encompassing all runners, and plenums, in a single control volume. Temperature profiles for the individual sub-sections of the exhaust manifold can be generated by the simulation, as well. The latter show wider amplitude oscillations, due to the smaller volume of each sub-section relative to the total exhaust system volume.

CHAPTER 10

SYSTEM PERFORMANCE RESULTS

The previous two chapters have described the calibration and subsequent validation procedure of the complete system model against data from a cooled engine, and demonstrated that the behavior of the individual sub-models adequately reflects the thermodynamic and heat transfer engine processes. Thus, we can now apply the full system simulation with considerable confidence to the study of the low-heat-rejection turbocompounded diesel system. The present chapter explores the effect of various degrees of reduction in heat loss to coolant on system performance.

10.1 Study Methodology

The simulation predictions depend on the underlying assumptions and constraints applied to the system. As the degree of insulation of the various system components increases, it is important to define which of the parameters that characterize system performance are held constant. Examples of such parameters include mass flow going through the system, volumetric efficiency, cyclic wall surface temperature variations, injection timing, shape and start of heat release, amount of fuel injected per cycle, degree of radiant heat transfer, maximum allowed cylinder pressure, compression ratio, compound turbine gear ratio, friction losses, turbomachinery performance, etc. Clearly, a universal answer to the problem of defining insulated engine performance does not exist. Our approach to the problem is the following: First, the sensitivity of the performance predictions to some of the above parameters is explored by comparing a baseline cooled engine against a partially insulated engine achieving a 50 percent reduction in heat loss. Then, based on these results, appropriate choices as to which parameters are

fixed for the subsequent studies of system performance with increased degree of insulation are made.

10.1.1 Sensitivity of radiative heat transfer to degree of insulation

Radiative heat transfer is expected to play a significant role in insulated diesel engines with low convective heat transfer. Hence, our ability to predict radiation as accurately as possible is critical. Figure 26 shows the distributions of the convective, radiative (based on the flame model), and total heat transfer rates over the duration of the expansion process for the insulated and the baseline system configurations. It is clear that radiative heat transfer as a percentage of the total heat transfer becomes considerably more important (47%) for the insulated engine relative to the cooled baseline engine (only 20%). This is largely due to the reduction in convective heat transfer that results from the introduction of insulation and not due to the increase (only about 5%) in radiative heat transfer. As shown in Fig. 27 and further explained in Section 10.2.2, the bulk gas temperature in the ceramic engine during the expansion process is only about 4% higher than in the cooled metal engine. Since the adiabatic flame temperature profile is almost insensitive to the reduction in heat loss, the characteristic radiant temperature profile in the ceramic engine is only 2% above the baseline profile, resulting in a modest increase in radiative heat transfer.

Figure 28 compares the radiation predictions based on the flame model against results from Annand's model (with a calibrating constant of 2.0). Annand's model predicts a greater relative increase in radiative heat transfer in the insulated engine over the baseline engine. However, the difference (9% versus 5%) between the predictions of the two models is relatively small. In the absence of any radiation measurements in insulated engines, the flame

radiation model, which does not require any calibration, is chosen for use in our studies of insulated system configurations.

10.1.2 Sensitivity of optimum injection timing to degree of insulation

Proper timing of the combustion process is essential to achieve optimum diesel engine operation. Early injection gives a very high rate of pressure rise, owing to the associated long ignition delay period. Retarded injection timing reduces the importance of heat transfer to the combustion chamber walls due to reduced peak gas temperature, etc. Hence, in order to achieve the maximum mean effective pressure, the injection timing must be adjusted for major changes in combustion chamber design and/or the engine operating conditions. In particular, several investigators have predicted a reduction in ignition delay in insulated engines [12,14]. This changes the combustion characteristics in these engines, and thus the injection timing needs to be adjusted for optimum performance. In order to explore the effect of insulation on the optimum injection timing, we have carried out two sets of calculations:

(i) The start of combustion was specified at 4 deg. crank-angle after the start of injection so that changes in the shape of the heat release profile with variations in ignition delay were suppressed. Then a series of cycle simulations was run to study the sensitivity of brake mean effective pressure (bmep) to changes in injection timing for both a cooled engine (baseline) and a partially insulated engine. Figure 29 (top) shows that, for optimum performance, the injection timing for the cooled engine must be set at 338.5 deg. crank angle while for the partially insulated engine it must be advanced slightly to 337 deg. crank-angle. However, it must be noted that over the range 334 to 340 deg. crank-angle, the predicted bmep is almost constant (within 0.3 percent of the maximum value for both the metal and the ceramic engine).

(ii) The ignition delay was predicted for each injection timing based on equations (4-12) and (4-13), so that changes in the heat release profile were taken into account, in addition to the changes in the rate of pressure rise and the rate of wall heat transfer. Figure 29 (bottom) shows the bmep versus injection timing profiles for the baseline and the ceramic engine, based on the predicted delay model. Again, the optimum injection timing for the ceramic engine (338 deg. crank-angle) is earlier than for the baseline engine (339.5 deg. crank-angle) but the effect on b.m.e.p. is small (less than 0.2 percent). In summary, although the injection timing must be optimized for each system configuration, predictions based on the optimum timing for the baseline engine are reasonable first estimates.

10.1.3 Sensitivity of optimum gear ratio to degree of insulation

Figure 30 shows the variation of power turbine brake power, reciprocator brake power, and total combined brake power with respect to the power turbine gear ratio for the cooled and the insulated system configurations. An increase in gear ratio, which is defined as the ratio of the power turbine speed to the reciprocator speed, translates into a higher power turbine speed. Thus more power is developed by the power turbine for a given reciprocator speed. However, the pressure ratio across the power turbine increase while the turbocharger turbine's expansion ratio decreases. As a result, the turbocharger boost and the mass flow going through the reciprocator are reduced. Obviously, to maximize the total power produced by the compound system, we must select a gear ratio that will optimize the trade-off between the power developed by the reciprocator and the power turbine. Figure 30 (top) indicates that the optimum gear ratio for both the metal and the ceramic engine lies in the range of 17 to 20. Since the two characteristic curves are fairly flat over this range (deviations from maximum value are less than 0.5

percent), we may conclude that the optimum gear ratio is not dramatically affected by the degree of insulation.

10.2 Effect of Insulation on System Performance

10.2.1 Assumptions

Given the conclusions of the previous sections, the following assumptions were used in our study of insulated system configurations:

1. Radiant heat transfer predictions are based on the flame radiation model.
2. The start of combustion (342 deg. crank-angle) and the amount of fuel injected per cycle per cylinder are fixed. (The shape of the heat release profile can change, however, due to changes in the overall equivalence ratio).
3. The compounded gear ratio is fixed at its optimum value (17) for the baseline engine.
4. Mass flow rates through the system components, and efficiencies of the turbomachinery components are obtained from the solution of the reciprocator-turbocharger matching problem.
5. Different degrees of insulation are simulated by specifying different wall surface temperatures (quasi-steady values) in the engine combustion chamber. The effect of cyclic surface temperature variations on system performance is assessed in a later section.
6. The compression ratio (14.5) is held constant. The peak cylinder pressure is not constrained.
7. Friction losses are based on reciprocator speed only.
8. All performance predictions are carried out at the reciprocator's rated speed, i.e., at 1900 RPM.

10.2.2. Effect of variation of combustion chamber surface temperature

Having stated the above assumptions, we can now use the simulation to study the effect of insulation on system performance. Several different levels of insulation are examined, covering a range from no insulation (baseline cooled engine) up to full insulation (96 percent reduction in heat loss to coolant over the baseline engine). This is simulated by varying the surface temperature of the combustion chamber from 400 K (baseline engine) up to 900 K (fully-insulated engine). The results are summarized in Table 7.

As the combustion chamber surface temperature increases, the fraction of the input fuel energy that would be lost in heat transfer to the walls decreases. Then, the first law of thermodynamics requires that more energy appears in the reciprocator exhaust and/or more useful work is extracted on the crankshaft. One of the important conclusions of our study is that reductions in heat transfer due to insulation are primarily traded for increased exhaust enthalpy, as evidenced by the higher mean temperatures (on a mass-averaged basis) of the reciprocator exhaust shown in Table 7. On the other hand, there is little change in shaft work so that a fully insulated engine achieves only a modest thermal efficiency benefit (less than 1 percent) over a baseline cooled engine.

This result can be explained in terms of the degradation in volumetric efficiency that occurs with increasing degree of insulation. The drop in volumetric efficiency (based on intake manifold density), by as much as 17 percentage points for a fully insulated engine, results from the decrease in charge density due to the heat transferred to the intake charge from the high temperature insulated walls. In a turbocharged engine, part of the extra available exhaust energy is used by the turbocharger turbine which supplies more power, thus increasing the speed of the turbocharger rotor. The

resulting higher boost pressure ratios partly compensate for the reduction in charge density so that the volumetric efficiency based on atmospheric conditions falls off more slowly than the volumetric efficiency based on intake manifold conditions. This is reflected in the mass flow inducted in the cylinder which drops linearly by 1 percentage point for every 20 percentage points reduction in the heat loss. It is important to note that the airflow into the engine does not remain constant with increasing insulation.

It can be concluded that the heating-up of the intake charge during the intake and early compression processes is detrimental to the system performance. First, because the intake charge starts from a higher temperature, and higher pressure (due to the higher boost pressure ratios), more compression work is required in an insulated engine compared to the baseline engine. Second, the heat that flows from the walls to the gas during intake and compression is absorbed by the walls from the gas during combustion, when that energy is most needed to produce useful work. Furthermore, since the intake airflow decreases while fuel flow rate remains constant, the overall equivalence ratio increases. Due to the resulting changes in the shape of the heat release profile and the increased combustion duration, the gas temperature and pressure distributions during expansion are close to those for the baseline engine. This can be seen from Fig. 27 and from the values of peak cylinder pressure tabulated in Table 7, which increase only slightly with increasing degree of insulation. Hence, there is little change in the expansion work compared to the baseline engine. Consequently, the gross indicated work (based on the compression and expansion work), and thus the gross i.m.e.p. and the gross indicated thermal efficiency are slightly reduced with increasing insulation (by as much as 1 percent for a fully insulated engine).

We may conclude that any thermal efficiency benefits from the use of insulation results from either a reduction in the pumping work requirement and/or a reduction in friction large enough to offset the decrease in gross indicated work. Indeed, our results show that the intake manifold pressure increases with insulation (due to the higher turbocharger boost pressure ratio) without a corresponding increase in the exhaust manifold pressure, thus leading to less pumping work. This can be seen from the decrease (in absolute value) of the pumping mean effective pressure with increasing insulation shown in Table 7, which is in agreement with experimental measurements taken at Cummins [13,14]. Assuming that mechanical friction is independent of the degree of insulation, the reduced pumping work causes an increase in b.m.e.p. and a corresponding modest improvement in cylinder brake thermal efficiency, which is approximately 1 percent with a 50 percent reduction in heat loss.

Another important conclusion is that the power developed by the power turbine does not show any substantial increase with increasing insulation, despite the fact that most of the conserved energy appears in the engine exhaust. The reason for this is twofold: First, most of the extra available high pressure and high temperature energy is used-up by the turbocharger turbine in order to provide the higher boost levels. This limits the pressure ratio across the compounded turbine so that the improvement in the power turbine work per unit mass flow is modest. Apparently, the power turbine cannot derive much benefit from the high temperature, low pressure, available energy, as evidenced by the increasing temperatures at the power turbine exhaust in Table 7. Second, the loss in volumetric efficiency reduces the mass flow going through the total system. As a result, the product of the (reduced) mass flow times the (increased) specific work -- i.e., the power turbine power, shows only a modest improvement (e.g., about 2 percent at 50

percent reduction in heat loss). Since both the reciprocator and the power turbine performance gains are small, the overall brake thermal efficiency improvement of even a fully insulated system is limited to 1 percentage point over the baseline cooled system.

At this point, the important distinction between a fully insulated system and an adiabatic system needs to be drawn. Neither of these systems transmit any heat to the coolant, i.e., they achieve 100 percent reduction in heat loss. However, the fully-insulated engine achieves zero gas to wall heat transfer only on a cycle-averaged basis. As shown on Fig. 31, the engine walls absorb a large amount of heat during combustion, where the flame temperature and the bulk gas temperature are appreciably above the wall surface temperature (900 K). To offset this positive (i.e., from gas to walls) heat transfer, heat must flow back to the gas during the rest of the cycle. Since the gas radiative heat transfer can only be positive, this requires that the net convective heat transfer is negative on a cycle-averaged basis. That is why so much heat is added to the gas during the intake process resulting in the large drop in volumetric efficiency.

In contrast, in an adiabatic system, the total heat transfer between the cylinder gases and the combustion chamber walls is zero at any instant, i.e., the walls absorb no heat. This effectively requires that the wall surface and the gas temperature are equal at any instant. Although it is difficult to approach this condition with current ceramic materials (see Chapter 11), the adiabatic case sets a useful limit on the potential gains that can be realized from the use of insulation. As shown in the last column of Table 7, the adiabatic engine has a very high volumetric efficiency (94.5 percent), more mass flow compared to the baseline case, requires less compression work (because the charge is not heated-up), and produces more expansion work.

Furthermore, the power from the compound turbine increases substantially due to more mass flow. As a result, the adiabatic engine realizes a significant gain in thermal efficiency: 6 percentage points.

10.2.3 Effect of variation of liner temperature on system performance

Several investigators, e.g., [12,14], have suggested that an optimum insulation strategy would maintain a cooler liner temperature compared to other parts of the combustion chamber. In order to evaluate this proposition, a series of simulation calculations was performed for liner temperatures ranging from 450 K (fully cooled liner) up to 800 K, while the piston and the cylinder head were maintained at 800 K. The results of these studies are summarized in Table 8.

As the liner insulation, and thus the liner temperature, is reduced, less heat is transferred to the intake charge from the walls. As a result, the volumetric efficiency based on intake manifold conditions improves substantially, by as much as 5 percentage points for a fully-cooled liner (at 450 K) compared to a liner maintained at 800 K. This translates into an increase in the airflow and a reduction in the compression work. The latter, coupled with little change in expansion work, causes an increase in the gross i.m.e.p. and the gross indicated efficiency with reduced liner insulation.

On the other hand, heat rejection is substantially increased, by approximately 3.5 percentage points for every 50 K reduction in the liner temperature. In turn, this reduces the available exhaust energy and hence the boost pressure ratio. Consequently, the pumping work is increased (due to the lower intake manifold pressures). This increase in the pumping work erodes most of the thermal efficiency benefit due to the increase in volumetric efficiency. Hence, the advantages of running the engine with cooled liner (half a percent improvement in efficiency, reduced lubrication problems) must be evaluated against the inconvenience of retaining a cooling system.

10.2.4 Effect of higher turbomachinery component efficiencies on system performance

The previous sections have demonstrated the critical importance of turbomachinery in compensating for the loss in volumetric efficiency in insulated engine configurations. In order to evaluate whether more efficient turbomachinery would further improve the performance of an insulated engine, a series of calculations was performed where, (a) one turbomachine at a time and (b) all three turbomachines at the same time were assumed to be 5 percent more efficient than the baseline components. Results are summarized in Table 9.

Increasing either the compressor or the turbine efficiency by 5 percent, results in a 3 percent increase in the boost pressure ratio, the volumetric efficiency (based on atmospheric conditions) and the mass flow going through the system. As a result, the brake thermal efficiency improves by 0.3 percentage points. Increasing the power turbine efficiency by 5 percent does not alter the reciprocator performance (as expected), but increases the power turbine power (by 4.5 percent) so that the overall thermal gain is still 0.3 percentage points. Then, a system using the more efficient compressor, turbine and power turbine achieves almost 1 percentage point higher thermal efficiency over the baseline (i.e., individual gains are compounded).

Table 10 examines the sensitivity of these gains to the degree of insulation. It is shown that a cooled engine gains relatively less (0.6 percentage points) from the use of more efficient turbomachinery compared to an insulated engine achieving a 50 percent reduction in heat loss over the baseline (0.9 percentage points).

CHAPTER 11

WALL CONDUCTION MODEL RESULTS

The purpose of this chapter is to demonstrate the use of the component wall conduction models for global system simulation and preliminary component heat transfer studies. First, the models are used to assess the effect of cyclic wall surface temperature variations on system performance. Then, the engineering trade-offs associated with the use of different ceramic materials to achieve a desired degree of insulation are illustrated. Subsequently, the dependence of the degree of insulation achieved with a specific material thickness on engine load and speed is examined. Finally, the relationship between the dimensions of the combustion chamber insulation and the resulting degree of insulation is explored for some alternative design configurations.

11.1 Effects of Wall Surface Temperature Variations on System Performance

In order to assess the effect of surface temperature variations on system performance, the transient wall conduction models were used to predict the performance of a cooled and a representative insulated engine. Results were then compared against predictions based on quasi-steady heat transfer. The wall construction details of the two configurations are as follows:

- (a) The cooled engine has an all cast-iron combustion chamber ($k = 54 \text{ W/m-K}$). The piston and the cylinder head are 12 mm thick, while the liner is 7 mm thick. The wall surface temperatures on the coolant side are set at 380 K for all components.
- (b) The partially-insulated engine has a 1.5 mm plasma-sprayed zirconia coating applied on the cylinder head and the piston. The coating has a thermal conductivity $k = 0.6 \text{ W/m-K}$ and a heat capacity $pc = 1.1 \times 10^6$

$\text{J/m}^3\text{-K}$ [70], and is supported by 10 mm of cast-iron substructure ($k = 54 \text{ W/m-K}$). The liner is non-insulated, 7 mm thick cast iron. The wall surface temperatures on the cold side (coolant or ambient) are set at 380 K for all components.

Figure 32 shows the temperature profiles of the mean bulk gas and the piston surface throughout the engine cycle for the insulated (solid curves) and the baseline (dashed curves) engines. As discussed in Chapter 10, the bulk gas temperature in the insulated engine is slightly higher than in the cooled engine. The surface temperature variations in the cast-iron engine are 18 K (peak-to-peak) which is in agreement with experimental measurements [36],[52]. The fluctuation around the quasi-steady surface temperature (800 K) in the insulated engine is considerably larger, i.e., 235 K (peak-to-peak). This fluctuation is still small compared to the variation in the bulk gas temperature during the engine cycle. However, the instantaneous wall surface temperatures are below the mean quasi-steady temperature during intake and the early part of compression, and above the mean during combustion. Both these effects reduce the gas to wall heat interchange during the cycle.

Table 11 summarizes the performance predictions for the two engines, based on the quasi-steady heat transfer and the transient wall conduction models. As expected, the results for the cooled engine are identical in both cases (due to the small temperature swings). In the insulated engine, the reduction in heat transfer during intake results in less degradation in volumetric efficiency (1%), and hence less compression work. Further, reduced heat transfer during combustion increases the expansion work. These effects lead to a small increase in the reciprocator brake work. Additionally, because the turbocharger turbine is required to provide less boost, the power turbine produces more power. The overall brake thermal efficiency of the

system is about 1% higher compared to the predictions based on quasi-steady heat transfer, i.e., 2.5% over the baseline engine performance. Thus, we may conclude that the higher the cyclic wall surface temperature variations, the more the expected improvement on the thermal efficiency of the total system.

11.2 Effects of Wall Surface Temperature Variations on Component Thermal Loading

The previous section has demonstrated that the zirconia-coated engine can achieve a moderate (2.5 percent) thermal efficiency benefit over the baseline cast-iron design. However, to realize this benefit, the zirconia-coated components must be able to withstand the resulting adverse thermal environment. First, the mean wall surface temperature (800 K) in the zirconia-sprayed engine is considerably higher than the temperature (450 K) in the cast-iron combustion chamber. Furthermore, the peak wall surface temperature approaches 1000 K due to the large fluctuations around the mean temperature. Thus, the zirconia-coating must have good high temperature strength and be able to maintain its stability under these conditions. Additionally, the coating must possess high fatigue durability in order to withstand the cyclic thermal loading caused by the large (235 K peak-to-peak) surface temperature variations.

Besides the surface temperature variations, a useful quantity to describe the component thermal loading is the penetration distance, or 'skin depth', of the cyclic transients. This is conveniently defined as the distance from the surface at which the difference between the maximum and minimum temperature over the cycle decays to 1% (or sometimes 5%) of its value at the wall surface. From the physics of the unsteady conduction problem, the skin depth ' δ ' is proportional to the square root of the ratio of the thermal diffusivity, α , over the engine speed, N , i.e.,

$$\delta \sim \sqrt{\alpha/N} \quad (11-1)$$

Figure 33 shows the penetration depth of the cyclic transients in the plasma-sprayed zirconia coating and in the cast-iron piston. Due to the low thermal diffusivity of plasma-sprayed zirconia ($\alpha = 0.545 \times 10^{-6} \text{ m}^2/\text{s}$), the cyclic transients penetrate into the wall structure for only a limited distance, i.e., 0.51 mm (or 0.28 mm to decay to 5% of value at surface). In contrast, the relevant skin depth of the cast-iron piston, which possesses a high thermal diffusivity ($\alpha = 15.741 \times 10^{-6} \text{ m}^2/\text{s}$), is 2.75 mm.

The combination of large surface temperature swings and short penetration depths in the zirconia-coated piston results in high thermal gradients, and thus high cyclic thermal loading. Figure 34 shows the perturbations from the quasi-steady temperature profiles in the insulated and the cast-iron engine at three instants (300 deg., 350 deg., and 450 deg. crank-angle) during the engine cycle. Although the profiles are qualitatively similar, the temperature and length scales are substantially different in these two cases for the reasons explained above. It is apparent that the plasma-sprayed zirconia must possess high thermal shock resistance to withstand the thermal stresses developed as a result of the steep thermal gradients.

11.3 Use of Alternative Ceramic Materials to Achieve a Desired Degree of Insulation

Current research into the use of ceramics in engines is directed towards developing new materials and characterizing their production processes and properties. Although most of these materials possess good high temperature strength, the family of ceramics covers a wide range of properties. Furthermore, the mechanical performance of any given ceramic can vary

considerably as a result of its production process. However, for the purpose of evaluating the potential of ceramics for engine applications, we will assume that the properties reported by Ricardo [69] in Table 12 are sufficiently representative of current practice. For comparison, the properties of certain metals which are commonly used in engines are given, too.

In order to illustrate the engineering trade-offs associated with the use of alternative ceramic materials to achieve a desired degree of insulation, the 1.5 mm plasma-sprayed zirconia coating ($k = 0.6 \text{ W/m-K}$ and $\rho c = 1.1 \times 10^6 \text{ J/m}^3\text{-K}$) of the previous example was replaced by:

- (a) A 3 mm coating of sprayed zirconia ($k = 1.2 \text{ W/m-K}$ and $\rho c = 3.8 \times 10^6 \text{ J/m}^3\text{-K}$) applied to the cylinder head and piston, supported by a 10 mm cast-iron substructure ($k = 54 \text{ W/m-K}$).
- (b) A monolithic Reaction Bonded Silicon Nitride, RBSN, ($k = 5 \text{ W/m-K}$ and $\rho c = 1.8 \times 10^6 \text{ J/m}^3\text{-K}$) cylinder head and piston, of thickness 13.4 mm. Similar monolithic ceramic components have been evaluated experimentally by Parker and Smart [71].

Obviously, the thickness of each ceramic material was adjusted to compensate for differences in conductivity so that the effective heat transfer coefficient was maintained constant ($U = 373 \text{ W/m-K}$). In all the above cases, the liner was non-insulated, 7 mm thick cast-iron, and the wall surface temperatures on the cold side were kept at 380 K. Thus, all three designs achieved the same degree of insulation (i.e., 45% reduction in heat transfer compared to the baseline cast-iron engine).

Figure 35 shows the cyclic variations from the mean temperature (800 K) at the surface of the piston for the three candidate materials. Clearly, the plasma-sprayed zirconia [70], which has the lowest conductivity and lowest

thermal capacity of the three materials, experiences the largest swings (235 K peak-to-peak) around the mean temperature. Consequently, it achieves the highest overall brake thermal efficiency (i.e., 46%). In contrast, the swings predicted for the zirconia coating (95 K peak-to-peak) and the RBSN (70 K peak-to-peak) are substantially smaller, leading to half a percentage point reduction in brake thermal efficiency (45.6% and 45.5%, respectively).

Although the swings for zirconia and RBSN are of the same order of magnitude, it must be noted that RBSN has a considerably greater conductivity ($k = 5 \text{ W/m-K}$) compared to zirconia ($k = 1.2 \text{ W/m-K}$), and thus experiences a steeper thermal gradient at the gas/wall boundary. However, zirconia has a greater thermal capacity ($\rho c = 3.8 \times 10^6 \text{ J/m}^3\text{-K}$) than RBSN ($\rho c = 1.8 \times 10^6 \text{ J/m}^3\text{-K}$), and thus stores a greater fraction of the heat flow that it receives. As a result, the surface temperature variations of the two materials are similar. We may conclude that the lower the thermal conductivity and the lower the thermal capacity of a material, the higher the wall surface temperature swings and hence the better the thermal efficiency of the overall system.

The above conclusions seem to imply that to achieve truly adiabatic engine operation, the insulating material must possess zero conductivity and zero thermal capacity, so that the wall surface temperature follows the gas temperature. However, it seems unlikely that such a combination of properties can be realized in any material which has, at the same time, the necessary strength and thermal shock and fatigue properties. In practice, the selection of an insulating material involves a strong trade-off between system performance improvement and component thermal loading. This is illustrated by means of Table 13 which summarizes the predicted cyclic surface temperature transients and their penetration into the wall structure for the three ceramic

materials considered above. For comparison, results for cast-iron are tabulated, too. In accordance with Eq. (11-1), the skin depth of each material was found to be proportional to its thermal diffusivity (the ratio $\delta/\sqrt{\alpha}$ was constant at a speed of 1900 RPM). Therefore, the plasma-sprayed zirconia, which leads to the highest overall thermal efficiency (46%), experiences the most adverse thermal gradients (a swing of 235 K decays to zero over 0.51 mm). In contrast, use of materials which experience reduced thermal loading (e.g., RBSN) is accompanied by a one percent reduction in thermal efficiency.

11.4 Effects of Speed and Load on Degree of Insulation

The purpose of this section is to explore whether the degree of insulation achieved with a given material thickness is significantly affected by variations in the reciprocator speed and load. As an illustrative case, we will consider again the engine with the 1.5 mm coating of plasma-sprayed zirconia applied on the cylinder head and piston,, and the standard (cooled) liner. This engine achieves a 45% reduction in heat losses over the baseline cast-iron engine at rated speed (1900 RPM) and full load conditions (see Section 11.3).

11.4.1 Effect of speed

When the insulated engine is run at a speed of 1500 RPM, the importance of heat transfer as a fraction of the fuel energy input increases. Therefore, both the mean and the cyclic variations around the mean wall surface temperature tend to increase. However, due to the reduced engine speed, Eq. (11-1) shows that the penetration depth of the cyclic transients is 27% more than their penetration at 1900 RPM. This compensates for the effect of increased heat transfer, so that the amplitude of the surface temperature

swings increases only slightly with the reduction in engine speed, as shown in Fig. 36. Furthermore, the mean wall surface temperature remains approximately constant (at 800 K). As a result, the insulated engine achieves a 42% reduction in heat loss over the baseline cast-iron engine at a speed of 1500 RPM. Hence, the degree of insulation is not significantly affected by engine speed.

11.4.2 Effect of load

In order to assess the effect of engine load on the degree of insulation, the insulated engine was run at a light load (75% of full load) while the speed was kept constant (1900 RPM). Due to the reduction in the overall equivalence ratio at light load, the bulk gas temperatures throughout the cycle are reduced. This leads to a reduction in the heat flux from the gas to the walls, and hence a reduction in the mean temperature at the piston and cylinder head surfaces (from 800 K down to 723 K). Furthermore, the surface temperature variations are reduced; as shown in Fig. 37, the peak-to-peak fluctuation is almost 75% of its value at full load. Since both the mean and the perturbations from the mean temperature at the piston and cylinder head surfaces depend on the level of heat transfer, the resultant surface temperature profiles are strongly dependent on the engine load. However, this fact allows the insulated engine to achieve a 41% reduction in heat loss over the baseline engine at light load, i.e., essentially the same degree of insulation as at full load conditions.

11.5 Effect of Material Thickness on Degree of Insulation

The previous sections have illustrated the use of alternative ceramic materials to achieve a given degree of insulation (45% reduction in heat loss). Different degrees of insulation can be obtained using any of these

materials by altering the thickness of insulation. This section explores the relationship between thickness of insulating material and resulting degree of insulation. The analysis is carried-out for the case of sprayed zirconia ($k = 1.2 \text{ W/m-K}$), but the results can be readily applied to other insulators, if scaled by the ratio of their respective conductivities to that of zirconia. The same basic assumptions as for the previous calculations are made, i.e., the insulation is applied on the cylinder head and piston, and it is backed by 10 mm of cast-iron substructure; the liner is maintained cooled (7 mm thick, cast iron); the wall surface temperatures on the cold side are kept at 380 K for all components.

Figure 38 (top) shows the surface temperature profiles for different material thicknesses of sprayed zirconia, ranging from 1 mm to 8 mm. As thickness increases, the effective heat transfer coefficient is reduced (see Table 14). Hence the mean temperature at the cylinder head and piston surfaces increases (from 650 K to 908 K), while the gas to wall heat transfer is reduced. The increase in the mean surface temperature with increasing insulating thickness is reflected on the surface temperature profiles shown in Fig. 38 (top). The other characteristics of these profiles (shape, peak-to-peak amplitude) are similar since the perturbations from the mean surface temperatures are essentially constant with insulating thickness. Actually, as thickness becomes very small (e.g., 1 mm) and the level of heat flow increases, the surface temperature variations are somewhat larger. Nevertheless, this effect is small.

Figure 39 shows graphically the relationship between insulating thickness of zirconia and resulting reduction in heat loss to the coolant. The rapid reduction in heat loss with an initial increase of thickness must be noted; a 3 mm insulating layer is sufficient to cut down heat losses by 48%. As more

insulation is added, the incremental benefit progressively diminishes; for instance, an additional 5 mm of insulation reduces losses by an extra 15 percentage points, only. The reason is that the fully-insulated condition for the piston and the cylinder head is approached. The rest of the heat losses (i.e., approx. 30%) are associated with the liner, which is not insulated for this example. The above results were compared with previously-published studies [13],[69],[72] and good agreement was found.

11.6 Effect of Air Gap on Degree of Insulation

The results of section 11.5 suggest that a fully insulated piston or cylinder head requires more than 8 mm of zirconia coating on the metal substructure. However, a coating of that thickness may suffer from fatigue during engine operation. Several investigators [69],[71],[73] have studied an alternative component design where an air gap is sandwiched between a relatively thin ceramic coating and the metal base of a component. To evaluate the merits of this approach, we first simulated an engine with a 2.5 mm of zirconia coating applied to the metallic cylinder head and piston (with no air gap). Then, keeping the thickness of zirconia constant, we introduced an air gap between the coating and the metal base. Table 15 shows the effect of various thicknesses of air gap on the degree of insulation. Due to the very low conductivity of air ($k = 0.02 \text{ W/m-K}$), the introduction of an air gap leads to a dramatic reduction in the heat transfer coefficient of the component, an increase in its surface temperature (see Fig. 40) and a corresponding marked reduction in heat loss. Once again, most of the benefits are derived with the incorporation of a relatively thin air gap (0.5 mm or less); as the fully-insulated condition is approached, an increase in the thickness of the air gap (say to 1 mm) has a minor impact. The results of

Tables 14 and 15 indicate the excellent insulation potential of composite ceramic/air gap/metal component designs. In practice, though, the air gap will pass some heat to the metal by radiation and by conduction through the supporting members. These effects would tend to increase the effective conductivity of the air, and thus the resulting heat transfer. However, the air gap would still reduce the thickness of required coating for a given level of insulation.

CHAPTER 12

SUMMARY AND CONCLUSIONS

This thesis has described the development and use of a computer simulation of the turbocharged turbocompounded diesel engine system for studies of low-heat-rejection engine performance and component thermal loading as major design parameters and materials are varied. The major conclusions are the following:

1. Comparison of model performance predictions with data from a cooled, turbocompounded engine shows very good agreement over the range of reciprocator speeds and loads examined. Thus, the computer simulation provides an effective means of analyzing coupled thermodynamic and heat transfer processes in an engine and through the component wall structures.

2. A new radiation model based on the adiabatic flame temperature has been developed for this work. Due to its expanded physical basis, the characteristic radiant temperature predicted by the model compares more favorably with measured data than the mean bulk gas temperature used in Annand's model. Additionally, the model does not require any calibration for different engine combustion chambers.

3. Radiative heat transfer as a percentage of the total heat transfer becomes considerably more important for low-heat-rejection engine configurations relative to the baseline cooled engine. This is largely due to the reduction in convective heat transfer and not due to the increase (modest) in radiative heat transfer with increasing insulation.

4. High combustion chamber wall surface temperatures due to insulation cause a significant drop in volumetric efficiency (by as much as 17 percentage points for a fully-insulated engine). This reduction in volumetric efficiency

based on inlet manifold density is partly offset by increased boost pressure from the turbocharger.

5. A fully-insulated engine has zero cycle-averaged heat transfer between the gas and the walls. However, heat is transferred from the gas to the walls during combustion, and flows back into the gas from the wall during the intake process.

6. A fully-insulated engine achieves only a modest thermal efficiency benefit (1 percentage point) over a baseline cooled engine. An additional benefit is the increased exhaust enthalpy. Other system configurations (e.g., Rankine compounding) should be considered in addition to, or instead of turbo-compounding to utilize more of this energy.

7. A partially-insulated engine with a cooled liner achieves a slight improvement in thermal efficiency (half a percent) over a fully insulated engine. This gain and the advantage of fewer lubrication problems must be evaluated against the inconvenience of retaining a cooling system.

8. Low-heat-rejection system configurations should be optimized with respect to injection timing and compounded turbine gear ratio in order to maximize the power produced. However, these effects are small (half a percent or less).

9. Incorporation of 5% more efficient turbomachinery components would improve the performance of an insulated engine by one percentage point. In the case of a cooled baseline engine, the gain would be smaller (0.6 percentage points).

10. The assumption of constant wall surface temperatures over the engine cycle is reasonable for conventional engines with cooled metal walls. In contrast, for ceramic insulated components, cyclic surface temperature variations are critical. The lower the thermal conductivity and the lower the

thermal capacity of a material, the higher the wall surface temperature variations, the smaller the degradation in volumetric efficiency and thus the better the thermal efficiency of the overall system.

11. Due to the low thermal diffusivities of ceramic materials, the cyclic transients penetrate into the wall structure for only a limited distance (of the order of 1 mm). The combination of large swings and short penetration depths results in high thermal gradients. Hence, selection of an insulating material involves a trade-off between system performance improvement and component thermal loading.

12. Substantial gains in thermal efficiency (6 percentage points) could only be achieved with truly adiabatic engine operation, i.e., if the wall surface temperatures exactly followed the gas temperatures. This requires that the insulating material has zero conductivity and zero thermal capacity, and therefore it is unlikely to be realized in practice.

13. The degree of insulation achieved with a specific material thickness is not significantly affected by variations in reciprocator speed or load. However, the surface temperature of the material is strongly dependent on reciprocator load.

14. Increasing the thickness of surface insulation, initially results in a rapid increase in the mean temperature of the surface and a corresponding reduction in the heat transfer losses. However, as more insulation is added, the incremental benefits progressively decrease.

15. Thick coatings provide increased insulation but may suffer from fatigue. Introducing an air gap (as small as 0.5 mm) between the ceramic insulation and the metallic base of a component can dramatically reduce the thickness of the coating for the same level of insulation.

REFERENCES

1. Katz, N.R. and Lencoe, E.M., "Ceramics for Diesel Engines: Preliminary Results of a Technology Assessment," Progress Report DOE/AMMRC IAG DE-AE 101-77 CS51017, 1981.
2. Watts, P.A. and Heywood, J.B., "Simulation Studies of the Effects of Turbocharging and Reduced Heat Transfer on Spark-Ignition Engine Operation," SAE Paper 800289, 1980; in The Adiabatic Engine: Past, Present and Future Developments, SAE, pp. 93-111, 1984.
3. Siegla, D. and Amann, C., "Exploratory Study of the Low-Heat-Rejection Diesel for Passenger Car Applications," SAE Paper 840435, 1984, in The Adiabatic Engine: Past, Present and Future Developments, SAE, pp. 113-137, 1984.
4. Kamo, R. and Bryzik, W., "Adiabatic Turbocompound Engine Performance Predictions," SAE Paper 780068, 1978.
5. Kamo, R. and Bryzik, W., "Cummins-TARADCOM Adiabatic Turbocompound Engine Program," SAE paper 810070, 1981.
6. Poulin, E., Demler, R., Krepchin, I. and Walker, D., "Steam Bottoming Cycle for an Adiabatic Diesel Engine," DOE/NASA 0300-1, NASA CR-168255, U.S. Department of Energy, Conservation and Renewable Engine, March 1984.
7. Koplrow, M.D., DiNanno, L.D., and DiBella, F.A., "Status Report on Diesel Organic Rankine Compound Engine for Long-Haul Trucks," Proceedings of the Twentieth Automotive Technology Development Contractors' Coordination Meeting, October 25-28, 1982, pp. 243-258.
8. Griffiths, W.J., "Thermodynamic Simulation of the Diesel Cycle to Show the Effect of Increasing the Combustion Chamber Wall Temperatures on Thermal Efficiency and Heat Rejection", Wellworthy Topics, No. 63, 1976-7.
9. Zapf, H., "Limitations and Possibilities of a Heat Tight Combustion Space in Diesel Engines," VDI Berichte, No. 238, pp. 85-87, 1975.
10. Kamo, R. and Bryzik, W., "Cummins/TACOM Advanced Adiabatic Engine," SAE Paper 840428, 1984; in The Adiabatic Engine: Past, Present and Future Developments, SAE, pp. 3-18, 1984.
11. Wallace, F.J., Way, R.J. and Vollmert, H., "Effect of Partial Suppression of Heat Loss to Coolant on the High Output Diesel Engine Cycle," SAE Paper 790823, 1979; in The Adiabatic Engine: Past, Present and Future Developments, SAE, pp. 139-148, 1984.
12. Watson, N., Kyrtatos, N.P. and Holmes, K., "The Performance Potential of Limited Cooled Diesel Engines," Paper 45/83, Proceedings of Institute of Mechanical Engineers, Vol. 197A, 1983.

13. Sudhakar, V., "Performance Analysis of Adiabatic Engine," SAE Paper 840431, 1984; in The Adiabatic Engine: Past, Present and Future Developments, SAE, pp. 85-92, 1984.
14. Hoag, K.L., Brands, M.C. and Bryzik, W., "Cummins/TACOM Adiabatic Engine Program," SAE Paper 850356, 1985.
15. Toyama, K., Yoshimitsu, T., Nishiyama, T., Shimauchi, T., Nakagaki, T., "Heat Insulated Turbocompound Engine," SAE paper 831345, 1983; in The Adiabatic Engine: Past, Present and Future Developments, SAE, pp. 413-424, 1984.
16. Watson, N. and Janota, M.S., Turbocharging the Internal Combustion Engine, John Wiley & Sons, New York, 1982.
17. Lyn, W.T., "Study of Burning Rate and Nature of Combustion in Diesel Engine," IX Symposium (International) on Combustion, Proceedings, pp. 1069-1082, The Combustion Institute, 1962.
18. Shipinski, J., Uyehara, O.A. and Myers, P.S., "Experimental Correlation Between Rate-of-Injection and Rate-of-Heat-Release in a Diesel Engine," ASME Paper 68-DGP-11, 1968.
19. Watson, N., Pilley, A.D. and Marzouk, M., "A Combustion Correlation for Diesel Engine Simulation," SAE Paper 800029, 1980.
20. Igura, S., Kadota, T., Hirozasu, H., "Spontaneous Ignition Delay of Fuel Sprays in High Pressure Gaseous Environment," Jap. Soc. Mech. Engrs., Vol. 41, No. 345, p. 1559, 1975.
21. Stringer, F.W., Clarke, A.E., Clarke, J.S., "The Spontaneous Ignition of Hydrocarbon Fuels in a Flowing System," Proc. Auto. Div., Institution of Mech. Eng., 1970.
22. Spadaccini, L.J. and TeVelde, J.A., "Autoignition Characteristics of Aircraft-Type Fuels," United Technologies Research Center, NASA report CR-159886, 1980.
23. Hardenberg, H.O. and Hase, F.W., "An Empirical Formula for Computing the Pressure Rise Delay of a Fuel from its Cetane Number and from the Relevant Parameters of Direct-Injection Diesel Engines," SAE paper 790493, SAE Trans., Vol. 88, 1979.
24. Dent, J.C. and Mehta, P.S., "Phenomenological Combustion Model for a Quiescent Chamber Diesel Engine," SAE Paper 811235, 1981.
25. Woschni, G., "A Universally Applicable Equation for the Instantaneous Heat Transfer Coefficient in the Internal Combustion Engine," SAE Paper 670931, SAE Trans., Vol. 76, 1967.
26. Annand, J.D., "Heat Transfer in the Cylinders of Reciprocating Internal Combustion Engines," Proceedings Institute of Mechanical Engineers, Vol. 177, No. 36, 1963.

27. Annand, J.D. and Ma, T.H., "Instantaneous Heat Transfer Rates to the Cylinder Head Surface of a Small Compression-Ignition Engine," Proceedings Institute of Mechanical Engineers, Vol. 185, Second Paper, No. 72, 1971.
28. Sitkei, G., Heat Transfer and Thermal Loading in Internal Combustion Engines, Akademiai Kiado, Budapest, 1974.
29. Kamel, M. and Watson, N., "Heat Transfer in the Indirect Injection Diesel Engine," SAE Paper 790826, 1979.
30. Oguri, T. and Shigewo, I., "Radiant Heat Transfer in Diesel Engines," SAE paper 720023, SAE Trans., Vol. 81, 1972.
31. Kunitomo, T., Matsuoka, K. and Oguri, T., "Prediction of Radiative Heat Flux in a Diesel Engine," SAE Paper 750786, SAE Trans., Vol. 84, 1975.
32. Ebersole, G.D., Myers, P.S., and Uyehara, O.A., "The Radiant and Convective Components of Diesel Engine Heat Transfer," SAE Paper 701C, 1963.
33. Sitkei, G. and Ramanaiah, G.V., "A Rational Approach for Calculation of Heat Transfer in Diesel Engines," SAE Paper 720027, 1972.
34. Overbye, V.D., Bennethum, J.E., Uyehara, O.A., and Myers, P.S., "Unsteady Heat Transfer in Engines," SAE Transactions, Vol. 69, 1961, pp. 461-494.
35. Dent, J.C. and Suliaman, S.J., "Convective and Radiative Heat Transfer in a High Swirl Direct Injection Diesel Engine," SAE Paper 770407, 1977.
36. LeFeuvre, T., Myers, P.S. and Uyehara, O.A., "Experimental Instantaneous Heat Fluxes in a Diesel Engine and Their Correlation," SAE Paper 690464, 1969.
37. Flynn, P., Mizusawa, M., Uyehara, O.A. and Myers, P.S., "An Experimental Determination of the Instantaneous Potential Radiant Heat Transfer Within an Operating Diesel Engine," SAE Paper 720022, 1972.
38. Hottel, H.C. and Broughton, F.P., "Determination of True Flame Temperature and Total Radiation from Luminous Gas Flames," Industrial and Engineering Chemistry, Analytical Edition, Vol. 41932, pp. 166-175.
39. Svehla, R.A. and McBride, B.J., "Fortran IV Computer Program Calculations of Thermodynamic and Transport Properties of Complex Chemical Systems," NASA Technical Note, NASA TN D-7056, 1973.
40. Mansouri, S.H., Heywood, J.B. and Radhakrishnan, K., "Divided-Chamber Diesel Engines, Part 1: A Cycle-Simulation which Predicts Performance and Emissions," SAE Paper 820273, SAE Trans., Vol. 91, 1982.
41. Poulos, S.G. and Heywood, J.B., "The Effect of Chamber Geometry on Spark-Ignition Engine Combustion," SAE paper 830334, SAE Trans., Vol. 92, 1983.
42. Tennekes, M. and Lumley, J.L., A First Course in Turbulence, M.I.T. Press, Cambridge, Mass., 1972.

43. Millington, B.W. and Hartles, E.R., "Frictional Losses in Diesel Engines," SAE paper 680590, SAE Trans., Vol. 77, 1968.
44. Rohsenow, W.M. and Choi, H.Y., Heat, Mass, and Momentum Transfer, Prentice-Hall, Englewood Cliffs, N.J., 1961.
45. Oldfield, S.G., and Watson, N., 'Exhaust Valve Geometry and Its Effect on Gas Velocity and Turbulence in an Exhaust Port', SAE 830151, 1983.
46. Caton, J.A., and Hewwood, J.B., "Models for Heat Transfer, Mixing and Hydrocarbon Oxidation in an Exhaust Port of a Spark-Ignition Engine", SAE Paper 800290, 1980.
47. Boelter, Young, and Iversen, NACA, TN 1451, 1948.
48. Seban, R.A., and McLaughlin, E.F., 'Heat Transfer in Tube Coils', Int. J. Heat-Mass Transfer, Vol. 6, 387-395, 1963.
49. Rogers, C.F., and Mayhew, Y.R., 'Heat Transfer and Pressure Loss in Helically Coiled Tubes', Int. J. Heat-Mass Transfer, Vol. 7, 1207-1216, 1964.
50. Primus, R.J., 'A Second Law Approach to Exhaust System Optimization', SAE 840033, 1984.
51. Streit, E. and Borman, G., "Mathematical Simulation of a Large Turbocharged Two-Stroke Diesel Engine, SAE Paper 710176, 1971.
52. Whitehouse, N.D., "Heat Transfer in a Quiescent Chamber Diesel Engine," Proceedings Institute of Mechanical Engineers, Vol. 185, First Paper, No. 72, 1971.
53. Morel, T., Keribar, R. and Blumberg, P.N., "Cyclical Thermal Phenomena in Engine Combustion Chamber Surfaces," SAE paper 850360, 1985.
54. Crandall, S.H., Engineering Analysis: A Survey of Numerical Procedures, McGraw-Hill, 1956.
55. Levinson, N. and Redheffer, R., Complex Variables, Holden'day Inc., 1970.
56. Dusinberre, G.M., Numerical Analysis of Heat Flow, McGraw-Hill, New York, 1949.
57. Shampine, L.F. and Gordon, M.K., Computer Solution of Ordinary Differential Equations: The Initial Value Problem, Freeman, 1974.
58. Caton, J.A., "Comparison of Thermocouple, Time-Averaged and Mass-Averaged Exhaust Gas Temperatures for a Spark-Ignited Engine," SAE Paper 820050, 1982.
59. Arcoumanis, C., Bicen, A.F. and Whitelaw, J.H., "Effect of Inlet Parameters on the Flow Characteristics in a Four-Stroke Model Engine," SAE Paper 820750, 1982.

60. Witze, O., "A Critical Comparison of Hot-Wire Anemometry and Laser Doppler Velocimetry for I.C. Engine Applications," SAE Paper 800132, SAE Transactions, Vol. 89, 1980.
61. Rask, R.B., "Laser Doppler Anemometer Measurements in an Internal Combustion Engine," SAE Paper 790094, SAE Transactions, Vol. 88, 1979.
62. Liou, T., Hall, M., Santavicca, D.A. and Bracco, F.V., "Laser Doppler Velocimetry Measurements in Valved and Ported Engines," SAE Paper 840375, 1984.
63. Wong, V.W. and Hoult, D.P., "Rapid Distortion Theory Applied to Turbulent Combustion," SAE Paper 790357, SAE Transactions, Vol. 88, 1979.
64. Morel, T., and Keribar, R., "A Model for Predicting Spatially and time Resolved Convective Heat Transfer in Bowl-in-Piston Combustion Chambers," SAE paper 850204, 1985.
65. Reynolds, W.C., "Modeling of Fluid Motion in Engines - An Introductory Overview," Combustion Modeling in Reciprocating Engines, Editors Mattavi, J.N. and Amann, C.A., pp. 69-124, Plenum Press, 1980.
66. Dent, J.C. and Salama, N.S., "The Measurement of the Turbulence Characteristics in an Internal Combustion Engine Cylinder," SAE Paper 750886, 1975.
67. Lancaster, D.R., "Effects of Engine Variables on Turbulence in a Spark-Ignition Engine," SAE Paper 760159, SAE Transactions, Vol. 85, 1976.
68. Wakisaka, T., Hamamoto, Y. and Kinoshita, S., "The Measurement of Turbulent Flow in the Combustion Chamber of an I.C. Engine," JSAE Review, Vol. 3, pp. 9-16, 1980.
69. French, C.C., "Ceramics in Reciprocating Internal Combustion Engines," SAE Paper 841135, 1984.
70. Cawley, J.D., "Overview of Zirconia with Respect to Gas Turbine Applications," NASA Technical Paper 2286, NASA Lewis Research Center, 1984.
71. Parker, D.A. and Smart, R.F., "An Evaluation of Silicon Nitride Diesel Pistons," The Mechanical Engineering Properties and Applications of Ceramics, Ed. Godfrey, D.J., Proceedings of the British Ceramic Society, pp. 167-181, 1978.
72. Bryzik, W. and Kamo, R., "TACOM/Cummins Adiabatic Engine Program," SAE paper 830314, 1983.
73. Cole, R.M. and Alkidas, A.C., "Evaluation of an Air-Gap-Insulated Piston in a Divided-Chamber Diesel Engine," SAE Paper 850359, 1985.
74. Hires, S.D., Ekchian, A., Heywood, J.B., Tabaczynski, R.J. and Wall, J.C., "Performance and NO_x Emissions Modelling of a Jet Ignition Prechamber Stratified Charge Engine," SAE Paper 760161, 1976.

75. Martin, M.K. and Heywood, J.B., "Approximate Relationships for the Thermodynamic Properties of Hydrocarbon-Air Combustion Products," *Combustion Science and Technology*, Vol. 15, pp. 1-10, 1977.
76. Rossini, F.D., Pitzer, K.S., Arnett, R.L., Braun, R.M. and Primentel, G.C., Selected Values of Physical and Thermodynamic Properties of Hydrocarbons and Related Compounds, Carnegie Press, Pittsburgh, PA, 1953.
77. Stull, D.R. and Prophet, H., JANAF Thermochemical Tables, Second Edition, National Bureau of Standards Publication, NSRDS-NBS 37, 1971.
78. Mansouri, S.H. and Heywood, J.B., "Correlations for the Viscosity and Prandtl Number of Hydrocarbon-Air Combustion Products," *Combustion Science and Technology*, Vol. 23, pp. 251-256, 1980.
79. Carslaw, H.S. and Jaeger, J.C., Conduction of Heat in Solids, Oxford University Press, London, Second Edition, 1959.

TABLE 1

Appropriate Heat Release Profile Constants
For Different Engine Designs

<u>ENGINE</u>	<u>A</u>	<u>B</u>	<u>C</u>
a	0.296	0.95	0.81
b	0.37	0.41	0.28
c	0.26	0.28	0.51
k_1	14.2	16.67	7.54
k_2	0.644	0.6	0.65
k_3	0.79	1.2	0.93
k_4	0.25	0.13	0.22

Engine A: 6-cylinder, in-line, turbocharged, 4 stroke, DI, with inlet port swirl generation, and deep bowl combustion chamber.

Engine B: V8, turbocharged and intercooled, DI, 4 stroke, diesel engine.

Engine C: Turbocharged and intercooled, but more highly rated than engine A or B.

Source: Ref. [19]

TABLE 2

Constants for Arrhenius Equation
for Ignition Delay [ms]

Fuel	A	n	E/R Kelvins	Ref.
diesel	3.45	1.02	2100	[19]
diesel	53.5	1.23	676.5	[20]
n-cetane	0.872	1.24	4050	[20]
n-heptane	0.748	1.44	5270	[20]
diesel	4.05×10^{-2}	0.757	5470	[21]
diesel	2.43×10^{-6}	2	20915.3	[22]
kerosene	1.68×10^{-5}	2	19008.7	[22]
cetane	4.04×10^{-10}	2	25383	[22]

TABLE 3

Relative Importance of Radiant Heat Flux

<u>Engine</u>	<u>Load Range</u>	\dot{Q}_r/\dot{Q}_w <u>Peak Values</u>	\dot{Q}_r/\dot{Q}_w <u>Mean Values</u>	<u>Ref.</u>
DI, 4 stroke	Mid-Full	9-15	10-30	[30]
DI, 2 stroke	Full		35-45	[32]
Prechamber	Idle-Full		7-23	[33]
DI, swirl	Light-Full		0-40	[34]
DI, swirl 4 stroke	80%-Full	12-18		[35]
DI, swirl 4 stroke	Light-Full	70-13	21-14	[36] [37]

TABLE 4
Engine Parameters

Bore	5.5 in
Stroke	6.0 in
Connecting rod length	12.0 in
Compression ratio	14.5
Number of cylinders	6
Engine swept volume	14.0 l
Intake manifold volume	5.5 l
Exhaust manifold volume	7.8 l
Injection timing	10 deg. BTC
Valve timings:	
Intake valve opens (IVO)	11 deg. BTC
Intake valve closes (IVC)	32 deg. ABC
Exhaust valve opens (EVO)	35 deg. BBC
Exhaust valve closes (EVC)	16 deg. ATC

TABLE 5

Calibration of Diffusion-Burning Shape Factor k_3

	*		
	Data	$k_3=0.79$	$k_3=1.05$
<u>Reciprocator</u>			
Peak cyl. pressure (atm)	121.7	153.7	123.7
Brake MEP (psi)	198.1	211.1	199.6
Brake SFC (lb/bhp-hr)	0.349	0.327	0.346
<u>Compressor</u>			
Mass flow (lb/min)	76.1	72.6	75.2
Speed (RPM)	64,800	63,175	65,193
Pressure ratio	2.66	2.53	2.63
<u>System</u>			
Diesel brake power (bhp)	406.7	433.6	410.1
Power turbine brake power (bhp)	45.9	42.8	46.9
Overall brake SFC (lb/bhp-hr)	0.313	0.298	0.310

*

Data obtained from Cummins Engine Company

TABLE 6

Comparison of Predictions with Data
Speed = 1900 RPM, Fuel Rate = 2.35 lb/min

	Pressure, atm	
	Data	Predictions
Compressor Inlet	0.94	0.94
Compressor Discharge	2.49	2.47
Intake Manifold	2.44	2.44
Exhaust Port	2.92	3.17
Turbine Inlet	3.04	3.16
Turbine Outlet	1.56	1.56
Power Turbine Inlet	1.57	1.54
Power Turbine Outlet	1.04	1.00

	Temperature, K	
	Data	Predictions
Compressor Inlet	303	303
Compressor Discharge	429	428
Intake Manifold	318	319
Exhaust Port	831	871
Turbine Inlet	864	853
Turbine Outlet	739	747
Power Turbine Inlet	---	737
Power Turbine Outlet	---	677

*
Data obtained from Cummins Engine Company

TABLE 7

Effect of Variation of Combustion Chamber
Surface Temperature on System Performance

Wall Temperature (K)	400	600	800	900	Adiabatic
Reduction in Heat Loss (%)	Base	40	77	96	100
<u>Reciprocator</u>					
Heat Transfer to Walls					
(% of Heat Input)	15.4	9.3	3.5	0.6	0
Mean Exhaust Temp. (K)	854	898	944	967	908
Int. Volumetric Eff. (%)*	92.9	85.3	79.0	76.3	94.5
Atm. Volumetric Eff. (%)**	218.1	214.0	209.3	207.1	240.2
Peak Cyl. Pressure (atm)	142.5	144.0	145.0	145.4	156.1
Pumping MEP (atm)	-1.15	-0.97	-0.79	-0.71	-1.30
Gross IMEP (atm)	16.56	16.48	16.41	16.38	18.25
Brake MEP (atm)	13.76	13.86	13.97	14.02	15.30
Gross Ind. Eff. (%)	48.6	48.4	48.2	48.1	53.6
Brake Thermal Eff. (%)	40.4	40.7	41.0	41.1	44.9
<u>Compressor</u>					
Boost Pressure Ratio	2.542	2.713	2.871	2.942	2.819
Mass Flow (kg/s)	0.527	0.517	0.506	0.500	0.581
Rotor Speed (RPM)	63,370	64,308	65,226	65,702	69,081
<u>System</u>					
Diesel Brake Power (hp)	415.3	418.3	421.5	423.0	461.8
P/Turbine Brake Power (hp)	44.3	45.0	45.3	45.4	57.1
P/Turbine Exhaust Temp (K)	670	700	731	747	723
Overall Brake Eff. (%)	44.7	45.1	45.4	45.6	50.5

*Volumetric efficiency based on intake manifold conditions.

**Volumetric efficiency based on atmospheric conditions.

TABLE 8

Effect of Variation of Liner Temperature on System Performance
(with Piston and Cylinder Head Temperatures at 800 K)

Liner Temperature (K)	450	500	550	600	700	800
Reduction in Heat Loss (%)	52	56	59	63	70	77
<u>Reciprocator</u>						
Heat Transfer to Walls (% of Heat Input)	7.4	6.8	6.3	5.7	4.6	3.5
Mean Exhaust Temp. (K)	899	904	912	917	932	944
Int. Volumetric Eff. (%)	84.9	84.0	83.1	82.3	80.6	79.0
Atm. Volumetric Eff. (%)	215.1	215.1	213.6	213.0	210.6	209.3
Peak Cyl. Pressure (atm)	144.7	145.2	144.9	145.0	144.7	145.0
Pumping MEP (atm)	-0.95	-0.94	-0.91	-0.88	-0.84	-0.79
Gross IMEP (atm)	16.62	16.60	16.56	16.54	16.47	16.41
Brake MEP (atm)	14.02	14.01	14.00	14.01	13.98	13.97
Gross Ind. Eff. (%)	48.8	48.7	48.6	48.5	48.4	48.2
Brake Thermal Eff. (%)	41.2	41.1	41.1	41.1	41.0	41.0
<u>Compressor</u>						
Boost Pressure Ratio	2.744	2.769	2.779	2.799	2.830	2.871
Mass Flow (kg/s)	0.520	0.520	0.516	0.515	0.509	0.506
Rotor Speed (RPM)	64,614	64,790	64,749	64,816	64,977	65,226
<u>System</u>						
Diesel Brake Power (hp)	423.3	422.8	422.7	422.7	422.0	421.5
P/Turbine Brake Power (hp)	45.5	45.8	45.4	45.3	45.3	45.3
P/Turbine Exhaust Temp (K)	701	703	709	713	722	731
Overall Brake Eff. (%)	45.6	45.6	45.5	45.5	45.4	45.4

TABLE 9

Effect of 5% Higher Turbomachinery Component Efficiencies
on the Performance of a Partially Insulated System Configuration*

Upgraded Component	Base	Comp.	Trb.	P/Trb.	All
<u>Reciprocator</u>					
Heat Transfer to Walls					
(% of Heat Input)	7.4	7.2	7.3	7.4	7.1
Mean Exhaust Temp. (K)	899	884	885	899	871
Int. Volumetric Eff. (%)	84.9	85.0	85.0	84.9	85.1
Atm. Volumetric Eff. (%)	215.1	221.8	221.6	215.1	229.0
Peak Cyl. Pressure (atm)	144.7	148.2	148.2	144.7	152.1
Pumping MEP (atm)	-0.95	-0.96	-0.95	-0.94	-0.96
Gross IMEP (atm)	16.62	16.68	16.67	16.62	16.73
Brake MEP (atm)	14.02	14.07	14.07	14.03	14.12
Gross Ind. Eff. (%)	48.4	49.0	49.0	48.4	49.2
Brake Thermal Eff. (%)	41.2	41.4	41.4	41.2	41.5
<u>Turbomachinery</u>					
Boost Pressure Ratio	2.744	2.832	2.832	2.741	2.927
Intake Air Flow (kg/s)	0.520	0.537	0.536	0.520	0.553
Rotor Speed (RPM)	64,614	66,194	66,226	64,554	67,958
Compressor Efficiency (%)	79.1	82.2	78.3	79.2	81.3
Turbine Efficiency (%)	77.6	77.3	81.2	77.6	80.3
Power Turbine Efficiency (%)	79.3	79.2	79.4	83.2	83.2
<u>System</u>					
Diesel Brake Power (hp)	423.4	424.7	424.8	423.5	426.2
P/Turbine Brake Power (hp)	45.5	46.9	46.5	47.5	50.7
P/Turbine Exhaust Temp (K)	701	688	683	699	667
Overall Brake Eff. (%)	45.6	45.9	45.9	45.9	46.5

*Piston and cylinder head surface temperatures at 800 K, liner at 450 K.

TABLE 10

Sensitivity of Performance Gains Due to More
Efficient Turbomachinery to Degree of Insulation

	Cooled *		Partially Insulated **	
	Base	Upgraded	Base	Upgraded
Int. Volumetric Eff.(%)	92.9	93.0	84.9	85.1
Atm. Volumetric Eff.(%)	218.1	229.7	215.1	229.0
Diesel Brake Power (hp)	415.3	417.1	423.4	426.2
P/Turbine Brake Power (hp)	44.3	48.8	45.5	50.7
P/Turbine Exhaust Temp.(K)	670	640	701	667
Overall Brake Eff. (%)	44.7	45.3	45.6	46.5

* Combustion chamber surface temperature at 400 K.

** Same as for Table 9, achieves 50% reduction in heat loss over baseline.

TABLE 11

Effect of Wall Surface Temperature Cyclic Variations
on System Performance

Wall Conduction Models	Cooled		Partially-Insulated	
	Steady	Transient	Steady	Transient
<u>Reciprocator</u>				
Heat Transfer to Walls (% of Heat Input)	13.7	13.7	7.6	7.7
Mean Exhaust Temp. (K)	861	864	895	889
Volumetric Eff. (%) (Intake ; Atmospheric)	90.9 218.5	91.0 218.1	85.2 216.0	86.2 217.3
Peak Cyl. Pressure (atm)	145.7	145.4	147.2	147.9
Pumping MEP (atm)	-1.10	-1.11	-0.95	-1.00
Gross IMEP (atm)	16.56	16.57	16.64	16.78
Brake MEP (atm)	13.80	13.80	14.03	14.13
Gross Ind. Eff. (%)	48.6	48.6	48.8	49.3
Brake Thermal Eff. (%)	40.5	40.5	41.2	41.5
<u>Compressor</u>				
Boost Pressure Ratio	2.600	2.592	2.740	2.731
Mass Flow (kg/s)	0.528	0.527	0.522	0.525
Rotor Speed (RPM)	63,867	63,773	64,612	64,745
<u>System</u>				
Diesel Brake Power (hp)	416.7	416.6	423.5	426.4
P/Turbine Brake Power (hp)	45.1	45.0	45.6	46.2
P/Turbine Exhaust Temp (K)	674	674	698	697
Overall Brake Eff. (%)	44.9	44.9	45.6	46.0

TABLE 12

PROPERTIES OF SELECTED MATERIALS FOR ENGINE APPLICATIONS

Material	Conductivity (k) W/m°C	Density (ρ) kg/m ³ x 10 ³	Specific Heat (Cp) J/kg °C	Temperature Fluctuation Factor $\sqrt{\rho C_p}$	Expansion (α) °C ⁻¹ x 10 ⁶	Strength N/m ² x 10 ⁶	Youngs Modulus N/m ² x 10 ⁹	Poisson Ratio	Webull Modulus	Equivalent Tensile Strength N/m ² x 10 ⁶	Fracture Toughness (K _{1c})	Fracture for $a=10^{-4}$ N/m ² x 10 ⁶	Allowable working Stress (MPa)	Hardness (Brinell) (K-Knoop)
Cast Iron (17)	54.4	7.2	480	13715	12	262 (UTS)	117			262			65	240
Steel (EN 32)	50.2	7.87	485	13842	13	586 (UTS)	206	0.27		586			141	450-650
Nimonic (80A)	12.1	8.2	461	6763	13	1100 (UTS)	200			1100			330	200-370
Aluminium (LM27)	155	2.75	915	19749	21	150 (UTS)	71	0.32		150			45	100-150
Hot Pressed Silicon Nitride	25	3.19	710	7524	2.8	840 (3F)	310		15-20	486	5	350	54-108	1800
Reaction Bonded Silicon Nitride	5-10	2.5	710	4213	2.8	220 (3F)	164		15	120	2.3	133-175	14-28	1000
Syalon	18-20	3.2	710	6793	3.0	862 (3F)	288	0.23	10	452	7.7	350	53-106	2000
Reaction Sintered Silicon Carbide	20°C 104 600°C 39	2.98	710 1087	14869 11211	3.4	383 (4F)	332	0.13	10	209	4.9	343	30-60	1860(K)
Alpha Silicon Carbide	20°C 87 600°C 49	3.14	669 1120	13526 13179	4.0	459 (4F)	406	0.14	12.3	276	4.6	322	36-72	2800(K)
Partially Stabilised Zirconia	2.0	5.78	543	2505	10.6	610 (4F)	200	0.3			9.5 4.6	665 322	49-98	1200(K)
Sprayed Zirconia	1.16	5.20	732	2100	8.0									400
Aluminium Oxide	2-73	3.3	1172	3251	8	380	360	0.27	10		585	409	25-50	1600
Sintered Silicon Nitride						742 385			21 12					

Source: Ref. [69]

TABLE 13

THERMAL LOADING OF SELECTED MATERIALS* FOR
ENGINE APPLICATIONS

Material	Thermal Diffusivity, α [$\times 10^{-6}$ m ² /s]	Skin Depth, δ [mm]	$\sqrt{\alpha/\delta}$ [\sqrt{s}]	Peak Temperature Swings, [K]
Plasma-Sprayed Zirconia**	0.545	0.51	1.447	235
Sprayed Zirconia	0.315	0.39	1.438	95
Reaction Bonded Silicon Nitride	2.817	1.16	1.447	70
Cast Iron	15.741	2.75	1.442	18

* Except otherwise noted, material properties taken from Table 12.

** Material properties taken from [70].

TABLE 14

EFFECT OF INSULATING THICKNESS OF ZIRCONIA
ON DEGREE OF INSULATION

Insulating* Thickness, mm	1	3	6	8
Effective Heat Transfer Coeff., W/m-k	983	373	193	146
Mean Piston/Head Surface Temp, K	650	800	881	908
Mean Liner** Surface Temp, K	434	435	436	436
% Reduction in Heat Loss	32	49	58	63

* Assumed to be applied on cylinder head and piston, backed by 10 mm of cast-iron.

** The liner is non-insulated, 7 mm thick cast-iron, with forced cooling.

TABLE 15

EFFECT OF VARIOUS THICKNESSES OF AIR-GAP* ON DEGREE OF INSULATION

Air-gap thickness,** mm	0	0.5	1.0
Effective Heat Transfer Coeffi., W/m-K	441	37	19
Mean Piston/Head Surface Temp., K	776	984	998
Mean Liner Surface Temp., K	435	437	437
% Reduction in Heat Loss	46	70	73

* Assumed that $K_{\text{air-gap}} = 0.02 \text{ W/m-K}$.

** Assumed that air-gap separates a 2.5 mm zirconia coating ($k = 1.2 \text{ W/m-K}$) from the 10 mm cast-iron base ($k = 54 \text{ W/m-K}$). The liner is not insulated.

TABLE A-1
Burned Gas Composition under 1000 K

i	Species	x_i (moles/mole O_2 reactant)	
		$\phi \leq 1$	$\phi > 1$
1	CO_2	$\epsilon\phi$	$\epsilon\phi - C$
2	H_2O	$2(1-\epsilon)\phi$	$2(1-\epsilon\phi) + C$
3	CO	0	C
4	H_2	0	$2(\phi-1) - C$
5	O_2	$1-\phi$	0
6	N_2	ψ	ψ
	Sum	$(1-\epsilon)\phi + 1 + \psi$	$(2-\epsilon)\phi + \psi$

Source: Ref. [74]

TABLE A-2

Coefficients for Polynomial Fit to Thermodynamic Properties

Coefficients for $100 \text{ K} < T \leq 500 \text{ K}$:

i	Species	a_{i1}	a_{i2}	a_{i3}	a_{i4}	a_{i5}	a_{i6}^*
1	CO ₂	4.7373	16.653	-11.232	2.8280	.006767	-93.75793
2	H ₂ O	7.8097	-.20235	3.4187	-1.1790	.001436	-57.08004
3	CO	6.9739	-.82383	2.9420	-1.1762	.0004132	-27.19597
4	H ₂	6.9919	.16170	-.21821	.29682	-.016252	-.118189
5	O ₂	6.2957	2.3884	-.031479	-.32674	.004359	.103637
6	N ₂	7.0922	-1.2958	3.2069	-1.2022	-.0003458	-.013967

Coefficients for $500 \text{ K} < T \leq 6000 \text{ K}$:

i	Species	a_{i1}	a_{i2}	a_{i3}	a_{i4}	a_{i5}	a_{i6}^*
1	CO ₂	11.940	2.0886	-.47029	.037363	-.58945	-97.1418
2	H ₂ O	6.1391	4.6078	-.93560	.066695	.033580	-56.62588
3	CO	7.0996	1.2760	-.28775	.022356	-.15987	-27.73464
4	H ₂	5.5557	1.7872	-.28813	.019515	.16118	.76498
5	O ₂	7.8658	.68837	-.031944	-.0026870	-.20139	-.893455
6	N ₂	6.8078	1.4534	-.32899	.025610	-.11895	-.331835

* picked to give enthalpy datum at 0 K

Source: Ref. [74]

TABLE B-1

Coefficients for Polynomial Fit
to Fuel Vapor Data from 300 to 1500 K

Fuel	A ₁	A ₂	A ₃	A ₄	A ₅	A ₆
C ₁₂ H ₂₆	-2.2294	277.87	-157.08	34.555	0.1970	-79.304
C ₁₃ H ₂₈	-2.1801	300.14	-169.86	37.398	0.2105	-85.098
C ₁₀ H ₂₀	-12.482	244.84	-142.04	31.844	0.0474	-56.788
C ₁₁ H ₂₂	-13.607	270.54	-158.25	35.806	0.0986	-62.192
C ₁₀ H ₁₄	-5.7610	196.29	-118.07	27.238	-.0483	-9.5171
C ₁₁ H ₁₆	-4.8244	215.96	-128.28	29.245	-.0630	-15.586
C _{10.84} H _{18.68}	-9.1063	246.97	-143.74	32.329	0.0518	-41.166

Source: Ref. [76]

TABLE B-2

Fuel Analysis of No. 2 Diesel Fuel

Carbon	86.47	% by weight
Hydrogen	12.41	% by weight
Average Molecular Weight	149.0	
Specific Gravity at 60 F	0.8480	
Lower Heating Value	42,910.0	kJ/kg
Paraffins (straight chain)	21.18	% by volume
Olefins	1.8	% by volume
Aromatics	25.22	% by volume
Monocycloparaffins (ring compound)	26.863	% by volume
Dicycloparaffins (ring compound)	16.919	% by volume
Indans and Tetralins	9.815	% by volume
Sulfur	0.31	% by weight

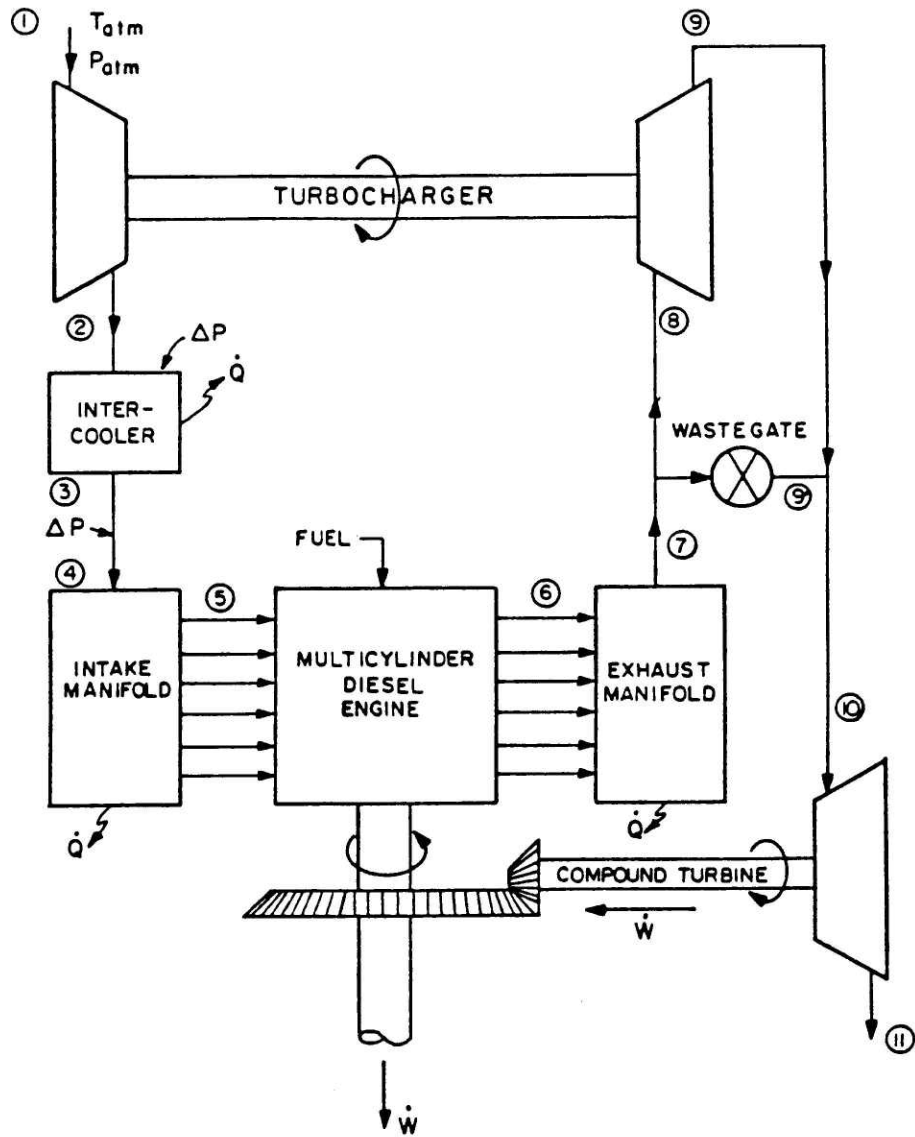


Figure 1. Turbocompounded diesel system configuration.

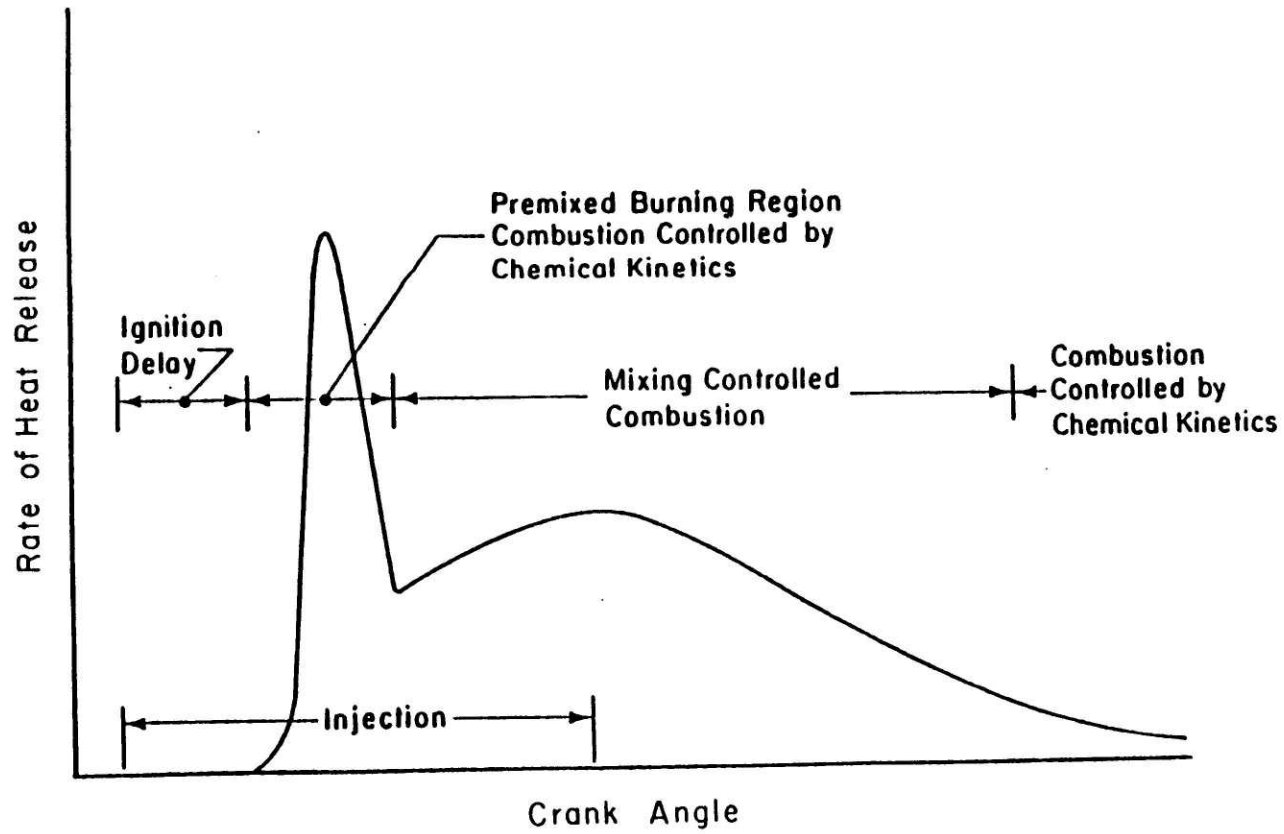


Figure 2. Typical rate of heat release diagram for a direct injection diesel engine.

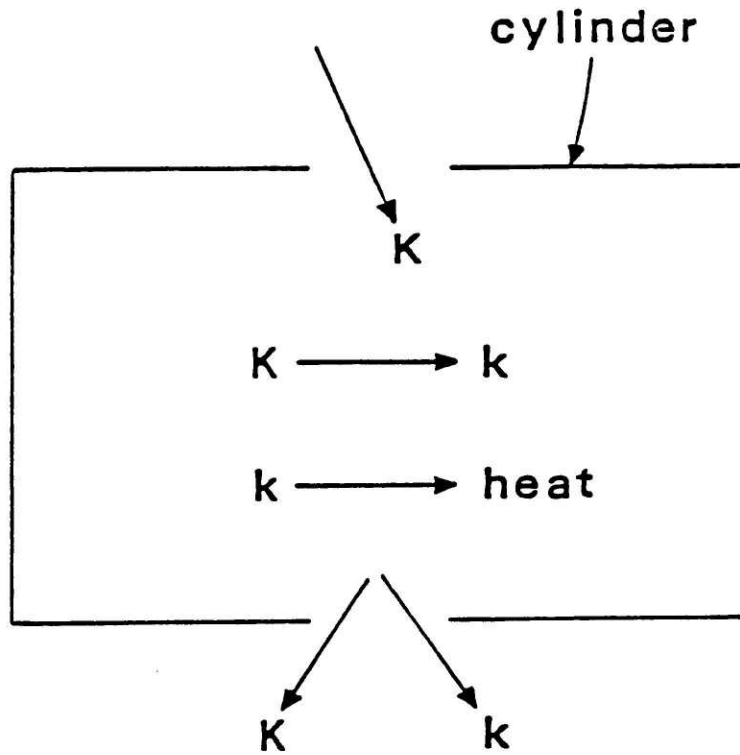


Figure 3. Turbulent energy cascade model. K: mean kinetic energy; k: turbulent kinetic energy.

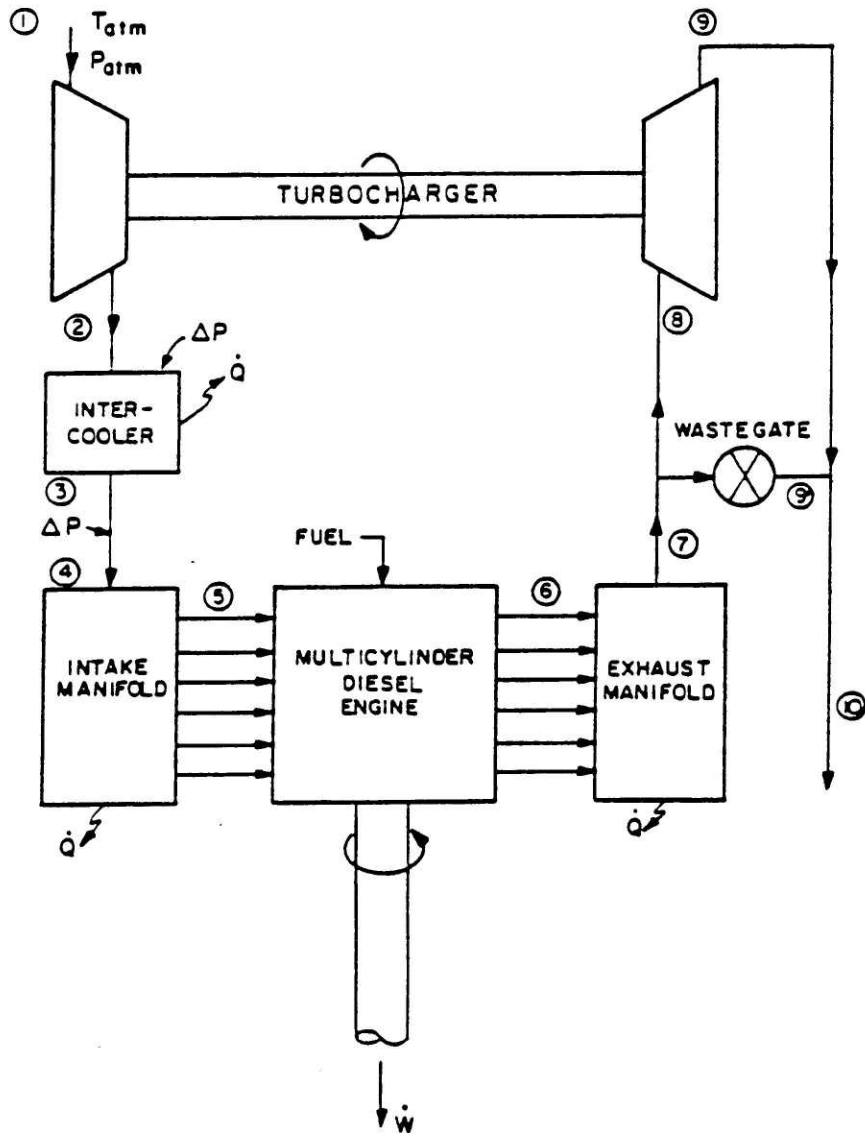


Figure 4. Single-stage turbocharged system configuration.

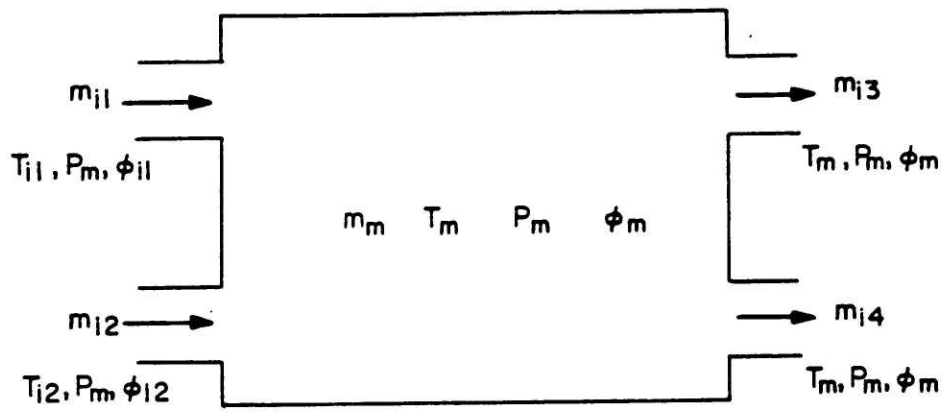


Figure 5. Generalized manifold open system.

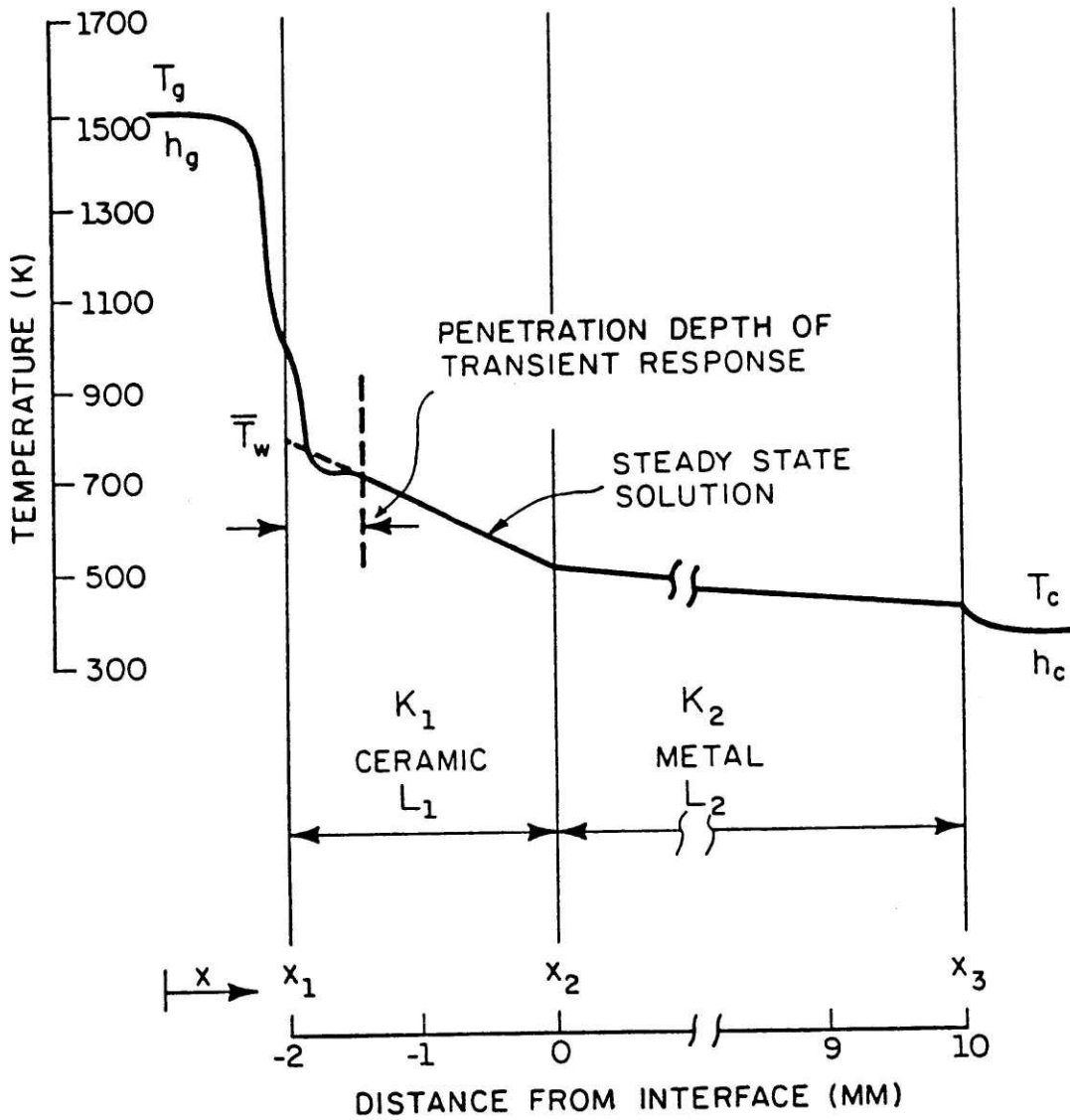


Figure 6. Typical temperature distribution within a ceramic/metal composite wall structure in the engine combustion chamber.

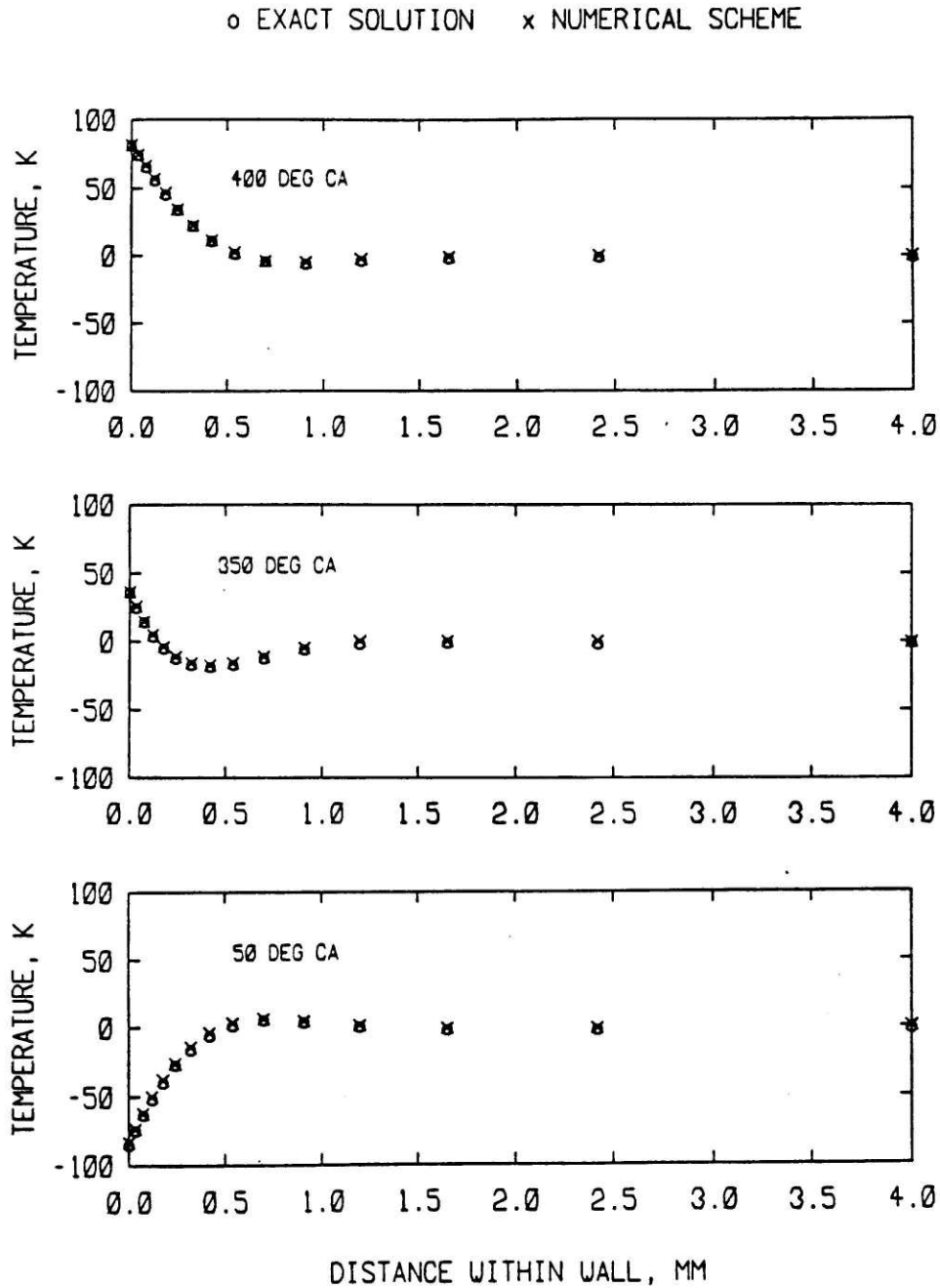


Figure 7. Comparison of exact and numerical solutions for the temperature profile in a 4 mm ceramic coating (with $k = 1 \text{ W/m-k}$ and $\alpha = 0.5 \times 10^{-5} \text{ m}^2/\text{s}$) exposed to a specified harmonically-varying gas temperature.

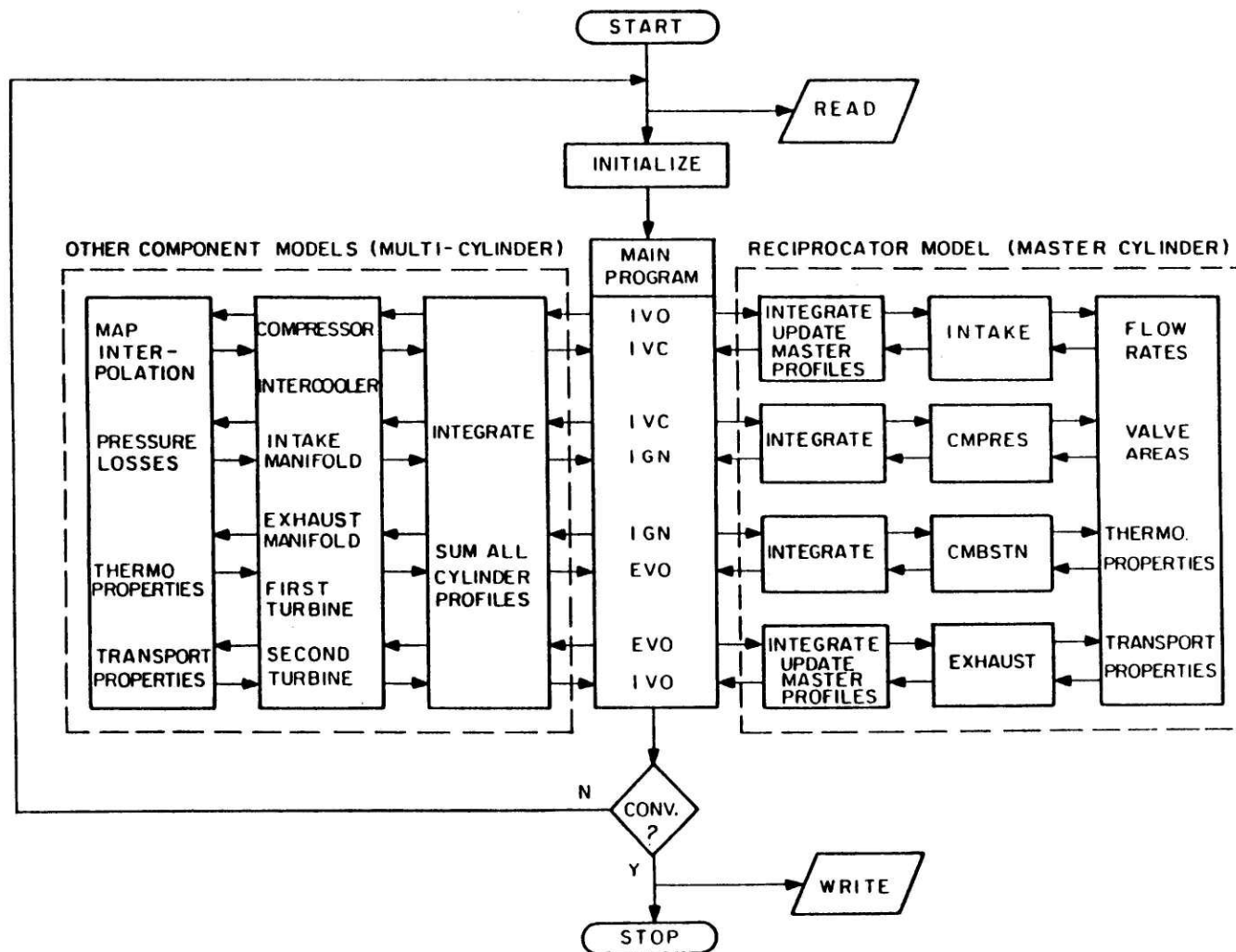


Figure 8. Flowchart of simulation program.

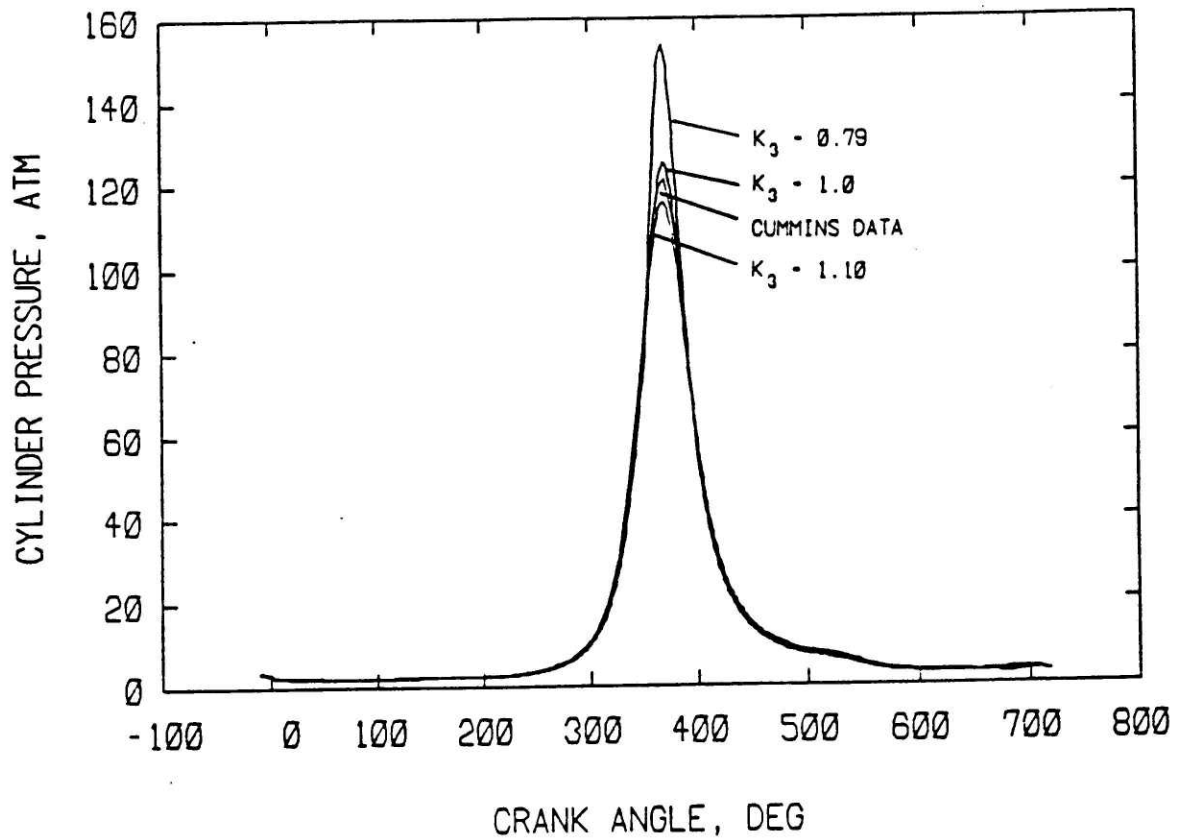


Figure 9. Comparison between cylinder pressure diagrams calculated for different values of the constant k_3 (used in the calculation of the diffusion burning shape factor C_{d2}) against experimental pressure trace obtained from Cummins.

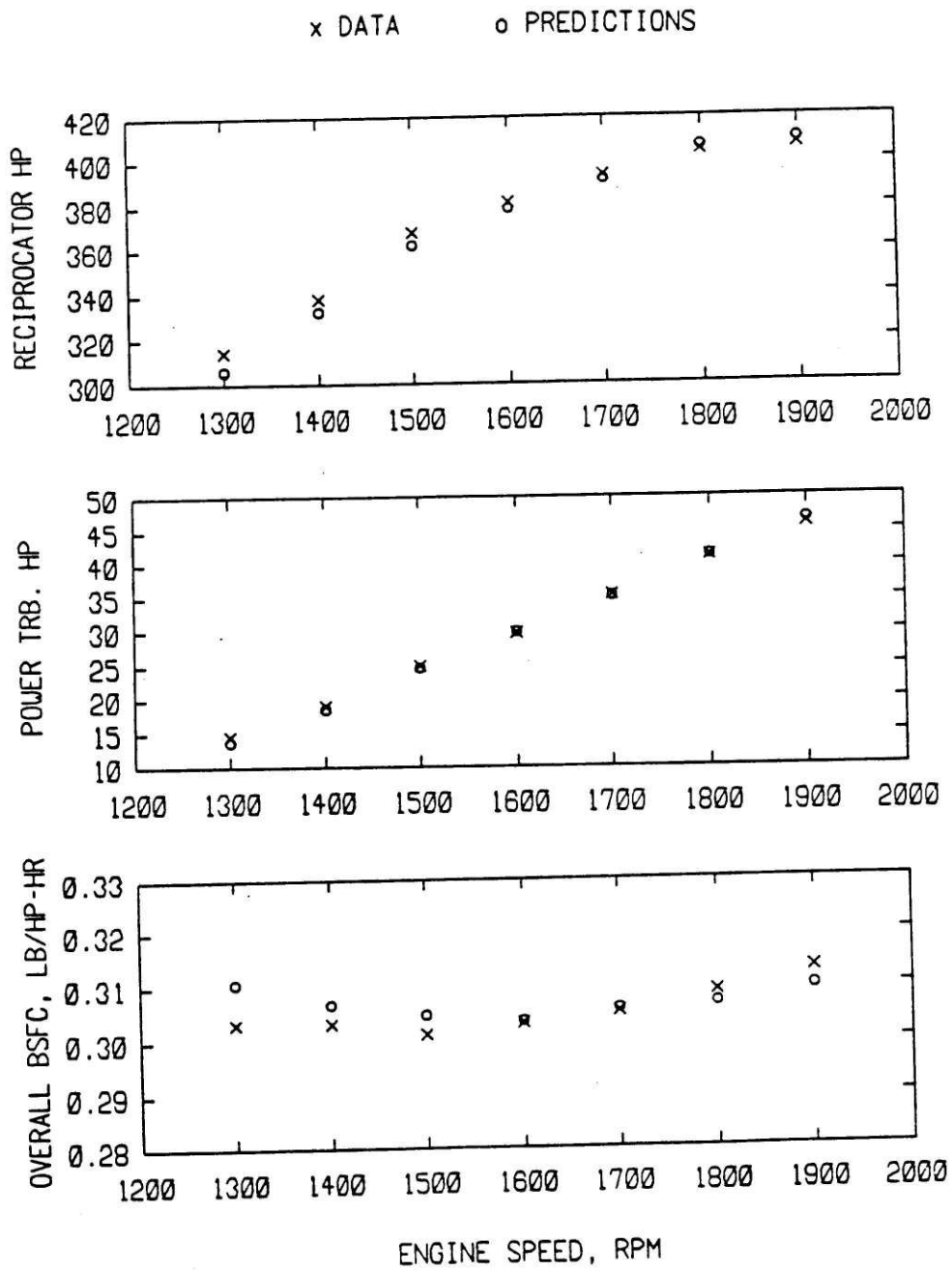


Figure 10. Measured and predicted reciprocator brake power, power turbine brake power and overall brake specific fuel consumption as a function of reciprocator brake speed for constant load operation.

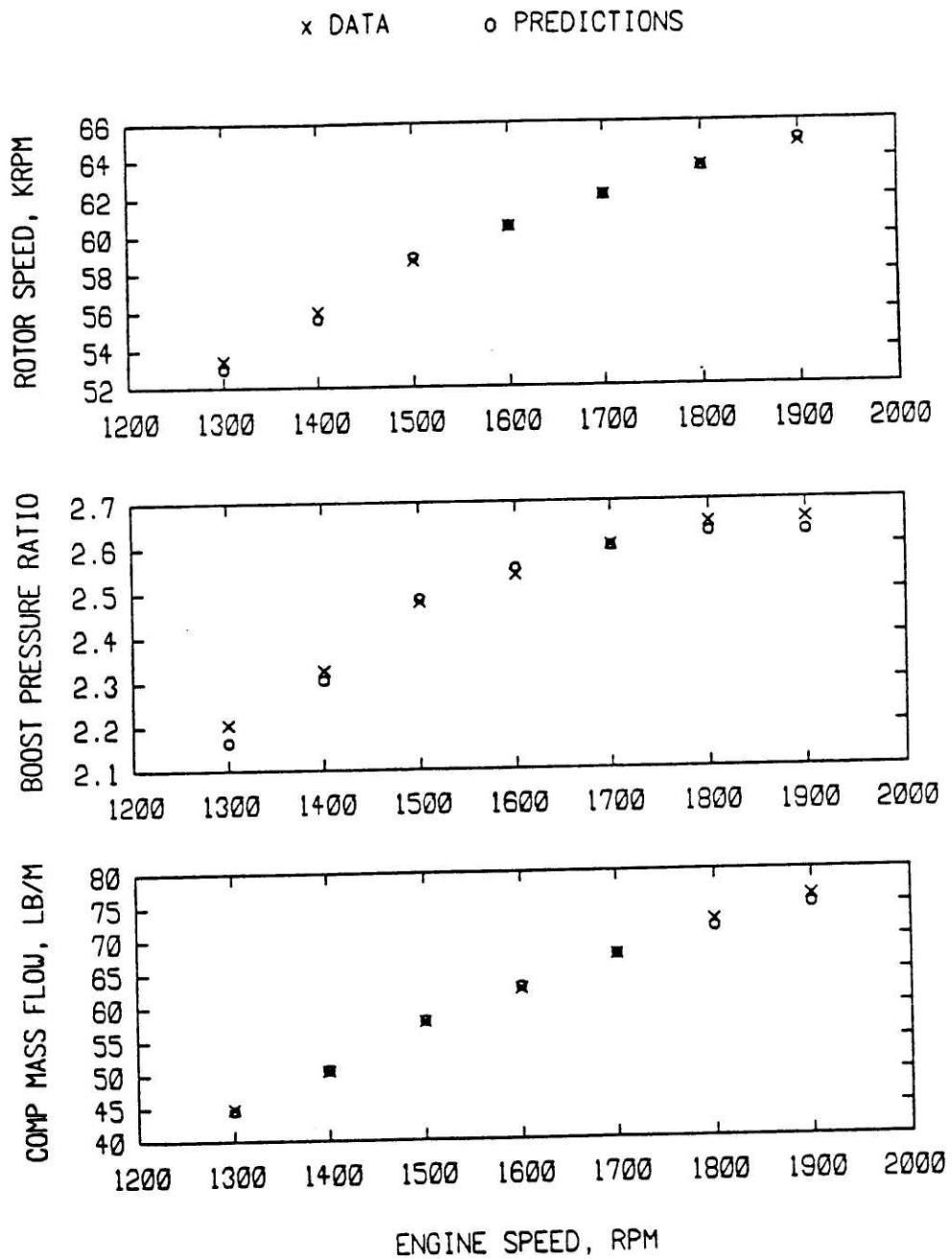


Figure 11. Measured and predicted turbocharger rotor speed, boost pressure ratio and mass flow through the compressor as a function of reciprocator speed for constant load operation.

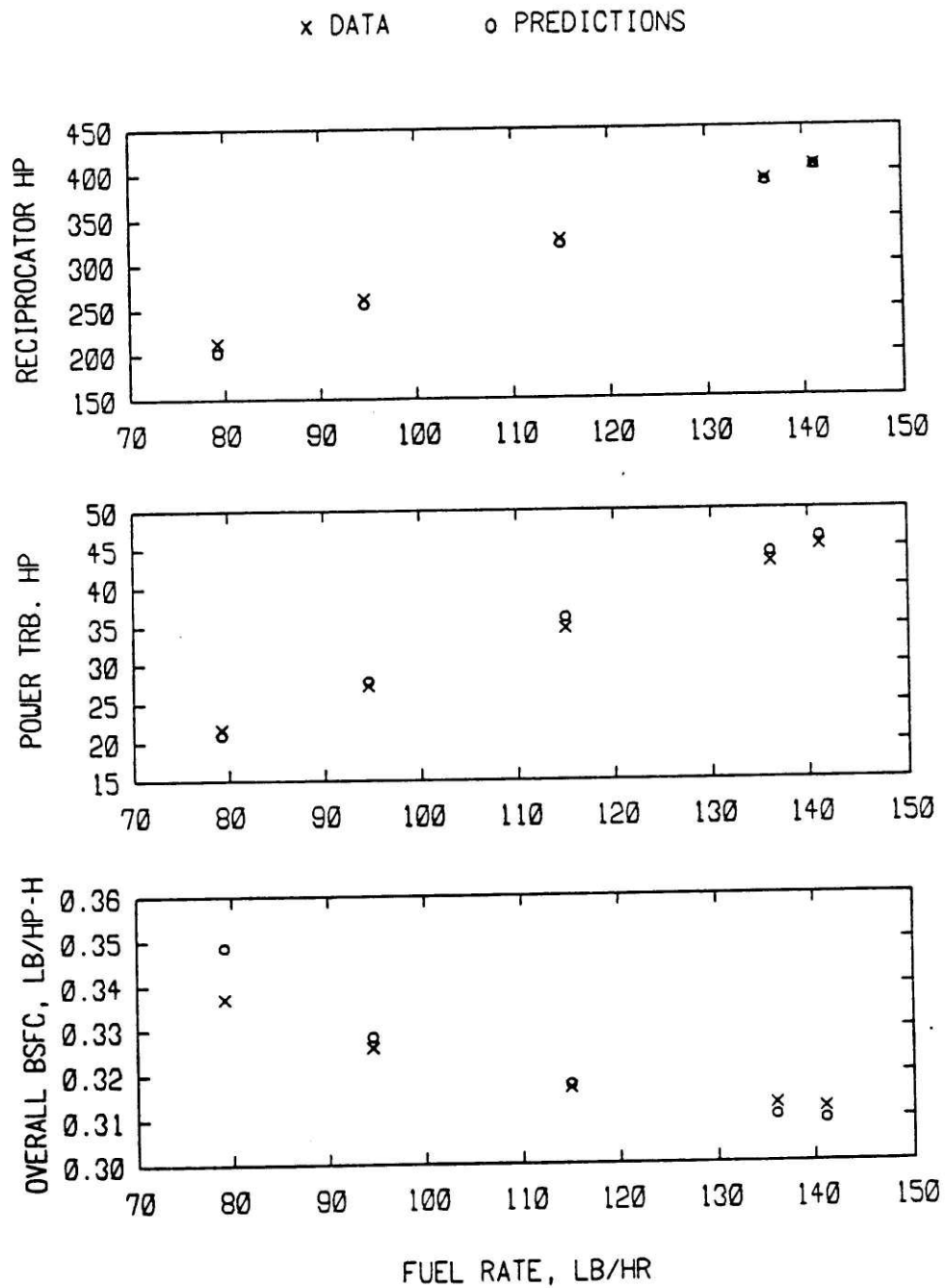


Figure 12. Measured and predicted reciprocator brake power, power turbine brake power and overall brake specific fuel consumption as a function of fueling rate (i.e., reciprocator load) for operation at a constant speed of 1900 RPM.

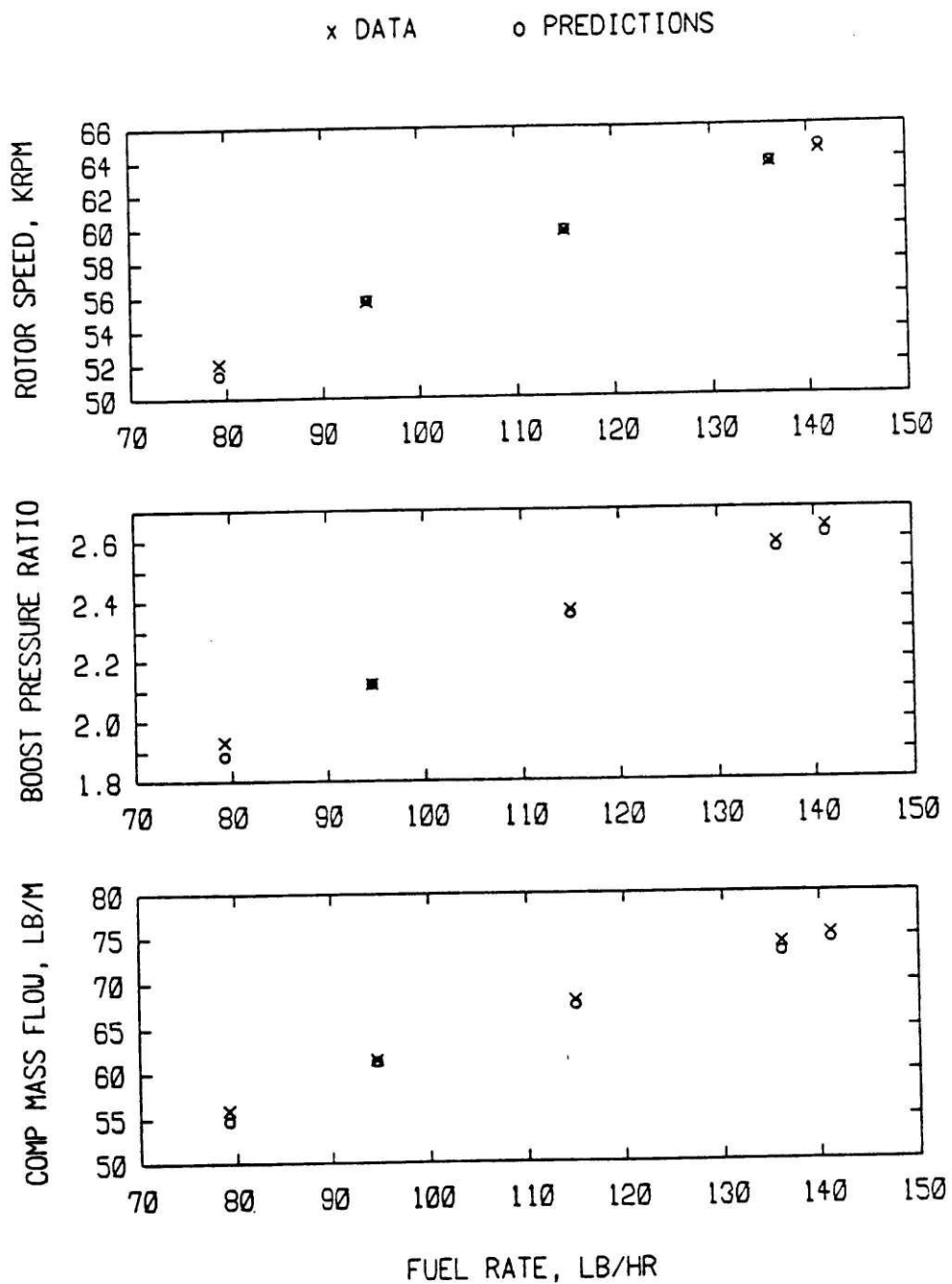


Figure 13. Measured and predicted turbocharger rotor speed, boost pressure ratio and mass flow through the compressor as a function of fueling rate (i.e., reciprocator load) for operation at a constant speed of 1900 RPM.

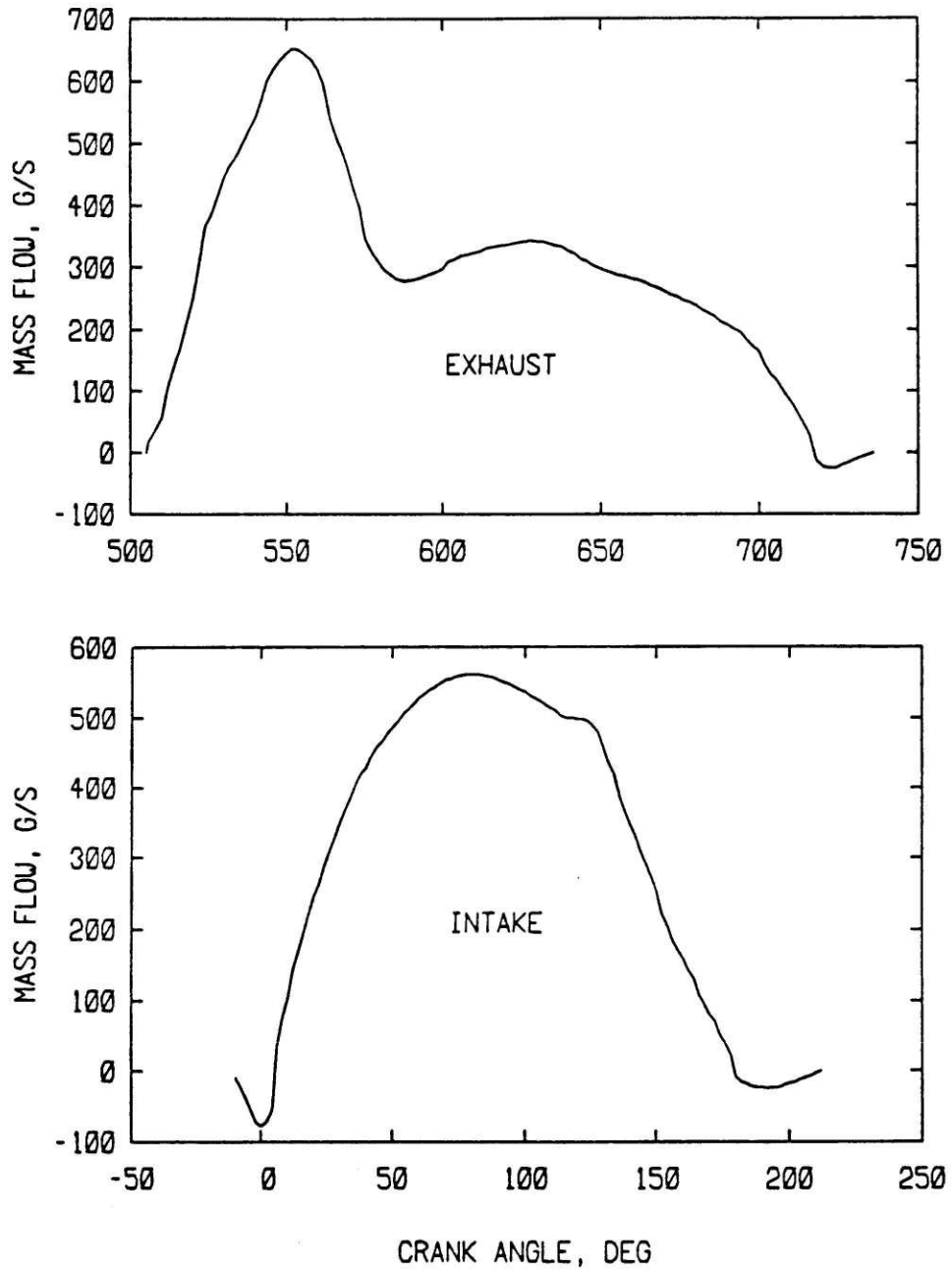


Figure 14. Mass flow rates through the intake (bottom) and exhaust (top) valves corresponding to the filling and emptying processes of the master cylinder.

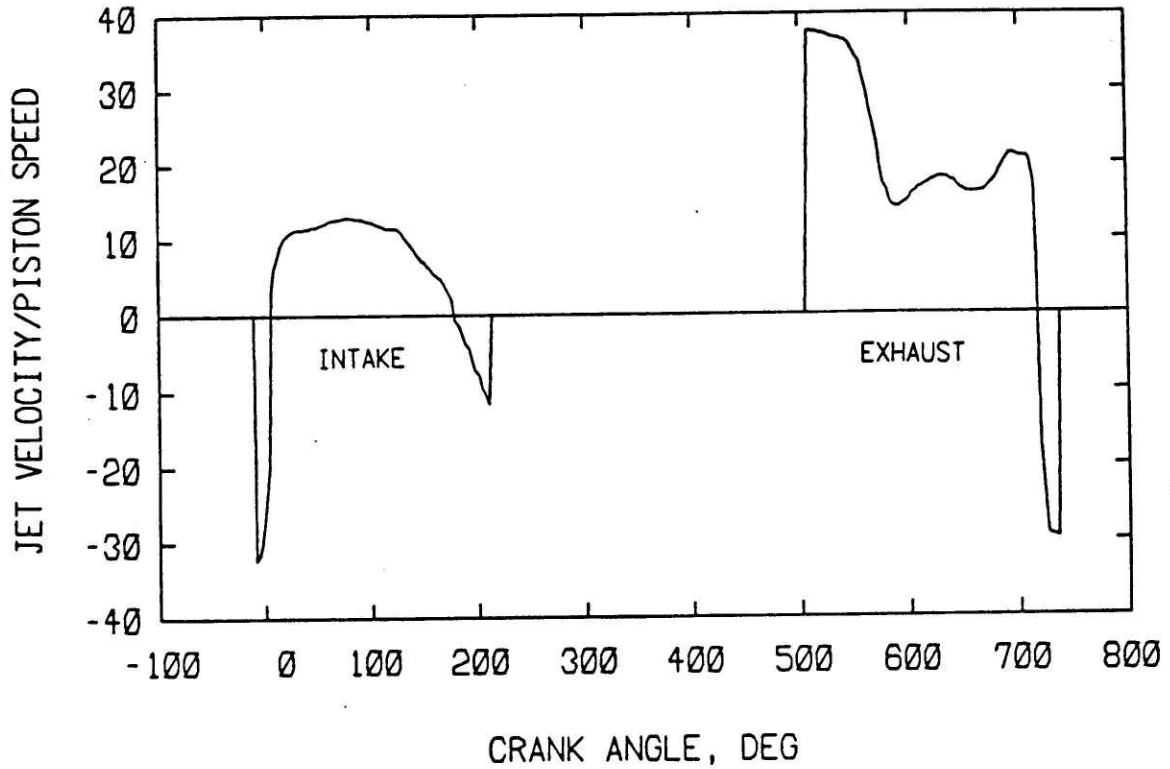


Figure 15. Velocity profiles of the conical jet flows through the intake and the exhaust valve opening, non-dimensionalized with respect to the mean piston speed. (i.e., two times the piston stroke times the rotational speed of the crankshaft).

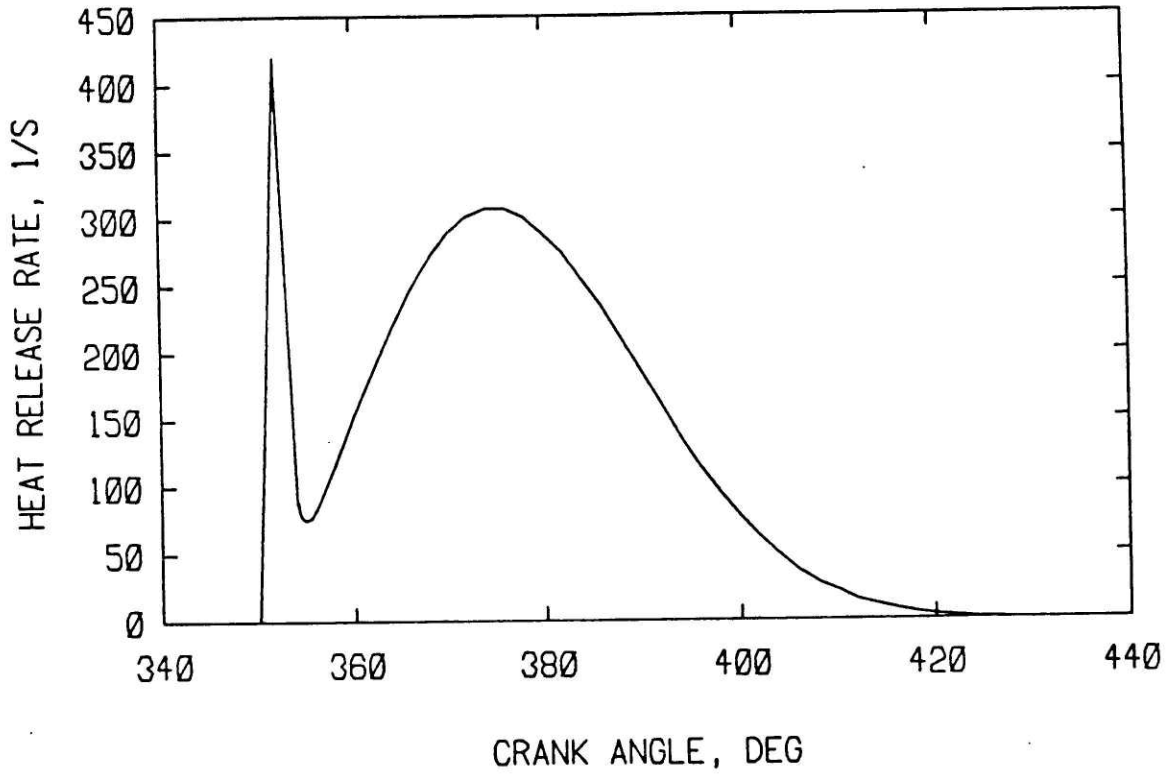


Figure 16. Predicted fuel burning rate profile normalized with respect to the total fuel injected per cycle per cylinder at rated speed and load.

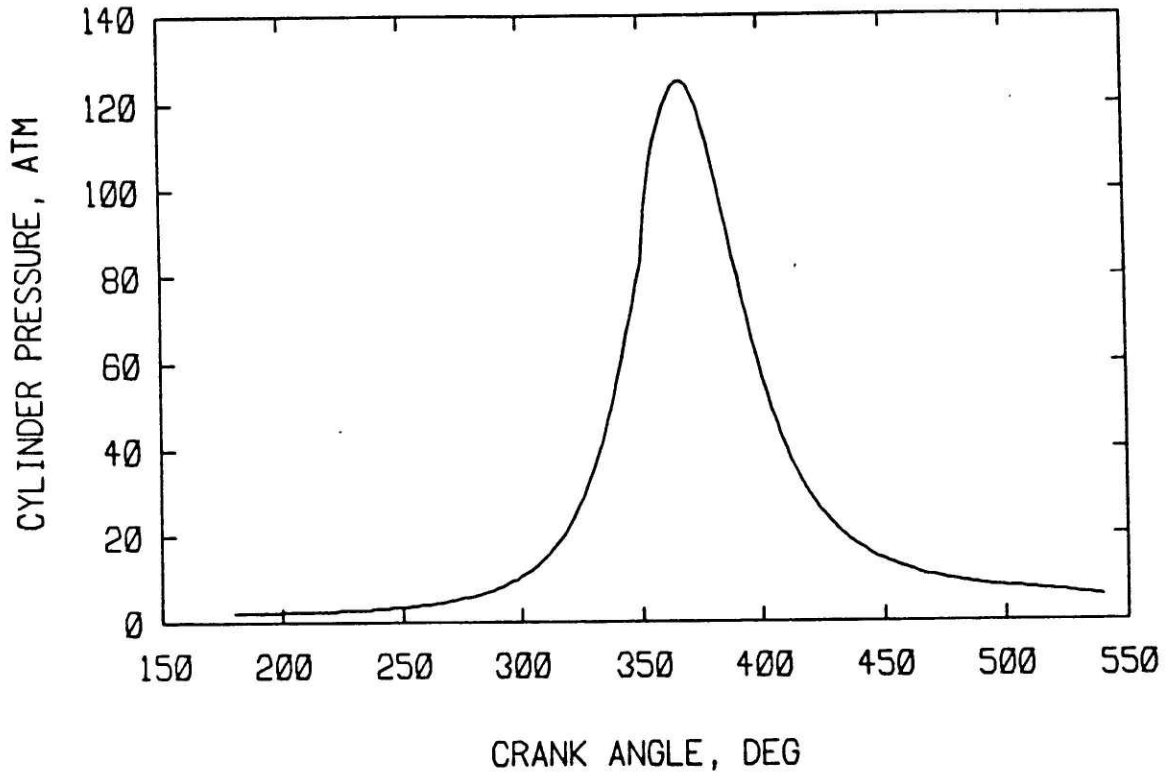


Figure 17. Pressure trace predicted by the simulation at rated speed and load.

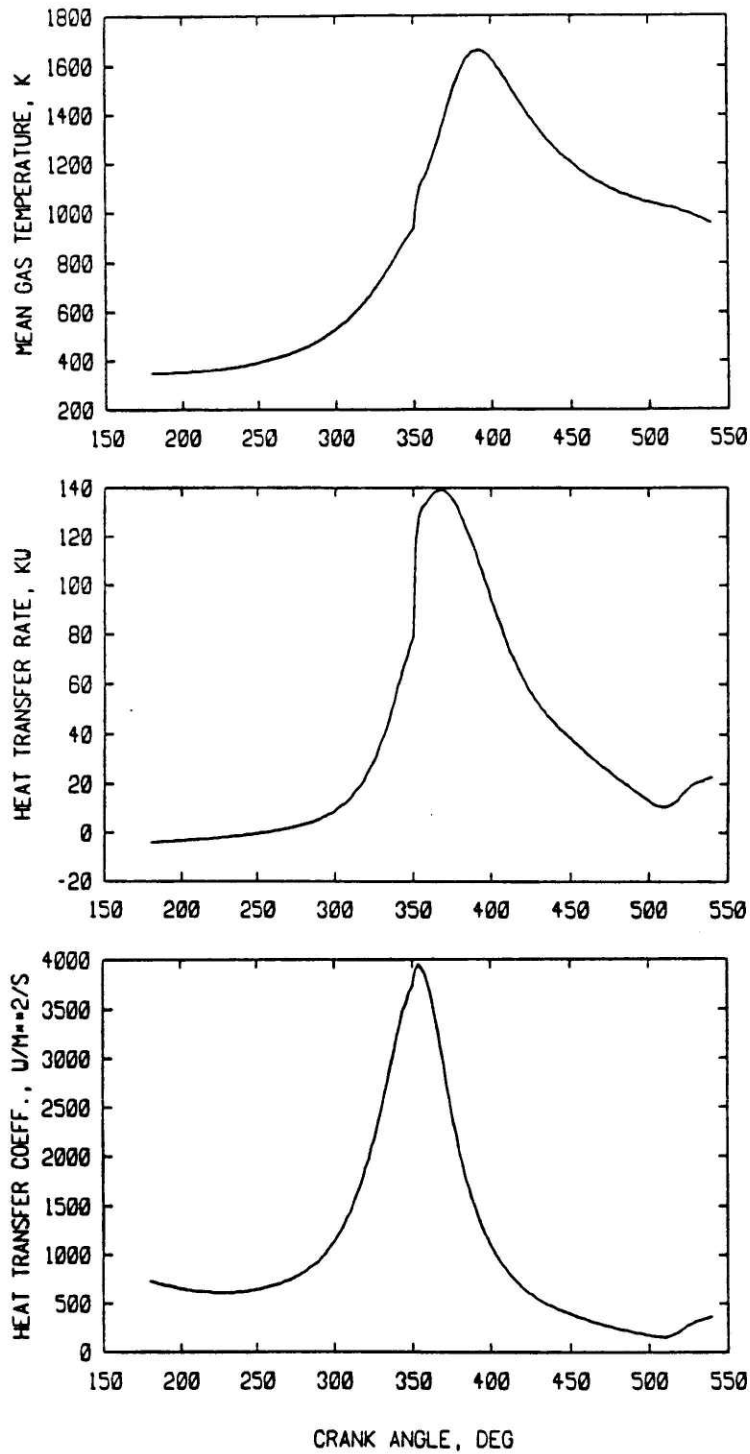


Figure 18. Bulk gas temperature (top), gas to wall heat transfer rate (middle) and convective heat transfer coefficient (bottom) as a function of crank-angle over the engine cycle.

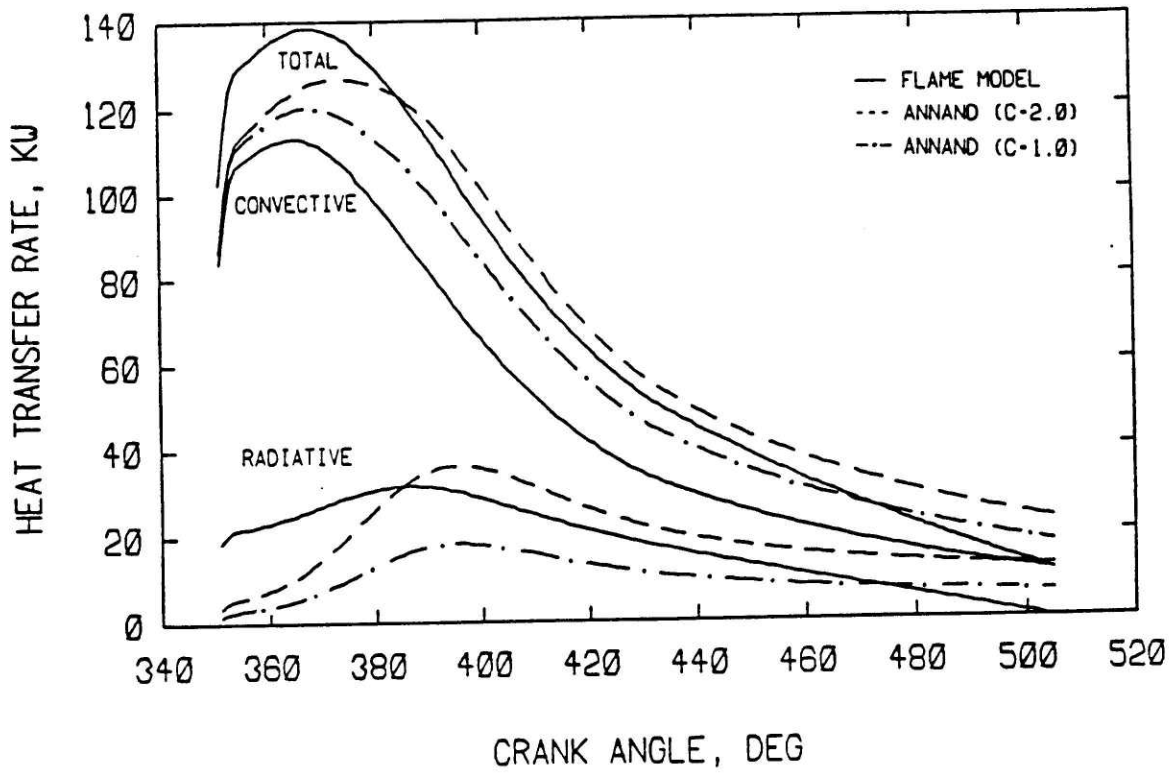


Figure 19. Simulation predictions of the radiative, convective, and total heat transfer rates over the duration of the expansion process in a cooled diesel engine. Results presented are based on the flame radiation model (continuous curves), and the Annand's radiation model with calibrating constants equal to 2.0 (dashed curves) and 1.0 (dotted-dashed curves).

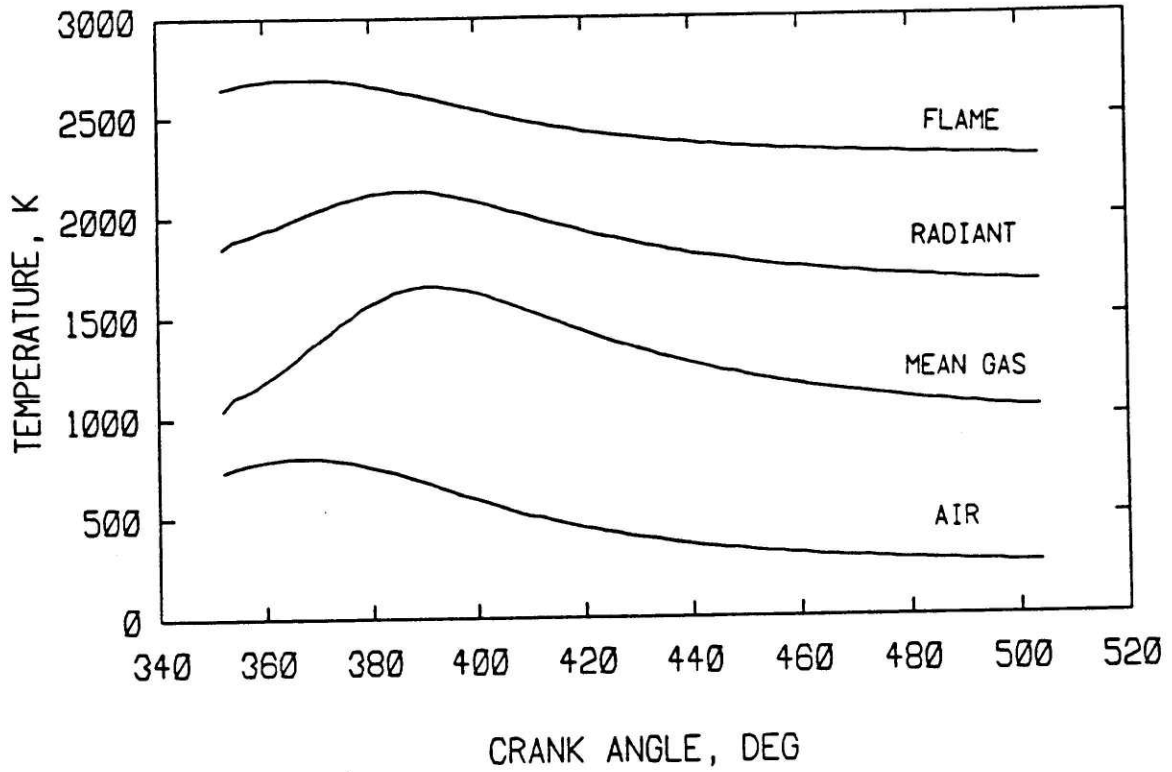


Figure 20. Temperature of air zones, temperature of bulk gas, characteristic radiant temperature and adiabatic flame temperature as a function of crank angle during the expansion process of a cooled metal engine.

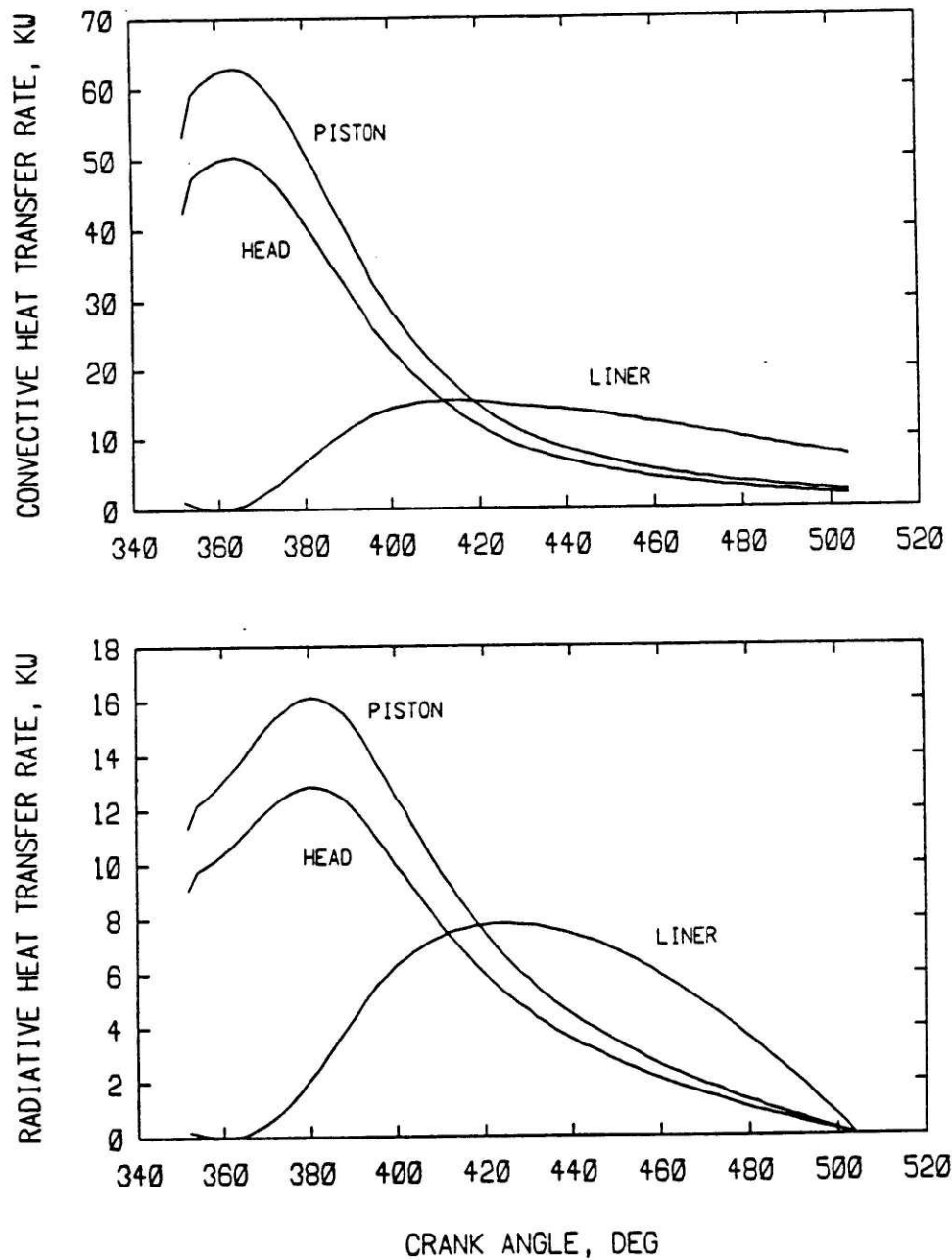


Figure 21. Breakdown of the convective (top) and radiative (bottom) heat transfer rates among cylinder head, piston, and liner over the duration of the expansion process.

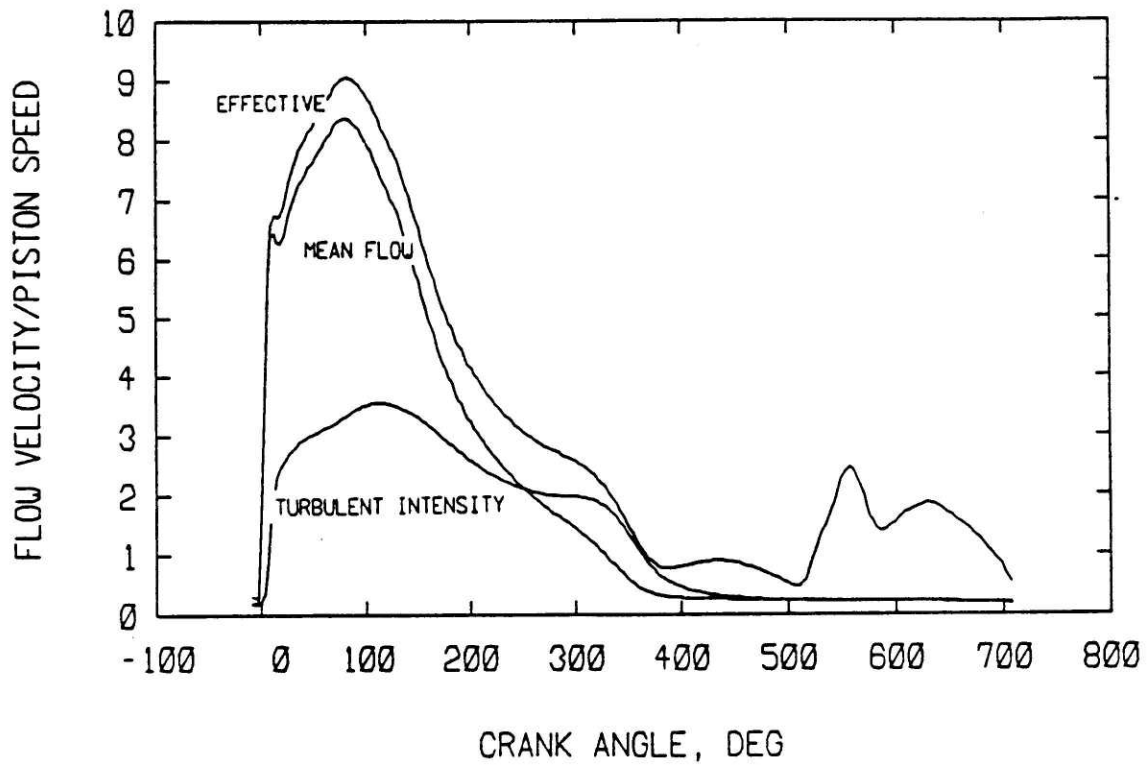


Figure 22. Variation of mean flow velocity, turbulent intensity, and resultant effective heat transfer velocity, defined by Eq. (4-18), with crank-angle. All velocity scales are normalized with respect to the mean piston speed.

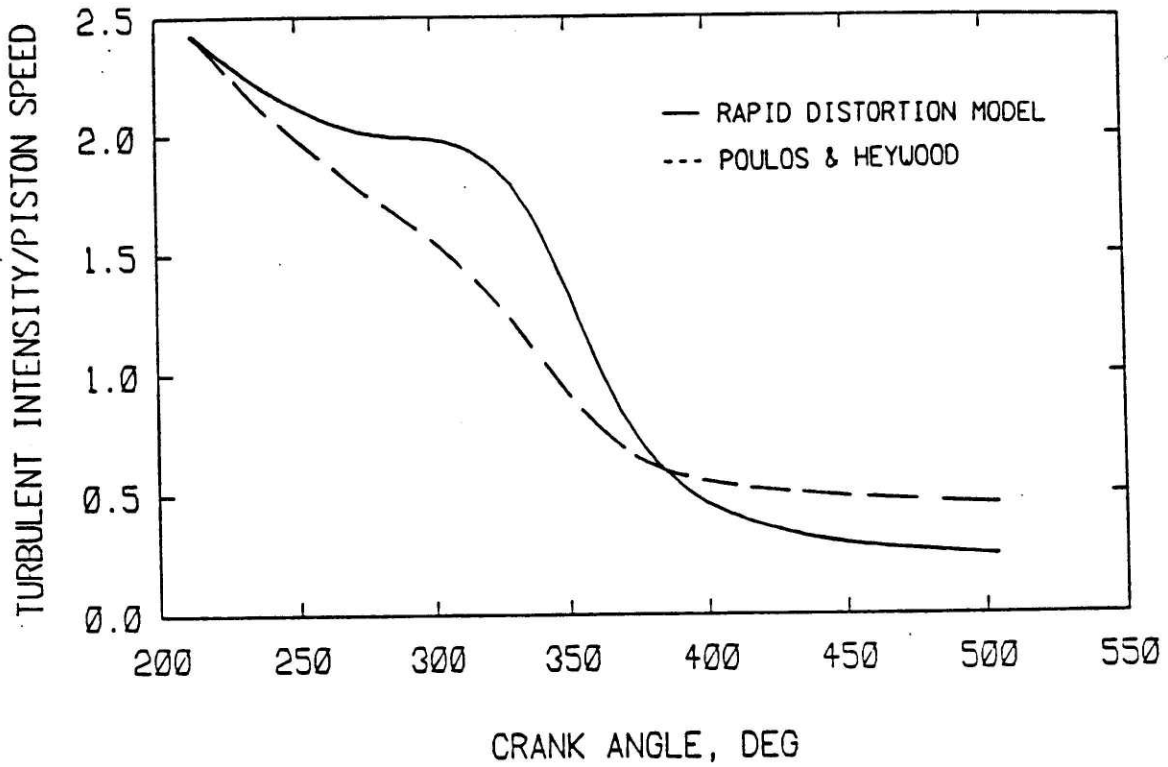


Figure 23. Predictions of the variation of non-dimensional turbulent intensity over the duration of the compression and expansion processes based on the Poulos and Heywood model and the extended model which includes the effects of rapid distortion.

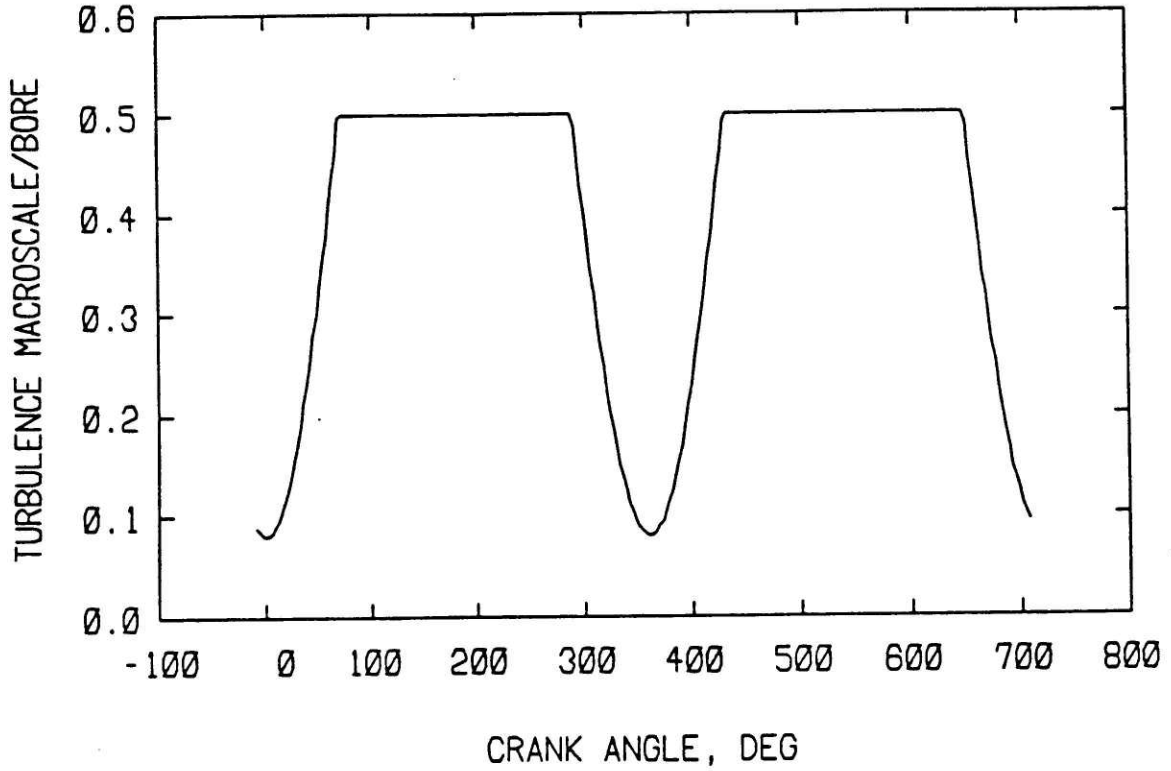


Figure 24. Predicted macroscale of turbulence, non-dimensionalized with respect to the cylinder bore, plotted against crank-angle throughout the engine cycle.

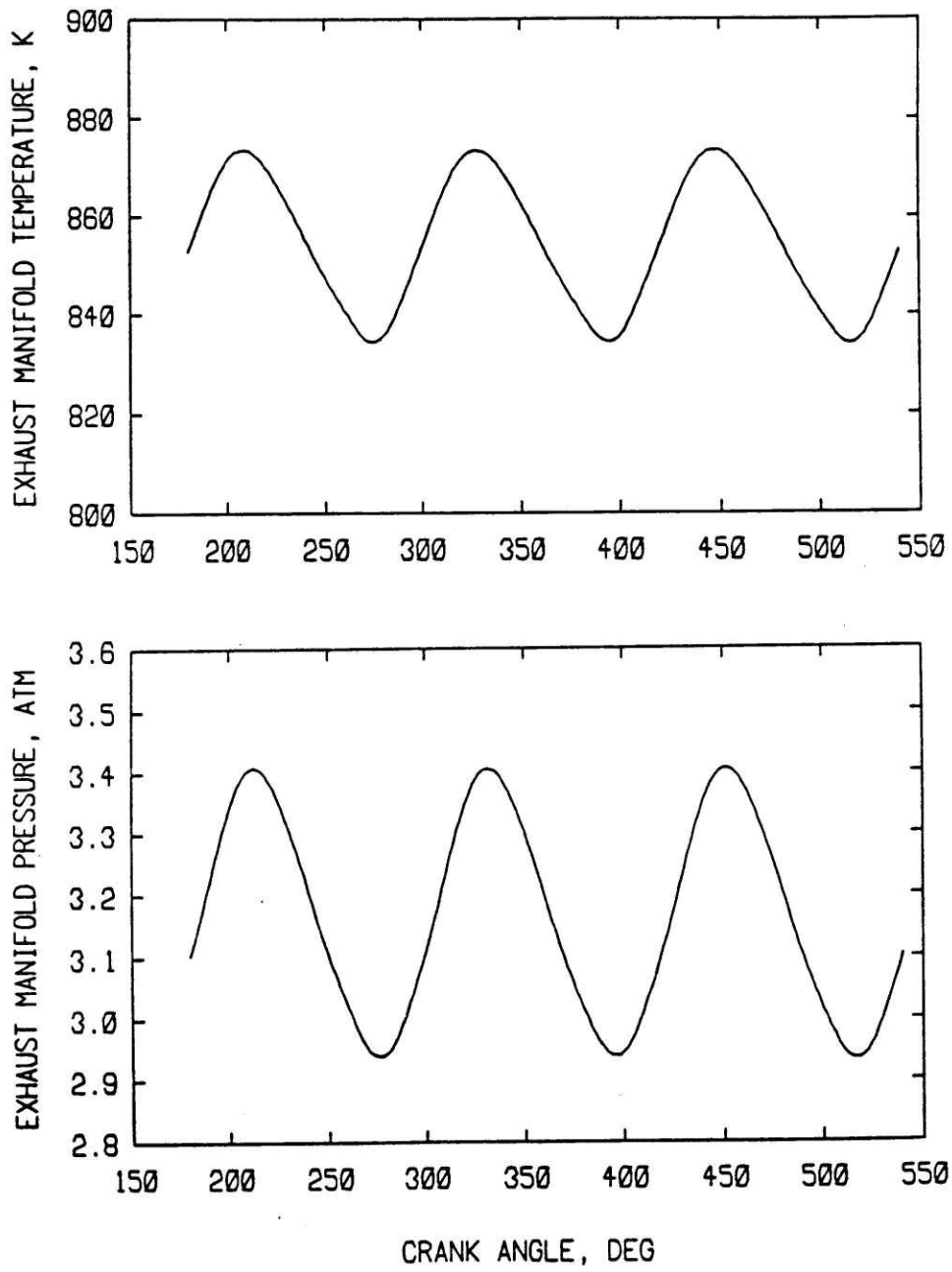


Figure 25. Exhaust manifold temperature and pressure crank-angle histories for a six cylinder turbocharged diesel engine.

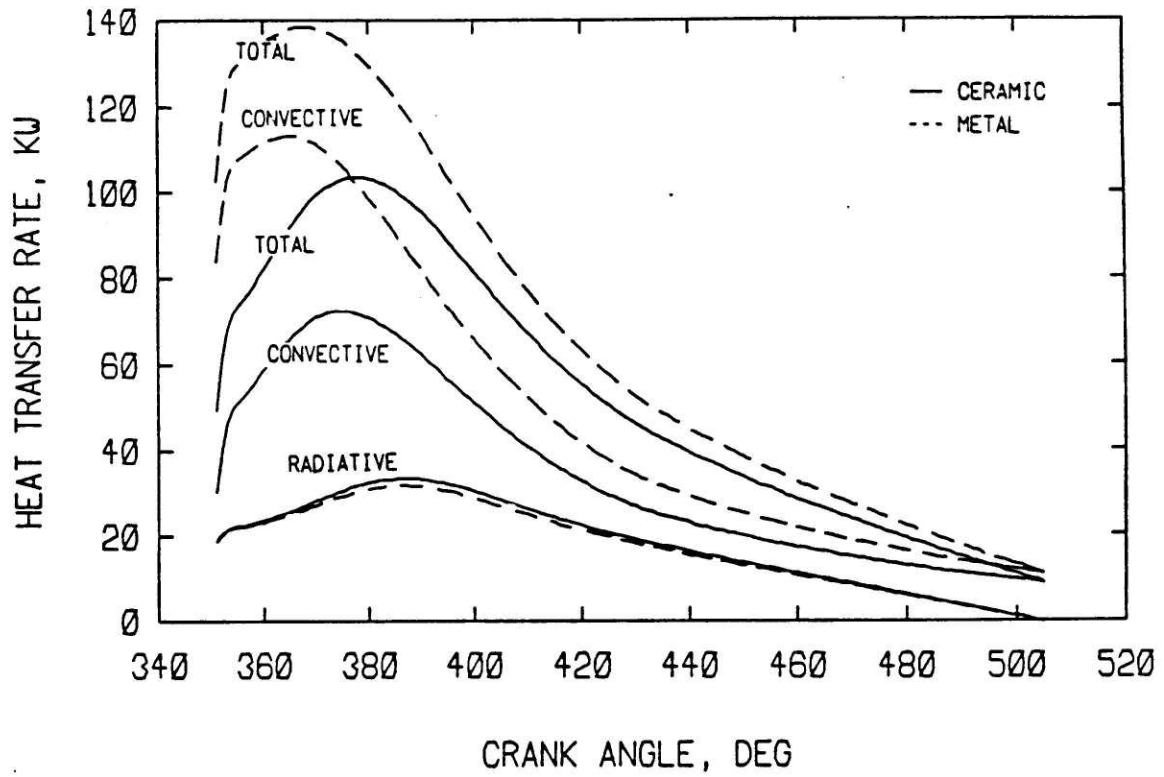


Figure 26. Comparison of the convective, radiative, and total heat transfer rates over the duration of the expansion process for the partially insulated (solid curves) and the baseline (dashed curves) system configurations.

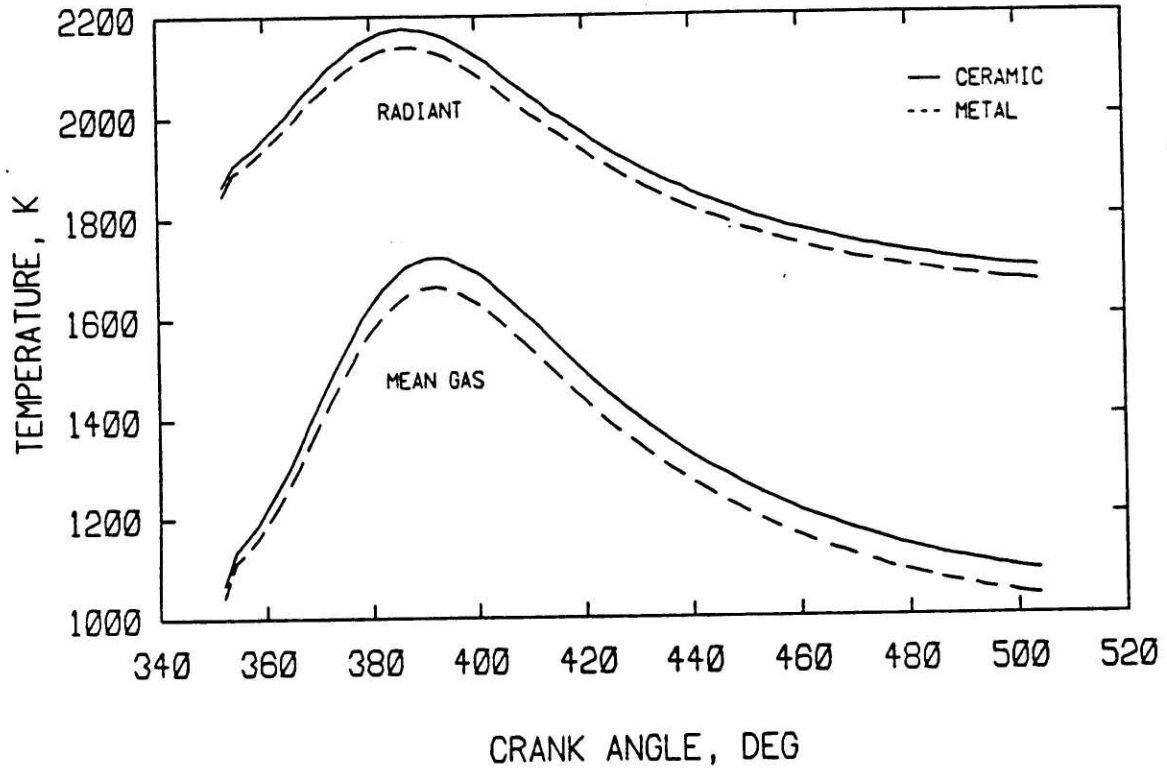


Figure 27. Comparison of mean bulk gas and characteristic radiant temperature profiles over the duration of the expansion process for the partially insulated (solid curves) and the baseline (dashed curves) engines.

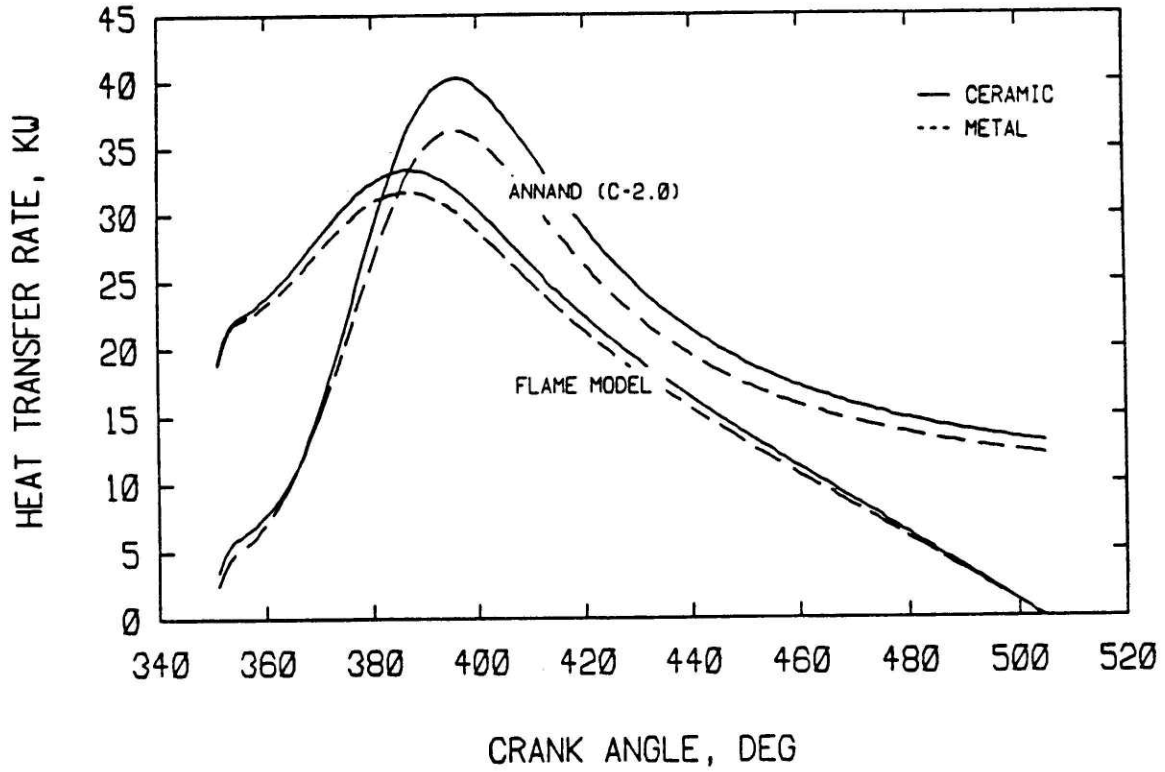


Figure 28. Predictions of radiative heat transfer rate against crank-angle based on the flame model and the Annand model (with $C_r = 2.0$) for the partially-insulated (solid curves) and the baseline (dashed curves) engines.

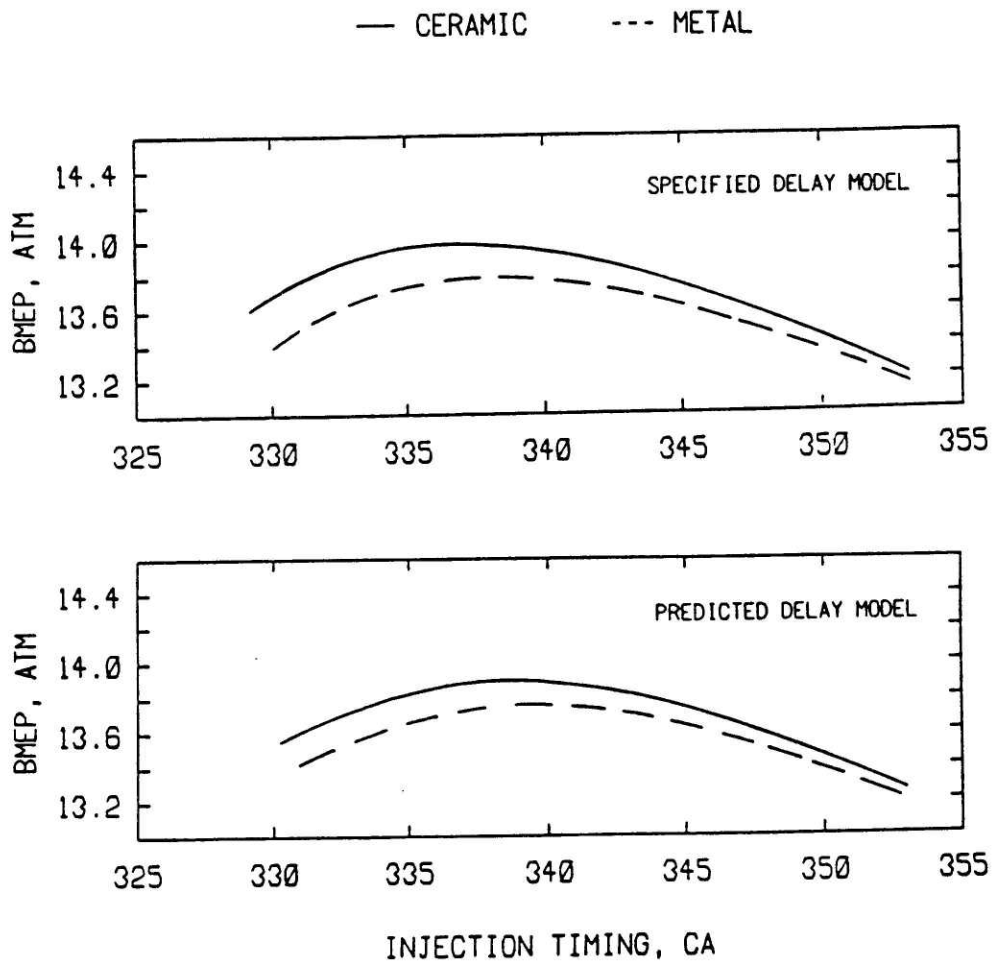


Figure 29. Variation of brake mean effective pressure with injection timing in a cooled (dashed curves) and a partially-insulated (solid curves) engine based on a specified ignition delay (top) and predicted ignition delay (bottom).

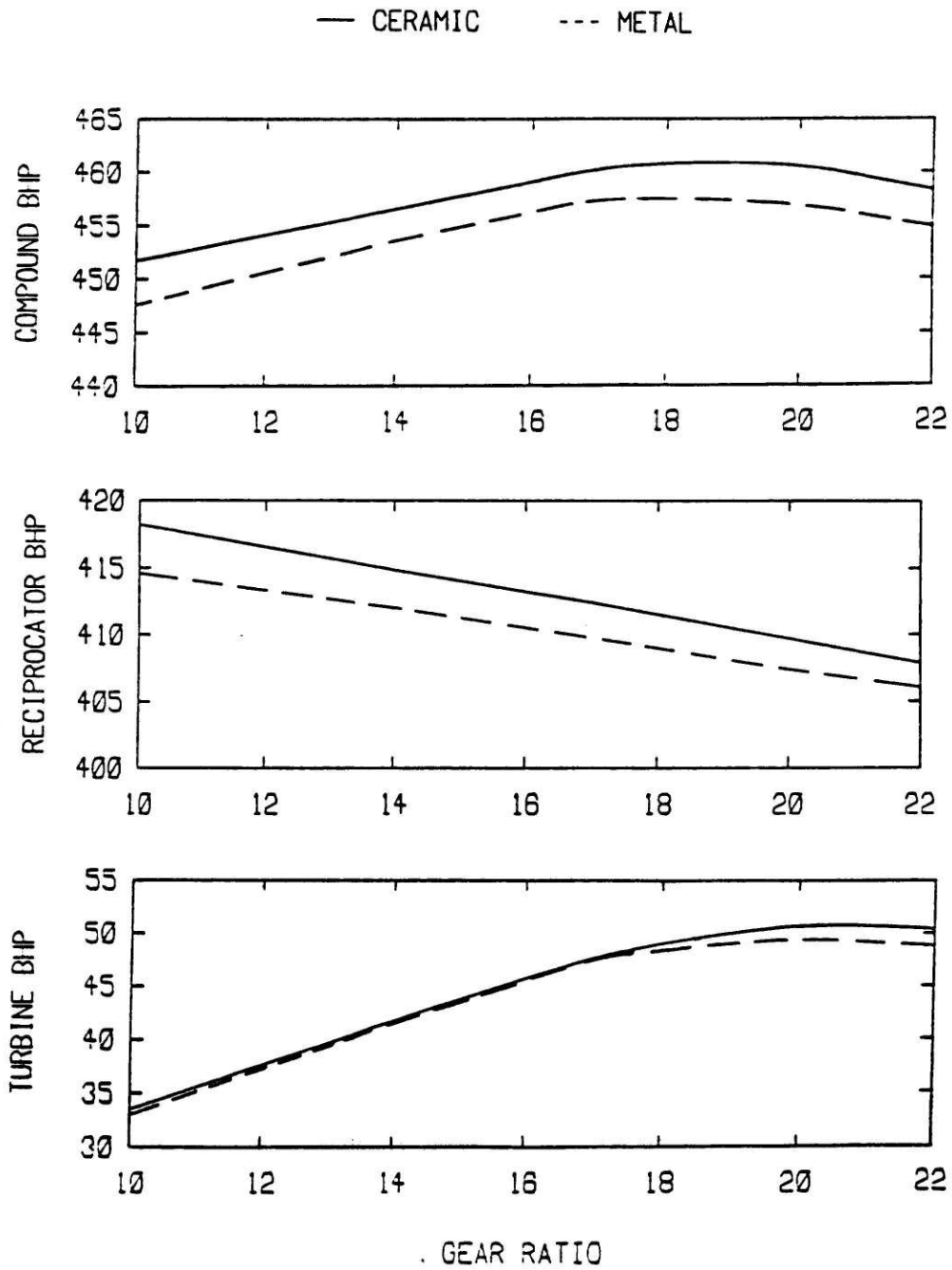


Figure 30. Variation of reciprocator brake power, power turbine brake power, and total brake power with power turbine gear ratio in a cooled and a partially-insulated engine.

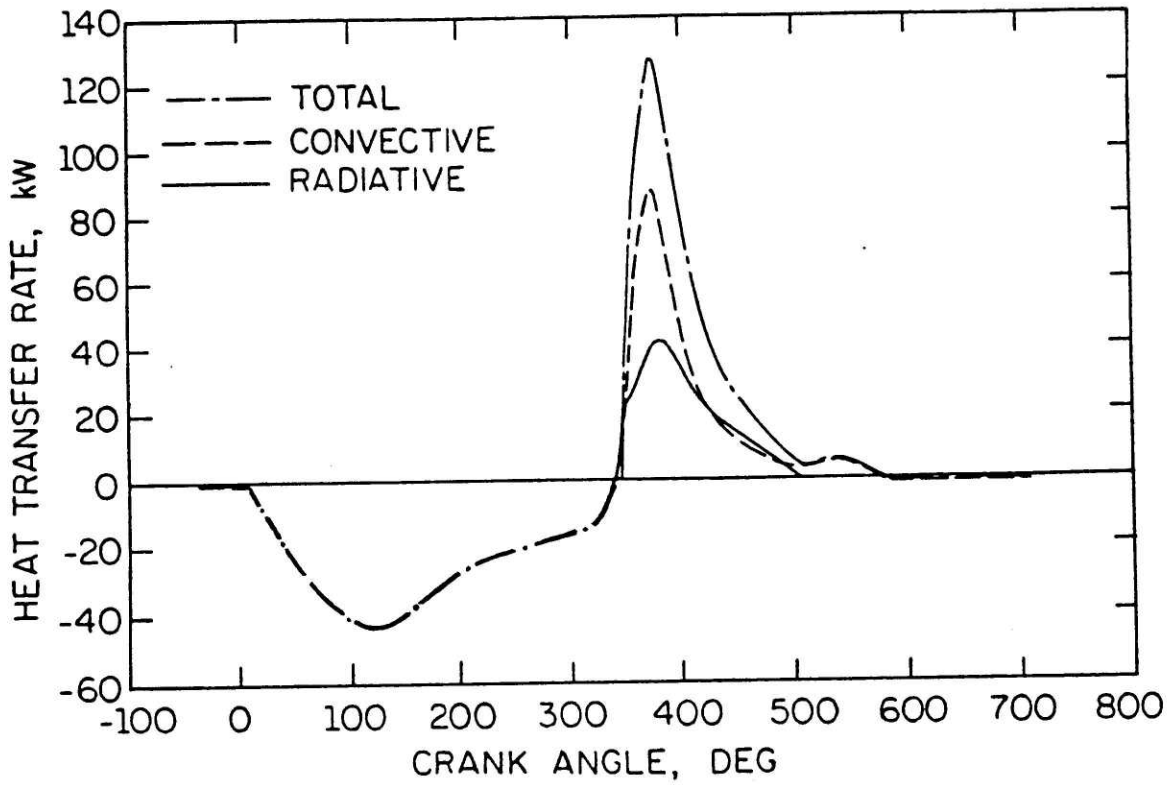


Figure 31. Simulation predictions of the radiative (solid curves), convective (dashed curves), and total (dashed-dotted curves) heat transfer rates throughout the cycle in a fully-insulated engine.

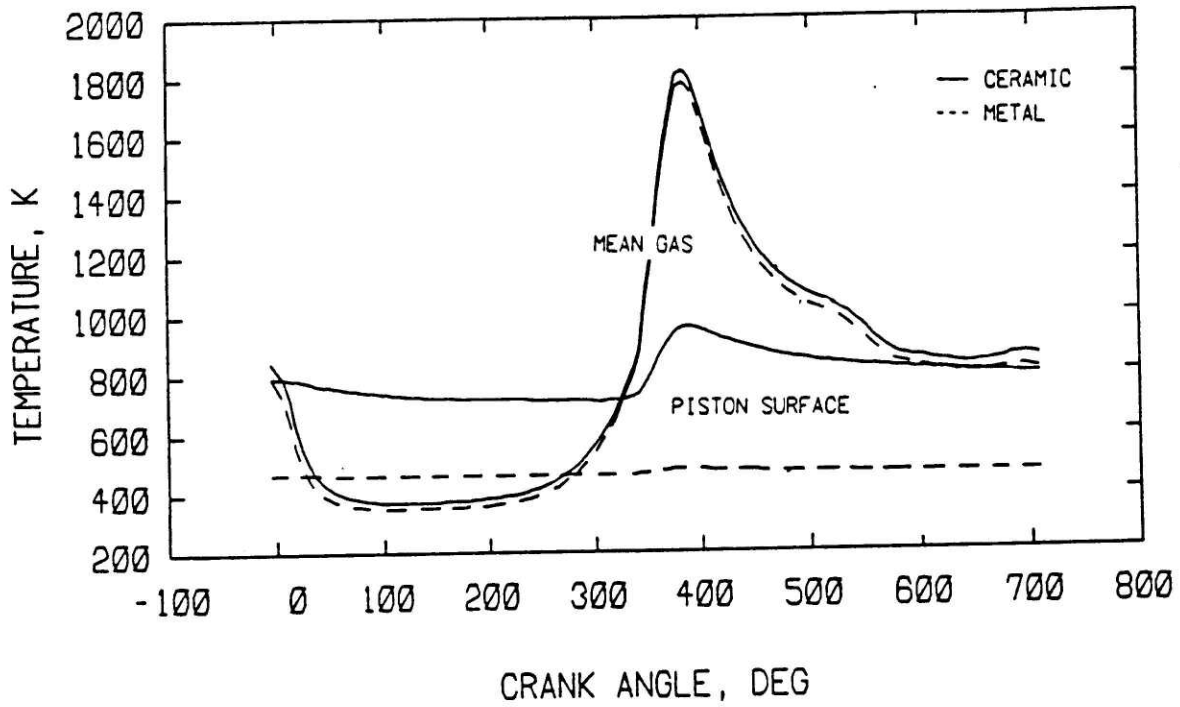


Figure 32. Temperature profiles of the mean bulk gas and the piston surface throughout the engine cycle for two system configurations. The dashed curves refer to a baseline engine with cooled, cast iron combustion chamber walls. The solid curves refer to a partially-insulated engine having 1.5 mm plasma-sprayed zirconia coating applied to the cylinder head and the piston, and a cooled, cast iron liner.

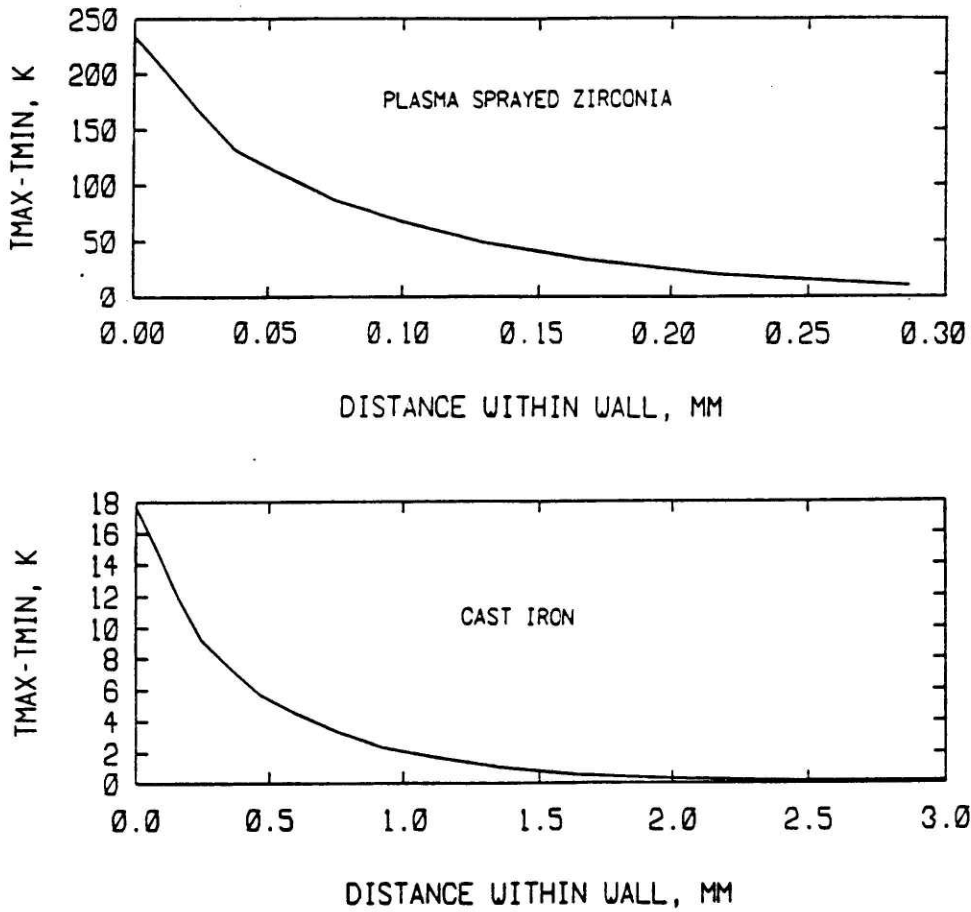


Figure 33. Penetration depth of the cyclic transients in a plasma-sprayed zirconia coated piston (top) and a cast-iron baseline piston (bottom) at a reciprocator speed of 1900 RPM.

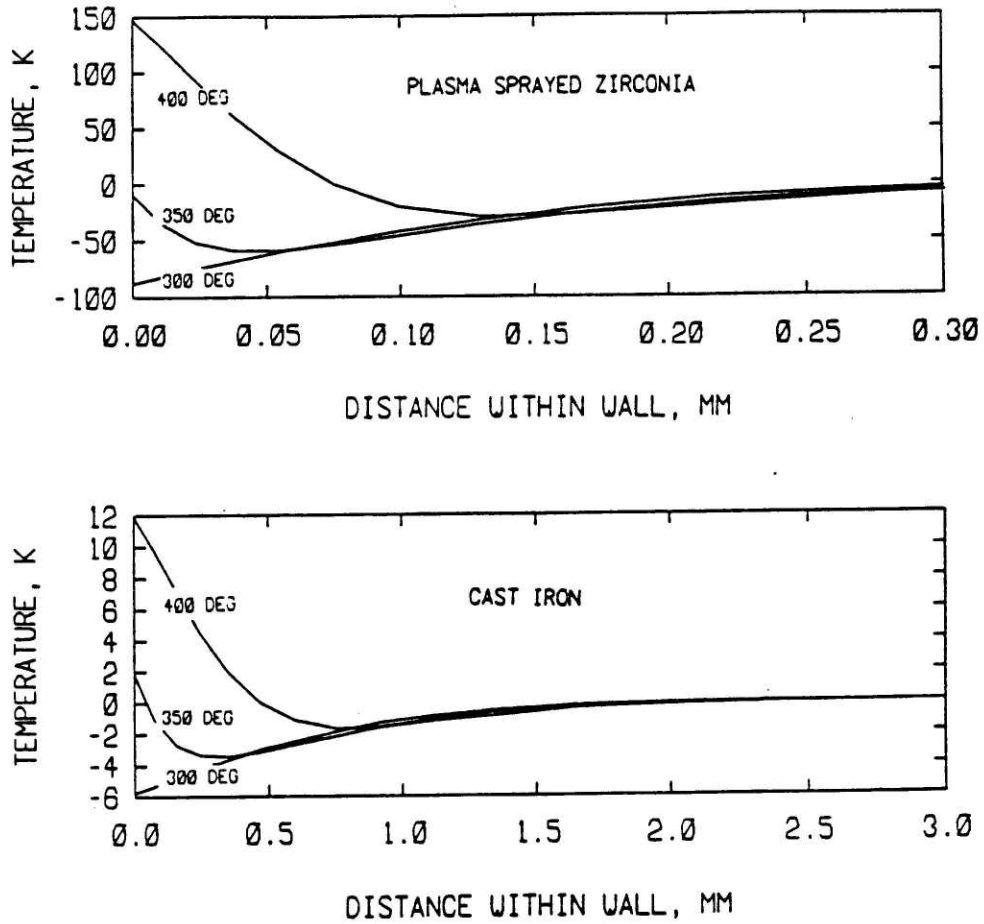


Figure 34. Perturbations from the quasi-steady temperature profiles at three instants (300 deg., 350 deg., and 400 deg. crank-angle) during the engine cycle for a cast-iron piston coated with a 1.5 mm layer of plasma sprayed zirconia (top) and an all cast-iron baseline piston (bottom).

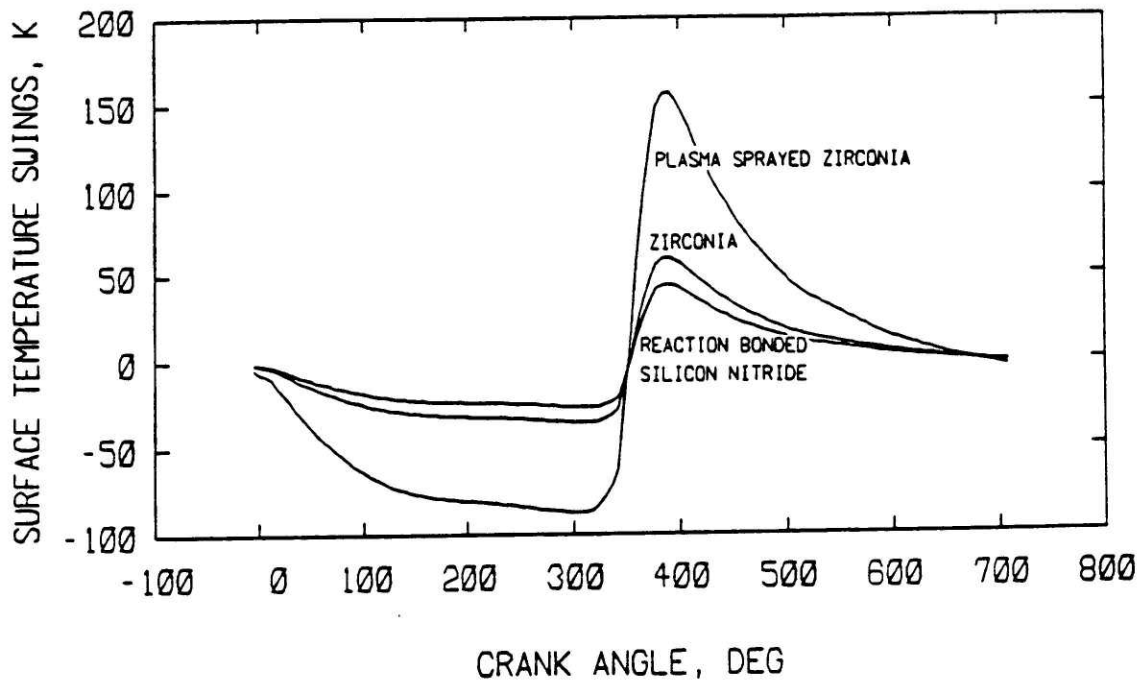


Figure 35. Cyclic variations from the mean temperature (800 K) at the surface of (i) a piston coated with a 1.5 mm layer of plasma-sprayed zirconia ($k = 0.6 \text{ W/m-K}$); (ii) a piston coated with a 3.0 mm layer of sprayed zirconia ($k = 1.2 \text{ W/m-K}$); (iii) a monolithic reaction-bonded silicon nitride piston ($k = 5 \text{ W/m-K}$) with an overall thickness of 13.4 mm. All designs achieve the same degree of insulation (55% reduction in heat loss).

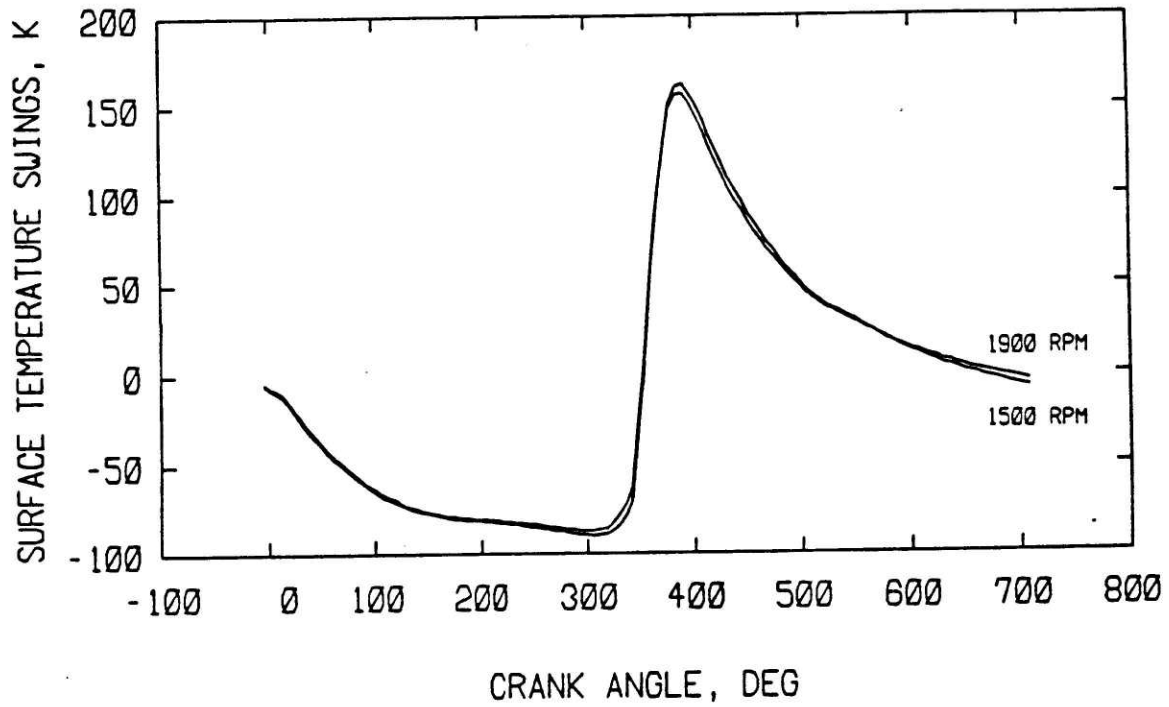


Figure 36. Cyclic variations from the mean surface temperature of a cast-iron piston coated with a 1.5 mm layer of plasma-sprayed zirconia at two reciprocator speeds: 1900 RPM (rated speed) and 1500 RPM (a medium speed).

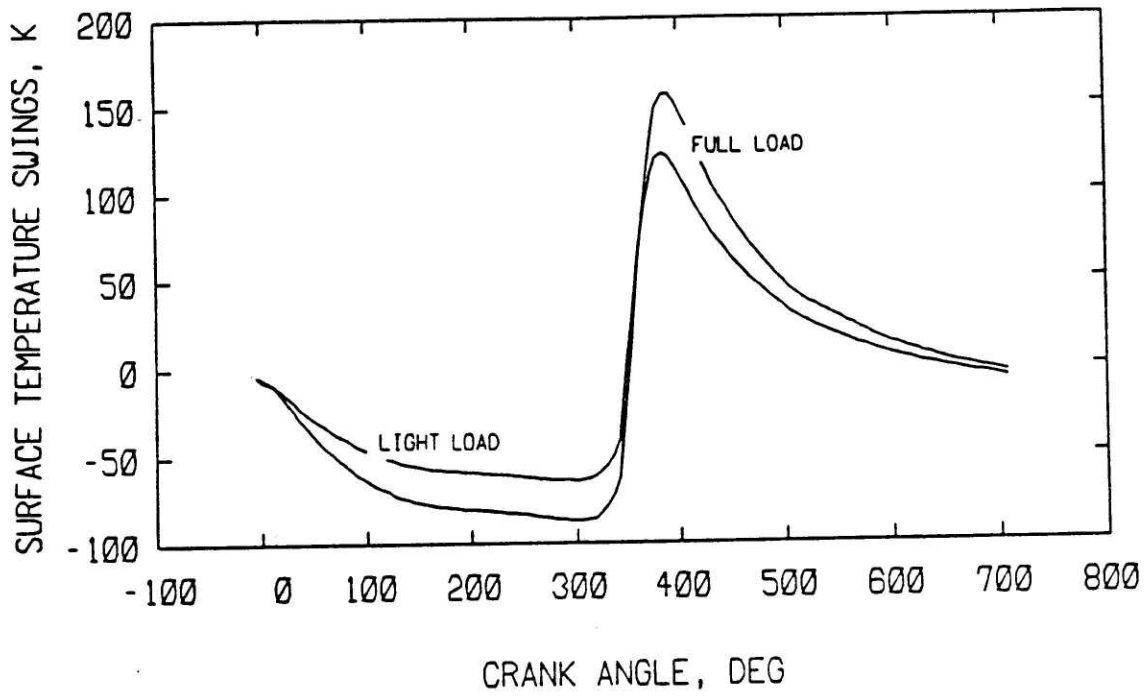


Figure 37. Cyclic variations from the mean surface temperature of a cast-iron piston coated with a 1.5 mm layer of plasma-sprayed zirconia at two reciprocator loads: full load and 75% of full load (light load).

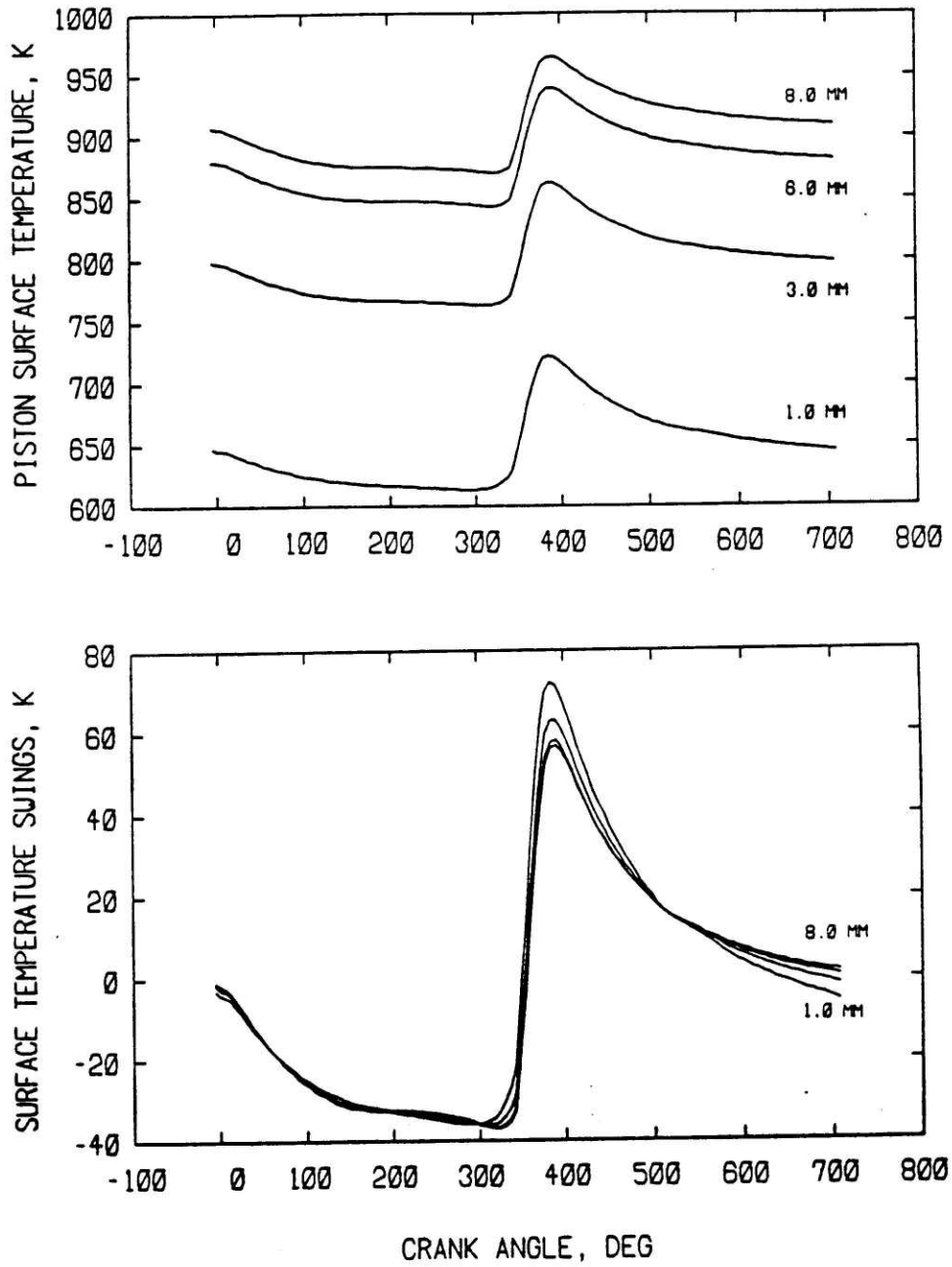


Figure 38. Instantaneous surface temperature (top) and cyclic variations from the mean surface temperatures (bottom) for various thicknesses of zirconia coatings applied to the piston and the cylinder head.

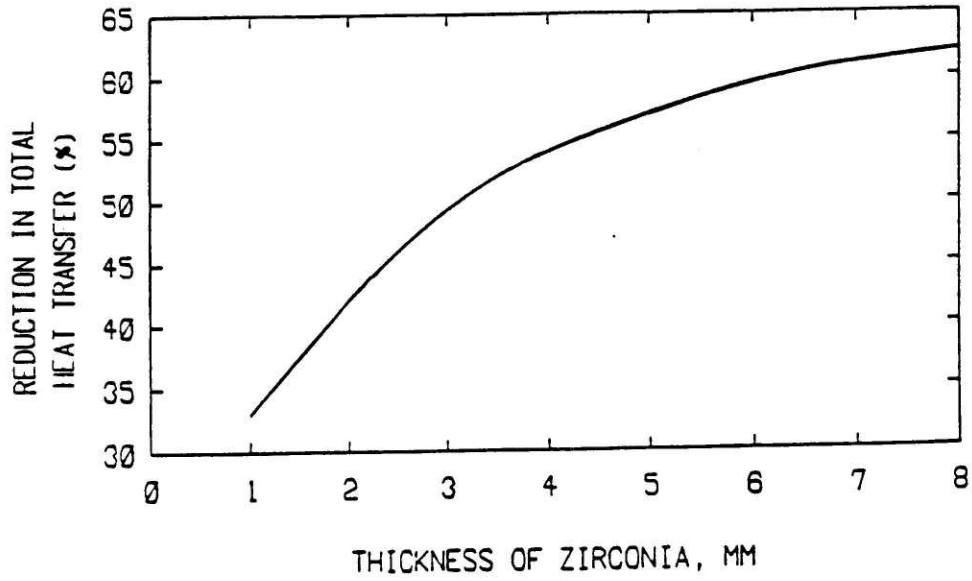


Figure 39. Reduction in total heat loss to the coolant as a function of the thickness of zirconia coating applied to the piston and the cylinder head. Results shown are for a non-insulated, cooled, cast-iron liner.

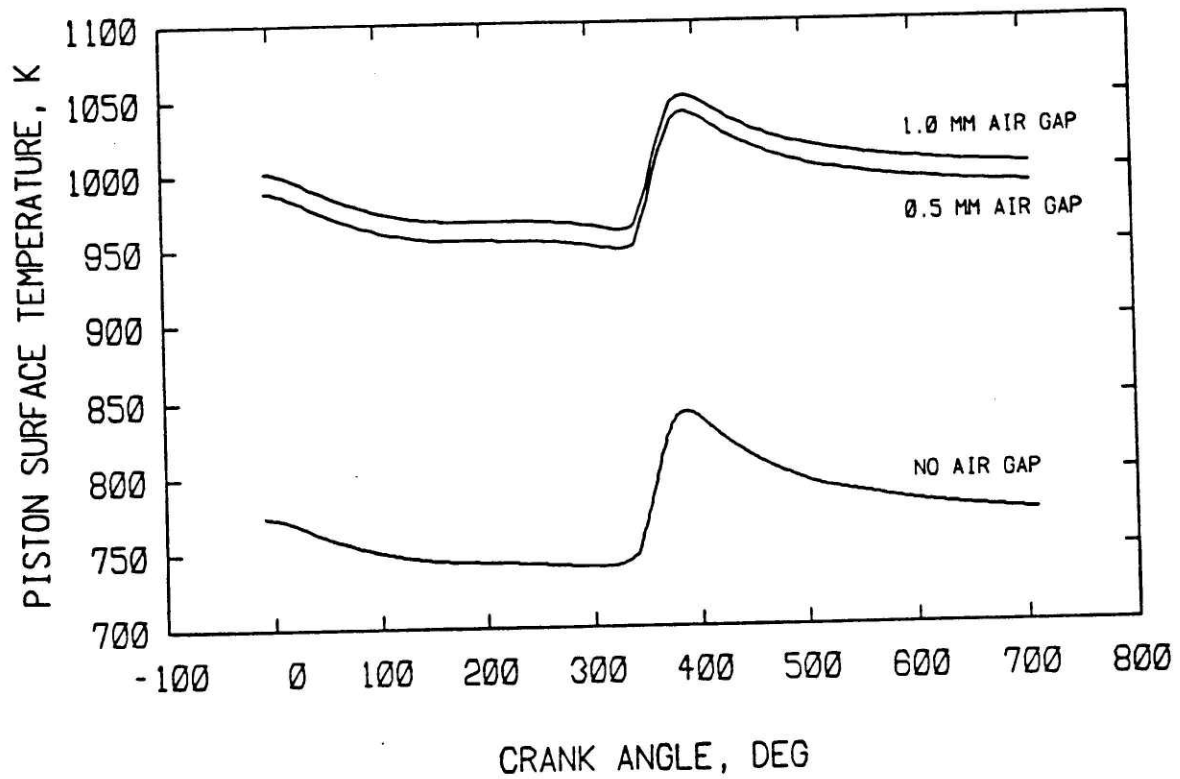


Figure 40. Predicted surface temperature profiles in a composite piston (ceramic/air-gap/metal) as a function of the thickness of air-gap separating the 2.5 mm zirconia crown from the cast-iron base.

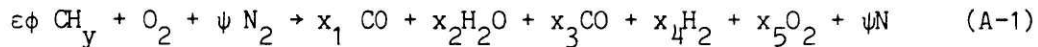
APPENDIX A

THERMODYNAMIC PROPERTIES

Our thermodynamic model assumes that the various open systems contain mixtures of air and combustion products throughout the total engine system. By utilizing the concept of the instantaneous average equivalence ratio defined in Section 4.1, the contents of any open system can be represented as one continuous medium. Furthermore, assuming ideal gas behavior and thermodynamic equilibrium, the instantaneous gas properties can be determined from a knowledge of pressure, temperature and average equivalence ratio in the open system.

When the temperature of the cylinder contents is below 1000 K, they are treated as a homogeneous mixture of non-reacting ideal gases, their properties being calculated using the procedure outlined below [74]:

The hydrocarbon-air combustion reaction is written as:



where ψ = the molar N:O ratio of the products,

y = the molar H:C ratio of the fuel,

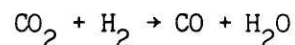
ϕ = the average equivalence ratio,

x_i = moles of species i per mole of O_2 reactant

$$\text{and } \epsilon = 4/(4+y) \quad (\text{A-2})$$

The quantities x_i are determined by using the following assumptions:

- a) for lean mixtures ($\phi \leq 1$) H_2 can be neglected.
- b) for rich mixtures ($\phi > 1$) O_2 can be neglected.
- c) for rich mixtures, the gas water reaction



is in equilibrium with equilibrium constant $K(T)$.

The solution for the x_i is shown in Table A-1, where C is obtained by solving equation (A-3) for its positive root.

$$(1 - K)C^2 + 2[1 - \epsilon\phi + K(\phi - 1 + \epsilon\phi)]C - 2K\epsilon\phi(\phi - 1) = 0 \quad (A-3)$$

The value of $K(T)$ is obtained by curve fitting JANAF table data over the temperature range 400 to 3200 K and is given by

$$\ln(K(T)) = 2.743 - 1.761/t - 1.611/t^2 + .2803/t^3 \quad (A-4)$$

where $t = T/1000$, and T is the temperature in Kelvins.

If the grams of products per mole of O_2 reactant is expressed as

$$M = (8\epsilon + 4)\phi + 32 + 28\psi \quad (A-5)$$

the specific enthalpy h and the specific heats at constant pressure and

constant composition, c_p and c_ϕ respectively, can be expressed by the

following relationships:

$$h = \frac{1}{M} \sum_{i=1}^6 x_i \sum_{j=1}^4 (a_{ij} \frac{t^j}{j} - \frac{a_{i5}}{t} + a_{i6}) \quad (A-6)$$

$$c_p = \frac{1}{M} \sum_{i=1}^6 x_i \sum_{j=1}^4 (a_{ij} t^{j-1} + \frac{a_{i5}}{t^2}) \quad (A-7)$$

$$c_\phi = \frac{1}{M} \sum_{i=1}^6 \frac{\partial x_i}{\partial \phi} \sum_{j=1}^4 (a_{ij} \frac{t^j}{j} - \frac{a_{i5}}{t} + a_{i6}) - \frac{\partial M / \partial \phi}{M^2} \sum_{i=1}^6 x_i \sum_{j=1}^4 (a_{ij} \frac{t^j}{j} - \frac{a_{i5}}{t} + a_{i6}) \quad (A-8)$$

The coefficients a_{ij} are obtained by curve fitting JANAF table data to the above functional form. The values of a_{ij} are given in Table A-2. The

resultant c_p is in cal/g-K, while h and c_ϕ are in kcal/g.

Since the cylinder contents are being treated as a mixture of non-reacting ideal gases, the density of the mixture is given by

$$\rho = \frac{p \bar{M}}{R_0 T} \quad (\text{A-9})$$

where

R_0 = the universal gas constant (1.9869 cal/mole-K)

and \bar{M} , the average molecular weight of the mixture, is given by

$$\bar{M} = M / ((1 - \epsilon)\phi + 1 + \psi) \quad \phi \leq 1 \quad (\text{A-10})$$

$$\bar{M} = M / ((2 - \epsilon)\phi + \psi) \quad \phi > 1$$

Then, the partial derivatives of the density with respect to temperature, pressure, and equivalence ratio are given by

$$\frac{\partial \rho}{\partial T} = - \frac{\rho}{T} \quad (\text{A-11})$$

$$\frac{\partial \rho}{\partial p} = \frac{\rho}{p} \quad (\text{A-12})$$

$$\frac{\partial \rho}{\partial \phi} = \frac{\partial \rho}{\partial \bar{M}} \frac{\partial \bar{M}}{\partial \phi} = \frac{\rho}{\bar{M}} \frac{\partial \bar{M}}{\partial \phi} \quad (\text{A-13})$$

When the temperature of the cylinder contents is above 1000 K, their properties are calculated with allowance for chemical dissociation, according to the calculation method described in [75]. This is an approximate method based on curve fitting data obtained from detailed thermochemical calculations [39] to a functional form obtained from a consideration of carbon air combustion. Although species concentrations within the burned gases are not calculated, the bulk thermodynamic properties needed for cycle analysis are accurately determined.

APPENDIX B

THERMODYNAMIC DATA FOR FUEL VAPOR

In the computer engine simulation code, the fuel vapor enthalpy is modelled by a polynomial of the form

$$H(T) = A_1 t + A_2 \frac{t^2}{2} + A_3 \frac{t^3}{3} + A_4 \frac{t^4}{4} - \frac{A_5}{t} + A_6 \quad (\text{B-1})$$

where $t = T/1000$, T is the temperature in Kelvins, and the units of $H(T)$ are kcal/gmole.

The value of A_6 for a particular fuel depends on the datum at which the elements C(graphite), H_2 , O_2 and N_2 are assigned zero enthalpy. Using a datum of 298 K, the coefficients A_i were obtained for various hydrocarbon fuels by curve fitting table data from Rossini et al [76] to the above functional form. The values of A_i for the fuels examined, including #2 Diesel fuel ($C_{10.84}H_{18.68}$) are given in Table B-1. A detailed fuel analysis of #2 Diesel fuel is given in Table B-2.

Our thermodynamic property computer codes, however, use a 0 K datum. To convert to a 0 K datum, a correction term A_8 must be added to the enthalpy given by (E-1) to account for the enthalpy difference of C and H_2 between 0 and 298 K. Using data from the JANAF Tables [77], the correction term for #2 Diesel fuel is:

$$\begin{aligned} A_8 &= n(H_0^O - H_{298}^O)_C + \frac{m}{2} (H_0^O - H_{298}^O) \\ &= 10.84 \times 0.252 + \frac{18.68}{2} \times 2.024 = 21.636 \text{ kcal/gmole} \end{aligned}$$

APPENDIX C

TRANSPORT PROPERTIES

The heat transfer correlations relate the heat transfer coefficient to the Reynolds and Prandtl numbers and the thermal conductivity. The calculation of the heat transfer rates will therefore require values for the viscosity and the Prandtl number (from which the thermal conductivity can be obtained). We have used the approximate correlations for the viscosity and the Prandtl number of hydrocarbon-air combustion products developed by Mansouri and Heywood [78].

The NASA equilibrium program [39] was used to compute the viscosity of hydrocarbon-air combustion products as a function of temperature, T , equivalence ratio, ϕ , and pressure p . It was shown that the viscosity of the combustion products was satisfactorily correlated by a power-law based on air viscosity data, corrected for the effect of equivalence ratio, i.e.,

$$\mu_{\text{prod}} \text{ [kg/ms]} = 3.3 \times 10^{-7} T^{0.7} / (1 + 0.027\phi) \quad (\text{C-1})$$

$$\text{for } 500 \text{ K} \leq T \leq 4000 \text{ K} \quad \text{and} \quad 0 \leq \phi \leq 4$$

Note that the viscosity of the combustion products is independent of the pressure.

The equilibrium Prandtl number of hydrocarbon-air combustion products was also calculated over the above ranges of temperature, pressure, and equivalence ratio. Using a second order polynomial of γ to curve fit the above data, it was shown that the following correlation for lean ($\phi < 1$) mixtures predicted values in good agreement (within 5%) with the data, i.e.,

$$\text{Pr} = 0.05 + 4.2(\gamma - 1) - 6.7(\gamma - 1)^2 \quad (\text{C-2a})$$

$$\text{for } 500 \text{ K} \leq T \leq 4000 \text{ K} \quad \text{and} \quad \phi \leq 1$$

For rich mixtures ($\phi > 1$), a reasonable fit (less than 10% error) to the equilibrium Prandtl number values calculated with the NASA program was found to be the following:

$$\text{Pr} = [0.05 + 4.2(\gamma - 1) - 6.7(\gamma - 1)^2] / [1 + 0.015 \times 10^{-6} (\phi T)^2]$$

for $2000 \text{ K} \leq T \leq 3500 \text{ K}$ and $1 < \phi \leq 4$ (C-2b)

APPENDIX D

LINEARIZATION OF TOTAL HEAT TRANSFER RATE AT THE GAS/WALL INTERFACE

The total instantaneous heat transfer rate, convective and radiative, per unit area, to the combustion chamber walls is given by

$$\dot{Q}_w = \dot{Q}_c + \dot{Q}_r \quad (D-1)$$

where $\dot{Q}_c = h(T_g - T_w)$ (D-2)

and $\dot{Q}_r = k_r(T_r^4 - T_w^4)$ (D-3)

where the symbols used have the same meaning as in Section 6.4.

The radiative heat transfer can be expressed as

$$\dot{Q}_r = k_r(T_r^4 - T_g^4) + k_r(T_g^4 - T_w^4) \quad (D-4)$$

or alternatively as

$$\dot{Q}_r = k_r \frac{(T_r^4 - T_g^4)}{T_g - T_w} (T_g - T_w) + k_r(T_g^3 + T_g^2 T_w + T_g T_w^2 + T_w^3)(T_g - T_w) \quad (D-5)$$

Combining equations (D-1), (D-2) and (D-5), the total instantaneous heat transfer rate per unit area can be expressed in linear form as

$$\dot{Q}_w = h_{\text{eff}}(T_g - T_w) \quad (D-6)$$

where h_{eff} is an effective linearized heat transfer coefficient defined as

$$h_{\text{eff}} = h + k_r(T_g^3 + T_g^2 T_w + T_g T_w^2 + T_w^3 + \frac{T_r^4 - T_g^4}{T_g - T_w}) \quad (D-7)$$

with the wall temperature taken as the value at the previous time step.

APPENDIX E

DERIVATION OF EXACT SOLUTION FOR A TWO-PARALLEL LAYER
COMPOSITE SLAB SUBJECT TO A TIME-PERIODIC BOUNDARY CONDITION

Consider the two parallel layer slab, shown in Fig. 6, where the thicknesses of the first and second layer are L_1 and L_2 , respectively, and the origin for the distance along the x-axis is taken at the interface between the two layers. Suppose that the slab is subject to a harmonically varying gas temperature, given by

$$T_g = \bar{T}_g + \Delta T_g \text{Re}(e^{i\omega t}) \quad (\text{E-1})$$

where \bar{T}_g is the mean gas temperature, and ω is the period of oscillations. Furthermore, assume that the heat transfer coefficient from the gas to the wall, h_g , the heat transfer coefficient from the wall to the outside, h_c , and the ambient temperature, T_c , are constant, independent of time.

The temperature distribution within each layer can be decomposed into a steady part (of no interest here), and a time-periodic part. The periodic part, induced due to the cyclic transients, will satisfy the unsteady heat conduction equation for each layer, i.e.,

$$\frac{1}{\alpha_1} \frac{\partial T_1}{\partial t} = \frac{\partial^2 T_1}{\partial x^2} \quad (\text{E-2})$$

$$\frac{1}{\alpha_2} \frac{\partial T_2}{\partial t} = \frac{\partial^2 T_2}{\partial x^2} \quad (\text{E-3})$$

where α_1 and α_2 are the thermal diffusivities for each layer.

Expressing the time-periodic temperatures as

$$T_1(x,t) = \theta_1(x) \text{Re}(e^{i\omega t}) \quad (\text{E-4})$$

$$T_2(x,t) = \theta_2(x) \text{Re}(e^{i\omega t}) \quad (\text{E-5})$$

where θ_1 and θ_2 are functions of position x only, and substituting into (E-2) and (E-3), we get

$$\frac{i\omega}{\alpha_1} \theta_1 = \frac{\partial^2 \theta_1}{\partial x^2} \quad (E-6)$$

$$\frac{i\omega}{\alpha_2} \theta_2 = \frac{\partial^2 \theta_2}{\partial x^2} \quad (E-7)$$

The solutions that satisfy (E-6) and (E-7) are of the form [79]:

$$\theta_1(x) = A_1 e^{x d_1} + B_1 e^{-x d_1} \quad (E-8)$$

$$\theta_2(x) = A_2 e^{x d_2} + B_2 e^{-x d_2} \quad (E-9)$$

where $d_1 = \sqrt{i\omega/\alpha_1}$ (E-10)

and $d_2 = \sqrt{i\omega/\alpha_2}$ (E-11)

The boundary conditions for the time-periodic solutions are the following:

At the gas side ($x = -L_1$),

$$-k_1 \frac{\partial \theta_1}{\partial x} = h_g (\Delta T_g - \theta_1) \quad (E-12)$$

At the ambient side ($x = L_2$),

$$-k_2 \frac{\partial \theta_2}{\partial x} = h_c \theta_2 \quad (E-13)$$

where k_1 and k_2 are the thermal conductivities of the first and second layer, respectively. Note that (E-12) and (E-13) do not contain \bar{T}_g or T_c , because we are interested, here, only in the time-periodic part of the solution. Finally, at the interface ($x=0$) between the two slabs, the requirements for continuity of temperature and heat flux give:

$$A_1 + B_1 = A_2 + B_2 \quad (\text{E-14})$$

$$k_1 d_1 (A_1 - B_1) = k_2 d_2 (A_2 - B_2) \quad (\text{E-15})$$

Substituting (E-8) into (E-12), and after some manipulation, we get

$$B_1 = S_1 A_1 + S_2 \quad (\text{E-16})$$

where
$$S_1 = \frac{k_1 d_1 - h_g}{k_1 d_1 + h_g} e^{-2L_1 d_1} \quad (\text{E-17})$$

and
$$S_2 = \frac{h_g \Delta T}{k_1 d_1 + h_g} e^{-L_1 d_1} \quad (\text{E-18})$$

Similarly, substituting (E-9) into (E-13), we get

$$B_2 = S_3 A_2 \quad (\text{E-19})$$

where
$$S_3 = \frac{k_2 d_2 + h_c}{k_2 d_2 - h_c} e^{2L_2 d_2} \quad (\text{E-20})$$

Equations (E-14), (E-15), (E-19) and (E-20) can be easily solved to determine the constants A_1 , A_2 , A_3 and A_4 that appear in Eqns. (E-8) and (E-9). Hence, the exact solutions for time periodic temperature distributions in the two slabs can be obtained from (E-4) and (E-5).

A COMPUTER SIMULATION OF THE
TURBOCHARGED TURBOCOMPOUNDED DIESEL ENGINE SYSTEM
FOR STUDIES OF LOW HEAT REJECTION ENGINE PERFORMANCE

Vol. 2
by

DIONISSIOS NIKOLAOU ASSANIS
"

B.Sc., Marine Engineering
University of Newcastle Upon Tyne
(1980)

S.M., Naval Architecture and Marine Engineering
S.M., Mechanical Engineering
Massachusetts Institute of Technology
(1983)

SUBMITTED IN PARTIAL FULFILLMENT
OF THE REQUIREMENTS FOR THE
DEGREE OF

DOCTOR OF PHILOSOPHY
IN
POWER AND PROPULSION

at the

MASSACHUSETTS INSTITUTE OF TECHNOLOGY

September 1985

VOLUME II

Signature of Author:

Dennis Assanis

Department of Ocean Engineering
September 1985

Certified by:

John B. Heywood

Thesis Supervisor
Prof. John B. Heywood
Dept. of Mechanical Engineering

Accepted by:

Prof. Douglas A. Carmichael, Chairman
Departmental Graduate Committee
Department of Ocean Engineering

MASSACHUSETTS INSTITUTE
OF TECHNOLOGY

MAR 27 1986

LIBRARIES

A COMPUTER SIMULATION OF THE
TURBOCHARGED TURBOCOMPOUNDED DIESEL ENGINE SYSTEM
FOR STUDIES OF LOW HEAT REJECTION ENGINE PERFORMANCE

Vol. 2
by

DIONISSIOS NIKOLAOU ASSANIS
"

B.Sc., Marine Engineering
University of Newcastle Upon Tyne
(1980)

S.M., Naval Architecture and Marine Engineering
S.M., Mechanical Engineering
Massachusetts Institute of Technology
(1983)

SUBMITTED IN PARTIAL FULFILLMENT
OF THE REQUIREMENTS FOR THE
DEGREE OF

DOCTOR OF PHILOSOPHY
IN
POWER AND PROPULSION

at the

MASSACHUSETTS INSTITUTE OF TECHNOLOGY

September 1985

VOLUME II

Signature of Author:

Signature redacted

Department of Ocean Engineering
September 1985

Signature redacted

Certified by:

Thesis Supervisor
Prof. John B. Heywood
Dept. of Mechanical Engineering

Accepted by:

Prof. Douglas A. Carmichael, Chairman
Departmental Graduate Committee
Department of Ocean Engineering

MASSACHUSETTS INSTITUTE
OF TECHNOLOGY

MAR 27 1986

LIBRARIES

APPENDIX F
TURBOCHARGED TURBOCOMPOUNDED
DIESEL ENGINE CYCLE SIMULATION CODE

C (M**3)
C DVOL NO YES TOTAL SWEEP VOLUME OF ENGINE (M**3)
C TIVO YES NO INTAKE VALVE OPENS (DEG)
C TIVC YES NO INTAKE VALVE CLOSES (DEG)
C TEVO YES NO EXHAUST VALVE OPENS (DEG)
C TEVC YES NO EXHAUST VALVE CLOSES (DEG)
C
C

3 MANIFOLD DESIGN PARAMETERS

(J=1 FOR INTAKE, J=2 FOR EXHAUST, J=3 FOR CONNECTING PIPE)

C ELNG(J) YES NO LENGTH (M)
C EDIAM(J) YES YES EFFECTIVE DIAMETER (M)
C EAREA(J) NO YES INTERNAL SURFACE AREA OF MANIFOLD
C (M**2)
C ECROSS(J) NO YES CROSS-SECTIONAL AREA OF MANIFOLD
C (M**2)
C EVOLME(J) NO YES VOLUME (M**3)
C

4 INTERCOOLER DESIGN

C HI(1) NO YES HEAT EXCHANGER EFFECTIVENESS
C HI(2) YES NO COOLANT INLET TEMPERATURE (K)
C HI(3) NO YES AIR TEMPERATURE AT
C INTERCOOLER OUTLET (K)
C HI(4) NO YES SPECIFIC ENTHALPY OF AIR
C AT T = HI(3) (J/kg/K)
C HI(5) YES NO HEAT TRANSFER COEFFICIENT x AREA
C (W/K)
C

5 TURBOCHARGER DATA

C B(1) YES NO ROTATIONAL INERTIA OF TURBOCHARGER
C ROTOR
C B(2) YES NO ROTATIONAL DAMPING OF TURBOCHARGER
C ROTOR
C

6 SYSTEM PRESSURE LOSSES (DELTA P'S) (PA)

C DP(1) YES NO COMPRESSOR EXIT - INTERCOOLER INLET
C DP(2) YES NO INTERCOOLER INLET - INTAKE MANIFOLD
C DP(3) YES NO EXHAUST MANIFOLD - TURBINE INLET
C DP(4) YES NO TURBINE EXIT - POWER TURBINE INLET
C DP(5) YES NO POWER TURBINE EXIT - ATMOSPHERIC
C

7 TURBULENCE SUB-MODEL CONSTANTS

C CBETA YES NO TURBULENT DISSIPATION CONSTANT
C

8 HEAT TRANSFER CONSTANTS: $NU = CONS'T * (REYNOLDS NO.)^{**EXP'NT}$

C

C	CONHT	YES	NO	CONS'T (FOR COMBUSTION CHAMBER)
C	ECONHT	YES	NO	CONS'T (FOR MANIFOLDS)
C	EXPHT	YES	NO	EXP'NT
C	CRAD	YES	NO	RADIATION CONS'T

9 FUEL AND AIR SPECIFICATIONS

C	CX	YES	NO	NUMBER OF CARBON ATOMS IN THE
C	-----	---	--	FUEL (8.0 FOR C8H18)
C	DEL	YES	NO	MOLAR C:H RATIO OF THE FUEL
C	PSI	YES	NO	MOLAR N:O RATIO OF AIR
C	QLOWER	YES	NO	LOWER HEATING VALUE OF FUEL (MJ/KG)

10 INITIAL GUESSES AT THE START OF INTAKE PROCESS

C	PSTART	YES	NO	INITIAL PRESSURE IN CYLINDER (ATM)
C	TSTART	YES	NO	INITIAL TEMPERATURE IN CYLINDER (K)
C	PHISTA	YES	NO	INITIAL AVERAGE CYLINDER EQUIVALENC
C	FSTART	NO	YES	OVERALL CYLINDER FUEL FRACTION
C	MKESTA	YES	NO	INITIAL MEAN K.E. (J)
C	TKESTA	YES	NO	INITIAL TURBULENT K.E. (J)
C	YO(1)	YES	NO	INTAKE MANIFOLD MASS (KG)
C	YO(2)	YES	NO	INTAKE MANIFOLD TEMPERATURE (K)
C	YO(3)	YES	NO	INTAKE MANIFOLD PRESSURE (PA)
C	YO(4)	YES	NO	INTAKE MANIFOLD FUEL FRACTION (-)
C	YO(5)	YES	NO	EXHAUST MANIFOLD MASS (KG)
C	YO(6)	YES	NO	EXHAUST MANIFOLD TEMPERATURE (K)
C	YO(7)	YES	NO	EXHAUST MANIFOLD PRESSURE (PA)
C	YO(8)	YES	NO	EXHAUST MANIFOLD FUEL FRACTION (-)
C	YO(9)	YES	NO	TURBOCHARGER SPEED (RPM * 1000.)

11 TIME INCREMENTS

C	TCALL	YES	NO	CRANK ANGLE INTERVAL AT WHICH
C	-----	---	--	ODERT IS TO BE CALLED
C	TPRINT	YES	NO	PRINTING INTERVAL FOR OUTPUT
C	-----	---	--	(HDCOPY FILE)
C	TSCREEN	YES	NO	PRINTING INTERVAL FOR OUTPUT
C	-----	---	--	(SCREEN)

12 ERROR TOLERANCES

C	AREROT	YES	NO	ERROR TOLERANCE FOR CALCULATING
C	-----	---	--	THE ROOT OF 'G' (SEE SUBROUTINE
C	-----	---	--	ODERT).
C	CIINTG	YES	NO	ERROR TOLERANCE FOR INTEGRATION
C	-----	---	--	DURING INTAKE PROCESS (SEE
C	-----	---	--	SUBROUTINE ODERT).
C	CCINTG	YES	NO	SAME, DURING COMPRESSION PROCESS
C	CBINTG	YES	NO	SAME, DURING COMBUSTION PROCESS

C	CEINTG	YES	NO	SAME, DURING EXHAUST PROCESS
C	REL	YES	NO	RELATIVE ERROR TOLERANCE IN
C	---	---	--	REACHING TEND
C	MAXITS	YES	NO	MAXIMUM NUMBER OF ITERATIONS OF
C	-----	---	--	COMPLETE CYCLE SIMULATION
C	MAXTRY	YES	NO	SEE SUBROUTINE ITRATE
C	MAXERR	YES	NO	SEE SUBROUTINE ITRATE

C*****

C
C DEFINITION OF SYSTEM STATE VARIABLES
C (ALL ARE DOUBLE PRECISION)

C	DT	TIME (DEG)
C	DY(1)	MASS INDUCTED INTO CHAMBER THROUGH
C	----	INTAKE VALVE (KG)
C	DY(2)	MASS EXHAUSTED FROM CHAMBER THROUGH
C	----	EXHAUST VALVE (KG)
C	DY(3)	-----
C	DY(4)	FRACTION OF FUEL MASS BURNED
C	DY(5)	-----
C	DY(6)	MEAN KINETIC ENERGY IN CHAMBER (J)
C	DY(7)	TURBULENT KINETIC ENERGY IN
C	----	CHAMBER (J)
C	DY(8)	HEAT TRANSFER - PISTON TOP (J)
C	DY(9)	HEAT TRANSFER - CYLINDER HEAD (J)
C	DY(10)	HEAT TRANSFER - CYLINDER WALL (J)
C	DY(11)	CYLINDER TEMPERATURE (K)
C	DY(12)	CYLINDER PRESSURE (PA)
C	DY(13)	ELAPSED/PREDICTED IGNITION DELAY TIME
C	DY(14)	-----
C	DY(15)	-----
C	DY(16)	TOTAL WORK TRANSFER (J)
C	DY(17)	TOTAL ENTHALPY EXHAUSTED (J)
C	DY(18)	-----
C	DY(19)	-----
C	DY(20)	BURNED FUEL FRACTION (-)
C	DY(21)	INTAKE MANIFOLD MASS (KG)
C	DY(22)	INTAKE MANIFOLD TEMPERATURE (K)
C	DY(23)	INTAKE MANIFOLD PRESSURE (PA)
C	DY(24)	INTAKE MANIFOLD AVERAGE FUEL FRACTION
C	DY(25)	EXHAUST MANIFOLD MASS (KG)
C	DY(26)	EXHAUST MANIFOLD TEMPERATURE (K)
C	DY(27)	EXHAUST MANIFOLD PRESSURE (PA)
C	DY(28)	EXHAUST MANIFOLD AVERAGE FUEL FRACTION
C	DY(29)	TURBOCHARGER SPEED (RPM * 1000.)
C	DY(30)	POWER TURBINE CUMULATIVE WORK TRANSFER
C	DY(31)	TOTAL MASS FLOWED FROM INTAKE MANIFOLD
C		TO ALL CYLINDERS
C	DY(32)	TOTAL MASS FLOWED FROM COMPRESSOR
C		TO INTAKE MANIFOLD
C	DY(33)	TOTAL MASS FLOWED FROM ALL CYLINDERS
C		TO EXHAUST MANIFOLD
C	DY(34)	TOTAL MASS FLOWED FROM EXHAUST MANIFOLD

C TO FIRST TURBINE
C DY(35) TIME-AVERAGED INTAKE MANIFOLD PRESSURE
C DY(36) TIME-AVERAGED EXHAUST MANIFOLD PRESSURE
C DY(37) TIME-AVERAGED COMPRESSOR DISCHARGE
C TEMPERATURE
C DY(38) TIME-AVERAGED INTERCOOLER OUTLET
C TEMPERATURE
C DY(39) TIME-AVERAGED INTAKE MANIFOLD
C TEMPERATURE
C DY(40) TIME-AVERAGED EXHAUST MANIFOLD
C TEMPERATURE
C DY(41) TIME-AVERAGED TURBOCHARGER TURBINE EXHAUST
C TEMPERATURE
C DY(42) TIME-AVERAGED POWER TURBINE EXHAUST
C TEMPERATURE
C DY(43) TIME-AVERAGED INTERCOOLER EFFECTIVENESS
C DY(44) TIME-AVERAGED COMPRESSOR MAP FLOW
C DY(45) TIME-AVERAGED TURBINE MAP FLOW
C DY(46) TIME-AVERAGED COMPRESSOR MAP SPEED
C DY(47) TIME-AVERAGED TURBINE MAP SPEED
C DY(48) TIME-AVERAGED POWER TURBINE MAP SPEED
C DY(49) TIME-AVERAGED TURBINE PRESSURE RATIO
C DY(50) TIME-AVERAGED COMPRESSOR EFFICIENCY
C DY(51) TIME-AVERAGED TURBINE EFFICIENCY
C DY(52) TIME-AVERAGED POWER TURBINE EFFICIENCY
C DY(53) TIME-AVERAGED POWER TURBINE MAP FLOW
C DY(54) TIME-AVERAGED EFFECTIVE LINEARIZED HEAT
C TRANSFER COEFF. FROM GAS TO PISTON
C DY(55) TIME-AVERAGED PRODUCT OF GAS/PISTON
C HEAT TRANSFER COEFF. TIMES GAS TEMPERATURE
C DY(56) TIME-AVERAGED EFFECTIVE LINEARIZED HEAT
C TRANSFER COEFF. FROM GAS TO CYL. HEAD
C DY(57) TIME-AVERAGED PRODUCT OF GAS/ HEAD
C HEAT TRANSFER COEFF. TIMES GAS TEMPERATURE
C DY(58) TIME-AVERAGED EFFECTIVE LINEARIZED HEAT
C TRANSFER COEFF. FROM GAS TO CYL. LINER
C DY(59) TIME-AVERAGED PRODUCT OF GAS/LINER
C HEAT TRANSFER COEFF. TIMES GAS TEMPERATURE
C DY(60) TIME-AVERAGED POWER TURBINE INLET TEMPEARTURE

C*****

C SYSTEM TEMPERATURE DEFINITIONS

C RTEMP(1) = COMPRESSOR INLET TEMPERATURE
C RTEMP(2) = COMPRESSOR DISCHARGE TEMPERATURE
C RTEMP(3) = TURBINE OUTLET TEMPERATURE
C RTEMP(4) = POWER TURBINE INLET TEMPERATURE
C RTEMP(5) = POWER TURBINE OUTLET TEMPERATURE

C SYSTEM PRESSURE DEFINITIONS

C PINLET = COMPRESSOR INLET PRESSURE
C PRSS(1) = COMPRESSOR DISCHARGE PRESSURE
C PRSS(2) = TURBINE INLET PRESSURE

C PRSS(3) = TURBINE OUTLET PRESSURE
 C PRSS(4) = POWER TURBINE INLET PRESSURE
 C PRSS(5) = POWER TURBINE OUTLET PRESSURE

C SYSTEM MASS FLOW RATE DEFINITIONS

C RMASS(1) = AVERAGE ENGINE INTAKE MASS FLOW
 C RMASS(2) = NOT USED
 C RMASS(3) = CORRECTED COMPRESSOR MASS FLOW (LB/MIN)
 C RMASS(4) = CORRECTED TURBINE MASS FLOW (LB/MIN)
 C RMASS(5) = CORRECTED POWER TURBINE MASS FLOW (LB/MIN)

C SYSTEM SPECIFIC ENTHALPY DEFINITIONS

C H(1) = SPECIFIC ENTHALPY AT ATMOSPHERIC CONDITIONS
 C H(2) = SPECIFIC ENTHALPY OF ENGINE EXHAUST
 C H(3) = SPECIFIC ENTHALPY CHANGE ACROSS COMPRESSOR
 C H(4) = SPECIFIC ENTHALPY CHANGE ACROSS TURBINE
 C H(5) = SPECIFIC ENTHALPY CHANGE ACROSS POWER TURBINE

C CONVERSION AND CORRECTION FACTORS

C RCORR(1) = POWER TURBINE GEAR RATIO, (TURBINE RPM/ RCP RPM)
 C RCORR(2) = MASS FLOW CONVERSION FACTOR FROM LB/MIN TO KG/DEG
 C 1 LB/MIN = 0.45359/60 KG/SEC = .00756 * ESPD KG/DEG
 C 1/RCORR(2)= CONVERTS FORM KG/DEG TO LB/MIN
 C RCORR(3) = TEMPERATURE CORRECTION FACTOR FOR COMPRESSOR MAP
 C RCORR(4) = TEMPERATURE CORRECTION FACTOR FOR TURBINE MAP
 C RCORR(5) = TEMPERATURE CORRECTION FACTOR FOR POWER TURBINE MAP

C*****

C REMARKS

C ALL CRANK ANGLE DATA ARE REFERENCED TO 0.0 DEG @ TDC
 C OF THE INTAKE STROKE (START OF THE INTAKE STROKE)

C SUBROUTINES AND FUNCTION SUBPROGRAMS REQUIRED:

C 1 WORKING SUBROUTINES

C INTAKE CMPRES CMBSTN EXHAUST
 C GCMP GIDEL

C 2 SPECIAL UTILITY SUBROUTINES

C VACDIN VACDEX CSAVDV

C 3 GENERAL UTILITY SUBROUTINES

C PARFIN PFDIF CYLPAR FLAME

```
C      DIFEQ      ICMAP      ITMAP      IPTMAP
C      DELH      THERMO     HPROP     CPROP
C      TRANSP     MFLRT     FUELDT    ENGPAP
C      QDP        SUMIT     FAHR      EQR
C      ODERT     DERT1     ROOT      ITRATE
C      ERRCHK     INTRP     STEP1     RESULT
C
C      METHOD
C      SEE D. N. ASSANIS, PH.D. THESIS, M.I.T., SEPTEMBER 1985
C
C      WRITTEN BY D. N. ASSANIS
C      EDITED BY D. N. ASSANIS
C
C      LOGICAL SPDEL, POWER, SPTEMP, ANNAND, TRANS
C      INTEGER SIZC, SIZT, SIZPT, SIZ1, SIZ2, SIZ3, FUELTP
C      REAL*8 DT, DY(60), TOUT, RELERR, ABSERR, WORK, REROOT, AEROOT
C      REAL MW, MWM, MSTART, MACRSC, MASS, MKESTA,
C      &      MAXERR, MFINAL, MASSIN, MASSEX, KIL, MIL
C
C      INTEGER IROW, EROW
C      PARAMETER (IROW = 46, EROW = 48)
C      DIMENSION TABLIN(IROW,2), TABLEX(EROW,2)
C      PARAMETER (PI=3.1415927, IO=0, I1=1, I2=2)
C      PARAMETER (SIZC=6, SIZT=6, SIZPT=6, SIZ1=7, SIZ2=8, SIZ3=11,
C      &      ITIVO = -11, ITEVC = 736, ITIVC = 212, ITEVO = 505)
C      PARAMETER (CEN = 1.E2, KIL = 1.E3, MIL = 1.E6, ERG = 1.E7,
C      &      ATPA = 1.01325E5, HGPA = 0.2953E-3, PSIPA = 6.8948E3,
C      &      CSFC = 1.644E-3, HPKW = 0.7457 )
C
C      DIMENSION YO(40), Y(60), WORK(1360), IWORK(5),
C      &      MASSIN(ITIVO:ITIVC), MASSEX(ITEVO:ITEVC),
C      &      FCYLIN(ITIVO:ITIVC), FCYLEX(ITEVO:ITEVC),
C      &      HCYLIN(ITIVO:ITIVC), HCYLEX(ITEVO:ITEVC)
C
C      DIMENSION EVOLME(3), ELNG(3)
C
C      DIMENSION CTNEW(6), NCLA(6)
C      DIMENSION PQGAS(2), PQSOL(2), PQSOLN(2), PQAvt(2), PTNEW(2)
C      DIMENSION PTW(2,3,51), NPLA(2)
C
C      COMMON/ITERAS/ ITERAS, ISTEDY
C      COMMON/VECTOR/ DY, DT, IFLAG
C      COMMON/PRINT/ TPRINT, TRES, TSCREEN
C      COMMON/SPTEMP/ SPTEMP
C      COMMON/ANNAND/ ANNAND
C
C      COMMON/RADIATION/ TCHTR, TRHTR, THTR, CHTRAP, CHTRAH, CHTRAW,
C      &      RHTRAP, RHTRAH, RHTRAW
C      COMMON/TOPO/ TOAIR, POAIR, GAMAIR
C      COMMON/FLAME/ TAIR, PAIR, TFLAME, TRAD, EMIS
C
C      COMMON/NCLA/ NCLA, NCC
C      COMMON/CYLPAR/ CDIAM(6), CTHIK(6,3), CCOND(6,3), CHCOOL(6),
C      &      CTCool(6), CUOVE(6)
```

```
COMMON/NPLA/ NPLA, NPC
COMMON/PARFIN/ PDELX(2,3),PCNUM(2,3),INNOD(2,3),PTHIK(2,3),
& PCOND(2,3), PHEFF(2,3), PDIFU(2,3), PHCOOL(2), PTCOOL(2),
& PUOVE(2)
COMMON/PFDIF/ PTW
COMMON/PHLIN/ PHLIN(2), TGAS
COMMON/PQSOL/ PQSOL
COMMON/PERFACT/ PERI, FACT, DELT
```

C

```
COMMON/POWER/POWER
COMMON/TABLIN/ TABLIN
COMMON/TABLEX/ TABLEX
COMMON/SUMIT/ ENGM(2), FMDOT(2), HMDOT(2)
COMMON/EHF/ENT(6), HAL(6), FAL(6), TFLAG, TAL(6)
COMMON/BURN/ FMIN
COMMON/D / ERPM
COMMON/DTDTH/ ESPD
COMMON/FUEL/ FUELTP, CX, HY, DEL, PSI, AFRAST, QLOWER, HFORM
COMMON/ARRAY/ MASSIN, MASSEX, FCYLIN, FCYLEX, HCYLIN, HCYLEX
COMMON/MSTA/ MSTART
COMMON/MA/ YPM(2), YPH
COMMON/RHMAS/ RHO, MASS, VOLUME, HH, GAMMA
COMMON/VALVE/ VIV, VEV
COMMON/B / CPM(2), HM(2), MWM(2), GM(2), RHOM(2)
COMMON/K /RTEMP(5), H(5), RMASS(5), RCORR(5)
COMMON/NEWDIF / ASP(3), PR(3), PRSS(5), DP(5), HI(5),
& TMAP(2), PTMAP(2), CMAP(2),
& CM(SIZC,SIZ1,3), TM(SIZT,SIZ2,3), PTM(SIZPT,SIZ3,3),
& CRPM(SIZC),TRPM(SIZT),PTRPM(SIZPT), PSTD(3), TSTD(3)
COMMON/PROFIL/ DTBRN, ALPHA, CSP1, CSP2, CSD1, CSD2
COMMON/FBRATE/ FBRATE
COMMON/HTRC/ CONHT, EXPHT
COMMON/CRAD/ CRAD
COMMON/TEMPS/ TPSTON, THEAD, TCW
COMMON/AREAS/ AHEAD, APSTON
COMMON/TURBU/ CBETA , MACRSC, UPRIME, VMKE, VPISTO
COMMON/HEATS/ CVHTRN, HTRCOE, HTPAPI, HTPAHD, HTPACW, HTRAPI,
& HTRAHD, HTRACW, THTRAN
COMMON/QP1/ EDIAM(3), EAREA(3), ECROSS(3), ETWALL(3), ECONHT(3)
COMMON/QP2/ EPRF(3), EVBLK(3), EREF(3), ENUF(3), EHTCOE(3),
& EQDOT(3)
COMMON/EMKT/ EMKT(3)
COMMON/I/ PINLET
COMMON/EPARAM/ BORE, STROKE, CONRL, CYLCA, CSATDC, CMRTIO, CLVTDC
COMMON/TCPAR/ B(2)
COMMON/TIMES/ TIVO, TEVC, TIVC, TINJ, TIGN, TEVO
COMMON/ITRLIM/ MAXTRY, MAXERR
```

C

```
NAMELIST/INPUT/ POWER, SPTEMP, TRANS, ANNAND, SPDEL, ERPM,
& FUELTP, FMIN, TINJ, TIGN, TIVO, TIVC, TEVO, TEVC, ICYL, BORE,
& CLVTDC, ELNG, EDIAM, HI, B, PTTEF, EMKT, DP, RCORR, CFR2,
& CFR3, TATM, PATM, PINLET, CFACTR, DTBRN, TPSTON, THEAD, TCW,
& ETWALL, EXPHT, CONHT, CRAD, CBETA, ECONHT, PSTART, TSTART,
& PHISTA, MKESTA, TKESTA, YO, PRSS, RTEMP, TCALL, TPRINT, TSCREN,
```

& CIINTG, CBINTG, CCINTG, CEINTG, REL, AREROT, MAXITS, MAXERR,
& MAXTRY, MINITS, FSEC1, FSEC2, CSC, TSC, PTSC

C

EXTERNAL INTAKE, CMPRES, CMBSTN, EXHAUST, GCMP, GIDEL

C

#####

C

STANDARD DATA SET -- OVERRIDE BY USING NAMELIST INPUT

C

ANNAND = .FALSE.
SPTMP = .FALSE.
POWER = .TRUE.
SPDEL = .TRUE.
TRANS = .FALSE.

C

ERPM = 1900.
FUELTP = 1
TINJ = 338.
TIGN = 342.
FMIN = 0.188

C

PINLET = 0.94
RTEMP(1) = 303.
PATM = 0.94
TATM = 303.

C

ICYL = 6
BORE = 13.97
CLVTDC = 173.035

C

TIVO = -11.0
TIVC = 212.0
TEVO = 505.0
TEVC = 736.0

C

CFR2 = 7.0
CFR3 = 1.5

C

ELNG(1) = 0.7
ELNG(2) = 1.0
ELNG(3) = 0.5
EDIAM(1) = 0.1
EDIAM(2) = 0.1
EDIAM(3) = 0.13

C

HI(1) = 0.9
HI(2) = 305.
HI(3) = 305.
HI(5) = 1200.

C

B(1) = 4.E-5
B(2) = 5.E-7
PTTEF = 0.90

RCORR(1)	=	0.017
CSC	=	1.0
TSC	=	1.0
PTSC	=	1.0
C-----		
CFACTR	=	1.05
CBETA	=	1.5
DTBRN	=	125.
C-----		
TPSTON	=	800.
THEAD	=	800.
TCW	=	450.
ETWALL(1)	=	305.
ETWALL(2)	=	750.
ETWALL(3)	=	600.
CONHT	=	.055
ECONHT(1)	=	.035
ECONHT(2)	=	.035
ECONHT(3)	=	.035
EXPHT	=	.8
CRAD	=	2.
C-----		
DP(1)	=	2000.
DP(2)	=	1000.
DP(3)	=	1000.
DP(4)	=	1000.
DP(5)	=	5000.
C-----		
EMKT(1)	=	1.0
EMKT(2)	=	2.0
EMKT(3)	=	1.0
C-----		
PRSS(4)	=	1.3E5
PRSS(5)	=	1.05E5
C-----		
PSTART	=	3.6
TSTART	=	800.
PHISTA	=	0.47
MKESTA	=	2.5E-3
TKESTA	=	1.1E-3
YO(2)	=	320.
YO(3)	=	240.E3
YO(4)	=	0.0
YO(6)	=	860.
YO(7)	=	330.E3
YO(8)	=	0.0336
YO(9)	=	64.
C-----		
TCALL	=	1.0
TPRINT	=	6.0
TSCREN	=	100.0
C-----		
REL	=	1.E-4
AREROT	=	1.E-4


```
      TM(I,J,2) = TM(I,J,2) * TSC
3     CONTINUE
4     CONTINUE
C
C       (POWER TURBINE)
C
      READ (5,*) PSTD(3), TSTD(3)
      DO 6 I = 1, SIZPT
      READ (5,*) PTRPM(I)
      DO 5 J = 1, SIZ3
      READ (5,*) (PTM(I,J,K), K = 1,3)
      PTM(I,J,2) = PTM(I,J,2) * PTSC
5     CONTINUE
6     CONTINUE
C
      DO 771 I = 1, IROW
      READ(75,*) (TABLIN(I,J), J=1,2)
771  CONTINUE
C
      DO 772 I = 1, EROW
      READ(76,*) (TABLEX(I,J), J=1,2)
772  CONTINUE

      CLOSE (UNIT=3)
      CLOSE (UNIT=4)
      CLOSE (UNIT=5)
      CLOSE (UNIT=8)
      CLOSE (UNIT=75)
      CLOSE (UNIT=76)
C
      CALL FUELDT
      FSTART = PHISTA / (PHISTA + AFRAST)
C
C       CONVERT INPUT PARAMETERS TO SI UNITS
C
      BORE   = BORE / 100.
      PSTART = PSTART * ATPA
      PATM   = PATM * ATPA
      PINLET = PINLET * ATPA
      CLVTDC = CLVTDC * 1.E-6
      FMIN   = FMIN * 1.E-3
C
C       READ IN CHAMBER GEOMETRY DATA AND CALCULATE BASIC
C       GEOMETRIC ENGINE PARAMETERS AND CONSTANTS
C
      CALL ENGPARG

      DVOLUM = PI * BORE * BORE * STROKE/4.
      DVOL   = FLOAT(ICYL) * DVOLUM
      CMRTIO = (CLVTDC + DVOLUM)/CLVTDC
      CYLCA  = .7853982 * BORE * BORE
      ESPD   = 1./(6. * ERPM)
C
      DELT = ESPD
```

```
PERI = 720. * DELT
C
IF(.NOT.SPTEMP) CALL PARFIN
IF(.NOT.SPTEMP) CALL CYLPAR
C
C   PERFORM GEOMETRIC CALCULATIONS FOR INTAKE AND EXHAUST
C   MANIFOLDS AND TURBINE CONNECTING PIPE.
C
DO 8 J = 1, 3
EAREA(J) = PI * EDIAM(J) * ELNG(J)
ECROSS(J) = PI * EDIAM(J) * EDIAM(J) / 4.
EVOLME(J) = ECROSS(J) * ELNG(J)
8 CONTINUE
C
C   APPROXIMATE AVERAGE ENGINE INTAKE MASS FLOW (LB/MIN):
C
CALL THERMO(YO(2),YO(3),YO(4),HM(1),CPM(1),G3,G4,RHOM(1),G5,
&           G6,G7,GM(1),MWM(1),G10,G11,G12)
RCORR(2) = .0075667 * ESPD
RMASS(1) = 0.9 * DVOL * RHOM(1) /720. /RCORR(2)
C
C   ASSIGN INITIAL VALUES TO ENTHALPIES, TEMPERATURES,
C   MASS FLOW RATES AND EQUIVALENCE RATIOS:
C
FR = FMIN * FLOAT(ICYL) / 720. /RCORR(2)
C
CALL THERMO ( YO(2), YO(3), 0., HGIN, XXB, XXC, XXD,
&           XXE, XXF, XXG, XXH, XXI, XXJ, XXK, XXL, XXM)
CALL THERMO ( YO(6), YO(7), FSTART, HGEX, XXB, XXC, XXD,
&           XXE, XXF, XXG, XXH, XXI, XXJ, XXK, XXL, XXM)
C
DO 777 I = ITIVO, ITIVC
AAA = FLOAT(I-ITIVO) /FLOAT(ITIVC-ITIVO) * PI
MASSIN(I) = 360. /ICYL /((TIVC-TIVO) * PI * RMASS(1)
&           * RCORR(2) * SIN(AAA))
FCYLIN(I) = 0.
HCYLIN(I) = HGIN,
777 CONTINUE
C
DO 778 I = ITEVO, ITEVC
BBB = FLOAT(I-ITEVO) /FLOAT(ITEVC-ITEVO) * PI
MASSEX(I) = 360. /ICYL /((TEVC-TEVO) * PI * (RMASS(1)+FR)
&           * RCORR(2) * SIN(BBB))
FCYLEX(I) = FSTART
HCYLEX(I) = HGEX
778 CONTINUE
C
TE = YO(6)
YO(8) = FSTART
C
CALL THERMO (RTEMP(1), YO(3), YO(4), H(1), X1, X2, X3,
&           X4, X5, X6, X7, X8, X9, X10, X11, X12)
CALL THERMO (TE, YO(7), YO(8), H(2), V1, V2, V3,
```

```
&          V4, V5, V6, V7, V8, V9, V10, V11, V12)
C
C      INITIALIZE SOME SYSTEM TEMPERATURES
C
RTEMP(3) = 0.85 * YO(6)
RTEMP(2) = YO(2)
RTEMP(4) = RTEMP(3)
RTEMP(5) = RTEMP(4)
C
C      INITIALIZE VARIOUS SYSTEM PRESSURES:
C
PRSS(1) = YO(3) + DP(1) + DP(2)
PRSS(2) = YO(7) - DP(3)
PRSS(5) = PATM + DP(5)
C
C      FIND COMPRESSOR, TURBINE AND POWER TURBINE MAP
C      TEMPERATURE CORRECTION FACTORS:
C
RCORR(3) = SQRT(TSTD(1)/RTEMP(1))
RCORR(4) = SQRT(TSTD(2)/YO(6))
RCORR(5) = SQRT(TSTD(3)/YO(6))
C
C
C      CALCULATE MANIFOLD MASSES FROM OTHER INITIAL STATES,
C      GIVEN VOLUME AND IDEAL GAS LAW, FOR EACH MANIFOLD:
C
14 CALL THERMO(YO(6),YO(7),YO(8),HM(2),CPM(2),Q3,Q4,RHOM(2),Q5,
&          Q6, Q7, GM(2), MWM(2), Q10, Q11, Q12)
YO(1) = RHOM(1) * EVOLME(1)
YO(5) = RHOM(2) * EVOLME(2)
C
C*****
C
C      START OF CURRENT CYCLE ITERATION
C*****
C
DO 470 ITERAS = 1, MAXITS
C
WRITE (7,880) ITERAS, MAXITS
C
C      CALCULATE MASS IN CYLINDER
C
CALL THERMO ( TSTART, PSTART, FSTART, HSTART, XXB, XXC, XXD,
&          RHO, XXE, XXF, XXG, XXH, XXI, XXJ, XXK, XXL)
CALL CSAVDV (TIVO, XXA, VOLUME, XXB)
MSTART = RHO * VOLUME
C
C      PREPARE ALL OUTPUT FILES FOR OUTPUT FROM THIS ITERATION
C
REWIND 6
REWIND 12
REWIND 13
REWIND 14
```

```
REWIND 36
REWIND 37
C
C   WRITE MAIN HEADINGS AND ECHO INPUT PARAMETERS
C
WRITE (6,222)
IF (.NOT. POWER) WRITE (6,2899)
IF (POWER) WRITE (6,2900)
C
WRITE (6,222)
WRITE (6,2901)
WRITE (6,222)
WRITE (6,2914)
IF (SPDEL) WRITE (6,2905)
IF (.NOT.SPDEL) WRITE (6,2906)
IF (SPTEMP) WRITE (6,2907)
IF (.NOT.SPTEMP .AND. ITERAS .LT. ISTEDY) WRITE (6,2908)
IF (.NOT.SPTEMP .AND. ITERAS .GT. ISTEDY) WRITE (6,2909)
IF (ANNAND) WRITE (6,2910)
IF (.NOT. ANNAND) WRITE (6,2911)
C
WRITE (6,222)
WRITE (6,2902)
IF (FUELTP .EQ. 1) WRITE (6,2903)
IF (FUELTP .EQ. 2) WRITE (6,2904)
WRITE (6,2913) ERPM, TINJ, FMIN*KIL, FR, PINLET/ATPA, RTEMP(1),
&          PATM/ATPA, TATM
WRITE (6,222)
C
WRITE (6,111)
WRITE (6,2918)
WRITE (6,2919) ICYL, BORE*CEN, STROKE*CEN, CONRL*CEN, CMRTIO,
&          DVOLUM*MIL, CLVTDC*MIL, DVOL*KIL, CFR2, CFR3,
&          TIVO, TIVC, TEVO, TEVC
WRITE (6,222)
C
WRITE (6,*) ' >>>> MANIFOLD DIMENSIONS           INTAKE',
& '          EXHAUST'
WRITE (6,*) ' '
WRITE (6,*) 'LENGTH                               (M) ',ELNG(1),ELNG(2)
WRITE (6,*) ' '
WRITE (6,*) 'DIAMETER                             (M)',EDIAM(1), EDIAM(2)
WRITE (6,*) ' '
WRITE (6,*) 'CROSS-SECTIONAL AREA                (M**2)',ECROSS(1),
&          ECROSS(2)
WRITE (6,*) ' '
WRITE (6,*) 'INTERNAL SURFACE AREA                (M**2)',EAREA(1),
&          EAREA(2)
WRITE (6,*) ' '
WRITE (6,*) 'VOLUME                               (LT) ',EVOLME(1)*1000.,
&          EVOLME(2)*1000.
WRITE (6,*) ' '
WRITE (6,222)
C
```

```
WRITE (6,*) '>>>> TURBINE CONNECTING PIPE DIMENSIONS'  
WRITE (6,*) ' '  
WRITE (6,*) 'LENGTH (M) ',ELNG(3)  
WRITE (6,*) ' '  
WRITE (6,*) 'DIAMETER (M) ',EDIAM(3)  
WRITE (6,*) ' '  
WRITE (6,*) 'CROSS-SECTIONAL AREA (M**2) ',ECROSS(3)  
WRITE (6,*) ' '  
WRITE (6,*) 'INTERNAL SURFACE AREA (M**2) ',EAREA(3)  
WRITE (6,*) ' '  
WRITE (6,*) 'VOLUME (LT) ',EVOLME(3)*1000.  
WRITE (6,*) ' '  
WRITE (6,222)
```

C

```
WRITE (6,111)  
WRITE (6,*) '>>>> TURBOMACHINERY DATA'  
WRITE (6,*) ' '  
WRITE (6,*) 'T/C INERTIA (KG-M**2) ',B(1)  
WRITE (6,*) ' '  
WRITE (6,*) 'T/C DAMPING (KG-M**2/S) ',B(2)  
WRITE (6,*) ' '  
WRITE (6,*) 'P.TURBINE TRANSMISSION EFFIC.',PTTEF  
WRITE (6,*) ' '  
WRITE (6,*) 'P.TURBINE GEAR RATIO', RCORR(1)  
WRITE (6,*) ' '  
WRITE (6,222)  
WRITE (6,*) '>>>> SYSTEM PRESSURE DROPS IN PA'  
WRITE (6,*) ' '  
WRITE (6,*) 'COMPRESSOR EXIT - INTERCOOLER INLET', DP(1)  
WRITE (6,*) ' '  
WRITE (6,*) 'INTERCOOLER INLET - INTAKE MANIFOLD', DP(2)  
WRITE (6,*) ' '  
WRITE (6,*) 'EXHAUST MANIFOLD - TURBINE INLET', DP(3)  
WRITE (6,*) ' '  
WRITE (6,*) 'TURBINE EXIT - POWER TURBINE INLET', DP(4)  
WRITE (6,*) ' '  
WRITE (6,*) 'POWER TURBINE EXIT - ATMOSPHERIC', DP(5)  
WRITE (6,222)
```

C

```
WRITE (6,2916)  
WRITE (6,2917) CONHT, ECONHT(1),ECONHT(2), ECONHT(3), EXPHT,  
& TPSTON, THEAD, TCW, ETWALL(1), ETWALL(2), ETWALL(3),  
& CBETA  
IF (ANNAND) WRITE (6,2930) CRAD  
WRITE (6,222)
```

C

```
IF (SPTMP) GO TO 191  
WRITE (6,111)  
WRITE (6,8861)  
DO 18 I = 1, NPC  
IF (I.EQ.1) WRITE (6,8862)  
IF (I.EQ.2) WRITE (6,8863)  
WRITE (6,8865) (ILAYER, ILAYER=1, NPLA(I))  
WRITE (6,8867) (PTHIK(I,J), J=1, NPLA(I))
```

```
WRITE (6,8868) (PCOND(I,J), J=1, NPLA(I))
WRITE (6,8869) (PDIFU(I,J), J=1, NPLA(I))
WRITE (6,8870) (INNODE(I,J), J=1, NPLA(I))
WRITE (6,8871) INT(FACT * INNODE(I,1))
WRITE (6,8872) (PCNUM(I,J), J=1, NPLA(I))
IF (PHCOOL(I).EQ.0.) WRITE (6,8880) PTCOOL(I), PUOVE(I)
IF (PHCOOL(I).NE.0.) WRITE (6,8881) PTCOOL(I),
& PHCOOL(I), PUOVE(I)
WRITE (6,*) ' '
18 CONTINUE
C
DO 19 I =1, NCC
WRITE (6,8864)
WRITE (6,8865) (ILAYER, ILAYER=1, NCLA(I))
WRITE (6,8866) CDIAM(I)
WRITE (6,8867) (CTHIK(I,J), J=1, NCLA(I))
WRITE (6,8868) (CCOND(I,J), J=1, NPLA(I))
IF (CHCOOL(I).EQ.0.) WRITE (6,8880) CTCOOL(I), CUOVE(I)
IF (CHCOOL(I).NE.0.) WRITE (6,8881) CTCOOL(I),
& CHCOOL(I), CUOVE(I)
WRITE (6,*) ' '
19 CONTINUE
C
WRITE (6,222)
C
191 CONTINUE
C
WRITE (6,111)
WRITE (6,2920)
WRITE (6,2921) MAXITS, ITERAS, TCALL, TPRINT, TSCREEN,
& CIINTG, CCINTG, CBINTG, CEINTG, AREROT,
& REL, MAXERR, MAXTRY
WRITE (6,222)
WRITE (6,111)
WRITE (6,2998)
WRITE (6,222)
WRITE (6,2999)
WRITE (6,222)
WRITE (6,3110)
WRITE (6,3596)
WRITE (6,222)
C
WRITE (12,111)
WRITE (12,6111)
WRITE (12,222)
WRITE (12,3110)
WRITE (12,6594)
WRITE (12,222)
C
WRITE (13,111)
WRITE (13,7111)
WRITE (13,222)
WRITE (13,3110)
WRITE (13,7592)
WRITE (13,222)
```

```
C      IF (.NOT. ANNAND) THEN
      WRITE (14,111)
      WRITE (14,8111)
      WRITE (14,8592)
      WRITE (14,222)
      ENDIF

C      IF (TRANS) THEN
      WRITE (36,111)
      WRITE (36,9111)
      WRITE (36,222)

C      WRITE (37,111)
      WRITE (37,9112)
      WRITE (37,222)
      ENDIF

C
C      INITIALIZE PARAMETERS FOR CALL TO SUBROUTINE ODERT
C
      DO 161 I = 1, 60
      Y(I) = 0.
161  CONTINUE

C      Y(6)  = MKESTA
      Y(7)  = TKESTA
      Y(11) = TSTART
      Y(12) = PSTART
      Y(20) = FSTART

C      DO 16 I = 1, 9
      Y(20+I) = Y0(I)
16  CONTINUE

C      HEATI = 0.0
      WORKI = 0.0
      VIV = 0.0

C      DO 17 I = 1, 60
      DY(I) = Y(I)
17  CONTINUE

C
C      WRITE(6,4210) TIVO,DY(12)/ATPA, DY(11), DY(1)*KIL, DY(2)*KIL,
      & EQR(DY(20)),DY(23)/ATPA,DY(22),DY(27)/ATPA,DY(26),IFLAG
      AEROT = AREROT
      REROT = AREROT

C
```

```
C#####  
C  
C      START OF INTAKE PROCESS (TIVO - TIVC)  
C  
C#####  
C  
C      20 I = 0  
C          NEQN = 60  
C          IFLAG = 1  
C          T = TIVO  
C          TEND = 180.  
C          DT = T  
C  
C      CALL SUMIT (T, DY(24), HM(1), 1., MASSIN, FCYLIN, HCYLIN,  
C      &          ITIVO, ITIVC, ENGM(1), FMDOT(1), HMDOT(1) )  
C  
C      AEX = T  
C      IF (T .LE. FLOAT(ITEVC - 720)) AEX = T + 720.  
C      CALL SUMIT (AEX, DY(28), HM(2), -1., MASSEX, FCYLEX, HCYLEX,  
C      &          ITEVO, ITEVC, ENGM(2), FMDOT(2), HMDOT(2) )  
C  
C      30 I = I + 1  
C          TCALL:   CRANK ANGLE INCREMENT AT WHICH ODERT  
C                  IS TO BE CALLED  
C  
C          NCALL = IFIX( ABS(TEND - T)/TCALL )  
C  
C          NCALL:   NO. OF TIMES INTEGRATING SUBROUTINE IS CALLED  
C  
C          DO 60 NC = 1, NCALL  
C              TOUT = T + TCALL  
C          50     ABSERR = CIINTG  
C              RELERR = CIINTG  
C  
C          CALL ODERT (INTAKE, NEQN, DY, DT, TOUT, RELERR, ABSERR,  
C          &          IFLAG, WORK, IWORK, GCMP, REROOT, AEROOT)  
C  
C          T = DT  
C  
C          IF(.NOT.SPTEMP .AND. ITERAS.GT.ISTEDY) THEN  
C              CALL PFDIF(1, TPIS)  
C              TPSTON = TPIS  
C              CALL PFDIF(2, THD)  
C              THEAD = THD  
C              ENDIF  
C  
C          MASSIN(IFIX(T)) = YPM(1)  
C          FCYLIN(IFIX(T)) = DY(20)  
C          HCYLIN(IFIX(T)) = YPH  
C          CALL SUMIT (T, DY(24), HM(1), 1., MASSIN, FCYLIN, HCYLIN,  
C          &          ITIVO, ITIVC, ENGM(1), FMDOT(1), HMDOT(1) )  
C  
C          IEX = IFIX(T) + 720  
C          IF (IEX.GT.ITEVC) GO TO 51
```

```
MASSEX(IEX) = YPM(2)
FCYLEX(IEX) = DY(20)
HCYLEX(IEX) = YPH
C
51  AEX = T
    IF (T .LE. FLOAT(ITEVC - 720)) AEX = T + 720.
    CALL SUMIT (AEX, DY(28), HM(2), -1., MASSEX,FCYLEX,HCYLEX,
&    ITEVO, ITEVC, ENGM(2), FMDOT(2), HMDOT(2) )
C
    CALL RESULT (1)
C
    IF (ABS(T/TEND - 1.0) .LE. REL) GO TO 190
    IF (IFLAG .NE. 2) GO TO 50
60  CONTINUE
C
190 CONTINUE
    IF (I .EQ. 2) GO TO 200
    HEATI = DY(8) + DY(9) + DY(10)
    WORKI = DY(16)
    TEND = TIVC
    GO TO 30
C
C#####
C
C    END OF INTAKE PROCESS
C
C#####
C
200 CONTINUE
C
    ZMAST = MSTART + DY(1) - DY(2)
C
C    CALCULATE TOTAL MASS OF AIR INDUCTED IN THIS CYCLE (AMIN)
C
    AMIN = DY(1)
C
C    CALCULATE VOLUMETRIC EFFICIENCY RELATIVE TO INTAKE MANIFOLD
C    CONDITIONS (VOLEFI) AND ATMOSPHERIC CONDITIONS (VOLEFA)
C
    TIM = DY(22)
    PIM = DY(23)
    VOLEFI = 100. * AMIN / ( DVOLUM * RHOM(1) )
    VOLEFA = VOLEFI * (PIM/PATM) * (TATM/TIM)
    WRITE (7,891) VOLEFI
C
    WRITE (6,222)
    WRITE (6,111)
    WRITE (6,3111)
    WRITE (6,3597)
    WRITE (6,222)
C
    WRITE (12,222)
    WRITE (12,111)
    WRITE (12,3111)
```

```
WRITE (12,6594)
WRITE (12,222)
C
WRITE (13,222)
WRITE (13,111)
WRITE (13,3111)
WRITE (13,7592)
WRITE (13,222)
C
QREL = 0.0
QIVC = DY(8) + DY(9) + DY(10)
C
C#####
C
C OPTION 1: START OF COMPRESSION PROCESS (TIVC - TINJ)
C OPTION 2: START OF COMPRESSION & IGNITION DELAY PROCESS(TIVC-TIGN)
C
C#####
C
C
NEQN = 60
IFLAG = 1
T = TIVC
TEND = TINJ
IF (SPDEL) TEND = TIGN
DT = T
NCALL = IFIX( ABS(TEND - T)/TCALL )
C
DO 220 NC = 1, NCALL
TOUT = T + TCALL
210 ABSERR = CCINTG
RELERR = CCINTG
C
CALL ODERT (CMPRES, NEQN, DY, DT, TOUT, RELERR, ABSERR,
& IFLAG, WORK, IWORK, GCMP, REROOT, AEROOT)
T = DT
C
IF(.NOT.SPTEMP .AND. ITERAS.GT.ISTEDY) THEN
CALL PFDIF(1, TPIS)
TPSTON = TPIS
CALL PFDIF(2, THD)
THEAD = THD
ENDIF
C
CALL SUMIT (T, DY(24), HM(1), 1., MASSIN, FCYLIN, HCYLIN,
& ITIVO, ITIVC, ENGM(1), FMDOT(1), HMDOT(1) )
C
AEX = T
CALL SUMIT (AEX, DY(28), HM(2), -1., MASSEX,FCYLEX,HCYLEX,
& ITEVO, ITEVC, ENGM(2), FMDOT(2), HMDOT(2) )
C
QREL = -( DY(8) + DY(9) + DY(10) - QIVC )/
& (FMIN * QLOWER)
C
CALL RESULT (2)
```

```
C
      IF (ABS(T/TEND - 1.0) .LE. REL) GO TO 250
      IF (IFLAG .NE. 2) GO TO 210
220 CONTINUE
C
250 CONTINUE
      IF (SPDEL) GO TO 227
C
C#####
C
C      OPTION 1: START OF IGNITION DELAY PERIOD (TINJ - TIGN)
C#####
C
251 NEQN = 60
      IFLAG = 1
      T = TINJ
      TEND = TEVO
      DT = T
      NCALL = IFIX( ABS(TEND - T)/TCALL )
C
      DO 225 NC = 1, NCALL
          TOUT = T + TCALL
215      ABSERR = CCINTG
          RELERR = CCINTG
C
          CALL ODERT (CMPRES, NEQN, DY, DT, TOUT, RELERR, ABSERR,
&                   IFLAG, WORK, IWORK, GIDEL, RERoot, AERoot)
C
          T = DT
C
          IF(.NOT.SPTEMP .AND. ITERAS.GT.ISTEDY) THEN
              CALL PFDIF(1, TPIS)
              TPSTON = TPIS
              CALL PFDIF(2, THD)
              THEAD = THD
              ENDIF
C
          IF (IFLAG .EQ. 8) GO TO 226
          CALL SUMIT (T, DY(24), HM(1), 1., MASSIN, FCYLIN, HCYLIN,
&                   ITIVO, ITIVC, ENGM(1), FMDOT(1), HMDOT(1) )
C
          AEX = T
          CALL SUMIT (AEX, DY(28), HM(2), -1., MASSEX, FCYLEX, HCYLEX,
&                   ITEVO, ITEVC, ENGM(2), FMDOT(2), HMDOT(2) )
C
          QREL = -( DY(8) + DY(9) + DY(10) - QIVC )/
&                (FMIN * QLOWER)
C
          CALL RESULT (2)
C
          IF (IFLAG .NE. 2) GO TO 215
225 CONTINUE
C
```

```
226 WRITE(7,882) DT, DY(12)/ATPA, IFLAG
    WRITE(6,4211) DT, DY(12)/ATPA, DY(11), EQR(DY(20)), DY(23)/ATPA,
    &    DY(22), DY(27)/ATPA, DY(26), IFLAG
    WRITE(12,6210) DT, DY(6), DY(7), VIV, VEV, VMKE,
    &    UPRIME, CVHTRN, MACRSC*CEN
    WRITE(13,7210) DT, HTRCOE, HTPAPI/KIL, HTPAHD/KIL,
    &    HTPACW/KIL, THTRAN/KIL
C
227 HEATC = DY(8) + DY(9) + DY(10) - HEATI
    WORKC = DY(16) - WORKI
C
C#####
C
C    END OF COMPRESSION PROCESS
C
C#####
C
C    REINITIALIZE 'ODERT' FOR START OF COMBUSTION
C
C
C    TIGN = T
C    TIDEL = TIGN - TINJ
C    DELMS = TIDEL * 1000. * ESPD
C
C
C    DY(4) = 0
C    MASS = MSTART + DY(1) - DY(2) + DY(4)
C    AIRMAS = MASS * (1. - DY(20))
C    PHIOVE = (FMIN / AIRMAS) * AFRAST
C    ALPHA = 0.
C    DELMIN = (0.926 * PHIOVE**0.37)**(1./0.26)
C    IF (DELMS .GT. DELMIN)
C    &    ALPHA = 1. - 0.926 * PHIOVE**0.37 / DELMS**0.26
C
C
C    THE FOLLOWING COMBUSTION CORRELATION CONSTANTS MUST BE
C    CALIBRATED AGAINST ENGINE CYLINDER PRESSURE DATA.
C
C
C    CSP1 = 2. + 1.25E-8 * (DELMS * ERPM)**2.4
C    CSP2 = 5000.
C
C
C    CSD1 = 14.2 / PHIOVE**0.644
C    CSD2 = CFACTR * CSD1**0.25
C
C
C    TOAIR = DY(11)
C    POAIR = DY(12)
C    CALL THERMO (TOAIR, POAIR, 0.,X1, X2, X3, X4, X5, X6, X7, X8,
C    &    GAMAIR, X9, X10, X11, X12)
C
C
C    WRITE (6,111)
C    WRITE (6,3112)
C    WRITE (6,3598)
C    WRITE (6,222)
C
C
C    WRITE (12,111)
C    WRITE (12,3112)
C    WRITE (12,6594)
```

```
WRITE (12,222)
C
WRITE (13,111)
WRITE (13,3112)
WRITE (13,7592)
WRITE (13,222)
C
IF (SPDEL) GO TO 256
C
C#####
C
START OF COMBUSTION PROCESS (TIGN - TEVO)
C
C#####
C
228 NEQN = 60
IFLAG = 1
T = DT
ITX = INT(T)
TX = REAL(ITX)
235 TOUT = TX + 1.0
245 ABSERR = CCINTG
RELERR = CCINTG
C
CALL ODERT (CMBSTN, NEQN, DY, DT, TOUT, RELERR, ABSERR,
& IFLAG, WORK, IWORK, GCMP, REROOT, AEROOT)
C
T = DT
C
IF(.NOT.SPTEMP .AND. ITERAS.GT.ISTEDY) THEN
CALL PFDIF(1, TPIS)
TPSTON = TPIS
CALL PFDIF(2, THD)
THEAD = THD
ENDIF
C
CALL SUMIT (T, DY(24), HM(1), 1., MASSIN, FCYLIN, HCYLIN,
& ITIVO, ITIVC, ENGM(1), FMDOT(1), HMDOT(1) )
C
AEX = T
CALL SUMIT (AEX, DY(28), HM(2), -1., MASSEX, FCYLEX, HCYLEX,
& ITEVO, ITEVC, ENGM(2), FMDOT(2), HMDOT(2) )
C
QREL = DY(4) - ( DY(8) + DY(9) + DY(10) - QIVC )/
& (FMIN * QLOWER)
C
CALL RESULT (3)
C
IF (ABS(T/TEND - 1.0) .LE. REL) GO TO 255
IF (IFLAG .NE. 2) GO TO 245
255 CONTINUE
C
256 NEQN = 60
IFLAG = 1
```

```
T = DT
IF (SPDEL) T = TIGN
TEND = TEVO
DT = T
NCALL = IFIX( ABS(TEND - T)/TCALL )
C
DO 350 NC = 1, NCALL
  TOUT = T + TCALL
340  ABSERR = CBINTG
  RELERR = CBINTG
C
  CALL ODERT (CMBSTN,NEQN,DY,DT,TOUT,RELERR,ABSERR,IFLAG,
&            WORK,IWORK,GCMP,REROOT,AEROOT)
  T = DT
C
  IF(.NOT.SPTEMP .AND. ITERAS.GT.ISTEDY) THEN
  CALL PFDIF(1, TPIS)
  TPSTON = TPIS
  CALL PFDIF(2, THD)
  THEAD = THD
  ENDIF
C
  CALL SUMIT (T, DY(24), HM(1), 1., MASSIN, FCYLIN, HCYLIN,
&            ITIVO, ITIVC, ENGM(1), FMDOT(1), HMDOT(1) )
C
  AEX = T
  CALL SUMIT (AEX, DY(28), HM(2), -1., MASSEX,FCYLEX,HCYLEX,
&            ITEVO, ITEVC, ENGM(2), FMDOT(2), HMDOT(2) )
C
  QREL = DY(4) - ( DY(8) + DY(9) + DY(10) - QIVC )/
&            (FMIN * QLOWER)
C
  CALL RESULT (3)
C
  IF (ABS(T/TEND - 1.0) .LE. REL) GO TO 380
  IF (IFLAG .NE. 2) GO TO 340
350 CONTINUE
C
380 CONTINUE
C
C#####
C
C      START OF EXHAUST PROCESS (TEVO - TIVO)
C
C#####
C
  WRITE (6,222)
  WRITE (6,111)
  WRITE (6,3113)
  WRITE (6,3599)
  WRITE (6,222)
C
  WRITE (12,222)
  WRITE (12,111)
```

```
WRITE (12,3113)
WRITE (12,6594)
WRITE (12,222)
C
WRITE (13,222)
WRITE (13,111)
WRITE (13,3113)
WRITE (13,7592)
WRITE (13,222)
C
VEV = 0.0
C
C      REINITIALIZE 'ODERT' FOR START OF EXHAUST
C
I = 0
NEQN = 60
IFLAG = 1
T = TEVO
TEND = 540.
DT = T
390 I = I + 1
    NCALL = IFIX( ABS(TEND - T)/TCALL )
C
DO 410 NC = 1, NCALL
    TOUT = T + TCALL
400   ABSERR = CEINTG
    RELERR = CEINTG
C
    CALL ODERT (EXHAUST,NEQN,DY,DT,TOUT,RELERR,ABSERR,IFLAG,
&              WORK,IWORK,GCMP,REROOT,AEROOT)
C
    T = DT
C
    IF(.NOT.SPTEMP .AND. ITERAS.GT.ISTEDY) THEN
    CALL PFDIF(1, TPIS)
    TPSTON = TPIS
    CALL PFDIF(2, THD)
    THEAD = THD
    ENDIF
C
    MASSEX(IFIX(T)) = YPM(2)
    FCYLEX(IFIX(T)) = DY(20)
    HCYLEX(IFIX(T)) = YPH
C
    CALL SUMIT (T, DY(24), HM(1), 1., MASSIN, FCYLIN, HCYLIN,
&              ITIVO, ITIVC, ENGM(1), FMDOT(1), HMDOT(1) )
C
    AEX = T
    CALL SUMIT (AEX, DY(28), HM(2), -1., MASSEX,FCYLEX,HCYLEX,
&              ITEVO, ITEVC, ENGM(2), FMDOT(2), HMDOT(2) )
C
    CALL RESULT (4)
C
    IF (ABS(T/TEND - 1.0) .LE. REL) GO TO 440
```

```

      IF (IFLAG .NE. 2) GO TO 400
410 CONTINUE
C
440 CONTINUE
      IF (I .EQ. 2) GO TO 450
C
      HEATCE = DY(8) + DY(9) + DY(10) - HEATI
      WORKCE = DY(16) - WORKI
      TEND = TIVO + 720.
      GO TO 390
C
C#####
C
      END OF EXHAUST PROCESS
C
C#####
C
450 CONTINUE
C
      HEATE = DY(8) + DY(9) + DY(10) - HEATCE - HEATI
      WORKE = DY(16) - WORKCE - WORKI
      WRITE (6,222)
C
      CONVERT STATE VARIABLES FROM DOUBLE TO SINGLE PRECISION:
C
      DO 454 J = 1, 60
      Y(J) = DY(J)
454 CONTINUE
C
      RE-INITIALIZE STATE VARIABLES FOR NEXT ITERATION:
C
      MKESTA = Y(6)
      TKESTA = Y(7)
      PSTART = Y(12)
      TSTART = Y(11)
      FSTART = Y(20)
C
      DO 466 J = 1, 40
      YO(J) = Y(J+20)
466 CONTINUE
C
      IF(SPTEMP) GO TO 1964
C
      PROCEED FOR PREDICTED WALL TEMPERATURE OPTIONS.
C
      CALCULATE CYCLE-AVERAGE QUANTITIES FOR WALL HEAT BALANCE:
C
      DY(54) = DY(54)/720.
      DY(55) = DY(55)/720.
      DY(56) = DY(56)/720.
      DY(57) = DY(57)/720.
      DY(58) = DY(58)/720.
      DY(59) = DY(59)/720.
C
```

```
C          CALCULATE APPARENT STEADY-STATE WALL TEMPERATURES,
C          BASED ON WALL HEAT BALANCE.
C
PTNEW(1) = (PUOVE(1)*PTCOOL(1) + DY(55))/(PUOVE(1)+DY(54))
PTNEW(2) = (PUOVE(2)*PTCOOL(2) + DY(57))/(PUOVE(2)+DY(56))
C
CTNEW(1) = (CUOVE(1)*CTCOOL(1) + DY(59))/(CUOVE(1)+DY(58))
C          CALCULATE AVERAGE HEAT FLUX FROM THE GAS TO THE SURFACE
C          OF THE PISTON AND THE HEAD:
C
PQGAS(1) = DY(8) /APSTON /ESPD /720.
PQGAS(2) = DY(9) /AHEAD /ESPD /720.
C
IF(ITERAS.GT.ISTEDY) GO TO 469
C
          DO THIS LOOP ONLY FOR QUASI STEADY-STATE CALCULATION
C
TPSTON = PTNEW(1)
THEAD  = PTNEW(2)
TCW    = CTNEW(1)
C
PQSOL(1) = PQGAS(1)
PQSOL(2) = PQGAS(2)
C
IF(ABS((PQSOL(1)-PQAVT(1))/PQSOL(1))+
& ABS((PQSOL(2)-PQAVT(2))/PQSOL(2)) .LT. FSEC1 .AND.
& ABS((DY(31)-DY(32))/DY(31)) .LE. 0.002 .AND.
& ABS((DY(33)-DY(34))/DY(33)) .LE. 0.002) GO TO 471
C
PQAVT(1) = PQSOL(1)
PQAVT(2) = PQSOL(2)
GO TO 1964
C
7811 CONTINUE
PQAVT(1) = PQSOL(1)
PQAVT(2) = PQSOL(2)
ISTEDY = ITERAS
C
          INITIALIZE TRANSIENT PROFILES TO ZERO
C
DO 7838 I = 1, 2
DO 7826 J = 1, NPLA(I)
DO 7822 K = 1, INNODE(I,J)
PTW(I,J,K)= 0.
7322 CONTINUE
7826 CONTINUE
7838 CONTINUE
C
GO TO 1964
C
469 CONTINUE
C
          DO THIS LOOP FOR TRANSIENT CALCULATION.
C          CALCULATE GAS-SIDE AVERAGE HEAT TRANSFER TO WALL
```

C

```
PQSOLN(1) = PQGAS(1)
PQSOLN(2) = PQGAS(2)
IF(ABS((PQSOLN(1)-PQAVT(1))/PQSOLN(1))
& + ABS((PQSOLN(2)-PQAVT(2))/PQSOLN(2)).LT.FSEC2) GO TO 471
PQAVT(1) = PQSOLN(1)
PQAVT(2) = PQSOLN(2)
```

C

```
1964 H(2) = DY(17) / DY(2)
```

C

C

C

```
OUTPUT DATA AT THE END OF MAXITS ITERATIONS
```

```
WRITE (6,111)
WRITE (6,*) '>>>> INSTANTANEOUS SYSTEM DATA AFTER', ITERAS,
& ' ENGINE CYCLES'
WRITE (6,*) ' '
WRITE (6,222)
WRITE (6,*) ' >>>> MANIFOLD HEAT TRANSFER DATA INTAKE',
& ' EXHAUST'
WRITE (6,*) ' '
WRITE (6,*) ' '
WRITE (6,*) 'MANIFOLD WALL TEMPERATURES (K)', ETWALL(1),
& ETWALL(2)
WRITE (6,*) ' '
WRITE (6,*) 'AVERAGE VELOCITY (M/S) ',EVBLK(1),EVBLK(2)
WRITE (6,*) ' '
WRITE (6,*) 'REYNOLDS NUMBER (FILM) ',EREF(1), EREF(2)
WRITE (6,*) ' '
WRITE (6,*) 'PRANDTL NUMBER ',EPRF(1), EPRF(2)
WRITE (6,*) ' '
WRITE (6,*) 'NUSSELT NUMBER ',ENUF(1), ENUF(2)
WRITE (6,*) ' '
WRITE (6,*) 'HEAT TRANSFER COEFF. (W/K/M**2) ', EHTCOE(1),
& EHTCOE(2)
WRITE (6,*) ' '
WRITE (6,*) 'HEAT TRANSFER RATE (W) ',EQDOT(1),EQDOT(2)
WRITE (6,*) ' '
WRITE (6,*) ' '
WRITE (6,222)
```

C

```
WRITE (6,*) ' >>>> TURBINE CONN. PIPE HEAT TRANSFER DATA'
WRITE (6,*) ' '
WRITE (6,*) ' '
WRITE (6,*) 'PIPE WALL TEMPERATURE (K)', ETWALL(3)
WRITE (6,*) ' '
WRITE (6,*) 'AVERAGE VELOCITY (M/S) ',EVBLK(3)
WRITE (6,*) ' '
WRITE (6,*) 'REYNOLDS NUMBER (FILM) ',EREF(3)
WRITE (6,*) ' '
WRITE (6,*) 'PRANDTL NUMBER (FILM) ',EPRF(3)
WRITE (6,*) ' '
WRITE (6,*) 'NUSSELT NUMBER ',ENUF(3)
WRITE (6,*) ' '
WRITE (6,*) 'HEAT TRANSFER COEFF. (W/K/M**2) ', EHTCOE(3)
```

```
WRITE (6,*) ' '
WRITE (6,*) 'HEAT TRANSFER RATE (W) ',EQDOT(3)
WRITE (6,*) ' '
WRITE (6,*) ' '
WRITE (6,222)
C
WRITE(7,*) 'TOTAL ENG. FLOWS (G/CYCLE)',DY(31)*KIL,DY(33)*KIL
WRITE(7,*) 'COMP FLOW, TRB FLOW (G/CYCLE)',DY(32)*KIL,DY(34)*KIL
C
      IF (SPTEMP .AND. ITERAS .GT. MINITS .AND.
&        ABS((DY(31)-DY(32))/DY(31)) .LE. 0.002 .AND.
&        ABS((DY(33)-DY(34))/DY(33)) .LE. 0.002) GO TO 471
470 CONTINUE
C
C*****
C
C      END OF CURRENT CYCLE ITERATION
C
C*****
C
C      CALCULATION RESULTS FOR THIS CYCLE
C
471 AVREXH = H(2)
   TGUESS = 900.
   PEM = DY(27)
   CALL ITRATE ( TGUESS, PEM, Y(20) , AVREXH, XXA, XXB, XXC,
&              XXD, XXE, XXF, XXG, XXH, XXI, XXJ, XXK, XXL)
   AVREXT = TGUESS
C
WRITE (6,111)
WRITE (6,*) '>>>> TIME-AVERAGED SYSTEM DATA AFTER', ITERAS -1,
&          ' ENGINE CYCLES'
WRITE (6,*) ' '
C
C      DEFINE THE FOLLOWING VARIABLES:
C
APCD = Y(35) + DP(2) + DP(1)
APTI = Y(36) - DP(3)
APTD = APTI / Y(49)
APPTI= APTD - DP(4)
APPTD= PATM + DP(5)
DELP = Y(35) - Y(36)
C
WRITE (6,222)
WRITE (6,*) ' >>>>PRESSURE DATA (ATM) (IN-HG)'
WRITE (6,*) ' '
WRITE (6,*) ' '
WRITE (6,*) 'COMPRESSOR INLET ',PINLET/ATPA , PINLET*HGPA
WRITE (6,*) ' '
WRITE (6,*) 'COMPRESSOR DISCHARGE',APCD/ATPA , APCD*HGPA
WRITE (6,*) ' '
WRITE (6,*) 'INTAKE MANIFOLD ',Y(35)/ATPA , Y(35)*HGPA
WRITE (6,*) ' '

```

```
WRITE (6,*) 'EXHAUST MANIFOLD      ',Y(36)/ATPA ,   Y(36)*HGPA
WRITE (6,*) ' '
WRITE (6,*) 'TURBINE INLET        ',APTI/ATPA,  APTI*HGPA
WRITE (6,*) ' '
WRITE (6,*) 'TURBINE DISCHARGE    ',APTD/ATPA,  APTD*HGPA
WRITE (6,*) ' '
IF (.NOT.POWER) GO TO 473
472 WRITE (6,*) 'POWER TURBINE INLET ',APPTI/ATPA,  APPTI*HGPA
WRITE (6,*) ' '
WRITE (6,*) 'P. TURBINE DISCHARGE',APPTD/ATPA,  APPTD*HGPA
WRITE (6,*) ' '
473 WRITE (6,*) 'DELTA P ENGINE      ',DELP/ATPA,  DELP*HGPA
WRITE (6,*) ' '
WRITE (6,*) ' '
WRITE (6,222)
```

C

```
WRITE (6,*) ' >>>>TEMPERATURE DATA      (K)              (F) '
WRITE (6,*) ' '
WRITE (6,*) ' '
WRITE (6,*) 'COMPRESSOR INLET      ', RTEMP(1), FAHR(RTEMP(1))
WRITE (6,*) ' '
WRITE (6,*) 'COMPRESSOR DISCHARGE', Y(37), FAHR(Y(37))
WRITE (6,*) ' '
WRITE (6,*) 'INTERCOOLER OUTLET   ', Y(38), FAHR(Y(38))
WRITE (6,*) ' '
WRITE (6,*) 'INTAKE MANIFOLD      ', Y(39), FAHR(Y(39))
WRITE (6,*) ' '
WRITE (6,*) 'ENGINE EXHAUST      ', AVREXT,FAHR(AVREXT)
WRITE (6,*) ' '
WRITE (6,*) 'EXHAUST MANIFOLD    ', Y(40), FAHR(Y(40))
WRITE (6,*) ' '
WRITE (6,*) 'TURBINE INLET       ', Y(40), FAHR(Y(40))
WRITE (6,*) ' '
WRITE (6,*) 'TURBINE EXHAUST     ', Y(41), FAHR(Y(41))
WRITE (6,*) ' '
IF (.NOT.POWER) GO TO 475
474 WRITE (6,*) 'POWER TURBINE INLET ', Y(60), FAHR(Y(60))
WRITE (6,*) ' '
WRITE (6,*) 'P. TURBINE EXHAUST  ', Y(42), FAHR(Y(42))
WRITE (6,*) ' '
475 WRITE (6,*) ' '
WRITE (6,222)
```

C

```
WRITE (6,111)
IF(.NOT.POWER) GO TO 477
476 WRITE (6,*) '>>>TURBOCHARGER DATA  COMPRESSOR      TURBINE ',
& '      P.TURBINE'
WRITE (6,*) ' '
WRITE (6,*) ' '
WRITE (6,*) 'MAP FLOW (LB/MIN)   ',Y(44), Y(45), Y(53)
WRITE (6,*) ' '
WRITE (6,*) 'MAP SPEED (KRPM)   ',Y(46), Y(47), Y(48)
WRITE (6,*) ' '
WRITE (6,*) 'PRESSURE RATIOS:   ',APCD/PINLET, Y(49), APPTI/APPTD
```

```
WRITE (6,*) ' '  
WRITE (6,*) 'EFFICIENCIES:      ',Y(50), Y(51), Y(52)  
WRITE (6,*) ' '  
GO TO 478
```

C

```
477 WRITE (6,*) '>>>>TURBOCHARGER DATA  COMPRESSOR      TURBINE '  
WRITE (6,*) ' '  
WRITE (6,*) ' '  
WRITE (6,*) 'MAP FLOW (LB/MIN)      ',Y(44), Y(45)  
WRITE (6,*) ' '  
WRITE (6,*) 'MAP SPEED (KRPM)        ',Y(46), Y(47)  
WRITE (6,*) ' '  
WRITE (6,*) 'PRESSURE RATIOS:          ',APCD/PINLET, Y(49)  
WRITE (6,*) ' '  
WRITE (6,*) 'EFFICIENCIES:            ',Y(50), Y(52)  
WRITE (6,*) ' '  
WRITE (6,*) ' '  
WRITE (6,222)
```

C

```
478 WRITE (6,*) ' >>>>> INTERCOOLER DATA  '  
WRITE (6,*) ' '  
WRITE (6,*) 'INTERCOOLER EFFECTIVENESS    ',Y(43)  
WRITE (6,*) ' '  
WRITE (6,*) 'COOLANT INLET TEMPERATURE      ',HI(2)  
WRITE (6,*) ' '  
WRITE (6,*) 'INTERCOOLER "A*U" (W/K)          ',HI(5)  
WRITE (6,*) ' '  
WRITE (6,222)
```

C

C

CALCULATE MASS REMAINING IN CYLINDER

C

C

```
480 CALL THERMO ( Y(11), Y(12), Y(20) , HFINAL, CSUBP, CSUBT, CSUBF,  
&      RHO, DRHODT,DRHODP,DRHODF, GAMMA, MW, ADUMY, BDUMY,CDUMY)  
CALL CSAVDV (TIVO, ACW, VOLUME, DVDT)  
MFINAL = RHO * VOLUME
```

C

C

CALCULATE NET AND GROSS THERMAL EFFICIENCIES

C

```
THREFN = 100. * DY(16)/(FMIN * QLOWER)  
THREFG = 100. * WORKCE/(FMIN * QLOWER)  
HEATX  = 100. * (DY(8) + DY(9) + DY(10))/(FMIN * QLOWER)  
ZPMEP  = (WORKI + WORKE)/DVOLUM  
ZIMEP  = WORKCE / DVOLUM  
ZISFC  = MIL * 3600. * FMIN/WORKCE
```

C

C

CALCULATE MEAN PISTON SPEED IN FPM . THEN, CALCULATE
FRICTION MEP BASED ON MILLINGTON & HARTLES CORRELATION.

C

C

```
VPFPM  = 2. * STROKE * ERPM  
CFR1   = CMRTIO - 4.  
ZFMEP  = (CFR1 + CFR2 * (ERPM/1000.) +  
&      CFR3 * (VPFPM/1000.)**2 ) * PSIPA  
FWORK  = ZFMEP * DVOLUM
```

BWORK = DY(16) - FWORK
THREFB = 100. * BWORK / (FMIN * QLOWER)
ZBMEP = ZIMEP + ZPMEP - ZFMEP
ZBSFC = MIL * 3600. * FMIN / BWORK

C
C
C

ENERGY BALANCE

CYHSTA = HSTART * MSTART
CYHIN = HM(1) * DY(1)
CYHEX = DY(17)
CYHEAT = HEATI + HEATCE + HEATE
CYWORK = WORKI + WORKCE + WORKE
CYHFIN = HFINAL * MFINAL
DECYCL = CYHFIN + CYHEX + CYHEAT + CYWORK - CYHIN - CYHSTA
DEONHI = 100.0 * DECYCL / (CYHIN + CYHSTA)
DEONQ = 100.0 * DECYCL / (FMIN * QLOWER)
WRITE (6,111)
WRITE (6,5910)
WRITE (6,222)
WRITE (6,5920) VOLEFI, VOLEFA, ZPMEP/ATPA, ZPMEP/PSIPA,
& ZIMEP/ATPA, ZIMEP/PSIPA, ZFMEP/ATPA, ZFMEP/PSIPA,
& ZBMEP/ATPA, ZBMEP/PSIPA, ZISFC, ZISFC*CSFC, ZBSFC, ZBSFC*CSFC,
& THREFG, THREFN, THREFB, HEATX, AVREXT
WRITE (6,222)

C

ENWORK = BWORK * FLOAT(ICYL)
ENHEAT = FLOAT(ICYL) * FMIN * QLOWER
PTWORK = DY(30) * PTTEF
ENBHP = ENWORK/KIL * ERPM/60. / 2.
PTBHP = PTWORK/KIL * ERPM/60. / 2.
TBSFC = MIL * 3600. * FLOAT(ICYL) * FMIN / (ENWORK + PTWORK)
BTHEFF = 100. * (ENWORK + PTWORK) / ENHEAT
WRITE (6,111)
WRITE (6,5922)
WRITE (6,222)
WRITE (6,5923) ENWORK/KIL, PTWORK/KIL, ENHEAT/KIL,
& ENBHP, ENBHP/HPKW, PTBHP, PTBHP/HPKW,
& TBSFC, TBSFC * CSFC, BTHEFF

C

WRITE (6,111)
WRITE (6,5939)
WRITE (6,5940) MSTART*KIL, ZMAST*KIL, AMIN*KIL, FMIN*KIL
WRITE (6,222)

C

WRITE (6,5960)
WRITE (6,5961) HEATI/KIL, WORKI/KIL
WRITE (6,5962) HEATC/KIL, WORKC/KIL
WRITE (6,5963) HEATCE/KIL, WORKCE/KIL
WRITE (6,5964) HEATE/KIL, WORKE/KIL
WRITE (6,222)
WRITE (6,5989)
WRITE (6,5990) CYHSTA/KIL, CYHIN/KIL, CYHEX/KIL, CYHEAT/KIL,
& WORK/KIL, BWORK/KIL, CYHFIN/KIL, DECYCL/KIL, DEONHI, DEONQ
WRITE (6,222)


```
2908 FORMAT (/,' PREDICTED QUASI-STEADY WALL TEMPERATURES')
2909 FORMAT (/,' PREDICTED TRANSIENT WALL TEMPERATURES')
2910 FORMAT (/,' ANNAND RADIATION MODEL')
2911 FORMAT (/,' FLAME RADIATION MODEL')
2913 FORMAT (/,' ENGINE SPEED = ',F7.1,' RPM',/
& /,' INJECTION TIMING = ',F7.1,' DEG CA',/
& /,' FUEL INJECTED /CYL /CYCLE = ',F7.4,' G',/
& /,' TOTAL FUELING RATE = ',F7.4,' LB/MIN',/
& /,' COMPRESSOR INLET PRESSURE = ',F10.4,' ATM',/
& /,' COMPRESSOR INLET TEMPERATURE = ',F8.2,' K',/
& /,' ATMOSPHERIC PRESSURE = ',F10.4,' ATM',/
& /,' ATMOSPHERIC TEMPERATURE = ',F8.2,' K',/)
```

C

```
2918 FORMAT (/,' >>>> ENGINE DESIGN PARAMETERS',/)
2919 FORMAT (/,' NUMBER OF CYLINDERS = ',I4,/
& /,' CYLINDER BORE = ',F9.3,' CM',/
& /,' CRANKSHAFT STROKE = ',F9.3,' CM',/
& /,' CONNECTING ROD LENGTH = ',F9.3,' CM',/
& /,' COMPRESSION RATIO = ',F9.3,/
& /,' DISPLACED VOLUME = ',F9.3,' CC',/
& /,' CLEARANCE VOLUME = ',F9.3,' CC',/
& /,' ENGINE DISPLACEMENT = ',F9.3,' LT',/
& /,' FRICTION CONSTANT 2 = ',F9.3,/
& /,' FRICTION CONSTANT 3 = ',F9.3,/
& /,' INTAKE VALVE OPENS = ',F7.1,' DEG CA',/
& /,' INTAKE VALVE CLOSES = ',F7.1,' DEG CA',/
& /,' EXHAUST VALVE OPENS = ',F7.1,' DEG CA',/
& /,' EXHAUST VALVE CLOSES = ',F7.1,' DEG CA',/)
```

C

```
2916 FORMAT (/,' >>>> HEAT TRANSFER AND TURBULENCE',
& ' PARAMETERS',/)
2917 FORMAT (/,' HEAT TRANSFER CONSTANT(CHAMBER)= ',F10.4,/
& /,' HEAT TRANSFER CONSTANT(INT MAN)= ',F10.4,/
& /,' HEAT TRANSFER CONSTANT(EXH MAN)= ',F10.4,/
& /,' HEAT TRANSFER CONSTANT(C. PIPE)= ',F10.4,/
& /,' HEAT TRANSFER EXPONENT = ',F10.4,/
& /,' PISTON TEMPERATURE = ',F9.2,' K',/
& /,' CYLINDER HEAD TEMPERATURE = ',F9.2,' K',/
& /,' CYLINDER WALL TEMPERATURE = ',F9.2,' K',/
& /,' INT. MANIFOLD WALL TEMPERATURE = ',F9.2,' K',/
& /,' EXH. MANIFOLD WALL TEMPERATURE = ',F9.2,' K',/
& /,' CONN. PIPE WALL TEMPERATURE = ',F9.2,' K',/
& /,' TURBULENT DISSIPATION CONSTANT = ',F10.4/)
```

C

```
2930 FORMAT (/,' RADIATION CONSTANT (ANNAND) = ',F10.4/)
```

C

```
2920 FORMAT (/,' >>>> COMPUTATIONAL PARAMETERS',/)
2921 FORMAT (/,' MAXIMUM # OF ITERATIONS = ',I4,/
& /,' OUTPUT AT ITERATION # = ',I4,/
& /,' TCALL = ',F9.2,/
& /,' TPRINT = ',F9.2,/
& /,' TSCREEN = ',F9.2,/
& /,' CIINTG = ',F13.6,/
& /,' CCINTG = ',F13.6,/)
```

```
&      /,'   CBINTG           = ',F13.6,/
&      /,'   CEINTG           = ',F13.6,/
&      /,'   AREROT           = ',F13.6,/
&      /,'   REL              = ',F13.6,/
&      /,'   MAXERR           = ',F13.6,/
&      /,'   MAXTRY           = ',I6,/'
```

C

```
2998 FORMAT (/,' >>>> OUTPUT DATA',/)
```

```
2999 FORMAT (/,' >>>> ENGINE CRANK-ANGLE BY CRANK-ANGLE RESULTS',/)
```

C

```
3110 FORMAT (///(1X,' >>>> START OF INTAKE PROCESS      '))//)
```

C

```
3111 FORMAT (///(1X,' >>>> START OF COMPRESSION PROCESS  '))//)
```

C

```
3112 FORMAT (///(1X,' >>>> START OF COMBUSTION AND EXPANSION PROCESSES
&      '))//)
```

C

```
3113 FORMAT (///(1X,' >>>> START OF EXHAUST PROCESS      '))//)
```

C

```
3596 FORMAT ((4X,'CA',8X,'P',8X,'TEMP',8X,'MIN',8X,'MEX',8X,
&      'PHI',8X,'PIM',8X,'TIM',8X,'PEM',8X,'TEM',4X,'IFG')/
&      (2X,'(DEG)',5X,'(ATM)',7X,'(K)',8X,'(G)',8X,'(G)',
&      8X,'(-)',7X,'(ATM)',7X,'(K)',7X,'(ATM)',7X,'(K)',
&      4X,'(-)'))
```

C

```
3597 FORMAT ((4X,'CA',7X,'P',9X,'TEMP',30X,'PHI',8X,'PIM',8X,
&      'TIM',8X,'PEM',8X,'TEM',4X,'IFG')/
&      (2X,'(DEG)',4X,'(ATM)',7X,'(K)',31X,'(-)',7X,'(ATM)',
&      7X,'(K)',7X,'(ATM)',7X,'(K)',4X,'(-)'))
```

C

```
3598 FORMAT ((4X,'CA',7X,'P',9X,'TEMP',30X,'PHI',
&      8X,'PIM',8X,'TIM',8X,'PEM',8X,'TEM',4X,'IFG')/
&      (2X,'(DEG)',4X,'(ATM)',8X,'(K)',30X,'(-)',7X,
&      '(ATM)',7X,'(K)',7X,'(ATM)',7X,'(K)',
&      4X,'(-)'))
```

C

```
3599 FORMAT ((4X,'CA',8X,'P',8X,'TEMP',19X,'MEX',8X,'PHI',
&      8X,'PIM',8X,'TIM',8X,'PEM',8X,'TEM',4X,'IFG')/
&      (2X,'(DEG)',5X,'(ATM)',7X,'(K)',19X,'(G)',8X,'(-)',
&      7X,'(ATM)',7X,'(K)',7X,'(ATM)',7X,'(K)',
&      4X,'(-)'))
```

C

```
4210 FORMAT (1X,F6.1,2X,F9.4,2X,F9.2,2X,F9.5,2X,F9.5,
&      2X,F9.5,2X,F9.4,2X,F9.2,2X,F9.4,2X,F9.2,2X,I2)
```

C

```
4211 FORMAT (1X,F6.1,2X,F9.4,2X,F9.2,24X,
&      F9.5,2X,F9.4,2X,F9.2,2X,F9.4,2X,F9.2,2X,I2)
```

C

```
4212 FORMAT (1X,F6.1,2X,F9.4,2X,F9.2,24X,F9.5,2X,F9.4,
&      2X,F9.2,2X,F9.4,2X,F9.2,2X,I2)
```

C

```
4213 FORMAT (1X,F6.1,2X,F9.4,2X,F9.2,13X,F9.5,2X,F9.5,
&      2X,F9.4,2X,F9.2,2X,F9.4,2X,F9.2,2X,I2)
```

C

5910 FORMAT (///(3X,'>>>> DIESEL ENGINE PERFORMANCE RESULTS '))//)

C

5920 FORMAT (/' VOLUMETRIC EFFICIENCY; (%) ')/
& (' BASED ON: INTAKE / ATM ',2(F9.1))//
& (' PUMPING MEAN EFF. PRESSURE ')/
& (' (ATM, PSI) : PMEP ',2(F10.2))//
& (' GROSS IND. MEAN EFF. PRESSURE ')/
& (' (ATM, PSI) : IMEP ',2(F10.2))//
& (' FRICTION MEAN EFF. PRESSURE ')/
& (' (ATM, PSI) : FMEP ',2(F10.2))//
& (' BRAKE MEAN EFF. PRESSURE ')/
& (' (ATM, PSI) : BMEP ',2(F10.2))//
& (' GROSS INDICATED S.F.C. ')/
& (' (G/KW/HR, LB/HP/HR) : ISFC ',2(F10.3))//
& (' BRAKE S.F.C. ')/
& (' (G/KW/HR, LB/HP/HR) : BSFC ',2(F10.3))//
& (' GROSS INDICATED THERMAL ')/
& (' EFFICIENCY; (%) ',F7.1)//
& (' NET INDICATED THERMAL ')/
& (' EFFICIENCY; (%) ',F7.1)//
& (' CYLINDER BRAKE THERMAL ')/
& (' EFFICIENCY; (%) ',F7.1)//
& (' (CYL. HEAT TRANSFER PER CYCLE)/ ')/
& (' (MASS OF FUEL TIMES LHV) : (%) ',F7.1)//
& (' MEAN EXHAUST ')/
& (' TEMPERATURE; (K) ',F7.1)//

5922 FORMAT (///(3X,'>>>> TOTAL SYSTEM PERFORMANCE RESULTS '))//)

5923 FORMAT (/' DIESEL WORK ')/
& (' PER CYCLE; (KJ) ',F10.6)//
& (' POWER TURBINE WORK ')/
& (' PER CYCLE (KJ) ',F10.6)//
& (' TOTAL HEAT INPUT ')/
& (' PER CYCLE (KJ) ',F10.6)//
& (' DIESEL BRAKE POWER ')/
& (' (KW, HP) : ENBHP ',2(F10.1))//
& (' POWER TRB. BRAKE POWER ')/
& (' (KW, HP) : PTBHP ',2(F10.1))//
& (' OVERALL BRAKE S.F.C. ')/
& (' (G/KW/HR, LB/HP/HR) : BSFC ',2(F10.3))//
& (' OVERALL BRAKE THERMAL ')/
& (' EFFICIENCY; (%) ',F7.1)//

C

5939 FORMAT (/, ' >>>> CYLINDER MASS SUMMARY', /)
5940 FORMAT (/ (' MASS IN CYLINDER AT TIVO = ',F8.5,' G')//
& (' MASS IN CYLINDER AT TIVC = ',F8.5,' G')//
& (' MASS OF AIR INDUCTED = ',F8.5,' G')//
& (' MASS OF FUEL INJECTED = ',F8.5,' G')//

C

5960 FORMAT (/, ' >>>> CYLINDER HEAT & WORK TRANSFERS', /)
5961 FORMAT (/ (' HEATI = ',F10.6,' KJ', ' (TIVO - 180)')//
& (' WORKI = ',F10.6,' KJ')//

C

5962 FORMAT (/ (' HEATC = ',F10.6,' KJ', ' (180 - TIGN)')//
& (' WORKC = ',F10.6,' KJ')//

```
C
5963 FORMAT ( / ( ' HEATCE = ',F10.6,' KJ',' (180 - 540)')/
&          ( ' WORKCE = ',F10.6,' KJ')/)

C
5964 FORMAT ( / ( ' HEATE = ',F10.6,' KJ',' (540 - TIVO)')/
&          ( ' WORKE = ',F10.6,' KJ')/)

C
5989 FORMAT (/,' >>>> CYLINDER ENERGY BALANCE',/)
5990 FORMAT ( / ( ' INITIAL ENTHALPY /CYL / CYCLE = ',F9.5,' KJ')//
&          ( ' TOTAL ENTHALPY IN /CYL/ CYCLE = ',F9.5,' KJ')//
&          ( ' TOTAL ENTHALPY OUT/CYL/ CYCLE = ',F9.5,' KJ')//
&          ( ' TOTAL HEAT LOSS / CYL / CYCLE = ',F9.5,' KJ')//
&          ( ' IND. WORK OUTPUT / CYL /CYCLE = ',F9.5,' KJ')//
&          ( ' BRAKE WORK OUTPUT /CYL /CYCLE = ',F9.5,' KJ')//
&          ( ' RESIDUAL ENTHALPY /CYL/ CYCLE = ',F9.5,' KJ')//
&          ( ' NET ENERGY GAIN / CYL/CYCLE = ',F9.5,' KJ')//
&          ( ' (ENERGY GAIN)/(H @ IVC) = ',F9.5,' % ')//
&          ( ' (ENERGY GAIN)/(MFUEL*LHV) = ',F9.5,' % ')//

C
5991 FORMAT (/,' >>>> COMBUSTION SUMMARY',/)
5992 FORMAT (//,' IGNITION DELAY PERIOD =', F8.3,' DEG CA',
&          //,' IGNITION TIMING =', F8.3,' DEG CA',
&          //,' BURN DURATION =',F8.3,' DEG CA',
&          //,' WEIGHTING FACTOR =',F8.3,
&          //,' PREMIXED CONSTANT 1 =',F8.3,
&          //,' PREMIXED CONSTANT 2 =',F8.3,
&          //,' DIFFUSION CONSTANT 1 =',F8.3,
&          //,' DIFFUSION CONSTANT 2 =',F8.3,
&          //,' CFACTR =',F8.3,/)

C
6111 FORMAT (///, ' >>>> TURBULENT FLOW MODEL')

C
6594 FORMAT (//(9X,'CA',7X,'MEANKE',8X,'TURBKE',10X,'VIV', 10X, 'VEV',
&          9X,'VMKE',9X,
&          'UPRIME',8X, 'CVHTRN', 9X, 'MACRSC')/
&          (8X,'(DEG)',6X,'(J)',12X,'(J)',9X,'(M/SEC)',6X, '(M/SEC)',
&          6X, '(M/SEC)',6X, '(M/SEC)', 7X, '(M/SEC)', 10X,'(CM)'))

C
6210 FORMAT (5X, F7.1, 4X, F9.5, 5X, F9.5, 4X, F10.3, 3X, F10.3, 3X,
&          F10.3, 3X, F10.3, 4X, F10.3, 4X, F10.3)

C
7111 FORMAT (///, ' >>>> HEAT TRANSFER DATA')

C
7592 FORMAT (//(9X,'CA', 8X, 'HTRCOE', 8X, 'HTPAPI', 8X, 'HTPAHD',
&          8X, 'HTPACW', 7X, 'THTRAN')/
&          (8X, '(DEG)', 4X, '(W/M**2/K)', 5X, '(KW/M**2)', 5X,
&          '(KW/M**2)', 5X, '(KW/M**2)', 6X, '(KW)'))

C
7210 FORMAT (5X, F7.1, 3X, F10.1, 3X, F11.3, 3X, F11.3, 3X, F11.3, 3X,
&          F10.3)

C
8111 FORMAT (///, ' >>>> RADIATIVE HEAT TRANSFER DATA')

C
8592 FORMAT (//(9X,'CA', 9X, 'PRES', 8X, 'TAIR', 8X, 'TGAS', 8X,
```

```
&      'TFLAME', 8X, 'TRAD', 10X, 'EMIS', 8X, 'QRAD',  
&      9X, 'QTOT')/  
&      (8X, '(DEG)', 7X, '(ATM)', 7X, '(K)', 9X, '(K)', 10X,  
&      '(K)', 10X, '(K)', 11X, '(-)', 9X, '(KW)', 9X, '(KW)'))
```

C

```
8210 FORMAT (5X, F7.1, 2X, F10.1, 3X, F10.1, 3X, F10.1, 3X, F10.1,  
&      3X, F10.1, 2X, F10.3, 3X, F10.3, 3X, F10.3)
```

C

```
8861 FORMAT (/,'>>>> WALL CONDUCTION MODELS')  
8862 FORMAT (/,'>>>> PISTON WALL STRUCTURE')  
8863 FORMAT (/,'>>>> CYL. HEAD WALL STRUCTURE')  
8864 FORMAT (/,'>>>> CYL. LINER WALL STRUCTURE')  
8865 FORMAT (/,' LAYER', 3X,3(I4,10X))  
8866 FORMAT (/,' INSIDE DIAMETER (M)', F10.5)  
8867 FORMAT (/,' THICKNESS (M)', 3(F10.5, 5X))  
8868 FORMAT (/,' THERMAL CONDUCTIVITY (W/M/K)', 3(F10.3, 5X))  
8869 FORMAT (/,' THERMAL DIFFUSIVITY (M2/SEC)', 3(E10.3, 5X))  
8870 FORMAT (/,' NUMBER OF NODES', 3X,3(I4, 10X))  
8871 FORMAT (/,' NODES WITHIN SKIN DEPTH', 3X, I4)  
8872 FORMAT (/,' COURANT NUMBER', 3(F10.3, 5X))  
8880 FORMAT (/,' OUTSIDE WALL TEMPERATURE (K)', F10.1,/  
&      /,' OVERALL CONDUCTIVITY (W/M/K)', F10.1,/  
8881 FORMAT (/,' AMBIENT TEMPERATURE (K)', F10.1,/  
&      /,' OUTSIDE HEAT TR. COEFF.(W/M2/K)', F10.1,/  
&      /,' OVERALL HEAT TR. COEFF.(W/M2)', F10.1,/  
9111 FORMAT (///,' >>>> TRANSIENT TEMPERATURE PROFILES WITHIN PISTON',/  
&      /,' UP TO FIRST 10 NODES '  
9112 FORMAT (///,' >>>> TRANSIENT TEMPERATURE PROFILES WITHIN HEAD',/  
&      /,' UP TO FIRST 10 NODES '  
C  
C  
C
```

612 CONTINUE

C IF(ITERAS.LT.MINITS) GO TO 1906

CLOSE(UNIT=36)

CLOSE(UNIT=37)

616 CLOSE(UNIT=6)

C

STOP

END

C***** VERSION 1.0 *****
C AUG 21, 1985

C SUBROUTINE RESULT

C PURPOSE

C WRITES CRANK-ANGLE BY CRANK-ANGLE RESULTS OF THE CYCLE
C SIMULATION TO THE APPROPRIATE OUTPUT FILES. THESE ARE
C RESULTS WHICH ARE RECORDED DEPENDING ON THE ENGINE PROCESS
C (SEE PROCESS LOOPS), AND RESULTS WHICH ARE RECORDED
C THROUGHOUT THE CYCLE (SEE COMMON SECTION).

C USAGE

C CALL RESULT (INDEX)

C DESCRIPTION OF PARAMETERS

PARAMETER	INPUT	OUTPUT	DESCRIPTION
INDEX	YES	NO	DETERMINES WHICH SET OF
-----	---	--	RESULTS ARE TO BE RECORDED

C REMARKS

C INDEX=1 MEANS THAT INTAKE LOOP RESULTS RECORDED
C INDEX=2 MEANS THAT CMPRES LOOP RESULTS RECORDED
C INDEX=3 MEANS THAT CMBSTN LOOP RESULTS RECORDED
C INDEX=4 MEANS THAT EXHAUST LOOP RESULTS RECORDED

C SUBROUTINE AND FUNCTION SUBPROGRAMS REQUIRED

C NONE

C WRITTEN BY D. N. ASSANIS

C EDITED BY D. N. ASSANIS

C SUBROUTINE RESULT (INDEX)

C LOGICAL SPTEMP, ANNAND

C INTEGER SIZC, SIZT, SIZPT, SIZ1, SIZ2, SIZ3

C REAL*8 DT, DY(60)

C REAL MWM, MACRSC, MASS, MASSIN, MASSEX, KIL, MIL

C DIMENSION Y(60), PTW(2,3,51)

C PARAMETER (PI=3.1415927)

C PARAMETER (SIZC=6, SIZT=6, SIZPT=6, SIZ1=7, SIZ2=8, SIZ3=11,

& ITIVO = -11, ITEVC = 736, ITIVC = 212, ITEVO = 505)

C PARAMETER (CEN = 1.E2, KIL = 1.E3, MIL = 1.E6, ERG = 1.E7,

& ATPA = 1.01325E5)

C DIMENSION MASSIN(ITIVO:ITIVC), MASSEX(ITEVO:ITEVC),

& FCYLIN(ITIVO:ITIVC), FCYLEX(ITEVO:ITEVC),
& HCYLIN(ITIVO:ITIVC), HCYLEX(ITEVO:ITEVC)

C

COMMON/SPTEMP/ SPTEMP
COMMON/ANNAND/ ANNAND
COMMON/RADIATION/ TCHTR, TRHTR,, THTR, CHTRAP, CHTRAH, CHTRAW,
& RHTRAP, RHTRAH, RHTRAW

C

COMMON/FLAME/ TAIR, PAIR, TFLAME, TRAD, EMIS

C

COMMON/PFDIF/ PTW
COMMON/PHLIN/ PHLIN(2), TGAS

C

COMMON/ITERAS/ ITERAS, ISTEDY
COMMON/VECTOR/ DY, DT, IFLAG
COMMON/PRINT/ TPRINT, TRES, TSCREEN

C

COMMON/D / ERPM
COMMON/DTDTH/ ESPD
COMMON/ARRAY/ MASSIN, MASSEX, FCYLIN, FCYLEX, HCYLIN, HCYLEX
COMMON/RHMAS/ RHO, MASS, VOLUME, HH, GAMMA
COMMON/VALVE/ VIV, VEV
COMMON/B / CPM(2), HM(2), MWM(2), GM(2), RHOM(2)
COMMON/K /RTEMP(5), H(5), RMASS(5), RCORR(5)
COMMON/NEWDIF / ASP(3), PR(3), PRSS(5), DP(5), HI(5),
& TMAP(2), PTMAP(2), CMAP(2),
& CM(SIZC,SIZ1,3), TM(SIZT,SIZ2,3), PTM(SIZPT,SIZ3,3),
& CRPM(SIZC),TRPM(SIZT),PTRPM(SIZPT), PSTD(3), TSTD(3)
COMMON/FBRATE/ FBRATE
COMMON/TURBU/ CBETA , MACRSC, UPRIME, VMKE, VPISTO
COMMON/HEATS/ CVHTRN, HTRCOE, HTPAPI, HTPAHD, HTPACW, HTRAPI,
& HTRAHD, HTRACW, THTRAN
COMMON/QP2/ EPRF(3), EVBLK(3), EREF(3), ENUF(3), EHTCOE(3),
& EQDOT(3)

C

T = DT

C

IF(INDEX .EQ. 1) GO TO 10
IF(INDEX .EQ. 2) GO TO 20
IF(INDEX .EQ. 3) GO TO 30
IF(INDEX .EQ. 4) GO TO 40

C

C***** INTAKE *****

C

10 CONTINUE
IF (AMOD(T, TSCREEN).EQ.0.0) WRITE (7,881)
& DT, DY(12)/ATPA, DY(11), IFLAG
IF (AMOD(T, TPRINT).EQ.0.0) WRITE(6,4210) DT, DY(12)/ATPA,
& DY(11),DY(1)*KIL,DY(2)*KIL, EQR(DY(20)), DY(23)/ATPA,
& DY(22), DY(27)/ATPA, DY(26), IFLAG
GO TO 50

```
C*****
C          COMPRESSION LOOP
C*****
C
  20 CONTINUE
    IF (AMOD(T, TSCREEN).EQ.0.0) WRITE(7,882) DT,
    &   DY(12)/ATPA, IFLAG
    IF (AMOD(T, TPRINT).EQ.0.0) WRITE(6,4211) DT, DY(12)/ATPA,
    &   DY(11), EQR(DY(20)),DY(23)/ATPA, DY(22), DY(27)/ATPA,
    &   DY(26), IFLAG
    GO TO 50
C
C*****
C          COMBUSTION LOOP
C*****
C
  30 CONTINUE
    IF(.NOT. ANNAND .AND. AMOD(T,TPRINT).EQ.0.)
    &   WRITE(14,8210) T, DY(12)/ATPA, TAIR, DY(11), TFLAME,
    &   TRAD, EMIS, TRHTR/KIL, THTR/KIL
C
    IF (AMOD(T, TSCREEN).EQ.0.0) WRITE(7,883) DT, DY(12)/ATPA,
    &   DY(4), IFLAG
    IF (AMOD(T, TPRINT).EQ.0.0) WRITE(6,4212) DT, DY(12)/ATPA,
    &   DY(11), EQR(DY(20)), DY(23)/ATPA,DY(22), DY(27)/ATPA,
    &   DY(26), IFLAG
    GO TO 50
C
C*****
C          EXHAUST LOOP
C*****
C
  40 CONTINUE
C
    IF (AMOD(T, TSCREEN).EQ.0.0) WRITE(7,882)
    &   DT, DY(12)/ATPA, IFLAG
    IF (AMOD(T, TPRINT).EQ.0.0) WRITE(6,4213) DT, DY(12)/ATPA,
    &   DY(11),DY(2)*KIL,EQR(DY(20)),
    &   DY(23)/ATPA, DY(22), DY(27)/ATPA, DY(26) ,IFLAG
C
C*****
C          COMMON SECTION FOLLOWS
C*****
C
  50 CONTINUE
C
    IF(.NOT. SPTEMP .AND. ITERAS.GT.ISTEDY .AND.
    & AMOD(T, TPRINT).EQ.0.0) THEN
      WRITE(36,991) T, (PTW(1,1,INOD), INOD =1,10)
      WRITE(37,991) T, (PTW(2,1,INOD), INOD =1,10)
    ENDIF
C
    IF(AMOD(T,TPRINT).EQ.0.) WRITE(12,6210)
    &   T, DY(6), DY(7), VIV, VEV, VMKE, UPRIME, CVHTRN, MACRSC*CEN
```

```
IF(AMOD(T,TPRINT).EQ.0.) WRITE(13,7210)
& T, HTRCOE, HTPAPI/KIL, HTPAHD/KIL, HTPACW/KIL, THTRAN/KIL
C
C*****
C
C          FORMAT STATEMENTS FOLLOW
C*****
C
C 881 FORMAT (1H ,2X,'CA = ',F6.2,10X,'P = ',F10.5,9X,'T = ',F10.2,
&          8X,'IFG = ',I2)
C
C 882 FORMAT (1H ,2X,'CA = ',F6.2,10X,'P = ',F10.5,28X,'IFG = ',I2)
C
C 883 FORMAT (1H ,2X,'CA = ',F6.2,10X,'P = ',F10.5,9X,'XB = ',F9.6,
&          5X,'IFG = ',I2)
C
C 991 FORMAT (1X,F10.2,10(F11.1))
C
C 4210 FORMAT (1X, F6.1, 2X, F9.4, 2X, F9.2, 2X, F9.5, 2X, F9.5,
& 2X, F9.5, 2X, F9.4, 2X, F9.2,2X,F9.4,2X,F9.2,2X,I2)
C
C 4211 FORMAT (1X, F6.1, 2X, F9.4, 2X, F9.2, 24X,
& F9.5, 2X, F9.4, 2X, F9.2, 2X, F9.4,2X,F9.2,2X,I2)
C
C 4212 FORMAT (1X, F6.1, 2X, F9.4, 2X, F9.2, 24X, F9.5, 2X, F9.4,
& 2X, F9.2,2X,F9.4,2X,F9.2,2X,I2)
C
C 4213 FORMAT (1X, F6.1, 2X, F9.4, 2X, F9.2, 13X, F9.5, 2X, F9.5,
& 2X, F9.4, 2X, F9.2, 2X,F9.4,2X,F9.2,2X,I2)
C
C 6210 FORMAT (5X, F7.1, 4X, F9.5, 5X, F9.5, 4X, F10.3, 3X, F10.3, 3X,
& F10.3, 3X, F10.3, 4X, F10.3, 4X, F10.3)
C
C 7210 FORMAT (5X, F7.1, 3X, F10.1, 3X, F11.3, 3X, F11.3, 3X, F11.3, 3X,
& F10.3)
C
C 8210 FORMAT (5X, F7.1, 2X, F10.1, 3X, F10.1, 3X, F10.1, 3X, F10.1,
& 3X, F10.1, 2X, F10.3, 3X, F10.3, 3X, F10.3)
C
C          RETURN
C          END
```

C***** VERSION 3.0 *****
C AUG 21, 1985

C SUBROUTINE INTAKE

C PURPOSE

C CALCULATES THE TIME RATE OF CHANGE OF PRESSURE, TEMPERATURE,
C FUEL EQUIVALENCE RATIO, MASS, HEAT TRANSFER, WORK TRANSFER,
C MEAN KINETIC ENERGY, AND TURBULENT KINETIC ENERGY IN THE
C THE MASTER CYLINDER DURING INTAKE.

C USAGE

C CALL INTAKE (DT, DY, DYP)

C DESCRIPTION OF PARAMETERS

PARAMETER	INPUT	OUTPUT	DESCRIPTION
DT	YES	NO	TIME (DEG)
DY(1)	YES	NO	MASS INDUCTED INTO CHAMBER THROUGH
----	---	--	INTAKE VALVE (KG)
DY(2)	YES	NO	MASS EXHAUSTED FROM CHAMBER THROUGH
----	---	--	EXHAUST VALVE (KG)
DY(6)	YES	NO	MEAN KINETIC ENERGY IN CHAMBER (J)
DY(7)	YES	NO	TURBULENT KINETIC ENERGY IN
----	---	--	CHAMBER (J)
DY(8)	YES	NO	HEAT TRANSFER - PISTON TOP (J)
DY(9)	YES	NO	HEAT TRANSFER - CYLINDER HEAD (J)
DY(10)	YES	NO	HEAT TRANSFER - CYLINDER WALL (J)
DY(11)	YES	NO	CYLINDER TEMPERATURE (K)
DY(12)	YES	NO	CYLINDER PRESSURE (PA)
DY(16)	YES	NO	TOTAL WORK TRANSFER (J)
DY(17)	YES	NO	TOTAL ENTHALPY EXHAUSTED (J)
DY(20)	YES	NO	BURNED FUEL FRACTION (-)

DYP(1)	NO	YES	RATE AT WHICH MASS IS INDUCTED
-----	--	---	THROUGH THE INTAKE VALVE (KG/DEG)
DYP(2)	NO	YES	RATE AT WHICH MASS IS EXHAUSTED
-----	--	---	THROUGH THE EXHAUST VALVE (KG/DEG)
DYP(6)	NO	YES	RATE OF CHANGE OF MEAN KINETIC
-----	--	---	ENERGY (J/DEG)
DYP(7)	NO	YES	RATE OF CHANGE OF TURBULENT KINETIC
-----	--	---	ENERGY (J/DEG)
DYP(8)	NO	YES	RATE OF HEAT TRANSFER -
-----	--	---	PISTON TOP (J/DEG)
DYP(9)	NO	YES	RATE OF HEAT TRANSFER -
-----	--	---	CYLINDER HEAD (J/DEG)
DYP(10)	NO	YES	RATE OF HEAT TRANSFER -
-----	--	---	CYLINDER WALL (J/DEG)
DYP(11)	NO	YES	RATE OF CHANGE OF CYLINDER
-----	--	---	TEMPERATURE (K/DEG)
DYP(12)	NO	YES	RATE OF CHANGE OF CYLINDER

C	-----	--	---	PRESSURE (PA/DEG)
C	DYP(16)	NO	YES	RATE OF TOTAL WORK TRANSFER (J/DEG)
C	DYP(17)	NO	YES	RATE AT WHICH TOTAL ENTHALPY IS
C	-----	--	---	EXHAUSTED (J/DEG)
C	DYP(20)	NO	YES	RATE OF CHANGE OF BURNED
C	-----	--	---	FUEL FRACTION (1/DEG)

REMARKS

UNITS CHANGED TO S.I.
DOCUMENTATION REVISED APRIL 20, 1985.

SUBROUTINE AND FUNCTION SUBPROGRAMS REQUIRED

THERMO	TRANSP	IVACD	MFLRT
CSAVDV	EVACD		

METHOD

SEE REPORT

WRITTEN BY D. N. ASSANIS AND S. G. POULOS
EDITED BY D. N. ASSANIS

SUBROUTINE INTAKE (DT, DY, DYP)

REAL*8 DT, DY(60), DYP(60)
 REAL MWM, MW, MWIM, MWEM, KINVIS, MASS, MDOT, MSTART, MACRSC
 DIMENSION Y(60), YP(60), Y1(40), YP1(40)
 COMMON/EPARAM/ BORE, STROKE, CONRL, CYLCA, CSATDC, CMRTIO, CLVTDC
 COMMON/HTRC/ CONHT, EXPHT
 COMMON/TEMPS/ TPSTON, THEAD, TCW
 COMMON/DTDTH/ ESPD
 COMMON/MA/ YPM(2), YPH
 COMMON/MSTA/ MSTART
 COMMON/TIMES/ TIVO, TEVC, TIVC, TINJ, TIGN, TEVO
 COMMON/B / CPM(2), HM(2), MWM(2), GM(2), RHOM(2)
 COMMON/HEATS/ CVHTRN, HTRCOE, HTPAPI, HTPAHD, HTPACW, HTRAPI,
 & HTRAHD, HTRACW, THTRAN
 COMMON/TURBU/ CBETA, MACRSC, UPRIME, VMKE, VPISTO
 COMMON/VALVE/ VIV, VEV
 COMMON/RHMAS/ RHO, MASS, VOLUME, H, GAMMA
 COMMON/AREAS/ AHEAD, APSTON
 COMMON/FUEL/ FUELTP, CX, HY, DEL, PSI, AFRAST, QLOWER, HFORM
 COMMON/EFFAR/ AREA, CD
 COMMON/PHLIN/ HLIN1, HLIN2, TG

VIV = 0.0

VEV = 0.0

DO 10 I = 1, 60
Y(I) = DY(I)

10 CONTINUE

T = DT

```
DO 20 I = 1, 20
  YP(I) = 0.0
20 CONTINUE
C
  PIM = Y(23)
  GIM = GM(1)
  MWIM = MWM(1)
  RHOIM = RHOM(1)
  FIM = Y(24)
  TIM = Y(22)
  HIM = HM(1)
C
  PEM = Y(27)
  GEM = GM(2)
  MWEM = MWM(2)
  RHOEM = RHOM(2)
  TEM = Y(26)
  FEM = Y(28)
  HEM = HM(2)
C
  C      FIND THERMODYNAMIC AND TRANSPORT PROPERTIES IN CYLINDER
  C
  C      FR = Y(20)
  C      CALL THERMO ( Y(11), Y(12), FR, H, CSUBP, CSUBT, CSUBF,
  C      & RHO, DRHODT, DRHODP, DRHODF, GAMMA, MW, ADUMY, BDUMY, CDUMY)
  C      CALL TRANSP (Y(11), FR, GAMMA, CSUBP, DYNVIS, THRCON)
  C      YPH = H
  C      KINVIS = DYNVIS/RHO
  C      MASS = MSTART + Y(1) - Y(2)
C
  C      FIND OUT IF INTAKE VALVE IS OPEN.
  C
  C      IF (T .GE. TIVC) GO TO 50
C
  C      YES IT IS.
  C      FIND OUT IF ANY MASS FLOWS ACROSS INTAKE VALVE.
  C
  C      IF (PIM - Y(12)) 30, 50, 40
C
  C      REVERSE FLOW PAST VALVE.
  C      CALCULATE CD AND EFFECTIVE AREA.
  C
30 PR = Y(12)/PIM
  CALL VACDIN (T, AREA, CD)
C
  C      CALCULATE MASS FLOW RATE FROM CYLINDER TO INTAKE MANIFOLD.
  C
  C      CALL MFLRT (CD, AREA, Y(12), MW, Y(11), PIM, GAMMA, FRAIV)
C
  C      CALCULATE RATES DUE TO THIS FLOW.
  C
  C      YP(1) = -FRAIV
  C      IF (AREA .LE. 0.0) GO TO 35
  C      VIV = -FRAIV/(RHO * AREA)
```

```
35 YP(6) = -FRAIV * (Y(6)/MASS)
    YP(7) = -FRAIV * (Y(7)/MASS)
    HIM = H
    GO TO 50
```

C
C
C
C

```
    FLOW INTO CYLINDER.
    CALCULATE CD AND AREA.
```

```
40 PR = PIM/Y(12)
    CALL VACDIN (T, AREA, CD)
```

C
C
C

```
    CALCULATE MASS FLOW RATE
```

```
    CALL MFLRT (CD, AREA, PIM, MWIM, TIM, Y(12), GIM, FRAIV)
```

C
C
C

```
    CALCULATE RATES DUE TO THIS FLOW
```

```
    YP(1) = FRAIV
    YP(20) = (FIM - Y(20)) * YP(1)/MASS
    IF (AREA .LE. 0.0) GO TO 45
    VIV = FRAIV/(RHOIM * AREA)
45 YP(6) = .5 * FRAIV * VIV*VIV
```

C
C
C

```
    IS EXHAUST VALVE STILL OPEN ?
```

```
50 IF ((T + 720.) .GE. TEVC) GO TO 80
```

C
C
C
C

```
    YES IT IS.
    ANY FLOW ACROSS IT ?
```

```
    IF (Y(12) - PEM) 60, 80, 70
```

C
C
C
C

```
    YES, FLOW INTO CYLINDER.
    FIND CD AND AREA FOR EXHAUST VALVE.
```

```
60 PR = PEM/Y(12)
```

C
C
C

```
    CONVERT TIME FOR EXHAUST VALVE
```

```
    TEX = T + 720.
    CALL VACDEX (TEX, AREA, CD)
```

C
C
C

```
    FIND MASS FLOW RATE.
```

```
    CALL MFLRT (CD, AREA, PEM, MWEM, TEM, Y(12), GEM, FRAEV)
```

C
C
C

```
    CALCULATE RATES DUE TO THIS FLOW.
```

```
    YP(2) = -FRAEV
    IF (AREA .LE. 0.0) GO TO 65
    VEV = -FRAEV/(RHOEM * AREA)
65 YP(6) = YP(6) + .5 * FRAEV * VEV*VEV
    YP(20) = YP(20) + ( FEM - Y(20) ) * FRAEV / MASS
    GO TO 80
```

```
C
C      FLOW FROM CYLINDER INTO EXHAUST MANIFOLD.
C      FIND AREA AND CD FOR EXHAUST VALVE.
C
70 PR = Y(12)/PEM
   TEX = T + 720.
   CALL VACDEX (TEX, AREA, CD)
C
C      FIND MASS FLOW RATE.
C
   CALL MFLRT (CD, AREA, Y(12), MW, Y(11), PEM, GAMMA, FRAEV)
C
C      CALCULATE RATES DUE TO THIS FLOW.
C
   YP(2) = FRAEV
   IF (AREA .LE. 0.0) GO TO 75
   VEV = FRAEV/(RHO * AREA)
75 YP(6) = YP(6) - FRAEV * (Y(6)/MASS)
   YP(7) = YP(7) - FRAEV * (Y(7)/MASS)
C
C      FIND SURFACE AREAS AND VOLUME OF CHAMBER
C
80 CALL CSAVDV (T, ACW, VOLUME, DVDT)
   MACRSC = VOLUME/(3.1415 * BORE * BORE/4.)
   IF (MACRSC .GE. (BORE/2.)) MACRSC = BORE/2.
   YP(6) = YP(6) - .3307 * CBETA/MACRSC * Y(6) *
&      SQRT( Y(7)/MASS)
   YP(7) = YP(7) + .3307 * CBETA/MACRSC * Y(6) *
&      SQRT( Y(7)/MASS)
&      - .5443 * Y(7)/MACRSC * SQRT( Y(7)/MASS)
   MDOT = YP(1) - YP(2)
C
C      CHARACTERISTIC VELOCITY IN CYLINDER; (M/SEC).
C
   PI      = 3.141592654
   CONSTR = CONRL/STROKE
   SINTH   = SIN( T*PI/180. )
   COSTH   = COS( T*PI/180. )
   VONVPM  = ABS( PI * SINTH * ( 1. + COSTH/SQRT( 4. * CONSTR*CONSTR
&      - SINTH*SINTH ) )/2. )
   VPMEAN  = STROKE/(180. * ESPD)
   VPISTO  = VPMEAN * VONVPM
   VMKE    = SQRT( 2. * Y(6)/MASS )
   UPRIME  = SQRT( .666667 * Y(7)/MASS )
   CVHTRN  = SQRT( 0.25*VPISTO*VPISTO + VMKE*VMKE + UPRIME*UPRIME )
C
C      CALCULATE HEAT TRANSFER RATES
C
   HTRCOE = CONHT*(ABS(CVHTRN*MACRSC/KINVIS)**EXPHT * THRCON/MACRSC)
C
85 HTPAPI = HTRCOE * ( Y(11) - TPSTON )
   HTPAHD = HTRCOE * ( Y(11) - THEAD )
   HTPACW = HTRCOE * ( Y(11) - TCW )
```

```
C      TG      = Y(11)
      HLIN1   = HTRCOE
      HLIN2   = HTRCOE
      HLIN3   = HTRCOE

C      HTGPI  = HTRCOE * Y(11)
      HTGHD  = HTRCOE * Y(11)
      HTGCW  = HTRCOE * Y(11)

C      HTRAPI = APSTON * HTPAPI
      HTRAHD = AHEAD * HTPAHD
      HTRACW = ACW * HTPACW

C      THTRAN = HTRAPI + HTRAHD + HTRACW

C      CALCULATE RATES OF CHANGE OF TEMPERATURE, PRESSURE,
C      AND FUEL EQUIVALENCE RATIO IN THE CYLINDER.
C      THEN CALCULATE RATE OF DOING WORK.
C
90 PHIDOT = AFRAST/(1.-FR)/(1.-FR) * YP(20)
   PHI    = FR * AFRAST / (1. - FR)
   YP(11) = (BDUMY/ADUMY)*((MDOT/MASS)*(1.-H/BDUMY) -
&          DVDT/VOLUME +(YP(1)*HIM -YP(2)*H -THTRAN)/(BDUMY*MASS)
&          - CDUMY/BDUMY * PHIDOT)

C      YP(12) = RHO/DRHODP * (-DVDT/VOLUME - YP(11)*DRHODT/RHO
&          - PHIDOT*DRHODF/RHO + MDOT/MASS)

C      YP(16) = Y(12) * DVDT

C
C      YP(8) = HTRAPI
      YP(9) = HTRAHD
      YP(10) = HTRACW

C      YP(17) = YP(2) * H

C
C      CONVERT ALL TIME DERIVATIVES TO RATE PER CRANK
C      ANGLE DEGREE.
C
      DO 100 I = 1, 20
         YP(I) = YP(I) * ESPD
100 CONTINUE

C      YPM(1) = YP(1)
      YPM(2) = YP(2)

C      DO 108 I = 1, 40
         Y1(I) = Y(20 +I)
108 CONTINUE

C      CALL DIFEQ (T, Y1, YP1)

C
```

```
      DO 110 I = 1, 40
      YP(20+I) = YP1(I)
110 CONTINUE
C
      YP(54) = HTRCOE
      YP(55) = HTGPI
      YP(56) = HTRCOE
      YP(57) = HTGHD
      YP(58) = HTRCOE
      YP(59) = HTGCW
C
      DO 111 I = 1, 60
      DYP(I) = YP(I)
111 CONTINUE
C
      RETURN
      END
```

C***** VERSION 3.0 *****
 C AUG 25, 1985

C SUBROUTINE CMPRES

C PURPOSE

C CALCULATES THE TIME RATE OF CHANGE OF PRESSURE, TEMPERATURE,
 C FUEL EQUIVALENCE RATIO, MASS, HEAT TRANSFER, WORK TRANSFER,
 C MEAN KINETIC ENERGY, AND TURBULENT KINETIC ENERGY IN THE
 C MASTER CYLINDER DURING COMPRESSION. ALSO USED TO PREDICT THE
 C LENGTH OF THE IGNITION DELAY PERIOD.

C USAGE

C CALL CMPRES (DT, DY, DYP)

C DESCRIPTION OF PARAMETERS

PARAMETER	INPUT	OUTPUT	DESCRIPTION
DT	YES	NO	TIME (DEG)
DY(1)	YES	NO	MASS INDUCTED INTO CHAMBER THROUGH
-----	---	---	INTAKE VALVE (KG)
DY(2)	YES	NO	MASS EXHAUSTED FROM CHAMBER THROUGH
-----	---	---	EXHAUST VALVE (KG)
DY(6)	YES	NO	MEAN KINETIC ENERGY IN CHAMBER (J)
DY(7)	YES	NO	TURBULENT KINETIC ENERGY IN
-----	---	---	CHAMBER (J)
DY(8)	YES	NO	HEAT TRANSFER - PISTON TOP (J)
DY(9)	YES	NO	HEAT TRANSFER - CYLINDER HEAD (J)
DY(10)	YES	NO	HEAT TRANSFER - CYLINDER WALL (J)
DY(11)	YES	NO	CYLINDER TEMPERATURE (K)
DY(12)	YES	NO	CYLINDER PRESSURE (PA)
DY(13)	YES	NO	ELAPSED/PREDICTED IGNITION DELAY (-)
DY(16)	YES	NO	TOTAL WORK TRANSFER (J)

DYP(1)	NO	YES	RATE AT WHICH MASS IS INDUCTED
-----	---	---	THROUGH THE INTAKE VALVE (KG/DEG)
DYP(2)	NO	YES	RATE AT WHICH MASS IS EXHAUSTED
-----	---	---	THROUGH THE EXHAUST VALVE (KG/DEG)
DYP(6)	NO	YES	RATE OF CHANGE OF MEAN KINETIC
-----	---	---	ENERGY (J/DEG)
DYP(7)	NO	YES	RATE OF CHANGE OF TURBULENT KINETIC
-----	---	---	ENERGY (J/DEG)
DYP(8)	NO	YES	RATE OF HEAT TRANSFER -
-----	---	---	CYLINDER HEAD (J/DEG)
DYP(9)	NO	YES	RATE OF HEAT TRANSFER -
-----	---	---	PISTON TOP (J/DEG)
DYP(10)	NO	YES	RATE OF HEAT TRANSFER -
-----	---	---	CYLINDER WALL (J/DEG)
DYP(11)	NO	YES	RATE OF CHANGE OF CYLINDER
-----	---	---	TEMPERATURE (K/DEG)
DYP(12)	NO	YES	RATE OF CHANGE OF CYLINDER

```
C      -----  --  ---  PRESSURE (PA/DEG)
C      DYP(13)  NO  YES  RATE OF CHANGE OF ELAPSED/PREDICTED
C      -----  --  ---  IGNITION DELAY FRACTION (1/DEG)
C      DYP(16)  NO  YES  RATE OF TOTAL WORK TRANSFER (J/DEG)
```

```
C  REMARKS
C    UNITS CHANGED TO S.I.
C    REVISED DOCUMENTATION
```

```
C  SUBROUTINE AND FUNCTION SUBPROGRAMS REQUIRED
C    THERMO      TRANSP      CSAVDV      DIFEQ
```

```
C  METHOD
C    SEE REPORT
```

```
C  WRITTEN BY D. N. ASSANIS AND S. G. POULOS
C  EDITED BY D. N. ASSANIS
```

```
C  SUBROUTINE CMPRES (DT,DY,DYP)
```

```
C
C  REAL*8 DT, DY(60), DYP(60)
C  REAL MW, KINVIS, MASS, MDOT, MDOTFR, MSTART, MACRSC
C  DIMENSION Y(20), YP(20), Y1(40), YP1(40)
C  PARAMETER (PI = 3.141592654)
C  COMMON/EPARAM/ BORE, STROKE, CONRL, CYLCA, CSATDC, CMRTIO, CLVTDC
C  COMMON/HTRC/ CONHT, EXPHT
C  COMMON/TEMPS/ TPSTON, THEAD, TCW
C  COMMON/DTDTH/ ESPD
C  COMMON/MSTA/ MSTART
C  COMMON/TIMES/ TIVO, TEVC, TIVC, TINJ, TIGN, TEVO
C  COMMON/HEATS/ CVHTRN, HTRCOE, HTPAPI, HTPAHD, HTPACW, HTRAPI,
C  &          HTRAHD, HTRACW, THTRAN
C  COMMON/TURBU/ CBETA, MACRSC, UPRIME, VMKE, VPISTO
C  COMMON/VALVE/ VIV, VEV
C  COMMON/RHMAS/ RHO, MASS, VOLUME, H, GAMMA
C  COMMON/AREAS/ AHEAD, APSTON
C  COMMON/PHLIN/ HLIN1, HLIN2, TG
```

```
C
C  DO 10 I = 1, 20
C    YP(I) = 0.0
C    Y(I) = DY(I)
10 CONTINUE
C    T = DT
```

```
C
C    FIND THERMODYNAMIC AND TRANSPORT PROPERTIES IN CYLINDER
```

```
C
C    FR = Y(20)
C    CALL THERMO ( Y(11), Y(12), FR, H, CSUBP, CSUBT, CSUBF,
C  & RHO, DRHODT, DRHODP, DRHODF, GAMMA, MW, ADUMY, BDUMY, CDUMY)
C    CALL TRANSP (Y(11), FR, GAMMA, CSUBP, DYNVIS, THRCON)
C    KINVIS = DYNVIS/RHO
C    MASS = MSTART + Y(1) - Y(2)
```

```
C
C      FIND SURFACE AREAS AND VOLUME OF CHAMBER
C
CALL CSAVDV (T, ACW, VOLUME, DVDT)
MACRSC = VOLUME/(3.1415 * BORE * BORE/4.)
IF (MACRSC.GE.(BORE/2.)) MACRSC = BORE/2.
YP(6) = -.3307 * CBETA/MACRSC * Y(6) * SQRT(Y(7)/MASS)

C
C      ADD TURBULENCE AMPLIFICATION TERM FOR RAPID DISTORTION
C
RDOT = DRHODT * YP11 + DRHODP * YP12
AMPL = 2./3. * Y(7)/RHO * RDOT
YP(7) = .3307 * CBETA/MACRSC * Y(6) * SQRT(Y(7)/MASS)
&      - .5443 * Y(7)/MACRSC * SQRT(Y(7)/MASS) + AMPL

C
C      CHARACTERISTIC VELOCITY IN CYLINDER; (M/SEC).
C
CONSTR = CONRL/STROKE
SINTH = SIN( T*PI/180. )
COSTH = COS( T*PI/180. )
VONVPM = ABS( PI * SINTH * ( 1. + COSTH/SQRT( 4. * CONSTR*CONSTR
&      - SINTH*SINTH ) )/2. )
VPMEAN = STROKE/(180. * ESPD)
VPISTO = VPMEAN * VONVPM
VMKE = SQRT( 2. * Y(6)/MASS )
UPRIME = SQRT( .666667 * Y(7)/MASS )
CVHTRN = SQRT( 0.25*VPISTO*VPISTO + VMKE*VMKE + UPRIME*UPRIME )

C
C      CALCULATE HEAT TRANSFER RATES
C
HTRCOE = CONHT*( (CVHTRN*MACRSC/KINVIS)**EXPHT ) * THRCON/MACRSC

C
85 HTPAPI = HTRCOE * ( Y(11) - TPSTON )
HTPAHD = HTRCOE * ( Y(11) - THEAD )
HTPACW = HTRCOE * ( Y(11) - TCW )

C
TG      = Y(11)
HLIN1  = HTRCOE
HLIN2  = HTRCOE
HLIN3  = HTRCOE

C
HTGPI  = HTRCOE * Y(11)
HTGHD  = HTRCOE * Y(11)
HTGCW  = HTRCOE * Y(11)

HTRAPI = APSTON * HTPAPI
HTRAHD = AHEAD * HTPAHD
HTRACW = ACW * HTPACW

C
THTRAN = HTRAPI + HTRAHD + HTRACW

C
C      CALCULATE RATES OF CHANGE OF TEMPERATURE, PRESSURE,
C      AND FUEL EQUIVALENCE RATIO IN THE CYLINDER.
C      THEN CALCULATE RATE OF DOING WORK.
```

```
C
30 YP(11) = -(BDUMY/ADUMY) * (DVDT/VOLUME + THTRAN/(BDUMY*MASS))
   YP11 = YP(11)
C
   YP(12) = RHO/DRHODP * (-DVDT/VOLUME - YP(11)*DRHODT/RHO)
   YP12 = YP(12)
C
   YP(16) = Y(12) * DVDT
C
   YP(8) = HTRAPI
   YP(9) = HTRAHD
   YP(10) = HTRACW
C
   IF(T.LT.TINJ) GO TO 32
C
      INTEGRATE PREDICTED CONTRIBUTIONS OF THE DURATION
C      OF THE IGNITION DELAY PERIOD
C
31 ATPA = 1.01325E+5
   PRATM= Y(12)/ATPA
C
   TPARMS = 3.45 * EXP(2100./Y(11))/ PRATM**1.02
   TPRED = TPRMS/1000.
   YP(13)= 1./TPRED
C
32 CONTINUE
C
      CONVERT ALL TIME DERIVATIVES TO RATE PER CRANK
C      ANGLE DEGREE.
C
   DO 40 I = 1, 20
   DYP(I) = YP(I) * ESPD
40 CONTINUE
C
   DO 41 I = 1, 40
41 Y1(I) = DY(20+I)
C
   CALL DIFEQ (T, Y1, YP1)
C
   DO 50 I = 1, 40
50 DYP(I+20) = YP1(I)
C
   DYP(54) = HTRCOE
   DYP(55) = HTGPI
   DYP(56) = HTRCOE
   DYP(57) = HTGHD
   DYP(58) = HTRCOE
   DYP(59) = HTGCW
C
   RETURN
   END
```

C***** VERSION 3.0 *****
C AUG 21, 1985

C SUBROUTINE CMBSTN

C PURPOSE

C CALCULATES THE TIME RATE OF CHANGE OF PRESSURE, TEMPERATURE,
C FUEL EQUIVALENCE RATIO, MASS, HEAT TRANSFER, WORK TRANSFER,
C MEAN KINETIC ENERGY, AND TURBULENT KINETIC ENERGY IN THE
C MASTER CYLINDER DURING COMBUSTION.

C USAGE

C CALL CMBSTN (DT, DY, DYP)

C DESCRIPTION OF PARAMETERS

PARAMETER	INPUT	OUTPUT	DESCRIPTION
DT	YES	NO	TIME (DEG)
DY(1)	YES	NO	MASS INDUCTED INTO CHAMBER THROUGH INTAKE VALVE (KG)
-----	---	---	
DY(2)	YES	NO	MASS EXHAUSTED FROM CHAMBER THROUGH EXHAUST VALVE (KG)
-----	---	---	
DY(4)	YES	NO	FUEL MASS BURNED (-)
DY(6)	YES	NO	MEAN KINETIC ENERGY IN CHAMBER (J)
DY(7)	YES	NO	TURBULENT KINETIC ENERGY IN CHAMBER (J)
-----	---	---	
DY(8)	YES	NO	HEAT TRANSFER - PISTON TOP (J)
DY(9)	YES	NO	HEAT TRANSFER - CYLINDER HEAD (J)
DY(10)	YES	NO	HEAT TRANSFER - CYLINDER WALL (J)
DY(11)	YES	NO	CYLINDER TEMPERATURE (K)
DY(12)	YES	NO	CYLINDER PRESSURE (PA)
DY(16)	YES	NO	TOTAL WORK TRANSFER (J)
DY(20)	YES	NO	BURNED FUEL FRACTION (-)

DYP(1)	NO	YES	RATE AT WHICH MASS IS INDUCTED THROUGH THE INTAKE VALVE (KG/DEG)
-----	---	---	
DYP(2)	NO	YES	RATE AT WHICH MASS IS EXHAUSTED THROUGH THE EXHAUST VALVE (KG/DEG)
-----	---	---	
DYP(4)	NO	YES	RATE OF BURNING OF FUEL MASS FRESH CHARGE (1/DEG)
-----	---	---	
DYP(6)	NO	YES	RATE OF CHANGE OF MEAN KINETIC ENERGY (J/DEG)
-----	---	---	
DYP(7)	NO	YES	RATE OF CHANGE OF TURBULENT KINETIC ENERGY (J/DEG)
-----	---	---	
DYP(8)	NO	YES	RATE OF HEAT TRANSFER - CYLINDER HEAD (J/DEG)
-----	---	---	
DYP(9)	NO	YES	RATE OF HEAT TRANSFER - PISTON TOP (J/DEG)
-----	---	---	
DYP(10)	NO	YES	RATE OF HEAT TRANSFER - CYLINDER WALL (J/DEG)
-----	---	---	
DYP(11)	NO	YES	RATE OF CHANGE OF CYLINDER


```
YP(I) = 0.0
Y(I) = DY(I)
10 CONTINUE
T = DT

C
C   FIND THERMODYNAMIC AND TRANSPORT PROPERTIES IN CYLINDER
C
FR = Y(20)
MFUEL = Y(4) * FMIN
CALL THERMO ( Y(11), Y(12), FR, H, CSUBP, CSUBT, CSUBF,
& RHO, DRHODT, DRHODP, DRHODF, GAMMA, MW, ADUMY, BDUMY, CDUMY)
CALL TRANSP (Y(11), FR, GAMMA, CSUBP, DYNVIS, THRCON)
KINVIS = DYNVIS/RHO
MASS = MSTART + Y(1) - Y(2) + MFUEL

C
C   FIND SURFACE AREAS AND VOLUME OF CHAMBER
C
CALL CSAVDV (T, ACW, VOLUME, DVDT)

C
TONDTB = (T - TIGN)/DTBRN
IF (TONDTB .GT. 1.0) TONDTB = 1.0
IF (TONDTB .GT. .15) GO TO 11
12 MDOPRE = CSP1 * CSP2 * TONDTB** (CSP1 -1.) * (1. - TONDTB**CSP1)**
&      (CSP2 -1.)
GO TO 13
11 MDOPRE = 0.0
13 MDODIF = CSD1*CSD2 *(TONDTB** (CSD2-1.)) * EXP(-CSD1*TONDTB**CSD2)
MDOTOT= ALPHA * MDOPRE + (1. - ALPHA) * MDODIF
YP(4) = MDOTOT/ (DTBRN * ESPD)
MDOTFU= YP(4) * FMIN

C
C
C   FBRATE = YP(4)

C
YP(20)= MDOTFU/MASS * (1.-Y(20))
YP20 = YP(20)

C
MACRSC = VOLUME/(3.1415 * BORE * BORE/4.)
IF (MACRSC.GE.(BORE/2.)) MACRSC = BORE/2.
YP(6) = -.3307 * CBETA/MACRSC * Y(6) * SQRT(Y(7)/MASS)

C
C   INCLUDE NEW TURBULENCE AMPLIFICATION TERM DUE TO RAPID DISTORTION
C
RDOT = DRHODT * YP11 + DRHODP * YP12 + DRHODF * YP20
AMPL = 2./3. * Y(7)/RHO * RDOT
YP(7) = .3307 * CBETA/MACRSC * Y(6) * SQRT(Y(7)/MASS)
&      - .5443 * Y(7)/MACRSC * SQRT(Y(7)/MASS) + AMPL

C
C   CHARACTERISTIC VELOCITY IN CYLINDER; (M/SEC).
C
CONSTR = CONRL/STROKE
SINTH = SIN( T*PI/180. )
COSTH = COS( T*PI/180. )
VONVPM = ABS( PI * SINTH * ( 1. + COSTH/SQRT( 4. * CONSTR*CONSTR
```

```
&      - SINTH*SINTH ) )/2. )
VPMEAN = STROKE/(180. * ESPD)
VPISTO = VPMEAN * VONVPM
VMKE   = SQRT( 2. * Y(6)/MASS )
UPRIME = SQRT( .666667 * Y(7)/MASS )
CVHTRN = SQRT( 0.25*VPISTO*VPISTO + VMKE*VMKE + UPRIME*UPRIME )

C
C      CALCULATE HEAT TRANSFER RATES
C
C      HTRCOE = CONHT*( (CVHTRN*MACRSC/KINVIS)**EXPHT ) * THRCON/MACRSC
C
C      CHTPAP = HTRCOE * (Y(11) - TPSTON)
C      CHTPAH = HTRCOE * (Y(11) - THEAD)
C      CHTPAW = HTRCOE * (Y(11) - TCW)
C
C      IF(ANNAND) THEN
C      TRAD = Y(11)
C      SIGMA IS STEPHANN-BOLTZMAN CONSTANT = 5.67E-8 W/M**2/K**4
C      CONRAD = CRAD * SIGMA
C      RTRAD = TRAD
C      GO TO 87
C      ENDIF
C
C      CALL FLAME (Y(11), Y(12), TAIR, TFLAME, TRAD)
C      EMIS = 0.9 - 0.9 * (T-TIGN)/(TEVO-TIGN)
C      IF (EMIS .LT. 0.) EMIS = 0.
C      CONRAD = EMIS * SIGMA
C      RTAIR = TAIR
C      RPAIR = Y(12)
C      RTFLAM= TFLAME
C      RTRAD = TRAD
C
C      87 RHTPAP = CONRAD * (TRAD**4 - TPSTON**4)
C      RHTPAH = CONRAD * (TRAD**4 - THEAD**4)
C      RHTPAW = CONRAD * (TRAD**4 - TCW**4)
C
C      CALCULATE EFFECTIVE LINEAR HEAT TRANSFER COEFFICIENTS
C      (CONVECTIVE + RADIATIVE)
C
C      TG = Y(11)
C      IF(TG.EQ.TPSTON) GO TO 92
C      HLIN1 = HTRCOE + CONRAD * (TG**3 + TG**2 * TPSTON +
&      TG * TPSTON**2 + TPSTON**3) +
&      CONRAD * (TRAD**4 - TG**4) / (TG - TPSTON)
C      92 CONTINUE
C      IF(TG.EQ.THEAD) GO TO 93
C      HLIN2 = HTRCOE + CONRAD * (TG**3 + TG**2 * THEAD +
&      TG * THEAD**2 + THEAD**3) +
&      CONRAD * (TRAD**4 - TG**4) / (TG - THEAD)
C      93 CONTINUE
C      IF(TG.EQ.TCW) GO TO 94
C      HLIN3 = HTRCOE + CONRAD * (TG**3 + TG**2 * TCW +
&      TG * TCW**2 + TCW**3) +
&      CONRAD * (TRAD**4 - TG**4) / (TG - TCW)
```

```
C
94 HTGPI = HLIN1 * TG
   HTGHD = HLIN2 * TG
   HTGCW = HLIN3 * TG

C
C   CALCULATE CONVECTIVE AND RADIATIVE HEAT TRANSFER RATES
C   TO EACH COMPONENT SURFACE:
C
   CHTRAP = CHTPAP * APSTON
   CHTRAH = CHTPAH * AHEAD
   CHTRAW = CHTPAW * ACW

C
   RHTRAP = RHTPAP * APSTON
   RHTRAH = RHTPAH * AHEAD
   RHTRAW = RHTPAW * ACW

C
C   CALCULATE COMBINED HEAT TRANSFER RATES:
C   I) TO EACH COMPONENT; II) TOTALS
C
   HTPAPI = CHTPAP + RHTPAP
   HTPAHD = CHTPAH + RHTPAH
   HTPACW = CHTPAW + RHTPAW

C
   HTRAPI = CHTRAP + RHTRAP
   HTRAHD = CHTRAH + RHTRAH
   HTRACW = CHTRAW + RHTRAW

C
   TCHTR  = CHTRAP + CHTRAH + CHTRAW
   TRHTR  = RHTRAP + RHTRAH + RHTRAW
   THTR   = TCHTR  + TRHTR

C
   THTRAN = HTRAPI + HTRAHD + HTRACW

C
C   CALCULATE RATES OF CHANGE OF TEMPERATURE AND PRESSURE IN
C   THE CYLINDER. THEN CALCULATE RATE OF DOING WORK.
C
30 PHIDOT = AFRAST/(1.-FR)/(1.-FR) * YP(20)
   PHI    = FR * AFRAST / (1. - FR)
   YP(11) = (BDUMY/ADUMY) * ((MDOTFU/MASS)*(1.-H/BDUMY)
&          - DVDT/VOLUME - CDUMY/BDUMY*PHIDOT
&          + (MDOTFU*HFORM - THTRAN)/(BDUMY*MASS))
   YP11   = YP(11)

C
   YP(12) = RHO/DRHODP * (-DVDT/VOLUME - YP(11)*DRHODT/RHO
&          -PHIDOT*DRHODF/RHO + MDOTFU/MASS)
   YP12   = YP(12)

C
   YP(16) = Y(12) * DVDT

C
   YP(8)  = HTRAPI
   YP(9)  = HTRAHD
   YP(10) = HTRACW

C
C   CONVERT ALL TIME DERIVATIVES TO RATE PER CRANK
```

```
C      ANGLE DEGREE.
C
      DO 40 I = 1, 20
          DYP(I) = YP(I) * ESPD
40 CONTINUE
C
      DO 41 I = 1, 40
          Y1(I) = DY(20+I)
41 CONTINUE
C
      CALL DIFEQ (T, Y1, YP1)
C
      DO 50 I = 1, 40
          DYP(I+20) = YP1(I)
50 CONTINUE
C
      DYP(54) = HLIN1
      DYP(55) = HTGPI
      DYP(56) = HLIN2
      DYP(57) = HTGHD
      DYP(58) = HLIN3
      DYP(59) = HTGCW
C
      RETURN
      END
```

C***** VERSION 3.0 *****
C AUG 21, 1985

C SUBROUTINE EXHAUST

C PURPOSE

C CALCULATES THE TIME RATE OF CHANGE OF PRESSURE, TEMPERATURE,
C FUEL EQUIVALENC RATIO, MASS, HEAT TRANSFER, WORK TRANSFER,
C MEAN KINETIC ENERGY, AND TURBULENT KINETIC ENERGY IN THE
C MASTER CYLINDER DURING EXHAUST.

C USAGE

C CALL EXHAUST (DT, DY, DYP)

C DESCRIPTION OF PARAMETERS

PARAMETER	INPUT	OUTPUT	DESCRIPTION
DT	YES	NO	TIME (DEG)
DY(1)	YES	NO	MASS INDUCTED INTO CHAMBER THROUGH
----	---	---	INTAKE VALVE (KG)
DY(2)	YES	NO	MASS EXHAUSTED FROM CHAMBER THROUGH
----	---	---	EXHAUST VALVE (KG)
DY(6)	YES	NO	MEAN KINETIC ENERGY IN CHAMBER (J)
DY(7)	YES	NO	TURBULENT KINETIC ENERGY IN
----	---	---	CHAMBER (J)
DY(8)	YES	NO	HEAT TRANSFER - PISTON TOP (J)
DY(9)	YES	NO	HEAT TRANSFER - CYLINDER HEAD (J)
DY(10)	YES	NO	HEAT TRANSFER - CYLINDER WALL (J)
DY(11)	YES	NO	CYLINDER TEMPERATURE (K)
DY(12)	YES	NO	CYLINDER PRESSURE (PA)
DY(16)	YES	NO	TOTAL WORK TRANSFER (J)
DY(17)	YES	NO	TOTAL ENTHALPY EXHAUSTED (J)

DYP(1)	NO	YES	RATE AT WHICH MASS IS INDUCTED
----	---	---	THROUGH THE INTAKE VALVE (KG/DEG)
DYP(2)	NO	YES	RATE AT WHICH MASS IS EXHAUSTED
----	---	---	THROUGH THE EXHAUST VALVE (KG/DEG)
DYP(6)	NO	YES	RATE OF CHANGE OF MEAN KINETIC
----	---	---	ENERGY (J/DEG)
DYP(7)	NO	YES	RATE OF CHANGE OF TURBULENT KINETIC
----	---	---	ENERGY (J/DEG)
DYP(8)	NO	YES	RATE OF HEAT TRANSFER -
----	---	---	CYLINDER HEAD (J/DEG)
DYP(9)	NO	YES	RATE OF HEAT TRANSFER -
----	---	---	PISTON TOP (J/DEG)
DYP(10)	NO	YES	RATE OF HEAT TRANSFER -
----	---	---	CYLINDER WALL (J/DEG)
DYP(11)	NO	YES	RATE OF CHANGE OF CYLINDER
----	---	---	TEMPERATURE (K/DEG)
DYP(12)	NO	YES	RATE OF CHANGE OF CYLINDER
----	---	---	PRESSURE (PA/DEG)

C	DYP(16)	NO	YES	RATE OF TOTAL WORK TRANSFER (J/DEG)
C	DYP(17)	NO	YES	RATE AT WHICH TOTAL ENTHALPY IS
C	-----	--	---	EXHAUSTED (J/DEG)

C REMARKS
 C UNITS CHANGED TO SI

C SUBROUTINE AND FUNCTION SUBPROGRAMS REQUIRED
 C THERMO TRANSP MFLRT
 C CSAVDV EVACD DIFEQ

C METHOD
 C SEE REPORT

C WRITTEN BY D. N. ASSANIS AND S. G. POULOS
 C EDITED BY D. N. ASSANIS

C SUBROUTINE EXAUST (DT, DY, DYP)

C
 C REAL*8 DT, DY(60), DYP(60)
 C REAL MW, MWEM, MWM, KINVIS, MASS, MDOT, MDOTFR, MSTART, MACRSC, MFUEL
 C DIMENSION Y(60), YP(60), Y1(40), YP1(40)
 C PARAMETER (PI = 3.141592654)
 C COMMON/EPARAM/ BORE, STROKE, CONRL, CYLCA, CSATDC, CMRTIO, CLVTDC
 C COMMON/BURN/ FMIN
 C COMMON/HTRC/ CONHT, EXPHT
 C COMMON/TEMPS/ TPSTON, THEAD, TCW
 C COMMON/DTDTH/ ESPD
 C COMMON/MA/ YPM(2), YPH
 C COMMON/MSTA/ MSTART
 C COMMON/TIMES/ TIVO, TEVC, TIVC, TINJ, TIGN, TEVO
 C COMMON/B/ CPM(2), HM(2), MWM(2), GM(2), RHOM(2)
 C COMMON/HEATS/ CVHTRN, HTRCOE, HTPAPI, HTPAHD, HTPACW, HTRAPI,
 C & HTRAHD, HTRACW, THTRAN
 C COMMON/TURBU/ CBETA, MACRSC, UPRIME, VMKE, VPISTO
 C COMMON/VALVE/ VIV, VEV
 C COMMON/RHMAS/ RHO, MASS, VOLUME, H, GAMMA
 C COMMON/AREAS/ AHEAD, APSTON
 C COMMON/PHLIN/ HLIN1, HLIN2, TG

C VEV = 0.0

C DO 10 I = 1, 60
 C Y(I) = DY(I)

C 10 CONTINUE

C DO 11 I = 1, 20
 C YP(I) = 0.0

C 11 CONTINUE

C T = DT

```
C
C      FIND THERMODYNAMIC AND TRANSPORT PROPERTIES IN CYLINDER
C
TEM = Y(26)
PEM = Y(27)
FEM = Y(28)
HEM = HM(2)
MWEM = MWM(2)
GEM = GM(2)
RHOEM = RHOM(2)
FR = Y(20)
MFUEL = Y(4) * FMIN
CALL THERMO ( Y(11), Y(12), FR, H, CSUBP, CSUBT, CSUBF,
& RHO, DRHODT, DRHODP, DRHODF, GAMMA, MW, ADUMY, BDUMY, CDUMY)
YPH = H
CALL TRANSP (Y(11), FR, GAMMA, CSUBP, DYNVIS, THRCON)
KINVIS = DYNVIS/RHO
MASS = MSTART + Y(1) - Y(2) + MFUEL

C
C      IS EXHAUST VALVE STILL OPEN ?
C
IF (T .GE. TEVC) GO TO 50

C
C      YES IT IS.
C      ANY FLOW ACROSS IT ?
C
IF (Y(12) - PEM) 30, 50, 40

C
C      YES, FLOW INTO CYLINDER.
C      FIND CD AND AREA FOR EXHAUST VALVE.
C
30 PR = PEM/Y(12)
CALL VACDEX (T, AREA, CD)

C
C      FIND MASS FLOW RATE.
C
CALL MFLRT (CD, AREA, PEM, MWEM, TEM, Y(12), GEM, FRAEV)

C
C      CALCULATE RATES DUE TO THIS FLOW.
C
YP(2) = -FRAEV
IF (AREA .LE. 0.0) GO TO 35
VEV = -FRAEV/(RHOEM * AREA)
35 YP(6) = .5 * FRAEV * VEV*VEV
YP(20) = (FEM - Y(20)) * FRAEV / MASS
GO TO 50

C
C      FLOW FROM CYLINDER INTO EXHAUST MANIFOLD.
C      FIND AREA AND CD FOR EXHAUST VALVE.
C
40 PR = Y(12)/PEM
CALL VACDEX (T, AREA, CD)

C
C      FIND MASS FLOW RATE.
```

```
C
CALL MFLRT (CD, AREA, Y(12), MW, Y(11), PEM, GAMMA, FRAEV)
C
C   CALCULATE RATES DUE TO THIS FLOW
C
  YP(2) = FRAEV
  IF (AREA .LE. 0.0) GO TO 45
  VEV = FRAEV/(RHO * AREA)
45 YP(6) = -FRAEV * (Y(6)/MASS)
  YP(7) = -FRAEV * (Y(7)/MASS)
  YP(20) = 0.
C
C   FIND SURFACE AREAS AND VOLUME OF CHAMBER
C
50 CALL CSAVDV (T, ACW, VOLUME, DVDT)
  MACRSC = VOLUME/(3.1415 * BORE * BORE/4.)
  IF (MACRSC .GE. (BORE/2.)) MACRSC = BORE/2.
  YP(6) = YP(6) - .3307 * CBETA/MACRSC * Y(6) * SQRT(Y(7)/MASS)
  YP(7) = YP(7) + .3307 * CBETA/MACRSC * Y(6) * SQRT(Y(7)/MASS)
&   - .5443 * Y(7)/MACRSC * SQRT(Y(7)/MASS)
  MDOT = -YP(2)
C
C   CHARACTERISTIC VELOCITY IN CYLINDER (M/SEC)
C
  CONSTR = CONRL/STROKE
  SINTH = SIN( T*PI/180. )
  COSTH = COS( T*PI/180. )
  VONVPM = ABS( PI * SINTH * ( 1. + COSTH/SQRT( 4. * CONSTR*CONSTR
&   - SINTH*SINTH ) )/2. )
  VPMEAN = STROKE/(180. * ESPD)
  VPISTO = VPMEAN * VONVPM
  VMKE = SQRT( 2. * Y(6)/MASS )
  UPRIME = SQRT( .666667 * Y(7)/MASS )
C
C   ADD VELOCITY TERM DUE TO BLOWDOWN
C
  VBDOWN = 4 * YP(2)/( 3.1415925 * RHO * BORE * BORE )
  IF ( YP(2) .LT. 0.0 ) VBDOWN = 0.0
  CVHTRN = SQRT( 0.25*VPISTO*VPISTO + VMKE*VMKE + UPRIME*UPRIME +
&   VBDOWN*VBDOWN )
C
C   CALCULATE HEAT TRANSFER RATES
C
  HTRCOE = CONHT*( ( CVHTRN*MACRSC/KINVIS)**EXPHT ) * THRCON/MACRSC
C
85 HTPAPI = HTRCOE * ( Y(11) - TPSTON )
  HTPAHD = HTRCOE * ( Y(11) - THEAD )
  HTPACW = HTRCOE * ( Y(11) - TCW )
C
  TG = Y(11)
  HLIN1 = HTRCOE
  HLIN2 = HTRCOE
  HLIN3 = HTRCOE
C
```

```
HTGPI = HTRCOE * Y(11)
HTGHD = HTRCOE * Y(11)
HTGCW = HTRCOE * Y(11)
C
HTRAPI = APSTON * HTPAPI
HTRAHD = AHEAD * HTPAHD
HTRACW = ACW * HTPACW
C
THTRAN = HTRAPI + HTRAHD + HTRACW
C
      CALCULATE RATES OF CHANGE OF TEMPERATURE AND PRESSURE IN
      THE CYLINDER. THEN CALCULATE RATE OF DOING WORK.
C
60 YP(11) = -(BDUMY/ADUMY)*( YP(2)/MASS + DVDT/VOLUME +
&          CDUMY/BDUMY * PHIDOT + THTRAN/(BDUMY*MASS) )
C
      YP(12) = RHO/DRHODP * ( -DVDT/VOLUME - PHIDOT*DRHODF/RHO
&          - YP(11)*DRHODT/RHO - YP(2)/MASS )
C
      YP(16) = Y(12) * DVDT
C
      YP(8) = HTRAPI
      YP(9) = HTRAHD
      YP(10) = HTRACW
C
      YP(17) = YP(2) * H
C
      CONVERT ALL TIME DERIVATIVES TO RATE PER CRANK
      ANGLE DEGREE.
C
      DO 70 I = 1, 20
          DYP(I) = YP(I) * ESPD
70 CONTINUE
      YPM(2) = DYP(2)
C
      DO 78 I = 1, 40
78 Y1(I) = Y(20+I)
      CALL DIFEQ (T, Y1, YP1)
      DO 79 I = 1, 40
79 DYP(20+I) = YP1(I)
C
      DYP(54) = HTRCOE
      DYP(55) = HTGPI
      DYP(56) = HTRCOE
      DYP(57) = HTGHD
      DYP(58) = HTRCOE
      DYP(59) = HTGCW
C
      RETURN
      END
```

```
C***** VERSION 1.0 *****  
C                               OCT 21, 1984  
C  
C   FUNCTION GCMP  
C  
C     CALLED BY 'ODERT' TO CHECK FOR ROOTS DURING INTAKE, COMPRESSION  
C     (EXCLUDING IGNITION DELAY PERIOD), COMBUSTION, AND EXHAUST.  
C     THIS A DUMMY FUNCTION (GCMP ALWAYS >0)  
C  
C     WRITTEN BY D.N. ASSANIS  
C  
C   FUNCTION GCMP (DT, DY, DYP)  
C   REAL*8 DT,DY(60),DYP(60),GCMP  
C  
C   GCMP =10.DO  
C  
C   RETURN  
C   END
```

```
C***** VERSION 2.0 *****  
C                                MAY 6, 1985  
C  
C      FUNCTION GIDEL  
C  
C          CALLED BY ODERT TO CALCULATE THE ROOT OF THE IGNITION  
C          DELAY FUNCTION, AND THUS PREDICT THE LENGTH OF THE IGNITION  
C          DELAY PERIOD.  
C  
C      WRITTEN BY D.N. ASSANIS  
C  
C      FUNCTION GIDEL (DT, DY, DYP)  
C      REAL*8 DT, DY(60), DYP(60), GIDEL  
C  
C          CONVERT DOUBLE PRECISION TIME TO SINGLE PRECISION.  
C  
C      T      = DT  
C      DELFR = DY(13)  
C      GIDEL = DELFR - 1.  
C  
C      RETURN  
C      END
```


- C (11) TOTAL MASS FLOWED FROM INTAKE
C MANIFOLD
C TO ALL CYLINDERS
- C (12) TOTAL MASS FLOWED FROM COMPRESSOR
C TO INTAKE MANIFOLD
- C (13) TOTAL MASS FLOWED FROM ALL
C CYLINDERS TO EXHAUST MANIFOLD
- C (14) TOTAL MASS FLOWED FROM EXHAUST
C MANIFOLD TO FIRST TURBINE
- C (15) TIME-AVERAGED INTAKE MANIFOLD
C PRESSURE
- C (16) TIME-AVERAGED EXHAUST MANIFOLD
C PRESSURE
- C (17) TIME-AVERAGED COMPRESSOR DISCHARGE
C TEMPERATURE
- C (18) TIME-AVERAGED INTERCOOLER OUTLET
C TEMPERATURE
- C (19) TIME-AVERAGED INTAKE MANIFOLD
C TEMPERATURE
- C (20) TIME-AVERAGED EXHAUST MANIFOLD
C TEMPERATURE
- C (21) TIME-AVERAGED TURBOCHARGER TURBINE
C EXHAUST
C TEMPERATURE
- C (22) TIME-AVERAGED POWER TURBINE
C EXHAUST TEMPERATURE
- C (23) TIME-AVERAGED INTERCOOLER
C EFFECTIVENESS
- C (24) TIME-AVERAGED COMPRESSOR MAP FLOW
- C (25) TIME-AVERAGED TURBINE MAP FLOW
- C (26) TIME-AVERAGED COMPRESSOR MAP SPEED
- C (27) TIME-AVERAGED TURBINE MAP SPEED
- C (28) TIME-AVERAGED POWER TURBINE MAP
C SPEED
- C (29) TIME-AVERAGED TURBINE PRESSURE
C RATIO
- C (30) TIME-AVERAGED COMPRESSOR
C EFFICIENCY
- C (31) TIME-AVERAGED TURBINE EFFICIENCY
- C (32) TIME-AVERAGED POWER TURBINE
C EFFICIENCY
- C (33) TIME-AVERAGED POWER TURBINE MAP
C FLOW
- C (40) TIME-AVERAGED POWER TURBINE INLET
C TEMP.

C REMARKS
C NONE

C SUBROUTINES AND FUNCTIONS SUBPROGRAMS REQUIRED

C THERMO DELH QDP
C ICMAP ITMAP IPTMAP

C METHOD

```
C          SEE NASA DIESEL REPORT, 1984
C
C          WRITTEN BY D. N. ASSANIS
C
C          SUBROUTINE DIFEQ (A, Y, YDOT)
C
C          LOGICAL POWER
C          INTEGER SIZC, SIZPT, SIZT, SIZ1, SIZ2, SIZ3
C          PARAMETER (I1=1, I2=2, I3=3, PI=3.1415927)
C          PARAMETER (SIZC=6, SIZ1=7, SIZT=6, SIZ2=8, SIZPT=6, SIZ3=11)
C          REAL MWM
C          DIMENSION Y(40), PHDOT(2),YDOT(40), ENGM(2),FMDOT(2),HMDOT(2)
C
C          COMMON/POWER/POWER
C          COMMON/SUMIT/ ENGM,FMDOT,HMDOT
C          COMMON/B / CPM(2), HM(2), MWM(2), GM(2), RHOM(2)
C          COMMON/D / ERPM
C          COMMON/DTDTH/ ESPD
C          COMMON/NEWDIF / ASP(3), PR(3), PRSS(5), DP(5), HI(5),
&          TMAP(2), PTMAP(2), CMAP(2),
&          CM(SIZC,SIZ1,3), TM(SIZT,SIZ2,3), PTM(SIZPT,SIZ3,3),
&          CRPM(SIZC), TRPM(SIZT), PTRPM(SIZPT), PSTD(3), TSTD(3)
C          COMMON/I /PINLET
C          COMMON/K /RTEMP(5), H(5), RMASS(5), RCORR(5)
C          COMMON/FUEL/ FUELTP, CX, HY, DEL, PSI, AFRAST, QLOWER, HFORM
C          COMMON/TCPAR/ B(2)
C
C          DO 10 I=1,40
10         YDOT(I) = 0.
C
C          FIND INTAKE MANIFOLD HEAT TRANSFER AND PRESSURE DROP:
C
C          CALL QDP(Y(2), Y(3), Y(4), RHOM(1), I1, ENGM(1), Q1, DP(2))
C
C          FIND COMPRESSOR DISCHARGE PRESSURE:
C
C          PRSS(1) = Y(3) + DP(2) + DP(1)
C
C          FIND COMPRESSOR MASS FLOW CHARACTERISTIC FROM MAP:
C
C          PR(1) = PRSS(1) / PINLET
C          ASP(1) = Y(9) * RCORR(3)
C          CALL ICMAP(ASP(1), PR(1), CM, CRPM, SIZC, SIZ1, CMAP)
C
C          NOTE THAT IF AN INCOMPATIBLE INPUT SET OF SPEED AND
C          PRESSURE RATIO IS SUPPLIED TO ICMAP, THE ROUTINE WILL
C          RETURN A NEW SPEED THAT IS COMPATIBLE WITH THE INPUT
C          PRESSURE RATIO, WHICH REMAINS UNCHANGED. THE NEW SPEED
C          WILL BE USED IN THE FOLLOWING STEPS OF THE MATCHING
C          PROCESS.
C
C          Y(9) = ASP(1) / RCORR(3)
C
C          CONVERT FROM LB/MIN, CORRECTED, TO KG/DEG, ACTUAL:
```

```
C
  RMASS(3) = CMAP(1)
  CMAP(1) = RMASS(3) * RCORR(2) * PINLET/PSTD(1) * RCORR(3)
C
  YDOT(11) = ENGM(1)
  YDOT(12) = CMAP(1)
C
      EVALUATE SPECIFIC ENTHALPY AND DISCHARGE TEMPERATURE
      FROM COMPRESSOR:
C
  CALL DELH(RTEMP(1), RTEMP(2), PINLET, PRSS(1), 0., CMAP(2),
&    RTEMP(2), H(1), HC, H(3))
C
      FIND MANIFOLD SPECIFIC ENTHALPY :
C
  CALL THERMO (Y(2), Y(3), Y(4), HM(1), CPM(1), CM1, CM2,
&    RHOM(1), CM4, CM5, CM6, GM(1), MWM(1), CM9, CM10, CM11)
C
      FIND INTERCOOLER DISCHARGE TEMPERATURE AND SPECIFIC
      ENTHALPY:
C
  TMI = (RTEMP(2) + HI(3))/2.
  CALL THERMO (TMI, PRSS(1), 0., XI1, CPI, XI2, XI3, XI4,
&    XI5, XI6, XI7, XI8, XI9, XI10, XI11, XI12)
  CMIN = CMAP(1) / ESPD * CPI
  HI(1) = 1. - EXP(-HI(5)/CMIN)
  HI(3) = RTEMP(2) - HI(1) * (RTEMP(2)-HI(2))
  CALL THERMO (HI(3), Y(3), 0., HI(4), CPHI, DM1, DM2, DM3,
&    DM4, DM5, DM6, DM7, DM8, DM9, DM10, DM11)
C
      FIND INDIVIDUAL AND TOTAL ENTHALPY FLUXES INTO THE
      INTAKE MANIFOLD CONTROL VOLUME:
C
  H11 = HI(4) * CMAP(1)
  HNET1 = H11 - HMDOT(1) + Q1
C
      FIND EXHAUST MANIFOLD HEAT TRANSFER AND PRESSURE DROP:
C
  CALL QDP (Y(6), Y(7), Y(8), RHOM(2), I2, ENGM(2), Q2, DP(3))
C
  IF (POWER) GO TO 20
C
      FOLLOW THIS SECTION OF THE PROGRAM FOR A SIMPLE
      TURBOCHARGED CALCULATION (NO POWER TURBINE):
C
      FIND TURBOCHARGER TURBINE INLET PRESSURE, OUTLET
      PRESSURE, AND HENCE PRESSURE RATIO:
C
18  PRSS(2) = Y(7) - DP(3)
    PRSS(3) = PRSS(5)
    PR(2)  = PRSS(2)/PRSS(3)
C
      FIND TURBINE MAP FLOW AND EFFICIENCY FROM MAP:
C
```

```
RCORR(4) = SQRT(TSTD(2)/Y(6))
ASP(2)   = Y(9) * RCORR(4)
CALL IPTMAP(ASP(2), PR(2), TM, TRPM, SIZT, SIZ2, TMAP)
RMASS(4) = TMAP(1)
C       CONVERT FROM CORRECTED LBS/MIN MAP FLOW TO ACTUAL
C       KG/DEG MASS FLOW:
TRBM     = RMASS(4) * RCORR(2) * PRSS(2) / PSTD(2) * RCORR(4)
C
YDOT(14) = TRBM
YDOT(13) = ENGM(2)
C
C       FIND TURBINE ENTHALPY CHANGE AND DISCHARGE TEMPERATURE:
C
CALL DELH (Y(6), RTEMP(3), PRSS(2), PRSS(3), Y(8), 1./TMAP(2),
&        RTEMP(3), HM(2), HT, H(4))
C
GO TO 40
C
C       FOLLOW THIS SECTION OF THE PROGRAM FOR A TURBOCHARGED
C       TURBOCOMPOUNDED CALCULATION.
20 CONTINUE
DO 25 II = 1 , 50
C
C       FIND FIRST TURBINE DOWNSTREAM PRESSURE AND EFFICIENCY
C       FROM TURBOCHARGER SPEED AND CORRECTED MASS FLOW:
C
RCORR(4) = SQRT(TSTD(2)/Y(6))
ASP(2)   = Y(9) * RCORR(4)
CALL ITMAP (ASP(2), RMASS(4), TM, TRPM, SIZT, SIZ2, TMAP)
PR(2)    = TMAP(2)
PRSS(2)  = Y(7) - DP(3)
PRSS(3)  = PRSS(2) / PR(2)
PRSS(4)  = PRSS(3) - DP(4)
PR(3)    = PRSS(4) / PRSS(5)
C       CONVERT FROM CORRECTED LBS/MIN MASS FLOW TO ACTUAL
C       KG/DEG MASS FLOW:
TRBM     = RMASS(4) * RCORR(2) * PRSS(2) / PSTD(2) * RCORR(4)
C
C       FIND POWER TURBINE MASS FLOW RATE, GIVEN ENGINE SPEED,
C       GEAR RATIO, AND POWER TURBINE PRESSURE RATIO.
C
RCORR(5) = SQRT(TSTD(3)/RTEMP(4))
ASP(3)   = ERPM * RCORR(1) * RCORR(5)
CALL IPTMAP (ASP(3), PR(3), PTM, PTRPM, SIZPT, SIZ3, PTMAP)
RMASS(5) = PTMAP(1)
PTRBM    = RMASS(5) * RCORR(2) * PRSS(4) / PSTD(3) * RCORR(5)
C
IF (ABS(TRBM - PTRBM) .GT. 1.E-3 * PTRBM) GO TO 24
TRBM = PTRBM
GO TO 30
C
C       NOTE THAT THE NEW GUESS FOR THE TURBINE MASS IS MORE
C       HEAVILY WEIGHTED TO THE OLD TURBINE MASS RATHER THAN
C       THE POWER TURBINE MASS. THIS IMPROVES THE STABILITY OF
C       THE MATCHING PROCESS AND REDUCES THE RUNNING TIME.
```

```
24 TRBM = 0.75*TRBM + 0.25*PTRBM
   RMASS(4) = TRBM / RCORR(2) / PRSS(2) / RCORR(4) * PSTD(2)
25 CONTINUE
C
C       EQUATE THE ACTUAL TURBINE AND POWER TURBINE MASS FLOWS
C       (ON A KG/DEG BASIS)
   TRBM = PTRBM
C
C 30 YDOT(14) = TRBM
C
   YDOT(13) = ENGM(2)
C
C       FIND TURBINE ENTHALPY CHANGE AND DISCHARGE TEMPERATURE:
C
   CALL DELH (Y(6), RTEMP(3), PRSS(2), PRSS(3), Y(8), 1./TMAP(1),
&    RTEMP(3), HM(2), HT, H(4))
C
C       FIND POWER TURBINE INLET TEMPERATURE:
C
   CPTEMP = RTEMP(3)
C
C       CALCULATE HEAT TRANSFER IN CONNECTING PIPE BETWEEN
C       THE TWO TURBINES
C
   CALL THERMO (CPTEMP, PRSS(3), Y(8), XX1, XX2, XX3, XX4,
&    RHOC, XX6, XX7, XX8, XX9, XX10, XX11, XX12, XX13)
C
   CALL QDP (CPTEMP, PRSS(3), Y(8), RHOC, I3, TRBM, QCP, DP(4))
C
   DENTH = QCP / TRBM
   HCP = HT + DENTH
C
   CALL ITRATE (RTEMP(4), PRSS(3), Y(8), HCP, XX1, XX2, XX3,
&    XX4, XX5, XX6, XX7, XX8, XX9, XX10, XX11, XX12)
C
C       FIND POWER TURBINE ENTHALPY CHANGE AND DISCHARGE
C       TEMPERATURE:
C
   CALL DELH (RTEMP(4), RTEMP(5), PRSS(4), PRSS(5), Y(8),
&    1./PTMAP(2), RTEMP(5), HPT, HOUT, H(5))
C
C       CALCULATE POWER TURBINE INSTANTANEOUS POWER (J/KG)
C       NOTE NEGATIVE SIGN DUE TO THE DEFINITION OF ENTHALPY
C       CHANGES IN DELH.
C
   YDOT(10) = - YDOT(14) * H(5)
C
C       THIS SECTION IS COMMON FOR BOTH OPTIONS.
C       FIND INDIVIDUAL AND TOTAL ENTHALPY FLUXES INTO
C       EXHAUST MANIFOLD CONTROL VOLUME:
C
40 H12 = - YDOT(14) * HM(2)
   HNET2 = H12 + HMDOT(2) + Q2
C
```

```
C           FIND PROPERTIES OF EXHAUST MANIFOLD:
C
C           CALL THERMO (Y(6), Y(7), Y(8), HM(2), CPM(2), EX1, EX2,
&           RHOM(2), EX4, EX5, EX6, GM(2), MWM(2), EX9,EX10,EX11)
C
C***** CALCULATE DERIVATIVES *****
C
C           APPLY CONSERVATION OF MASS TO FIND INTAKE MANIFOLD
C           MASS DERIVATIVE:
C
C           YDOT(1) = CMAP(1) - ENGM(1)
C           AY1 = YDOT(1) / Y(1)
C
C           FIND EQUIVALENCE RATIO DERIVATIVES:
C
C           FF = Y(4)
C           AA = - FMDOT(1) + YDOT(12) * ( 0. - Y(4))
C           FDOT = AA / Y(1)
C           YDOT(4) = FDOT
C           PHDOT(1) = FDOT * AFRAST / (1. - FF)**2
C
C           FF = Y(8)
C           AA = FMDOT(2)
C           FDOT = AA / Y(5)
C           YDOT(8) = FDOT
C           PHDOT(2) = FDOT * AFRAST / (1. - FF)**2
C
C           CALCULATE TEMPERATURE AND PRESSURE DERIVATIVES FOR
C           INTAKE MANIFOLD:
C
C           YDOT(2) = (AY1*(CM10-HM(1)) - CM11*PHDOT(1) + HNET1/Y(1))/CM9
C           YDOT(3) = (AY1 * RHOM(1) - CM6 * PHDOT(1) - CM4 *YDOT(2))/CM5
C
C           APPLY CONSERVATION OF MASS TO FIND EXHAUST MANIFOLD
C           MASS DERIVATIVE:
C
C           YDOT(5) = ENGM(2) - YDOT(14)
C           AY2 = YDOT(5) / Y(5)
C
C           CALCULATE TEMPERATURE AND PRESSURE DERIVATIVES FOR
C           EXHAUST MANIFOLD:
C
C           YDOT(6) = (AY2*(EX10-HM(2)) - EX11*PHDOT(2) + HNET2/Y(5))/EX9
C           YDOT(7) = (AY2 * RHOM(2) - EX6 * PHDOT(2) - EX4 *YDOT(6))/EX5
C
C           CALCULATE TURBOCHARGER SPEED DERIVATIVE:
C
C           WDOT = - (H(4) * YDOT(14) + H(3) * CMAP(1)) * 9.E-4 / PI**2
C           YDOT(9) = (WDOT/Y(9) - B(2) * Y(9) * ESPD) / B(1)
C
C           PERFORM TIME-AVERAGING OF PRESSURES, TEMPERATURES,
C           AND TURBOMACHINERY VARIABLES.
C
C           YDOT(15) = Y(3) / 720.
```

YDOT(16) = Y(7) / 720.
YDOT(17) = RTEMP(2) / 720.
YDOT(18) = HI(3) / 720.
YDOT(19) = Y(2) / 720.
YDOT(20) = Y(6) / 720.
YDOT(21) = RTEMP(3) / 720.
YDOT(22) = RTEMP(5) / 720.
YDOT(23) = HI(1) / 720.
YDOT(24) = RMASS(3) / 720.
YDOT(25) = TRBM /RCORR(2) /PRSS(2) /RCORR(4) * PSTD(2) /720.
YDOT(26) = ASP(1) /720.
YDOT(27) = ASP(2) /720.
YDOT(28) = ASP(3) /720.
YDOT(29) = PR(2) /720.
YDOT(30) = CMAP(2) /720.
YDOT(31) = TMAP(1) /720.
YDOT(32) = PTMAP(2) /720.
YDOT(33) = PTRBM /RCORR(2) /PRSS(4) /RCORR(5) * PSTD(3) /720.
YDOT(40) = RTEMP(4) / 720.

C

RETURN
END

```
C***** VERSION 2.0 *****
C                                     AUG 12, 1985
C
C   SUBROUTINE SUMIT
C
C   PURPOSE
C     CALCULATES TOTAL AND FUEL MASS FLOW RATES AND ENTHALPY FLUXES
C     THAT ENTER INTAKE AND EXHAUST MANIFOLDS.
C
C   METHOD
C     THE ALGORITHM SUMS THE MASS FLOW RATES (TOTAL AND FUEL), AND
C     THE ENTHALPY FLUXES CONTRIBUTED BY EACH CYLINDER EVERY INSTANT.
C     THE MASS FLOW RATE AND ENTHALPY FLUX PROFILES OF THE MASTER
C     CYLINDER DURING THE INTAKE AND THE EXHAUST PROCESS ARE GENERATED
C     BY THE SIMULATION AND STORED IN APPROPRIATE ARRAYS (MASSIN, MASSEX,
C     FCYLIN, FCYLEX, HCYLIN, HCYLEX).
C     THE PROFILES OF THE OTHER CYLINDERS ARE ASSUMED TO BE ECHOES OF
C     THE MASTER CYLINDER PROFILES, SHIFTED BY THE APPROPRIATE
C     PHASE ANGLES.
C
C   WRITTEN BY D. N. ASSANIS
C
C
C   SUBROUTINE SUMIT (A, FFR, HM, FLAG, AMASS, AF, AH, ITVO, ITVC,
C   &                ENGM, FMDOT, HMDOT)
C   DIMENSION AMASS(ITVO:ITVC), AF(ITVO:ITVC), AH(ITVO:ITVC)
C   PARAMETER(ICYL=6)
C   COMMON/EHF/ENT(6),H(6),F(6),TFLAG,T(6)
C
C
C     SUM UP MASS FLOW RATES, ENTHALPY FLUXES, FUEL FRACTION
C     FLUXES CONTRIBUTED BY EACH CYLINDER AT THAT INSTANT.
C
C   ENGM = 0.
C   FMDOT = 0.
C   HMDOT = 0.
C   TVO = FLOAT(ITVO)
C   TVC = FLOAT(ITVC)
C
C
C     FOR EACH CYLINDER, CHECK IF IT IS ENGAGED IN THE PROCESS.
C
C   DO 20 I = 1, ICYL
C     T(I) = 0.
C     ENT(I) = 0.
C     F(I) = 0.
C     H(I) = HM
C     T(I) = A - FLOAT((I-1)*720/ICYL)
C     IF ( T(I) .LE. (TVC - 720.)) T(I) = T(I) + 720.
C
C
C     IF THE CRANK ANGLE LIES BEFORE OR AFTER THE CYLINDER'S
C     PROCESS PERIOD, MOVE ON TO NEXT CYLINDER.
C
C     IF ((T(I) .GT. TVC) .OR. (T(I) .LT. TVO)) GO TO 20
```

```
C      IT = INT(T(I))
C
      ENT(I) = AMASS(IT)
      IF (ENT(I) * FLAG .GT. 0.) GO TO 17
      F(I) = AF(IT) - FFR
      H(I) = AH(IT)
C
17     FMDOT = FMDOT + ENT(I) * F(I)
      HMDOT = HMDOT + ENT(I) * H(I)
      ENGM  = ENGM  + ENT(I)
20 CONTINUE
C
      RETURN
      END
```

C***** VERSION 1.0 *****
C APR 20, 1985

C SUBROUTINE ICMAP

C PURPOSE

C INTERPOLATES COMPRESSOR MAP; GIVEN THE VALUE OF TWO
C MAP VARIABLES, CALCULATES THE VALUE OF THE TWO REMAINING
C MAP VARIABLES.

C USAGE

C CALL ICMAP (X, Y, AM, RPM, SIZ1, SIZ2, AMAP)

C DESCRIPTION OF PARAMETERS

PARAMETER	INPUT	OUTPUT	DESCRIPTION
X	YES	NO	CORRECTED SPEED (THOUSANDS RPM)
Y	YES	NO	PRESSURE RATIO
AM	YES	NO	MAP ARRAY (CM)
RPM	YES	NO	SPEED ARRAY (THOUSANDS OF RPM) CORRESPONDING TO AM (CRPM)
SIZ1	YES	NO	DIMENSION OF RPM ARRAY AND FIRST DIMENSION OF AM ARRAY
SIZ2	YES	NO	SECOND DIMENSION OF AM ARRAY
AMAP(1)	NO	YES	CORRECTED MASS FLOW RATE (LB/MIN)
AMAP(2)	NO	YES	EFFICIENCY

C REMARKS

C SUBROUTINE AND FUNCTION SUBPROGRAMS REQUIRED

C NONE

C METHOD

- C 1) GIVEN A CORRECTED SPEED, A SEARCH OF THE RPM ARRAY IS
C PERFORMED FROM THE LOWEST SPEED VALUE UNTIL A SPEED GREATER
C THAN THE INPUT SPEED IS FOUND. USING THAT GREATER SPEED AND
C THE SPEED JUST PREVIOUS TO THAT (THE LESSER SPEED), AN
C INTERPOLATION PARAMETER, "QI", IS CALCULATED.
- C 2) USING THE SPEED INTERPOLATION PARAMETER, VALUES OF
C PRESSURE RATIO AT THE INPUT SPEED ARE CALCULATED, UNTIL A
C PRESSURE RATIO GREATER THAN THE INPUT PRESSURE RATIO IS
C FOUND. USING THE GREATER AND LESSER PRESSURE RATIOS, A
C PRESSURE RATIO INTERPOLATION PARAMETER, "QJ", IS CALCULATED.
- C 3) USING THE SPEED AND PRESSURE RATIO INTERPOLATION
C PARAMETERS, CALCULATE THE MASS FLOW RATE AND EFFICIENCY
C CORRESPONDING TO THE INPUT VALUES OF SPEED AND PRESSURE
C RATIO.

C WRITTEN BY D. N. ASSANIS

C SUBROUTINE ICMAP (X, Y, AM, RPM, SIZ1, SIZ2, AMAP)

```
INTEGER SIZ2, SIZ1
DIMENSION AMAP(2), RPM(SIZ1), AM(SIZ1,SIZ2,3), A(15)
C
C     SEARCH FOR RPM-VALUE THAT IS JUST GREATER THAN THE
C     GIVEN X, AND STOP SEARCH:
C
DO 10 I2 = 2,SIZ1
IF(RPM(I2).GT.X) GO TO 20
10 CONTINUE
C
C     IF THE SEARCH WENT TO THE END OF THE SPEED ARRAY,
C     SET I2 TO INDICATE THE HIGHEST SPEED:
C
I2 = SIZ1
20 I1 = I2-1
C
C     DEFINE X (SPEED) INTERPOLATION PARAMETER:
C      $QI = (X-RPM(I1)) / (RPM(I2)-RPM(I1))$ 
C
C     SIMILARLY, SEARCH FOR MAP VALUE, INTERPOLATED BETWEEN
C     HIGH AND LOW RPM CURVES, THAT IS JUST GREATER THAN
C     THE GIVEN Y-VALUE:
C
DO 30 J2= 2,SIZ2
C
C     SET UP ARRAY OF INTERPOLATED VALUES OF PRESSURE RATIO
C
C      $A(J2) = QI * (AM(I2,J2,3)-AM(I1,J2,3)) + AM(I1,J2,3)$ 
C
C     CHECK IF INTERPOLATED PRESSURE RATIO IS GREATER THAN
C     INPUT VALUE:
C
IF((A(J2).GT.Y).AND.(J2.NE.1)) GO TO 40
C
30 CONTINUE
C
C     IF THE SEARCH WENT TO END OF THE MAP ARRAY, THE GIVEN SPEED
C     IS TOO LOW FOR THE GIVEN PRESSURE RATIO. FIND THE LOWEST
C     POSSIBLE SPEED THAT IS COMPATIBLE WITH THAT PRESSURE RATIO,
C     AND RETURN THAT SPEED TO MAIN PROGRAM.
C
35 I2 = I2 +1
I1 = I1 + 1
C      $QI = (Y-AM(I1,SIZ2,3)) / (AM(I2,SIZ2,3)-AM(I1,SIZ2,3))$ 
IF (I2 .EQ. SIZ1) GO TO 37
36 IF (QI.GT.1.0) GO TO 35
37 X = QI *(RPM(I2)-RPM(I1)) + RPM(I1)
J2 = SIZ2
A(J2) = Y
C
40 J1 = J2 - 1
IF (J1.EQ.1) A(J1)=QI*(AM(I2,J1,3)-AM(I1,J1,3)) + AM(I1,J1,3)
C
C     DEFINE Y INTERPOLATION PARAMETER :
```

```
QJ = (Y-A(J1)) / (A(J2)-A(J1))
C
DO 70 K = 1, 2
C
C     FIND THE OTHER MAP-VARIABLE VALUES WHICH CORRESPOND
C     TO THE INDICIES OF THE HIGH AND LOW Y-VALUES:
C
Z1 = QI*(AM(I2,J1,K)-AM(I1,J1,K)) + AM(I1,J1,K)
Z2 = QI*(AM(I2,J2,K)-AM(I1,J2,K)) + AM(I1,J2,K)
C
C     AND INTERPOLATE BETWEEN EACH PAIR OF VALUES TO FIND
C     THE MAP VALUES WHICH CORRESPOND TO THE ACTUAL MAP VALUES:
C
AMAP(K) = QJ * (Z2-Z1) + Z1
70 CONTINUE
C
RETURN
END
```

C***** VERSION 1.0 *****
C APR 20, 1985

C SUBROUTINE ITMAP

C PURPOSE

C INTERPOLATES TURBINE MAP; GIVEN THE VALUE OF TWO
C MAP VARIABLES, CALCULATES THE VALUE OF THE TWO REMAINING
C MAP VARIABLES.

C USAGE

C CALL ITMAP (X, Y, AM, RPM, SIZ1, SIZ2, AMAP)

C DESCRIPTION OF PARAMETERS

PARAMETER	INPUT	OUTPUT	DESCRIPTION
X	YES	NO	CORRECTED SPEED (THOUSANDS RPM)
Y	YES	NO	CORRECTED MASS FLOW RATE (LB/MIN)
AM	YES	NO	MAP ARRAY (TM)
RPM	YES	NO	SPEED ARRAY (THOUSANDS OF RPM) CORRESPONDING TO AM (TRPM)
SIZ1	YES	NO	DIMENSION OF RPM ARRAY AND FIRST DIMENSION OF AM ARRAY
SIZ2	YES	NO	SECOND DIMENSION OF AM ARRAY
AMAP(1)	NO	YES	EFFICIENCY
AMAP(2)	NO	YES	PRESSURE RATIO

C REMARKS

C THIS SUBROUTINE REPLACES TCMAP FOR THE TURBOCHARGER TURBINE.

C SUBROUTINE AND FUNCTION SUBPROGRAMS REQUIRED

C NONE

C METHOD

- C 1) GIVEN A CORRECTED SPEED, A SEARCH OF THE RPM ARRAY IS
C PERFORMED FROM THE LOWEST VALUE UNTIL A SPEED GREATER THAN
C THE INPUT SPEED IS FOUND. USING THAT GREATER SPEED AND THE
C SPEED JUST PREVIOUS TO THAT (THE LESSER SPEED), AN
C INTERPOLATION PARAMETER, "QI", IS CALCULATED.
- C 2) USING THE SPEED INTERPOLATION PARAMETER, VALUES OF MASS
C FLOW RATE AT THE INPUT SPEED ARE CALCULATED, UNTIL A MASS
C FLOW RATE GREATER THAN THE INPUT MASS FLOW RATE IS FOUND.
C USING THE GREATER AND LESSER MASS FLOW RATES, A MASS FLOW
C RATE INTERPOLATION PARAMETER, "QJ" IS CALCULATED.
- C 3) USING THE SPEED AND MASS FLOW RATE INTERPOLATION
C PARAMETERS, CALCULATE THE EFFICIENCY AND PRESSURE RATIO
C CORRESPONDING TO THE INPUT VALUES OF SPEED AND MASS FLOW
C RATE.

C WRITTEN BY D. N. ASSANIS

C SUBROUTINE ITMAP (X, Y, AM, RPM, SIZ1, SIZ2, AMAP)

```
INTEGER SIZ2, SIZ1
DIMENSION AMAP(2),RPM(SIZ1),AM(SIZ1,SIZ2,3),A(15)
C
C SEARCH FOR RPM-VALUE THAT IS JUST GREATER THAN THE
C GIVEN X, AND STOP SEARCH:
C
DO 10 I2 = 2,SIZ1
IF(RPM(I2).GT.X) GO TO 20
10 CONTINUE
C
C IF THE SEARCH WENT TO THE END OF THE SPEED ARRAY,
C SET I2 TO INDICATE THE HIGHEST SPEED:
C
I2 = SIZ1
20 I1 = I2-1
C
C DEFINE X (SPEED) INTERPOLATION PARAMETER:
C
QI = (X-RPM(I1)) / (RPM(I2)-RPM(I1))
C
C SIMILARLY, SEARCH FOR MAP VALUE, INTERPOLATED BETWEEN
C HIGH AND LOW RPM CURVES, THAT IS JUST GREATER THAN
C THE GIVEN Y-VALUE:
C
DO 30 J2= 2,SIZ2
C
C SET UP ARRAY OF INTERPOLATED VALUES OF MASS FLOW RATE
C
A(J2) = QI*(AM(I2,J2,1)-AM(I1,J2,1)) + AM(I1,J2,1)
C
C CHECK IF INTERPOLATED ARRAY VARIABLE (MASS FLOW RATE)
C IS GREATER THAN INPUT VALUE:
C
IF((A(J2).GT.Y).AND.(J2.NE.1)) GO TO 40
C
30 CONTINUE
C
C IF THE SEARCH WENT TO END OF THE MAP ARRAY, THE TURBINE
C HAS CHOKED. RETURN THE VALUES CORRESPONDING TO THE CHOKED
C CONDITIONS AT THIS SPEED.
C
J2 = SIZ2
Y = A(J2)
C
40 J1 = J2 - 1
C
C DEFINE Y INTERPOLATION PARAMETER:
C
QJ = (Y-A(J1)) / (A(J2)-A(J1))
C
DO 70 K = 1, 2
C
C FIND THE OTHER MAP-VARIABLE VALUES WHICH CORRESPOND
C TO THE INDICIES OF THE HIGH AND LOW Y-VALUES:
```

```
C
Z1 = QI*(AM(I2,J1,K+1)-AM(I1,J1,K+1)) + AM(I1,J1,K+1)
Z2 = QI*(AM(I2,J2,K+1)-AM(I1,J2,K+1)) + AM(I1,J2,K+1)
C
C      AND INTERPOLATE BETWEEN EACH PAIR OF VALUES TO FIND
C      THE MAP VALUES WHICH CORRESPOND TO THE ACTUAL MAP VALUES:
C
      AMAP(K) = QJ*(Z2-Z1) + Z1
70 CONTINUE
C
      RETURN
      END
```

C***** VERSION 1.1 *****

C MAY 6, 1985

C SUBROUTINE IPTMAP

C PURPOSE

C INTERPOLATES POWER TURBINE MAP(TURBOCOMPOUNDED CASE), OR TURBINE
C MAP(TURBOCHARGED ONLY CASE) ; GIVEN THE VALUE OF TWO MAP
C VARIABLES CALCULATES THE VALUE OF THE TWO REMAINING MAP
C VARIABLES.

C USAGE

C CALL IPTMAP (X, Y, AM, RPM, SIZ1, SIZ2, AMAP)

C DESCRIPTION OF PARAMETERS

PARAMETER	INPUT	OUTPUT	DESCRIPTION
X	YES	NO	CORRECTED SPEED (THOUSANDS OF RPM)
Y	YES	NO	PRESSURE RATIO
AM	YES	NO	MAP ARRAY (PTM)
RPM	YES	NO	SPEED ARRAY (THOUSANDS OF RPM) CORRESPONDING TO AM (PTRPM)
SIZ1	YES	NO	DIMENSION OF RPM ARRAY AND FIRST DIMENSION OF AM ARRAY
SIZ2	YES	NO	SECOND DIMENSION OF AM ARRAY
AMAP(1)	NO	YES	CORRECTED MASS FLOW RATE (LB/MIN)
AMAP(2)	NO	YES	EFFICIENCY

C REMARKS

C THIS SUBROUTINE REPLACES TCMAP FOR THE POWER TURBINE.

C SUBROUTINE AND FUNCTION SUBPROGRAMS REQUIRED

C NONE

C METHOD

- 1) GIVEN A CORRECTED SPEED, A SEARCH OF THE RPM ARRAY IS PERFORMED, FROM THE LOWEST SPEED VALUE UNTIL A SPEED GREATER THAN THE INPUT SPEED IS FOUND. USING THAT GREATER SPEED AND THE SPEED JUST PREVIOUS TO THAT (THE LESSER SPEED), A SPEED INTERPOLATION PARAMETER, "QI", IS CALCULATED.
- 2) USING THE SPEED INTERPOLATION PARAMETER, VALUES OF PRESSURE RATIO AT THE INPUT SPEED ARE CALCULATED, UNTIL A PRESSURE RATIO GREATER THAN THE INPUT PRESSURE RATIO IS FOUND. USING THE GREATER AND LESSER PRESSURE RATIOS, A PRESSURE RATIO INTERPOLATION PARAMETER "QJ" IS CALCULATED.
- 3) USING THE SPEED AND PRESSURE RATIO INTERPOLATION PARAMETERS, CALCULATE THE MASS FLOW RATE AND EFFICIENCY CORRESPONDING TO THE INPUT VALUES OF SPEED AND PRESSURE RATIO.

C WRITTEN BY D. N. ASSANIS

C SUBROUTINE IPTMAP (X, Y, AM, RPM, SIZ1, SIZ2, AMAP)

```
C
  INTEGER SIZ2, SIZ1
  DIMENSION AMAP(2), RPM(SIZ1), AM(SIZ1,SIZ2,3), A(15)
C
C   SEARCH FOR RPM-VALUE THAT IS JUST GREATER THAN THE
C   GIVEN X, AND STOP SEARCH:
C
  DO 10 I2 = 2,SIZ1
  IF(RPM(I2).GT.X) GO TO 20
10 CONTINUE
C
C   IF THE SEARCH WENT TO THE END OF THE SPEED ARRAY, SET I2 TO
C   INDICATE THE HIGHEST SPEED:
C
  I2 = SIZ1
20 I1 = I2-1
C
C   DEFINE X (SPEED) INTERPOLATION PARAMETER:
C
  QI = (X-RPM(I1)) / (RPM(I2)-RPM(I1))
C
C   SIMILARLY, SEARCH FOR MAP VALUE, INTERPOLATED BETWEEN
C   HIGH AND LOW RPM CURVES, THAT IS JUST GREATER THAN
C   THE GIVEN Y-VALUE:
C
  DO 30 J2= 2,SIZ2
C
C   SET UP ARRAY OF INTERPOLATED VALUES OF PRESSURE RATIO
C
  A(J2) = QI * (AM(I2,J2,3)-AM(I1,J2,3)) + AM(I1,J2,3)
C
C   CHECK IF INTERPOLATED PRESSURE RATIO IS GREATER THAN
C   INPUT VALUE:
C
  IF((A(J2).GT.Y).AND.(J2.NE.1)) GO TO 40
  GO TO 30
C
30 CONTINUE
C
C   IF THE SEARCH WENT TO END OF THE MAP ARRAY, THE TURBINE IS
C   CHOKED. RETURN THE VALUES CORRESPONDING TO CHOKED CONDITIONS
C   AT THIS SPEED.
C
  J2 = SIZ2
  Y = A(SIZ2)
C
40 J1 = J2 - 1
C
C   DEFINE Y INTERPOLATION PARAMETER:
C
50 QJ = (Y-A(J1)) / (A(J2)-A(J1))
C
  DO 70 K=1,2
C
```

```
C      FIND THE OTHER MAP-VARIABLE VALUES WHICH CORRESPOND
C      TO THE INDICIES OF THE HIGH AND LOW Y-VALUES:
C
C      Z1 = QI * (AM(I2,J1,K)-AM(I1,J1,K)) + AM(I1,J1,K)
C      Z2 = QI * (AM(I2,J2,K)-AM(I1,J2,K)) + AM(I1,J2,K)
C
C      AND INTERPOLATE BETWEEN EACH PAIR OF VALUES TO FIND
C      THE MAP VALUES WHICH CORRESPOND TO THE ACTUAL MAP VALUES:
C
C      AMAP(K) = QJ * (Z2-Z1) + Z1
70 CONTINUE
C
C      RETURN
C      END
```

C***** VERSION 3.0 *****
C AUG 13, 1985

C SUBROUTINE QDP

C PURPOSE

C CALCULATES HEAT TRANSFER FROM MANIFOLD AND PRESSURE DROP
C ACROSS MANIFOLD

C USAGE

C CALL QDP (TB, P, FFR, RHOB, J, ENGM, Q, PDROP)

C DESCRIPTION OF PARAMETERS

PARAMETER	INPUT	OUTPUT	DESCRIPTION
TB	YES	NO	MANIFOLD GAS TEMPERATURE (K)
P	YES	NO	MANIFOLD AVERAGE PRESSURE (PA)
FFR	YES	NO	MANIFOLD FUEL FRACTION (-)
RHOB	YES	NO	BULK DENSITY(KG/M**3)
J	YES	NO	INDEX (INTAKE: J=1, EXHAUST: J=2 CONNECTING PIPE: J=3)
ENGM	YES	NO	TOTAL ENGINE MASS FLOW RATE (KG/DEG)

Q	NO	YES	HEAT TRANSFER (W)
PDROP	NO	YES	PRESSURE DROP (PA)

C REMARKS

C REVISED VERSION.

C SUBROUTINE AND FUNCTION SUBPROGRAMS REQUIRED

C THERMO TRANSP

C METHOD

C HEAT TRANSFER CALCULATED FROM CORRELATION OF REYNOLDS,
C PRANDTL, AND NUSSELT NUMBERS FOR TURBULENT FORCED CONVECTION
C IN CIRCULAR TUBES.

C PRESSURE DROP CALCULATED BASED ON EMPIRICAL DATA.

C SEE ROSHENOW & CHOI, 'HEAT, MASS AND MOMENTUM TRANSFER'.

C WRITTEN BY D. N. ASSANIS

C EDITED BY D. N. ASSANIS

C SUBROUTINE QDP (TB, P, FFR, RHOB, J, ENGM, Q, PDROP)

C COMMON/EMKT/ EMKT(3)

C COMMON/DTDTH/ ESPD

C COMMON/QP1/ EDIAM(3), EAREA(3), ECROSS(3), ETWALL(3), ECONHT(3)

C COMMON/QP2/ EPRF(3), EVBLK(3), EREF(3), ENUF(3), EHTCOE(3),

C & EQDOT(3)

C IF (ENGM .GT. 0.) GO TO 20

C PDROP = 0.

C Q = 0.

C RETURN

```
C
C      DEFINE WALL AND FILM TEMPERATURES:
C
C      20 TW = ETWALL(J)
      TF = (TB + TW) / 2.
C
C      CALCULATE FILM DENSITY, SPECIFIC HEAT AND GAMMA:
C
C      CALL THERMO (TF, P, FFR, HF, CPF, Z1, Z2, RHOF, Z3,
&                Z4, Z5, GAMF, Z6, Z7, Z8, Z9)
      CALL TRANSP (TF, FFR, GAMF, CPF, UF, TKF)
C
C      CALCULATE BULK VELOCITY, FILM REYNOLDS NUMBER,
      FILM PRANDTL NUMBER:
C
      EVBLK(J) = ENGM / ESPD / RHOB / ECROSS(J)
      EREF(J)  = EVBLK(J) * EDIAM(J) * RHOF / UF
      EPRF(J)  = CPF * UF / TKF
C
C      CALCULATE NUSSELT NUMBER, HEAT TRANSFER COEFFICIENT
C
      ENUF(J) = ECONHT(J) * EREF(J)**.8 * EPRF(J)**.3
      EHTCOE(J) = ENUF(J) * TKF / EDIAM(J)
C
C      CALCULATE HEAT TRANSFER RATE:
      EQDOT(J) IS HEAT TRANSFER FROM FLUID TO WALL
C
      EQDOT(J) = EHTCOE(J) * EAREA(J) * (TB - TW)
C
C      Q IS HEAT TRANSFER FROM WALL TO FLUID IN [J/DEG]
C
      Q = - EQDOT(J) * ESPD
C
C      CALCULATE PRESSURE DROP:
C
      PDROP = EMKT(J) * RHOB * EVBLK(J) * EVBLK(J) / 2.
      RETURN
      END
```

C***** VERSION 1.0 *****
C OCT 21, 1984

C SUBROUTINE DELH

C PURPOSE

C TO CALCULATE THE CHANGE IN SPECIFIC ENTHALPY OF A MIXTURE
C OF AIR AND PRODUCTS OF COMBUSTION ACROSS AN ADIABATIC
C SHAFT WORK DEVICE (COMPRESSOR OR TURBINE) GIVEN THE UPSTREAM
C AND DOWNSTREAM PRESSURES AND GAS TEMPERATURES.

C USAGE

C CALL DELH (T1, T2, P1, P2, F, EF, TOUT, H1, H2, DH)

C DESCRIPTION OF PARAMETERS

PARAMETER	INPUT	OUTPUT	DESCRIPTION
T1	YES	NO	UPSTREAM TEMPERATURE (K)
T2	YES	NO	DOWNSTREAM TEMPERATURE ESTIMATE (K)
P1	YES	NO	UPSTREAM PRESSURE (PA)
P2	YES	NO	DOWNSTREAM PRESSURE (PA)
F	YES	NO	UPSTREAM FUEL FRACTION
EF	YES	NO	COMPRESSOR EFFICIENCY OR TURBINE RECIPROCAL EFFICIENCY

TOUT	NO	YES	ACTUAL DOWNSTREAM TEMPERATURE (K)
H1	NO	YES	SPECIFIC ENTHALPY OF INLET FLOW
H2	NO	YES	SPECIFIC ENTHALPY OF OUTLET FLOW
DH	NO	YES	CHANGE IN SPECIFIC ENTHALPY FROM INLET TO OUTLET

C REMARKS

C ENTHALPY UNITS ARE (J/KG)

C SUBROUTINES AND FUNCTIONS REQUIRED

C THERMO

C METHOD

C A MEAN SPECIFIC HEAT (CPM) IS CALCULATED BY THERMO USING A
C MEAN PRESSURE AND AN ESTIMATED MEAN TEMPERATURE. THE
C ACTUAL OUTLET TEMPERATURE AND THE UPSTREAM AND DOWNSTREAM
C SPECIFIC ENTHALPIES ARE THEN CALCULATED.

C SEE D.G. WILSON, 'THE DESIGN OF HIGH-EFFICIENCY TURBO-
C MACHINERY AND GAS TURBINES', CHAPTER 2;

C ALSO CRAVALHO & SMITH, 'THERMODYNAMICS', CHAPTER 11.

C WRITTEN BY K. K. REPLOGLE

C EDITED BY D. N. ASSANIS

C SUBROUTINE DELH (T1, T2, P1, P2, F, EF, TOUT, H1, H2, DH)

C DEFINE MEAN TEMPERATURE, MEAN PRESSURE AND PRESSURE RATIO:

C $TM = (T1 + T2) / 2.$

$$PM = (P1 + P2) / 2.$$

$$PR = P2 / P1$$

C
C
C

CALCULATE MEAN SPECIFIC HEAT:

CALL THERMO (TM, PM, F, HM, CPM, X1, X2, X3, X4, X5, X6,
& GAM, RMW, X9, X10, X11)

C
C
C

CALCULATE TEMPERATURE CHANGE:

$$DT = T1 / EF * (PR^{((GAM-1)/GAM)} - 1.)$$

C
C
C
C

CALCULATE OUTPUTS: INLET SPECIFIC ENTHALPY, EXIT
TEMPERATURE, ENTHALPY CHANGE AND EXIT SPECIFIC ENTHALPY:

CALL THERMO (T1, P1, F, H1, CP1, Y1, Y2, Y3, Y4, Y5, Y6,
& Y7, Y8, Y9, Y10, Y11)

$$TOUT = T1 + DT$$

$$DH = DT * CPM$$

$$H2 = H1 + DH$$

C

RETURN

END

C***** VERSION 1.0 *****

C AUG 21, 1985

C SUBROUTINE FLAME

C PURPOSE

C CALCULATES APPARENT RADIANT TEMPERATURE BASED ON ADIABATIC
C FLAME TEMPERATURE. THIS SUBROUTINE IS CALLED ONLY WHEN
C THE NEW RADIATION MODEL OPTION IS SELECTED (I.E. NOT WITH
C ANNAND'S MODEL OPTION)

C USAGE

C CALL FLAME (TG, P, TAIR, TFLAME, TRAD)

C DESCRIPTION OF PARAMETERS

PARAMETER	INPUT	OUTPUT	DESCRIPTION
TG	YES	NO	BULK GAS TEMPERATURE
P	YES	NO	BULK GAS PRESSURE
TAIR	NO	YES	TEMPERATURE OF AIR ZONES
TFLAME	NO	YES	ADIABATIC FLAME TEMPERATURE
TRAD	NO	YES	APPARENT RADIANT TEMPERATURE

C SUBROUTINE AND FUNCTION SUBPROGRAMS REQUIRED

C NONE

C METHOD

C SEE D. N. ASSANIS, PH.D. THESIS

C WRITTEN BY D. N. ASSANIS

C EDITED BY D. N. ASSANIS

C SUBROUTINE FLAME (TG, P, TAIR, TFLAME, TRAD)

C COMMON/TOPO/ TO, PO, GAM

C PARAMETER (ATPA=1.01325E5)

C ESTIMATE AIR TEMPERATURE ASSUMING ADIABATIC COMPRESSION
C FROM START OF IGNITION

C TAIR = TO * (P / PO)**(GAM - 1.)/GAM
C CALL THERMO (TAIR, P, O., X1, X2, X3, X4, X5, X6, X7, X8,
& GAM, X9, X10, X11, X12)

C ESTIMATE ADIABATIC FLAME TEMPERATURE AS A FUNCTION OF
C AIR TEMPERATURE AND PRESSURE, BASED ON CORRELATION
C DERIVED BY CURVE-FITTING RESULTS OF NASA EQUILIBRIUM CODE.

C PC = P /ATPA
C IF(TG .GT. 800.) GO TO 20
C TFLAME = (1. + 0.000249 * (TAIR - 650.)) *
& (2497.3 + 4.7521 * PC - 0.11065 *PC**2 + 0.000898 * PC**3)
C GO TO 30

```
C
20  TFLAME = (1. + 0.0002317 * (TAIR - 950.)) *
    &      (2726.3 + 0.9306 * PC - 0.003233 * PC**2)
C
30  CONTINUE
C
C      ESTIMATE RADIANT TEMPERATURE AS THE MEAN OF THE GAS
C      AND THE ADIABATIC FLAME TEMPERATURE.
C
    TRAD = 0.5 * TFLAME + 0.5 * TG
C
    RETURN
    END
```



```
UOVE = PUOVE(INDEX)
QSOL = PQSOL(INDEX)
C
DO 88 J = 1, 3
DELX(J) = PDELX(INDEX,J)
CNUM(J) = PCNUM(INDEX,J)
NNODE(J) = INNODE(INDEX,J)
THIK(J) = PTHIK(INDEX,J)
COND(J) = PCOND(INDEX,J)
HEFF(J) = PHEFF(INDEX,J)
DIFU(J) = PDIFU(INDEX,J)
DO 86 K = 1, NNODE(J)
86 TW(J,K) = PTW(INDEX,J,K)
88 CONTINUE
C
C          CALCULATE PARAMETERS REQUIRED TO OPTIMIZE GRID SPACING
C
SKIN = SQRT(DIFU(1)*PERIOD)
ALPHA = 1./THIK(1)
GAMMA = (SKIN*ALPHA - FACT) / (SKIN-THIK(1))/FACT
C
NNOD1 = NNODE(1)
NNOD2 = NNODE(2)
NNOD3 = NNODE(3)
C
C          CALCULATE TEMPERATURES AT INTERIOR NODES. NOTE TRANSFORMATION
C          INTRODUCED IN FIRST LAYER TO MAP VARIABLY-SPACED NODES INTO
C          CORRESPONDING UNIFORMLY-SPACED NODES.
C
IF (NNOD1.EQ.2) GO TO 15
DO 10 I = 2, (NNOD1 - 1)
YMID = (I-1.)/(NNOD1-1.)
XMID = (1.-YMID)/(GAMMA*YMID - ALPHA)
DYDXM = (ALPHA - GAMMA)/(GAMMA*XMID+1.)**2
C
YLEF = (I-1.5)/(NNOD1-1.)
XLEF = (1.-YLEF)/(GAMMA*YLEF - ALPHA)
DYDXL = (ALPHA - GAMMA)/(GAMMA*XLEF+1.)**2
C
YRIT= (I-0.5)/(NNOD1-1.)
XRIT = (1.-YRIT)/(GAMMA*YRIT - ALPHA)
DYDXR = (ALPHA - GAMMA)/(GAMMA*XRIT+1.)**2
C
TNW(1,I)= TW(1,I)+((TW(1,I+1)-TW(1,I))*DYDXR-(TW(1,I)-
& TW(1,I-1))*DYDXL)*DIFU(1)*DELT*DYDXM*(NNOD1-1.)**2
10 CONTINUE
15 CONTINUE
C
IF (NNOD2.EQ.2) GO TO 25
C
DO 20 I = 2, (NNOD2 - 1)
TNW(2,I)= (TW(2,I-1) + TW(2,I+1) + (CNUM(2)-2.)*TW(2,I))/CNUM(2)
20 CONTINUE
C
```

```
25  CONTINUE
C
  IF (NNOD3.EQ.2) GO TO 28
C
  DO 26 I = 2, (NNOD3 - 1)
    TNW(3,I) = (TW(3,I-1) + TW(3,I+1) + (CNUM(3)-2.)*TW(3,I))/CNUM(3)
26  CONTINUE
C
28  CONTINUE
C
  UPDATE INTERIOR NODES
C
  IF (NNOD1.EQ.2) GO TO 35
C
  DO 30 I = 2, (NNOD1 - 1)
30  TW(1,I) = TNW(1,I)
C
35  CONTINUE
C
  IF (NNOD2.EQ.2) GO TO 45
C
  DO 40 I = 2, (NNOD2 - 1)
40  TW(2,I) = TNW(2,I)
C
45  CONTINUE
C
  IF (NNOD3.EQ.2) GO TO 60
C
  DO 50 I = 2, (NNOD3 - 1)
50  TW(3,I) = TNW(3,I)
C
60  CONTINUE
C
  CALCULATE STEADY-STATE WALL SURFACE TEMPERATURE.
C
  STW = QSOL/UOVE + TCOOL
C
  CALCULATE WALL TEMPERATURE AT GAS SIDE:
C
  DYDX = (ALPHA-GAMMA)/(1.-GAMMA*THIK(1))**2
  FF = DYDX * (NNOD1-1.) * COND(1) / HTRCOE
  FG = FF * HTRCOE / 2.
  TW(1,1) = ((4.*TW(1,2) - TW(1,3))*FG - QSOL +
&  HTRCOE*(TGAS-STW))/ (3.*FG + HTRCOE)
C
  CALCULATE TEMPERATURE AT INTERFACE BETWEEN FIRST AND
  SECOND LAYER:
C
  DYDX = (ALPHA-GAMMA)
  FF = (NNOD2-1.)/(NNOD1-1.) /THIK(2) * COND(2)/COND(1)/DYDX
  TW(1,NNOD1) = (2.*TW(1,NNOD1-1) - 0.5*TW(1,NNOD1-2) -
&  FF*(0.5*TW(2,3) - 2.*TW(2,2)))/1.5/(1.+FF)
C
  TW(2,1) = TW(1,NNOD1)
```

```
C
C      CALCULATE TEMPERATURE AT INTERFACE BETWEEN SECOND AND
C      THIRD LAYER:
C
      FF = (NNOD3-1.)/(NNOD2-1.) *THIK(2)/THIK(3) * COND(3)/COND(2)
      TW(2,NNOD2) = (2.*TW(2,NNOD2-1) - 0.5*TW(2,NNOD2-2) -
&      FF*(0.5*TW(3,3) - 2.*TW(3,2)))/1.5/(1.+FF)
C
      TW(3,1) = TW(2,NNOD2)
C
C      CALCULATE WALL TEMPERATURE AT COOLANT SIDE:
C
      IF (HCOOL .EQ. 0.) GO TO 70
C
      STW2 = QSOL/HCOOL + TCOOL
      FG = HEFF(3)/ 2.
      TW(3,NNOD3) = ((4.*TW(3,NNOD3-1) - TW(3,NNOD3-2))*FG + QSOL +
&      HCOOL*(TCOOL-STW2))/ (3.*FG + HCOOL)
      GO TO 75
C
70      TW(3,NNOD3) = TCOOL
C
75      TWALL = TW(1,1) + STW
C
      DO 988 J = 1, 3
      DO 986 K = 1, NNODE(J)
986      PTW(INDEX,J,K) = TW(J,K)
988      CONTINUE
C
      RETURN
      END
```

C***** VERSION 1.0 *****
C AUG 21, 1985

C SUBROUTINE PARFIN

C PURPOSE

C READS IN WALL CONSTRUCTION DATA , GIVEN IN "PHEAT.DAT", FOR
C THE PISTON AND THE CYLINDER HEAD. ALSO, CALCULATES THE
C COURRANT NUMBER FOR EACH MATERIAL LAYER AND THE OVERALL
C HEAT TRANSFER COEFFICIENT FOR EACH COMPONENT.

C USAGE

C CALL PARFIN

C DESCRIPTION OF PARAMETERS

PARAMETER	INPUT	OUTPUT	DESCRIPTION
NPC	YES	NO	TOTAL NUMBER OF COMPONENTS WITH PARALLEL COMPOSITE WALL STRUCTURES
-----	---	--	
NPLA(I)	YES	NO	NUMBER OF MATERIAL LAYERS OF ITH COMPONENT
-----	---	--	
PHCOOL(I)	---	--	HEAT TRANSFER COEFFICIENT FROM THE OUTSIDE WALL SURFACE OF ITH COMPONENT TO THE COOLANT OR AMBIENT (W/M2/K)
-----	---	--	
PTCOOL(I)	YES	NO	AMBIENT, COOLANT, OR SPECIFIED OUTSIDE WALL TEMPERATURE
PTHIK(I,J)	YES	NO	THICKNESS OF JTH LAYER OF ITH COMPONENT(M)
PCOND(I,J)	YES	NO	THERMAL CONDUCTIVITY OF JTH LAYER OF ITH COMPONENT(W/M/K)
-----	---	--	
PDIFU(I,J)	YES	NO	THERMAL DIFFUSIVITY OF JTH LAYER OF ITH COMPONENT (M2/SEC)
-----	---	--	
INNOD(I,J)	YES	NO	NUMBER OF NODES PLACED IN JTH LAYER OF ITH COMPONENT
FACT	YES	NO	FRACTION OF NODES OF FIRST LAYER WITHIN THE PENETRATION DEPTH

C REMARKS

C FIRST ARRAY DIMENSION : COMPONENT DESCRIPTION
C SECOND ARRAY DIMENSION : LAYER DESCRIPTION

C SUBROUTINE AND FUNCTION SUBPROGRAMS REQUIRED

C NONE

C WRITTEN BY D. N. ASSANIS

C EDITED BY D. N. ASSANIS

C SUBROUTINE PARFIN

C COMMON/PARFIN/PDELX(2,3),PCNUM(2,3),INNOD(2,3),PTHIK(2,3),
& PCOND(2,3), PHEFF(2,3), PDIFU(2,3), PHCOOL(2), PTCOOL(2),

```
& PUOVE(2)
COMMON/PERFACT/ PERI, FACT, DELT
COMMON/DTDTH/ ESPD
COMMON/NPLA/ NPLA(2), NPC
C
  NAMELIST/PHEAT/ FACT, NPC, NPLA, PTCOOL, PHCOOL, PTHIK, PCOND,
&
  PDIFU, INNODE
  OPEN (UNIT=10, FILE='PHEAT.DAT', STATUS='OLD', READONLY)
  READ (10, PHEAT)
  CLOSE (UNIT =10)
C
  DELT = ESPD
C
  DO 10 I = 1, NPC
  SUM = 0.
  DO 20 J = 1, NPLA(I)
  PDELX(I,J) = PTHIK(I,J)/(INNODE(I,J)-1.)
  PCNUM(I,J) = PDELX(I,J)**2 / (PDIFU(I,J)*DELT)
  PHEFF(I,J) = PCOND(I,J) / PDELX(I,J)
  SUM = SUM + PTHIK(I,J)/PCOND(I,J)
20 CONTINUE
  IF (PHCOOL(I) .NE.0.) SUM = SUM + 1./PHCOOL(I)
  PUOVE(I) = 1./SUM
10 CONTINUE
C
  RETURN
  END
```

C***** VERSION 1.0 *****
C AUG 21, 1985

C SUBROUTINE CYLPAR

C PURPOSE

C READS IN WALL CONSTRUCTION DATA GIVEN IN "CHEAT.DAT", FOR
C UP TO 6 COMPONENTS WITH CYLINDRICAL COMPOSITE LAYERS, SUCH
C AS THE CYLINDER LINER. ALSO, IT CALCULATES THE OVERALL
C HEAT TRANSFER COEFFICIENT FOR EACH COMPONENT.

C USAGE

C CALL CYLPAR

C DESCRIPTION OF PARAMETERS

PARAMETER	INPUT	OUTPUT	DESCRIPTION
NCC	YES	NO	TOTAL NUMBER OF COMPONENTS WITH CYLINDRICAL COMPOSITE WALL STRUCTURES
-----	---	--	
CDIAM(I)	YES	NO	INSIDE PARAMETER OF ITH COMPONENT (M)
NCLA(I)	YES	NO	NUMBER OF MATERIAL LAYERS OF ITH COMPONENT
CHCOOL(I)	YES	NO	HEAT TRANSFER COEFFICIENT FROM THE OUTSIDE WALL SURFACE OF ITH COMPONENT TO THE COOLANT OR AMBIENT (W/M2/K)
CTCOOL(I)	YES	NO	AMBIENT TEMPERATURE, COOLANT TEMPERATURE, OR SPECIFIED OUTSIDE WALL TEMPERATURE
-----	---	--	
CTHIK(I,J)	YES	NO	THICKNESS OF JTH LAYER OF ITH COMPONENT (M)
-----	---	--	
CCOND(I,J)	YES	NO	THERMAL CONDUCTIVITY OF JTH LAYER OF ITH COMPONENT (W/M/K)
CUOVE(I)	NO	YES	OVERALL HEAT TRANSFER COEFFICIENT OF ITH COMPONENT (W/M**2/K)

C REMARKS

C FIRST ARRAY DIMENSION : COMPONENT DESCRIPTION
C SECOND ARRAY DIMENSION : LAYER DESCRIPTION

C SUBROUTINES AND FUNCTIONS REQUIRED

C NONE

C WRITTEN BY D. N. ASSANIS

C EDITED BY D. N. ASSANIS

C SUBROUTINE CYLPAR

C DIMENSION CDIAM(6), NCLA(6), CTHIK(6,3), CCOND(6,3),
& CHCOOL(6), CTCOOL(6), CUOVE(6)

```
C
COMMON/NCLA/ NCLA, NCC
COMMON/CYLPAR/ CDIAM, CTHIK, CCOND, CHCOOL, CTCOOL, CUOVE
C
NAMELIST/CHEAT/ CDIAM, NCLA, NCC, CTHIK, CCOND, CHCOOL, CTCOOL
C
OPEN (UNIT=9, FILE = 'CHEAT.DAT', STATUS='OLD', READONLY)
READ (9, CHEAT)
CLOSE (UNIT = 9)
C
DO 10 I = 1, NCC
C
C          CALCULATE INSIDE RADIUS OF COMPONENT
C
RADI = CDIAM(I) /2.
C
C          CALCULATE NET WALL THERMAL RESISTANCE
C
SUM = 0.
RAD1 = RADI
DO 20 J = 1, NCLA(I)
C
C          SUM THERMAL RESISTANCE FOR EACH LAYER
C
RAD2 = RAD1 + CTHIK(I,J)
RES = LOG(RAD2/RAD1) /CCOND(I,J)
SUM = SUM + RES
RAD1 = RAD2
20  CONTINUE
C
C          ADD THERMAL RESISTANCE AT OUTSIDE WALL SURFACE
C
IF (CHCOOL(I).NE. 0.0) SUM = SUM + 1. /RAD2 /CHCOOL(I)
C
CUOVE(I) = 1. /RADI /SUM
C
10  CONTINUE
C
RETURN
END
```

C***** VERSION 1.0 *****
C OCT 21, 1984

C SUBROUTINE ENGPARG

C PURPOSE

C 'ENGPARG' READS IN NON-DIMENSIONAL RATIOS OF VARIOUS ENGINE
C PARAMETERS WITH RESPECT TO THE ENGINE BORE. THEN, ALL DATA IS
C DENORMALIZED BY MULTIPLYING BY APPROPRIATE FACTORS OF THE
C ENGINE BORE. THE BORE IS READ IN BY THE MAIN PROGRAM AND
C TRANSFERRED TO 'ENGPARG' VIA A COMMON BLOCK.

C USAGE

C CALL ENGPARG

C DESCRIPTION OF PARAMETERS

PARAMETER	INPUT	OUTPUT	DESCRIPTION
STROKE	NO	YES	ENGINE STROKE (M)
CONRL	NO	YES	CONNECTING ROD LENGTH (M)
AHEAD	NO	YES	CYLINDER HEAD SURFACE AREA (M**2)
APSTON	NO	YES	PISTON TOP SURFACE AREA (M**2)
CSATDC	NO	YES	CHAMBER SURFACE AREA @ TDC (M**2)

C REMARKS

C UNITS CHANGED TO SI.

C SUBROUTINES AND FUNCTION SUBPROGRAMS REQUIRED

C METHOD

C SEE PURPOSE, ABOVE

C WRITTEN BY D. N. ASSANIS
C EDITED BY D. N. ASSANIS

C SUBROUTINE ENGPARG

C COMMON/EPARAM/ BORE, STROKE, CONRL, CYLCA, CSATDC, CMRTIO, CLVTDC
C COMMON/AREAS/ AHEAD, APSTON

C READ NORMALIZED STROKE, AND CONNECTING ROD LENGTH.

C STBRAT = 1.09091
C CTBRAT = 2.18182
C STROKE = BORE * STBRAT
C CONRL = BORE * CTBRAT

C READ IN NORMALIZED VALUES FOR THE CONSTANT SURFACE AREAS

C AHEAD = 0.983023
C APSTON = 0.785393

```
C      DE-NORMALIZE THE VALUES OF THE CONSTANT SURFACE AREAS
C
AHEAD = AHEAD * BORE * BORE
APSTON = APSTON * BORE * BORE
C
C      THE SURFACE AREA OF THE CYL. WALLS @ TDC IS ZERO.
C
ACWTDC = 0.0
C
C      CALCULATE CHAMBER SURFACE AREA @ TDC
C
CSATDC = AHEAD + APSTON + ACWTDC
C
C
RETURN
END
```

C***** VERSION 2.0 *****
C AUG 21, 1985

C SUBROUTINE FUELDT

C PURPOSE

C THIS SUBROUTINE IS CALLED TO SET THE VALUES OF THE FUEL
C RELATED PARAMETERS AT THE START OF PROGRAM EXECUTION. THE
C ONLY INPUT REQUIRED IS THE FUEL TYPE. THE PARAMETERS WHICH
C ARE SET ARE: I) THE ATOM RATIOS WHICH SPECIFY THE PROPERTIES
C OF THE FUEL AIR MIXTURE
C II) THE FUEL HEATING VALUE AND STOICHIOMETRIC FUEL/AIR RATIO;

C USAGE

C CALL FUELDT

C DESCRIPTION OF PARAMETERS

PARAMETER	INPUT	OUTPUT	DESCRIPTION
FUELTP	YES	NO	FUEL TYPE
PSI	NO	YES	MOLAR N2 TO O2 RATIO FOR AIR
CX	NO	YES	# OF CARBON ATOMS/FUEL MOLECULE
HY	NO	YES	# OF HYDROGEN ATOMS/FUEL MOLECULE
DEL	NO	YES	CARBON/HYDROGEN RATIO OF FUEL
QLOWER	NO	YES	LOWER HEATING VALUE OF THE FUEL (J/KG)
HFORM	NO	YES	ABSOLUTE ENTHALPY OF FUEL WRT. ITS CONSTITUENT ELEMENTS AT 0 K.
AFRAST	NO	YES	STOICHIOMETRIC AIR/FUEL RATIO

C REMARKS

C ONLY DIESEL FUEL AND ISOCTANE ARE AVAILABLE
C FOR USE AS FUELS.

C SUBROUTINES AND FUNCTION SUBPROGRAMS REQUIRED

C METHOD

C SEE PURPOSE, ABOVE

C WRITTEN BY D. N. ASSANIS

C EDITED BY D. N. ASSANIS

C SUBROUTINE FUELDT

C INTEGER FUELTP

C COMMON/FUEL/ FUELTP, CX, HY, DEL, PSI, AFRAST, QLOWER, HFORM

C PSI = 3.76

C IF (FUELTP .GT. 1) GO TO 10

C FOLLOWING DATA FOR DIESEL #2 FUEL (FUELTP = 1)

```
C
  CX = 10.84
  HY = 18.68
  DEL = 10.84 / 18.68
C
  UNITS: J/KG
C
  QLOWER = 42.910E+6
C
  NOTE THAT HFUEL = HF(298) + DHF(298-0)
  HF(298)=-0.844E+6, DHF=0.608E+6
  VARIABLE HFORM DENOTES REALLY HFUEL REL TO ELEMENTS AT 0 K.
C
  HFORM = -0.236E+6
  AFRAST = 137.9 * (DEL+.25) / (12.*DEL +1.)
C
C
  GO TO 20
C
  FOLLOWING DATA FOR ISOCTANE (FUELTP = 2)
C
10 CX = 8.0
  HY = 18.0
  DEL = 8.0/18.0
  QLOWER = 44.39E+6
  AFRAST = 15.11
C
20 RETURN
  END
```

C***** VERSION 1.0 *****
C OCT 21, 1984

C SUBROUTINE MFLRT

C PURPOSE

C CALCULATES MASS FLOW RATE THROUGH AN ORIFICE.

C USAGE

C CALL MFLRT (CD, AREA, PO, MW, TO, PS, GAMMA, FLRT)

C DESCRIPTION OF PARAMETERS

PARAMETER	INPUT	OUTPUT	DESCRIPTION
CD	YES	NO	DISCHARGE COEFFICIENT
AREA	YES	NO	AREA OF RESTRICTION (M**2)
PO	YES	NO	UPSTREAM PRESSURE (PA)
PS	YES	NO	DOWNSTREAM PRESSURE (PA)
MW	YES	NO	MOLECULAR WEIGHT (KG/KMOLE)
TO	YES	NO	UPSTREAM TEMPERATURE (K)
GAMMA	YES	NO	RATIO OF SPECIFIC HEATS, CP/CV
FLRT	NO	YES	MASS FLOW RATE (KG/S)

C REMARKS

C UNITS CHANGED TO SI

C SUBROUTINE AND FUNCTION SUBPROGRAM REQUIRED

C NONE

C METHOD

C FLOW THROUGH THE ORIFICE IS TREATED AS ONE-DIMENSIONAL,
C QUASI-STEADY, AND ISENTROPIC (MODIFIED BY A DISCHARGE
C COEFFICIENT)

C WRITTEN BY S. H. MANSOURI AND D. N. ASSANIS

C EDITED BY D. N. ASSANIS

C SUBROUTINE MFLRT (CD, AREA, PO, MW, TO, PS, GAMMA, FLRT)

C REAL MW

C FLRT = 0.0
C IF (PO .EQ. PS) GO TO 20
C GI = 1.0/GAMMA
C SUM = GAMMA * MW/TO
C PROD = 1./91.1767 * CD * AREA * PO * SQRT(SUM)

C RATIO = PS/PO
C CRIT = (2./((GAMMA + 1.))** (GAMMA/(GAMMA - 1.)))

C CHECK IF FLOW IS CHOKED

```
IF (RATIO .LT. CRIT) GO TO 10
C
C   SUBSONIC FLOW
C
SUN = 2./(GAMMA - 1.) * ( RATIO**(GI + GI) - RATIO**(GI + 1.) )
FLRT = PROD * SQRT(SUN)
GO TO 20
C
C   CHOKED FLOW
C
10 FLRT = PROD * CRIT**( 0.5 * (1.0 + GI) )
C
20 RETURN
END
```

```
C***** VERSION 1.0 *****
C                               OCT 21, 1984
C
C   SUBROUTINE VACDIN
C
C   PURPOSE
C       CALCULATES AREA AND DISCHARGE COEFFICIENT OF INTAKE VALVE
C       BY INTERPOLATING IN A TABLE OF EFFECTIVE INTAKE VALVE FLOW
C       AREAS, SUPPLIED BY CUMMINS.
C
C   WRITTEN BY D.N. ASSANIS
C
C   SUBROUTINE VACDIN (X, AREA, CD)
C   INTEGER IROW
C   PARAMETER (IROW=46)
C   DIMENSION TABLIN (IROW,2)
C   COMMON/TABLIN/ TABLIN
C   IF (X .LT. TABLIN(1,1) .OR. X .GT. TABLIN(IROW,1)) RETURN
5   DO 10 I2 = 2, IROW
C   IF (TABLIN(I2,1) .GT. X) GO TO 20
10  CONTINUE
C   I2 = IROW
20  I1 = I2 - 1
C
C   Q = (X - TABLIN(I1,1)) / (TABLIN(I2,1) - TABLIN(I1,1))
C   EFFAR = TABLIN(I1,2) + Q * (TABLIN(I2,2) - TABLIN(I1,2))
C
C   CONVERT AREAS FROM SQ.FEET INTO SQ.METERS
C
C   EFFAR = EFFAR * 0.092903
C   AREA = EFFAR
C   CD = 1.0
C
C   30 RETURN
C   END
```

```
C***** VERSION 1.0 *****
C                               OCT 21, 1984
C
C   SUBROUTINE VACDEX
C
C   PURPOSE
C       CALCULATES AREA AND DISCHARGE COEFFICIENT OF EXHAUST VALVE
C       BY INTERPOLATING IN A TABLE OF EFFECTIVE EXHAUST VALVE FLOW
C       AREAS, SUPPLIED BY CUMMINS.
C
C   WRITTEN BY D.N. ASSANIS
C
C   SUBROUTINE VACDEX (X, AREA, CD)
C   INTEGER EROW
C   PARAMETER (EROW=48)
C   DIMENSION TABLEX (EROW,2)
C   COMMON/TABLEX/ TABLEX
C   IF (X .LT. TABLEX(1,1) .OR. X .GT. TABLEX(EROW,1)) RETURN
5   DO 10 I2 = 2, EROW
C   IF (TABLEX(I2,1) .GT. X) GO TO 20
10  CONTINUE
C   I2 = EROW
20  I1 = I2 - 1
C
C   Q = (X - TABLEX(I1,1)) / (TABLEX(I2,1) - TABLEX(I1,1))
C   EFFAR = TABLEX(I1,2) + Q * (TABLEX(I2,2) - TABLEX(I1,2))
C
C   CONVERT AREAS FROM SQ.FEET INTO SQ.METERS
C
C   EFFAR = EFFAR * 0.092903
C   AREA = EFFAR
C   CD = 1.0
C
C   30 RETURN
C   END
```

```
C***** VERSION 1.0 *****
C                               OCT 21, 1984
C
C   SUBROUTINE CSAVDV
C
C   PURPOSE
C     CALCULATES THE SURFACE AREA OF THE CYL. WALLS, AND THE VOLUME
C     AND TIME RATE OF CHANGE OF THE VOLUME OF THE COMBUSTION CHAMBER
C
C   USAGE
C     CALL CSAVDV (T, ACW, VOLUME, DVDT)
C
C   DESCRIPTION OF PARAMETERS
C
C     PARAMETER  INPUT  OUTPUT  DESCRIPTION
C
C     T          YES    NO       TIME (DEG)
C     ACW        NO     YES      SURFACE AREA OF CYL. WALLS (M**2)
C     VOLUME     NO     YES      VOLUME OF THE CHAMBER (M**3)
C     DVDT       NO     YES      TIME RATE OF CHANGE OF VOLUME OF
C     -----    --    ---      CHAMBER (M**3/SEC)
C
C   REMARKS
C     UNITS CHANGED TO SI
C
C   SUBROUTINE AND FUNCTION SUBPROGRAMS REQUIRED
C     NONE
C
C   METHOD
C     SEE REPORT
C
C   WRITTEN BY D. N. ASSANIS
C   EDITED BY D. N. ASSANIS
C
C   SUBROUTINE CSAVDV (T, ACW, VOLUME, DVDT)
C
C   COMMON/EPARAM/ BORE, STROKE, CONRL, CYLCA, CSATDC, CMRTIO, CLVTDC
C   COMMON/DTDTH/ ESPD
C
C   CONVERT ANGLE MEASURE FROM DEGREES TO RADIANS.
C   THETA = T * 0.0174533
C   COSC  = 0.5 * STROKE * COS(THETA)
C   SINC  = 0.5 * STROKE * SIN(THETA)
C   CI    = SQRT( CONRL * CONRL - SINC * SINC )
C
C   CYLL: CYLINDER LENGTH FROM PISTON POSITION AT TDC
C   CYLL  = CONRL + 0.5 * STROKE - COSC - CI
C   IF (CYLL .LT. 0.0) CYLL = 0.0
C   ACW   = 3.141593 * BORE * CYLL
C   VOLUME = CLVTDC + CYLCA * CYLL
C   DVDT  = CYLCA * SINC * (1.0 + COSC/CI) * .0174533 / ESPD
C
C   RETURN
C   END
```

```
C***** VERSION 1.0 *****  
C                               OCT 21, 1984  
C  
C   FUNCTION EQR  
C  
C   PURPOSE  
C     TO CONVERT FUEL FRACTION INTO EQUIVALENCE RATIO  
C  
C   DESCRIPTION OF PARAMETERS  
C   INPUT:  FFR      FUEL FRACTION (THE RATIO OF MASS OF PRODUCTS  
C             OF COMBUSTION TO TOTAL MASS OF AIR AND  
C             COMBUSTION PRODUCTS)  
C   OUTPUT: EQR      EQUIVALENCE RATIO (THE RATIO OF THE  
C             ACTUAL FUEL-AIR RATIO TO THE STOICHIOMETRIC  
C             FUEL-AIR RATIO)  
C   COMMON: AFRAST   STOICHIOMETRIC AIR-FUEL RATIO  
C  
C   REMARKS  
C     NONE  
C  
C   SUBROUTINE AND FUNCTION SUBPROGRAMS REQUIRED  
C     NONE  
C  
C   WRITTEN BY D.N. ASSANIS  
C  
C   FUNCTION EQR (FFR)  
C  
C   COMMON/FUEL/ FUELTP, CX, HY, DEL, PSI, AFRAST, QLOWER, HFORM  
C  
C   EQR = FFR * AFRAST / (1.- FFR)  
C  
C   RETURN  
C   END
```

```
C***** VERSION 1.0 *****
C                               OCT 21, 1984
C
C   FUNCTION FAHR
C
C   PURPOSE
C     CONVERTS TEMPERATURE IN DEGREES K TO DEGREES F.
C
C   PARAMETERS
C   INPUT: T           TEMPERATURE IN DEGREES KELVIN
C   OUTPUT: FAHR      TEMPERATURE IN DEGREES FAHRENHEIT
C
C   REMARKS
C     NONE
C
C   SUBROUTINE AND FUNCTION SUBPROGRAMS REQUIRED
C     NONE
C
C   WRITTEN BY D.N. ASSANIS
C
C   FUNCTION FAHR (T)
C   FAHR = 9./5. * (T - 273.16) + 32.
C
C   RETURN
C   END
```

C***** VERSION 1.0 *****
C OCT 21, 1984

C SUBROUTINE ITRATE

C PURPOSE

C THIS SUBROUTINE IS CALLED TO OBTAIN T GIVEN P, H, FR,
C AND A GUESS FOR T. 'ITRATE' CALLS 'THERMO' WITH TGUSS.
C 'THERMO' RETURNS WITH THE ENTHALPY CORRESPONDING TO THE
C GIVEN TGUSS. THEN A NEW CORRECTED VALUE FOR TGUSS
C IS CALCULATED BY USING THE DEFINITION OF CSUBP AND THE
C KNOWN VALUES OF CORRECT H AND RETURNED HGUESS. THIS PRO-
C CEDURE IS REPEATED AT MOST MAXTRY TIMES, OR FEWER TIMES
C IF ACCURACY MAXERR IS ACHIEVED.

C USAGE

C CALL ITRATE (TGUSS, P, FR, ENTHLP, CSUBP, CSUBT, CSUBF,
C & RHO, DRHODT, DRHODP, DRHODF, GAMMA, MW, ADUMY,
C & BDUMY, CDUMY)

C DESCRIPTION OF PARAMETERS

PARAMETER	INPUT	OUTPUT	DESCRIPTION
TGUSS	YES	YES	TEMPERATURE GUESS (K)
-----	---	---	(CORRECTED VALUE IS RETURNED)
P	YES	NO	PRESSURE (PA)
FR	YES	NO	BURNED FUEL FRACTION (-)
ENTHLP	YES	NO	ENTHALPY ON WHICH TO ITERATE (J/KG)
HGUESS	NO	NO	ENTHALPY GUESS (J/KG)
CSUBP	NO	YES	DH/DT @ CONSTANT P (J/KG-DEG K)
CSUBT	NO	YES	DH/DP @ CONSTANT T (M**3/KG)
CSUBF	NO	YES	DH/DPHI @ CONSTANT T,P (J/KG)
RHO	NO	YES	DENSITY (KG/M**3)
DRHODT	NO	YES	PARTIAL OF RHO WITH RESPECT TO T (KG/M**3-DEG K)
DRHODP	NO	YES	PARTIAL OF RHO WITH RESPECT TO P (KG/M**3-PA)
DRHODF	NO	YES	PARTIAL OF RHO WITH RESPECT TO PHI (KG/M**3)
MW	NO	YES	MOLECULAR WEIGHT
GAMMA	NO	YES	RATIO OF SPECIFIC HEATS
ADUMY	NO	YES	DEFINED IN THERMO
BDUMY	NO	YES	DEFINED IN THERMO
CDUMY	NO	YES	DEFINED IN THERMO

C REMARKS

C UNITS CHANGED TO S.I.

C SUBROUTINES AND FUNCTION SUBPROGRAMS REQUIRED
C THERMO

C METHOD

C SEE PURPOSE, ABOVE
C

```
C   WRITTEN BY D. N. ASSANIS AND S. G. POULOS
C   EDITED BY D. N. ASSANIS
C
C   SUBROUTINE ITRATE ( TGUSS, P, FR, ENTHLP, CSUBP, CSUBT, CSUBF,
&   &           RHO, DRHODT, DRHODP, DRHODF, GAMMA, MW, ADUMY,
&   &           BDUMY, CDUMY)
C
C   REAL MW, MAXERR
COMMON/ITRLIM/ MAXTRY, MAXERR
C
C   DO 10 I = 1, MAXTRY
      CALL THERMO ( TGUSS, P, FR, HGUSS, CSUBP, CSUBT, CSUBF, RHO,
&   &           DRHODT, DRHODP, DRHODF, GAMMA, MW, ADUMY, BDUMY, CDUMY)
      TOLD = TGUSS
      TGUSS = TOLD + (ENTHLP - HGUSS)/CSUBP
      IF( ABS((TGUSS - TOLD)/TGUSS ) .LE. MAXERR ) GO TO 20
10 CONTINUE
C
20 CALL THERMO ( TGUSS, P, FR, HGUSS, CSUBP, CSUBT, CSUBF, RHO,
&   &           DRHODT, DRHODP, DRHODF, GAMMA, MW, ADUMY, BDUMY, CDUMY)
C
      RETURN
      END
```

C***** VERSION 1.0 *****
C OCT 21, 1984

C SUBROUTINE THERMO

C PURPOSE

C 'THERMO' IS CALLED BY THE THE 4 PROCESS ROUTINES AND BY
C 'MAIN' AND RETURNS WITH THE REQUIRED THERMODYNAMIC PROPER-
C TIES IN EACH CASE. IT CALLS 'HPROP',
C AND THEN CALCULATES FROM THE RETURNED DATA ANY
C ADDITIONAL PROPERTIES OF INTEREST. THERMO ALSO CONVERTS ALL
C VALUES TO UNITS THAT ARE CONSISTENT WITH THOSE USED IN
C THE REST OF THE PROGRAM.

C USAGE

C CALL THERMO (TEMP, P, FR, ENTHLP, CSUBP, CSUBT, CSUBF, RHO
C DRHODT, DRHODP, DRHODF, GAMMA, MW, ADUMY, BDUMY, CDUMY)

C DESCRIPTION OF PARAMETERS

PARAMETER	INPUT	OUTPUT	DESCRIPTION
TEMP	YES	NO	TEMPERATURE (K)
P	YES	NO	PRESSURE (PA)
FR	YES	NO	BURNED FUEL FRACTION
ENTHLP	NO	YES	ENTHALPY (J/KG)
CSUBP	NO	YES	PARTIAL OF H WITH RESPECT TO T (J/KG-DEG K)
CSUBT	NO	YES	PARTIAL OF H WITH RESPECT TO P (M**3/KG)
CSUBF	NO	YES	PARTIAL OF H WITH RESPECT TO PHI (J/KG)
RHO	NO	YES	DENSITY (KG/M**3)
DRHODT	NO	YES	PARTIAL OF RHO WITH RESPECT TO T (KG/M**3-DEG K)
DRHODP	NO	YES	PARTIAL OF RHO WITH RESPECT TO P (KG/M**3-PA)
DRHODF	NO	YES	PARTIAL OF RHO WITH RESPECT TO PHI (KG/M**3)
MW	NO	YES	MOLECULAR WEIGHT
GAMMA	NO	YES	RATIO OF SPECIFIC HEATS
ADUMY	NO	YES	SEE ASSIGNMENT STATEMENTS BELOW (J/KG-DEG K)
BDUMY	NO	YES	SEE ASSIGNMENT STATEMENTS BELOW (J/KG)
CDUMY	NO	YES	SEE ASSIGNMENT STATEMENTS BELOW (J/KG)

C REMARKS

C UNITS CHANGED TO SI

C SUBROUTINES AND FUNCTION SUBPROGRAMS REQUIRED

C HPROP

C METHOD

```
C      SEE PURPOSE, ABOVE
C
C      WRITTEN BY D. N. ASSANIS
C      EDITED BY D. N. ASSANIS
C
C      SUBROUTINE THERMO (TEMP, P, FR, ENTHLP, CSUBP, CSUBT, CSUBF, RHO,
&      DRHODT,DRHODP,DRHODF, GAMMA, MW, ADUMY, BDUMY, CDUMY)
C
C      REAL MW
C
C      PRES = P/1.01325E+5
C      CALL HPROP (TEMP, PRES, FR, ENTHLP, CSUBP, CSUBT, CSUBF,
&      RHO, DRHODT, DRHODP, DRHODF)
C
C      CONVERT TO UNITS NEEDED IN MAIN PROGRAM
C
C      ENTHLP= ENTHLP* 4.184E+6
C      CSUBP = CSUBP * 4.184E+3
C      CSUBT = CSUBT / 1000.
C      CSUBF = CSUBF * 4.184E+6
C
C      RHO   = RHO   * 1000.
C      DRHODT= DRHODT * 1000.
C      DRHODP= DRHODP / 101.325
C      DRHODF= DRHODF * 1000.
C
C      CALCULATE GAS CONSTANT, MOLECULAR WEIGHT, DUMMY VARIABLES
C
C      ADUMY = CSUBP + ( DRHODT/DRHODP )*( 1./RHO - CSUBT )
C      BDUMY = (1. - RHO * CSUBT) / DRHODP
C      CDUMY = CSUBF + ( DRHODF/DRHODP )*( 1./RHO - CSUBT )
C
C      R      = P / (RHO * TEMP)
C      MW     = 8.3145E+3/R
C      GAMMA = CSUBP/( CSUBP - R )
C
C      RETURN
C      END
```

C***** VERSION 1.0 *****
C OCT 21, 1984

C SUBROUTINE HPROP

C PURPOSE

C TO CALCULATE THE PROPERTIES OF THE PRODUCTS OF HYDROCARBON-
C AIR COMBUSTION AS A FUNCTION OF TEMPERATURE AND PRESSURE,
C USING AN APPROXIMATE CORRECTION FOR DISSOCIATION.
C H AND RHO ARE CALCULATED AS FUNCTIONS OF P, T, AND PHI.
C THE PARTIAL DERIVATIVES OF H AND RHO WITH RESPECT TO
C P AND T ARE ALSO CALCULATED.

C USAGE

C CALL HPROP (T,P,FR, H,CP,CT,CF, RHO,DRHODT,DRHODP,DRHODF)

C DESCRIPTION OF PARAMETERS

C GIVEN:

C P : ABSOLUTE PRESSURE OF PRODUCTS (ATM)
C T : TEMPERATURE OF PRODUCTS (DEG K)
C FR : AVERAGE FUEL FRACTION
C DEL : MOLAR C:H RATIO OF PRODUCTS
C PSI : MOLAR N:O RATIO OF PRODUCTS

C RETURNS:

C H : SPECIFIC ENTHALPY OF PRODUCTS (KCAL/G)
C UNITS CHECKED ON 9/26/83.
C CP : PARTIAL DERIVATIVE OF H WITH RESPECT TO T
C (CAL/G-DEG K) - UNITS CHECKED ON 9/26/83.
C CT : PARTIAL DERIVATIVE OF H WITH RESPECT TO P (CC/G)
C CF : PARTIAL DERIVATIVE OF H WITH RESPECT TO PHI (KCAL/G)
C SAME UNITS WITH ENTHALPY - CHECKED ON 9/26/83.
C CONSISTENCY WITH UNITS OF CF IN CPROP.
C RHO : DENSITY OF THE PRODUCTS (G/CC)
C DRHODT: PARTIAL DERIVATIVE OF RHO WITH RESPECT TO T
C (G/CC-DEG K)
C DRHODP: PARTIAL DERIVATIVE OF RHO WITH RESPECT TO P
C (G/CC-ATM)
C DRHODF: PARTIAL DERIVATIVE OF RHO WITH RESPECT TO PHI
C (G/CC)

C REMARKS

- C 1) ENTHALPY DATUM STATE IS AT T = 0 ABSOLUTE WITH
C O₂, N₂, H₂ GASEOUS AND C SOLID GRAPHITE
C 2) MULTIPLY ATM-CC BY 0.0242173 TO CONVERT TO CAL
C 3) MODIFIED VERSION OF MIKE MARTIN'S PROGRAM
C BY DENNIS ASSANIS (253-2453)
C ADDED PARTIAL DERIVATIVES OF ENTHALPY AND DENSITY
C WITH RESPECT TO EQUIVALENCE RATIO

C SUBROUTINES AND FUNCTION SUBPROGRAMS REQUIRED
C CPROP

C METHOD

C SEE MARTIN AND HEYWOOD 'APPROXIMATE RELATIONSHIPS FOR THE

```
C      THERMODYNAMIC PROPERTIES OF HYDROCARBON-AIR COMBUSTION
C      PRODUCTS'
C
C      SUBROUTINE HPROP (T,P,FR, H, CP,CT,CF, RHO, DRHODT,DRHODP,DRHODF)
C
C      LOGICAL RICH, LEAN, NOTHOT, NOTWRM, NOTCLD
C      REAL MCP, MWT, K1, K2
C      COMMON/FUEL/ FUELTP, CX, HY, DEL, PSI, AFRAST, QLOWER, HFORM
C
C      INITIALIZE PARAMETERS USED IN THE CALCULATION
C      NOTE THAT R DENOTES THE UNIVERSAL GAS CONSTANT
C      GIVEN BY R = 1.9869 CAL / MOLE-DEG K
C
C      DATA R,ROVER2 /1.9869,0.99345/, PSCALE /2.42173E-2/
C      DATA TCOLD,THOT /1000.,1100./
C
C      PHI      = FR * AFRAST / (1. - FR)
C      RICH     = PHI .GE. 1.0
C      LEAN     = .NOT. RICH
C      NOTHOT   = T .LT. THOT
C      NOTCLD   = T .GT.TCOLD
C      NOTWRM   = .NOT. (NOTCLD .AND. NOTHOT)
C      EPS      = (4.*DEL)/(1. + 4.*DEL)
C
C      USE SIMPLE ROUTINE FOR LOW TEMPERATURE MIXES
C
C      IF (NOTCLD) GO TO 5
C      CALL CPRP (T,P,FR, H, CP,CT,CF, RHO, DRHODT,DRHODP,DRHODF)
C      RETURN
C
C      CALCULATE EQUILIBRIUM CONSTANTS FOR DISSOCIATION (EQS. 3.9
C      & 3.10) (NOTE THAT THESE HAVE UNITS ATM**(0.5) )
C
C      5 K1 = 5.819E-6 * EXP(0.9674*EPS + 35810./T)
C      K2 = 2.961E-5 * EXP(2.593*EPS + 28980./T)
C
C      CALCULATE A, X, Y, & U AS IN EQS. 5.24, 3.6, 5.25, 3.7, 2.18,
C      2.19, & 3.8
C
C      C5 = 2.- EPS + PSI
C      A  = (C5/(4.*P*K1*K1*EPS))**(0.33333333)
C
C      C6 = EPS + 2.*C5
C      X  = A*EPS*(3.*C5 + C6*A)/(3.*(1.+ 2.*A)*C5 + 2.*C6*A*A)
C
C      Z  = ABS(1.-PHI)/X
C      IF (LEAN) Y = X/SQRT(1.+ .666667*Z + 1.3333333*(1.-PHI))
C      IF (RICH) Y = X/(1.+0.666667*Z + 0.3333333*Z*Z -0.666667*(PHI-1.))
C      U  = C5*(EPS - 2.*X)/(4.*K1*K2*P*X)
C
C      CALCULATE THE ENTHALPY OF FORMATION FOR THIS APPROXIMATE
C      COMPOSITION AS IN EQS. 3.21, 3.22, & 5.7. ALSO GET THE
C      COEFFICIENTS FOR T & TV TERMS IN 3.15 USING 5.3 & 5.4
```

```
C
HF = 1000.*((121.5 + 29.59*EPS)*Y + 117.5*U)
HF = HF + (20372.*EPS - 114942.)*PHI
C1 = 7.*PSI + 5.*Y + 3.*U
C2 = 2.*(PSI - 3.*Y - U)

C
IF (LEAN) GO TO 10

C
C   RICH CASE
C
HF = HF + 1000.*(134.39 - 6.5/EPS)*(PHI - 1.)
C1 = 2. + 2.*(7.- 4.*EPS)*PHI + C1
C2 = 8. + 2.*(2.- 3.*EPS)*PHI + C2
GO TO 20

C
C   LEAN CASE

10 C1 = 7. + (9.- 8.*EPS)*PHI + C1
   C2 = 2. + 2.*(5.- 3.*EPS)*PHI + C2

C
C   ADD IN TRANSLATIONAL, VIBRATIONAL, AND ROTATIONAL TERMS
C   TO GET TOTAL ENTHALPY, USING EQS. 3.16, 5.6, 3.11, & 3.15
C
20 TV = (3256.- 2400.*EPS + 300.*PSI)/(1.- .5*EPS + .09*PSI)
   EXPTVT = EXP(TV/T)
   TVTIL = TV/(EXPTVT - 1.)
   MCP = (8.*EPS + 4.)*PHI + 32. + 28.*PSI

C
C   NOTE MULTIPLICATION OF H BY 0.001 TO CONVERT UNITS
C   FROM CAL/G TO KCAL/G.
C   NOW, UNITS OF H ARE SAME IN HPROP AND CPROP.
C
H = 0.001*ROVER2*(C1*T + C2*TVTIL + HF)/MCP

C
C   CALCULATE THE AVERAGE MOLECULAR WEIGHT, AND GET DENSITY
C   BY USING THE PERFECT GAS LAW - EQS. 3.12, 3.13, & 3.14
C
IF (LEAN) MWT = MCP/(1. + (1.- EPS)*PHI + PSI + Y + U)
IF (RICH) MWT = MCP/( (2.- EPS)*PHI + PSI + Y + U)

C
RHO = MWT*P*PSCALE/(R*T)

C
C   GET PARTIAL DERIVATIVES IF DESIRED
C
C   THE FOLLOWING USES IN ORDER EQS. 5.8, 5.9, 5.32, 5.31, 5.30,
C   5.29, 5.28, & 5.26
C
C3 = (121.5 + 29.59*EPS)*1000.
C4 = 1.175E5

C
DUDTPX = 64790.*U/(T*T)
DUDPTX = -U/P
DUDXPT = -U*EPS/(X*(EPS - 2.*X))

C
```

DADTP = 23873.*A/(T*T)
DADPT = -A/(3.*P)

C

T5 = 3.*C5
DXDA = T5*EPS*(T5 + 2.*C6*A)/(T5*(1. + 2.*A) + 2.*C6*A*A)**2

C

C

FOLLOWING USES EQS. 5.23, 5.19-5.22, 5.18-5.14, 5.12, & 5.13

C

IF (LEAN) DYDX = (Y*Y*Y)/(X*X*X) * (1.+ Z + 1.333333*(1.-PHI))
IF (RICH) DYDX = (Y*Y)/(X*X)*(1.+ 4.*Z/3. + Z*Z -2.*(PHI-1.)/3.)

C

DYDTP = DYDX*DXDA*DADTP
DYDPT = DYDX*DXDA*DADPT
DUDTP = DUDXPT*DXDA*DADTP + DUDTPX
DUDPT = DUDXPT*DXDA*DADPT + DUDPTX

C

DHFDPT = C3*DYDPT + C4*DUDPT
DC2DPT = -2.*(3.*DYDPT + DUDPT)
DC1DPT = 5.*DYDPT + 3.*DUDPT
DHFDTP = C3*DYDTP + C4*DUDTP
DC2DTP = -2.*(3.*DYDTP + DUDTP)
DC1DTP = 5.*DYDTP + 3.*DUDTP

C

DTVDTPT = (TVTIL*TVTIL)/(T*T)*EXPTVT

C

C

FOLLOWING USES EQS. 5.10, & 5.11

C

C

CP = ROVER2/MCP*(C1 + T*DC1DTP + C2*DTVDTPT + TVTIL*DC2DTP
& + DHFDTP)
CT = ROVER2/MCP*(T*DC1DPT + TVTIL*DC2DPT + DHFDPT)*PSCALE

C

C

DMCPDF = 8. * EPS + 4.
IF (RICH) GO TO 55

C

C

LEAN CASE

C

DYDF = 1./3. * (Y/X)**3 * (1.+2.*X)
DC1DF = (9.-8*EPS) + 5.*DYDF
DC2DF = 2.*(5.-3.*EPS) - 6.*DYDF
DHFDFF = 20732.*EPS - 114942. + C3*DYDF

C

D = 1. + (1.-EPS)*PHI + PSI + Y + U
DDDF = (1.-EPS) + DYDF
GO TO 65

C

C

RICH CASE

C

55 DYDF = -2./3. * (Y/X)**2 * (1.+Z-X)
DC1DF = 2.*(7.-4.*EPS) + 5.*DYDF
DC2DF = 2.*(2.-3.*EPS) - 6.*DYDF
DHFDFF = 20732.*EPS + 19448. + C3*DYDF - 6500./EPS

C

D = (2.-EPS)*PHI + PSI + Y + U
DDDF = (2.-EPS) + DYDF

C
C
C
C
C
C

NOTE MULTIPLICATION OF CF BY 0.001 TO CONVERT UNITS
FROM CAL/G TO KCAL/G , NEEDED BY THERMO.
NOW, UNITS OF CF ARE SAME IN HPROP AND CPROP.
NOTE ALSO THAT CF HAS SAME UNITS WITH ENTHALPY.

65 CF = 0.001 * ROVER2/MCP * ((DC1DF - C1/MCP*DMCPDF)*T +
& (DC2DF-C2/MCP*DMCPDF)*TVTIL + (DHFDF-HF/MCP*DMCPDF))

C

G = -MCP / (D*D)
DMWDT = G * (DYDTP + DUDTP)
DMWDP = G * (DYDPT + DUDPT)
DMWDF = -MCP/D/D* (DDDF - D/MCP*DMCPDF)

C

DRHODT = PSCALE * P * (DMWDT - MWT/T) / (R*T)
DRHODP = PSCALE * (MWT + P*DMWDP) / (R*T)
DRHODF = PSCALE * P * DMWDF / (R*T)

C
C
C
C
C

IF CALCULATING FOR AN INTERMEDIATE TEMPERATURE, USE A
WEIGHTED AVERAGE OF THE RESULTS FROM THIS ROUTINE AND
THOSE FROM THE SIMPLE ROUTINE

IF (NOTWRM) RETURN

C

CALL CPROP (T,P,FR, TH, TCP, TCT, TCF, TRHO, TDRT, TDRP, TDRF)
W1 = (T - TCOLD)/(THOT - TCOLD)
W2 = 1.0 - W1

C

H = W1*H + W2*TH
RHO = W1*RHO + W2*TRHO
CP = W1*CP + W2*TCP
CT = W1*CT + W2*TCT
CF = W1*CF + W2*TCF
DRHODT = W1*DRHODT + W2*TDRT
DRHODP = W1*DRHODP + W2*TDRP
DRHODF = W1*DRHODF + W2*TDRF

C

RETURN
END


```
C      SUBROUTINES AND FUNCTION SUBPROGRAMS REQUIRED
C      NONE
C
C      METHOD
C      SEE SAE PAPER BY HIRES ET AL (APPENDIX)
C      SEE MARTIN & HEYWOOD 'APPROXIMATE RELATIONSHIPS FOR THE
C      THERMODYNAMIC PROPERTIES OF HYDROCARBON-AIR COMBUSTION
C      PRODUCTS'
C
C      SUBROUTINE CPROP (T, P, FR, ENTHLP, CSUBP, CSUBT, CSUBF,
&      RHO, DRHODT, DRHODP, DRHODF)
C
C      LOGICAL RICH, LEAN
C      REAL*4 MBAR, K
C
C      DECLARE MCP
C      REAL MCP
C      DIMENSION A(6,6,2), X(6), DX(6)
C      DIMENSION A1(36), A2(36)
C      COMMON/FUEL/ FUELTP, CX, HY, DEL, PSI, AFRAST, QLOWER, HFORM
C      EQUIVALENCE (A1(1), A(1,1,1)), (A2(1), A(1,1,2))
C
C      INITIALIZE PARAMETERS, AND CHECK TO SEE IN WHAT TEMPERATURE
C      RANGE WE ARE SO THAT THE CORRECT FITTED COEFFICIENTS WILL BE
C      USED. FLAG TEMPERATURES TOO HIGH OR TOO LOW.
C
C      DATA A1/11.94033,2.088581,-0.47029,.037363,-.589447,-97.1418,
1  6.139094,4.60783,-.9356009,6.669498E-02,.0335801,-56.62588,
2  7.099556,1.275957,-.2877457,.022356,-.1598696,-27.73464,
3  5.555680,1.787191,-.2881342,1.951547E-02,.1611828,.76498,
4  7.865847,.6883719,-.031944,-2.68708E-03,-.2013873,-.893455,
5  6.807771,1.453404,-.328985,2.561035E-02,-.1189462,-.331835/
C      DATA A2/4.737305,16.65283,-11.23249,2.828001,6.76702E-03,
1  -93.75793,7.809672,-.2023519,3.418708,-1.179013,1.43629E-03,
2  -57.08004,6.97393,-.8238319,2.942042,-1.176239,4.132409E-04,
3  -27.19597,6.991878,.1617044,-.2182071,.2968197,-1.625234E-02,
4  -.118189,6.295715,2.388387,-.0314788,-.3267433,4.35925E-03,
5  .103637,7.092199,-1.295825,3.20688,-1.202212,-3.457938E-04,
6  -.013967/
C
C      PHI = FR * AFRAST / (1.-FR)
C      RICH = PHI .GT. 1.0
C      LEAN = .NOT. RICH
C      EPS = 4.*DEL/(1. + 4.*DEL)
C      IR = 1
C      IF (T .LT. 500.) IR = 2
C
C      GET THE COMPOSITION IN MOLES/MOLE OXYGEN
C
C      IF (RICH) GO TO 10
C      X(1) = EPS*PHI
C      X(2) = 2.*(1.- EPS)*PHI
C      X(3) = 0.
```

```

X(4) = 0.
X(5) = 1.- PHI
C
DX(1)= EPS
DX(2)= 2.*(1.-EPS)
DX(3)= 0.
DX(4)= 0.
DX(5)=-1.
C
GO TO 20
10 K      = 3.5
ALPHA = 1. - K
BETA  = (2.*(1.-EPS*PHI) + K*(2.*(PHI - 1.) + EPS*PHI))
GAMMA = 2.*K*EPS*PHI*(PHI - 1.)
C      = ( -BETA + SQRT(BETA*BETA + 4.*ALPHA*GAMMA))/(2.*ALPHA)
X(1)  = EPS*PHI - C
X(2)  = 2.*(1. - EPS*PHI) + C
X(3)  = C
X(4)  = 2.*(PHI - 1.) - C
X(5)  = 0.
C
C      WORK-OUT DERIVATIVES DX(1) UNTIL DX(5) FOR RICH CASE
C      AT A LATER DATE, AND REPLACE THE FOLLOWING ZEROES BY THE
C      CORRECT EXPRESIONS. NOT NECESSARY FOR MY CASE.
C
DX(1) = 0.
DX(2) = 0.
DX(3) = 0.
DX(4) = 0.
DX(5) = 0.
C
20 X(6) = PSI
DX(6) = 0.
C
C      CONVERT COMPOSITION TO MOLE FRACTIONS AND CALCULATE AVERAGE
C      MOLECULAR WEIGHT
C
IF (LEAN) TMOLES = 1. + PSI + PHI*(1.-EPS)
IF (RICH) TMOLES = PSI + PHI*(2.-EPS)
DO 30 J = 1, 6
    X(J) = X(J)/TMOLES
30 CONTINUE
MBAR = ((8.*EPS + 4.)*PHI + 32. + 28.*PSI)/TMOLES
C
MCP = (8.*EPS+4.)*PHI + 32. + 28.*PSI
DMCPDF = (8.*EPS+4.)
C
C      CALCULATE H, CP, CT, AND CF, AS IN WRITEUP,
C      USING FITTED COEFFICIENTS FROM JANAF TABLES.
C
ENTHLP = 0.
CSUBP  = 0.
CSUBT  = 0.
CSUBF  = 0.

```

```
ST      = T/1000.
DO 40 J = 1,6
  TH     = ((( A(4,J,IR)/4.*ST + A(3,J,IR)/3.)*ST
&        + A(2,J,IR)/2.)*ST + A(1,J,IR) )*ST
  TCP    = (( A(4,J,IR)*ST + A(3,J,IR) )*ST
&        + A(2,J,IR) )*ST + A(1,J,IR)
  TH     = TH - A(5,J,IR)/ST + A(6,J,IR)
  TCP    = TCP + A(5,J,IR)/ST**2
  ENTHLP = ENTHLP + TH*X(J)
  CSUBP  = CSUBP + TCP*X(J)
  CSUBF  = CSUBF + 1./MCP * ( TH*DX(J) - DMCPDF/MCP*TH*X(J) )
40 CONTINUE
  ENTHLP = ENTHLP/MBAR
  CSUBP  = CSUBP/MBAR
C
C      NOW CALCULATE RHO AND ITS PARTIAL DERIVATIVES
C      USING PERFECT GAS LAW
C
  RHO    = .012187*MBAR*P/T
  DRHODT = -RHO/T
  DRHODP = RHO/P
C
  IF (RICH) GO TO 60
C
  LEAN CASE
C
50 D     = 1. + (1.-EPS)*PHI + PSI
  DDDF   = (1.-EPS)
  GO TO 70
C
  RICH CASE
C
60 D     = (2.-EPS)*PHI + PSI
  DDDF   = (2.-EPS)
C
70 DMWDF = -MCP/D/D*(DDDF - D/MCP*DMCPDF)
  DRHODF = 0.012187 * P * DMWDF / T
C
  RETURN
  END
```

C***** VERSION 1.0 *****
C OCT 21, 1984

C SUBROUTINE TRANSP

C PURPOSE

C CALCULATES DYNAMIC VISCOSITY AND THERMAL CONDUCTIVITY
C OF BURNED PRODUCTS

C USAGE

C CALL TRANSP (TEMP, FR, GAMMA, CP, DYNVIS, THRCON)

C DESCRIPTION OF PARAMETERS

PARAMETER	INPUT	OUTPUT	DESCRIPTION
TEMP	YES	NO	TEMPERATURE (K)
FR	YES	NO	AVERAGE FUEL FRACTION
GAMMA	YES	NO	RATIO OF SPECIFIC HEATS
CP	YES	NO	HEAT CAPACITY AT CONSTANT PRESSURE
---	---	---	OF COMBUSTION PRODUCTS (J/KG-DEG K)
DYNVIS	NO	YES	DYNAMIC VISCOSITY OF
-----	---	---	COMBUSTION PRODUCTS (KG/SEC-M)
THRCON	NO	YES	THERMAL CONDUCTIVITY OF
-----	---	---	COMBUSTION PRODUCTS (J/SEC-M-DEG K)

C REMARKS

C UNITS CHANGED TO S.I.

C SUBROUTINE AND FUNCTION SUBPROGRAMS REQUIRED

C NONE

C METHOD

C SEE S. H. MANSOURI AND J. B. HEYWOOD, "CORRELATIONS FOR THE
C VISCOSITY AND PRANDTL NUMBER OF HYDROCARBON-AIR COMBUSTION
C PRODUCTS", COMBUSTION SCIENCE AND TECHNOLOGY, 1980, VOL. 23,
C PP. 251-256.

C WRITTEN BY S. H. MANSOURI AND D. N. ASSANIS

C EDITED BY D. N. ASSANIS

C SUBROUTINE TRANSP (TEMP, FR, GAMMA, CP, DYNVIS, THRCON)

C COMMON/FUEL/ FUELTP, CX, HY, DEL, PSI, AFRAST, QLOWER, HFORM

C PHI = FR * AFRAST / (1.-FR)
C DYNVIS = 3.3E-7 * (TEMP**.7)/(1.0 + .027 * PHI)
C PRNDTL = 0.05 + 4.2 * (GAMMA - 1.0) - 6.7 * (GAMMA - 1.0) *
C & (GAMMA - 1.0)
C THRCON = DYNVIS * CP/PRNDTL
C IF ((PHI .LE. 1.0) .OR. (TEMP .LE. 1500.)) RETURN
C PRNDTL = PRNDTL/(1.0 + 1.5E-8 * PHI * PHI * TEMP * TEMP)
C THRCON = DYNVIS * CP/PRNDTL

C

RETURN
END

```

C * * * * *
C
C SANDIA MATHEMATICAL PROGRAM LIBRARY
C APPLIED MATHEMATICS DIVISION 2613
C SANDIA LABORATORIES
C ALBUQUERQUE, NEW MEXICO 87115
C CONTROL DATA 6600/7600 VERSION 7.2 SEPTEMBER 1977
C
C * * * * *
C *
C * ISSUED BY SANDIA LABORATORIES *
C * A PRIME CONTRACTOR TO THE *
C * UNITED STATES DEPARTMENT OF ENERGY *
C *
C * * * * * NOTICE * * * * *
C *
C * THIS REPORT WAS PREPARED AS AN ACCOUNT OF WORK SPONSORED BY THE *
C * UNITED STATES GOVERNMENT. NEITHER THE UNITED STATES NOR THE *
C * UNITED STATES DEPARTMENT OF ENERGY NOR ANY OF THEIR EMPLOYEES, *
C * NOR ANY OF THEIR CONTRACTORS, SUBCONTRACTORS, OR THEIR EMPLOYEES *
C * MAKES ANY WARRANTY, EXPRESS OR IMPLIED, OR ASSUMES ANY LEGAL *
C * LIABILITY OR RESPONSIBILITY FOR THE ACCURACY, COMPLETENESS OR *
C * USEFULNESS OF ANY INFORMATION, APPARATUS, PRODUCT OR PROCESS *
C * DISCLOSED, OR REPRESENTS THAT ITS USE WOULD NOT INFRINGE *
C * OWNED RIGHTS. *
C *
C * * * * *
C * THE PRIMARY DOCUMENT FOR THE LIBRARY OF WHICH THIS ROUTINE IS *
C * PART IS SAND77-1441. *
C *
C * * * * *
C
C WRITTEN BY M. K. GORDON, 5122
C
C*****
C ABSTRACT
C*****
C SUBROUTINE ODERT INTEGRATES A SYSTEM OF NEQN FIRST ORDER
C ORDINARY DIFFERENTIAL EQUATIONS OF THE FORM
C DY(I)/DT = F(T,Y(1),...,Y(NEQN))
C Y(I) GIVEN AT T.
C THE SUBROUTINE INTEGRATES FROM T IN THE DIRECTION OF TOUT UNTIL
C IT LOCATES THE FIRST ROOT OF THE NONLINEAR EQUATION
C G(T,Y(1),...,Y(NEQN),YP(1),...,YP(NEQN)) = 0.
C UPON FINDING THE ROOT, THE CODE RETURNS WITH ALL PARAMETERS IN THE
C CALL LIST SET FOR CONTINUING THE INTEGRATION TO THE NEXT ROOT OR
C THE FIRST ROOT OF A NEW FUNCTION G . IF NO ROOT IS FOUND, THE
C INTEGRATION PROCEEDS TO TOUT . AGAIN ALL PARAMETERS ARE SET TO
C CONTINUE.
C
C THE DIFFERENTIAL EQUATIONS ARE ACTUALLY SOLVED BY A SUITE OF CODES,
C DERT1 ,STEP1 , AND INTRP . ODERT ALLOCATES VIRTUAL STORAGE IN

```

C THE WORK ARRAYS WORK AND IWORK AND CALLS DERT1 . DERT1 IS A
C SUPERVISOR WHICH DIRECTS THE INTEGRATION. IT CALLS ON STEP1 TO
C ADVANCE THE SOLUTION AND INTRP TO INTERPOLATE THE SOLUTION AND
C ITS DERIVATIVE. STEP1 USES A MODIFIED DIVIDED DIFFERENCE FORM OF
C THE ADAMS PECE FORMULAS AND LOCAL EXTRAPOLATION. IT ADJUSTS THE
C ORDER AND STEP SIZE TO CONTROL THE LOCAL ERROR PER UNIT STEP IN A
C GENERALIZED SENSE. NORMALLY EACH CALL TO STEP1 ADVANCES THE
C SOLUTION ONE STEP IN THE DIRECTION OF TOUT . FOR REASONS OF
C EFFICIENCY ODERT INTEGRATES BEYOND TOUT INTERNALLY, THOUGH
C NEVER BEYOND $T+10*(TOUT-T)$, AND CALLS INTRP TO INTERPOLATE THE
C SOLUTION AND DERIVATIVE AT TOUT . AN OPTION IS PROVIDED TO STOP
C THE INTEGRATION AT TOUT BUT IT SHOULD BE USED ONLY IF IT IS
C IMPOSSIBLE TO CONTINUE THE INTEGRATION BEYOND TOUT .

C AFTER EACH INTERNAL STEP, DERT1 EVALUATES THE FUNCTION G AND
C CHECKS FOR A CHANGE IN SIGN IN THE FUNCTION VALUE FROM THE
C PRECEDING STEP. SUCH A CHANGE INDICATES A ROOT LIES IN THE
C INTERVAL OF THE STEP JUST COMPLETED. DERT1 THEN CALLS SUBROUTINE
C ROOT TO REDUCE THE BRACKETING INTERVAL UNTIL THE ROOT IS
C DETERMINED TO THE DESIRED ACCURACY. SUBROUTINE ROOT USES A
C COMBINATION OF THE SECANT RULE AND BISECTION TO DO THIS. THE
C SOLUTION AND DERIVATIVE VALUES REQUIRED ARE OBTAINED BY
C INTERPOLATION WITH INTRP . THE CODE LOCATES ONLY THOSE ROOTS
C FOR WHICH G CHANGES SIGN IN (T,TOUT) AND FOR WHICH A
C BRACKETING INTERVAL EXISTS. IN PARTICULAR, IT WILL NOT DETECT A
C ROOT AT THE INITIAL POINT T .

C THE CODES STEP1 , INTRP , ROOT , AND THAT PORTION OF DERT1
C WHICH DIRECTS THE INTEGRATION ARE EXPLAINED AND DOCUMENTED IN THE
C TEXT, COMPUTER SOLUTION OF ORDINARY DIFFERENTIAL EQUATIONS, THE
C INITIAL VALUE PROBLEM, BY L. F. SHAMPINE AND M. K. GORDON.

C DETAILS OF THE USE OF ODERT ARE GIVEN IN SAND-75-0211.

C*****

C THE PARAMETERS FOR ODERT ARE

C*****

C F -- SUBROUTINE F(T,Y,YP) TO EVALUATE DERIVATIVES $YP(I)=DY(I)/DT$
C NEQN -- NUMBER OF EQUATIONS TO BE INTEGRATED
C Y(*) -- SOLUTION VECTOR AT T
C T -- INDEPENDENT VARIABLE
C TOUT -- ARBITRARY POINT BEYOND THE ROOT DESIRED
C RELERR,ABSERR -- RELATIVE AND ABSOLUTE ERROR TOLERANCES FOR LOCAL
C ERROR TEST. AT EACH STEP THE CODE REQUIRES
C $ABS(LOCAL ERROR) \leq ABS(Y)*RELERR + ABSERR$
C FOR EACH COMPONENT OF THE LOCAL ERROR AND SOLUTION VECTORS
C IFLAG -- INDICATES STATUS OF INTEGRATION
C WORK,IWORK -- ARRAYS TO HOLD INFORMATION INTERNAL TO THE CODE
C WHICH IS NECESSARY FOR SUBSEQUENT CALLS
C G - FUNCTION OF T, Y(*), YP(*) WHOSE ROOT IS DESIRED.
C REROOT, AEROOT -- RELATIVE AND ABSOLUTE ERROR TOLERANCES FOR
C ACCEPTING THE ROOT. THE INTERVAL CONTAINING THE ROOT IS
C REDUCED UNTIL IT SATISFIES
C $0.5*ABS(LENGTH OF INTERVAL) \leq REROOT*ABS(ROOT)+AEROOT$

```
C      WHERE ROOT IS THAT ENDPOINT YIELDING THE SMALLER VALUE OF
C      G IN MAGNITUDE. PURE RELATIVE ERROR IS NOT RECOMMENDED
C      IF THE ROOT MIGHT BE ZERO.
C*****
C      FIRST CALL TO ODERT ---
C*****
C      THE USER MUST PROVIDE STORAGE IN HIS CALLING PROGRAM FOR THE
C      ARRAYS IN THE CALL LIST,
C          Y(NEQN), WORK(100+21*NEQN), IWORK(5)
C      AND DECLARE F , G IN AN EXTERNAL STATEMENT. HE MUST SUPPLY THE
C      SUBROUTINE F(T,Y,YP) TO EVALUATE
C          DY(I)/DT = YP(I) = F(T,Y(1),...,Y(NEQN))
C      AND THE FUNCTION G(T,Y,YP) TO EVALUATE
C          G = G(T,Y(1),...,Y(NEQN),YP(1),...,YP(NEQN)).
C      NOTE THAT THE ARRAY YP IS AN INPUT ARGUMENT AND SHOULD NOT BE
C      COMPUTED IN THE FUNCTION SUBPROGRAM. FINALLY THE USER MUST
C      INITIALIZE THE PARAMETERS
C      NEQN --- NUMBER OF EQUATIONS TO BE INTEGRATED
C      Y(*) --- VECTOR OF INITIAL CONDITIONS
C      T --- STARTING POINT OF INTEGRATION
C      TOUT --- ARBITRARY POINT BEYOND THE ROOT DESIRED
C      RELERR,ABSERR --- RELATIVE AND ABSOLUTE LOCAL ERROR TOLERANCES
C                      FOR INTEGRATING THE EQUATIONS
C      IFLAG --- +1,-1. INDICATOR TO INITIALIZE THE CODE. NORMAL INPUT
C                      IS +1. THE USER SHOULD SET IFLAG=-1 ONLY IF IT IS
C                      IMPOSSIBLE TO CONTINUE THE INTEGRATION BEYOND TOUT .
C      REROOT,AEROOT --- RELATIVE AND ABSOLUTE ERROR TOLERANCES FOR
C                      COMPUTING THE ROOT OF G
C
C      ALL PARAMETERS EXCEPT F, G, NEQN, TOUT, REROOT AND AEROOT MAY BE
C      ALTERED BY THE CODE ON OUTPUT SO MUST BE VARIABLES IN THE CALLING
C      PROGRAM.
C*****
C      OUTPUT FROM ODERT ---
C*****
C      NEQN --- UNCHANGED
C      Y(*) --- SOLUTION AT T
C      T --- LAST POINT REACHED IN INTEGRATION. NORMAL RETURN HAS
C          T = TOUT OR T = ROOT
C      TOUT --- UNCHANGED
C      RELERR,ABSERR --- NORMAL RETURN HAS TOLERANCES UNCHANGED. IFLAG=3
C                      SIGNALS TOLERANCES INCREASED
C      IFLAG = 2 --- NORMAL RETURN. INTEGRATION REACHED TOUT
C          = 3 --- INTEGRATION DID NOT REACH TOUT BECAUSE ERROR
C                      TOLERANCES TOO SMALL. RELERR , ABSERR INCREASED
C                      APPROPRIATELY FOR CONTINUING
C          = 4 --- INTEGRATION DID NOT REACH TOUT BECAUSE MORE THAN
C                      500 STEPS NEEDED
C          = 5 --- INTEGRATION DID NOT REACH TOUT BECAUSE EQUATIONS
C                      APPEAR TO BE STIFF
C          = 6 --- INTEGRATION DID NOT REACH TOUT BECAUSE SOLUTION
C                      VANISHED MAKING PURE RELATIVE ERROR IMPOSSIBLE.
C                      MUST USE NON-ZERO ABSERR TO CONTINUE
C          = 7 --- INVALID INPUT PARAMETERS (FATAL ERROR)
```



```
4  WORK(ITOLD),WORK(IDELSN),WORK(IGX),WORK(ITROOT),IWORK(1),  
5  NORND,IWORK(3),IWORK(4),IWORK(5))  
   WORK(ISTART) = -1.0  
   IF(START) WORK(ISTART) = 1.0  
   WORK(IPHASE) = -1.0  
   IF(PHASE1) WORK(IPHASE) = 1.0  
   IWORK(2) = -1  
   IF(NORND) IWORK(2) = 1  
   RETURN  
   END
```

C * * * * *
C
C SANDIA MATHEMATICAL PROGRAM LIBRARY
C APPLIED MATHEMATICS DIVISION 2613
C SANDIA LABORATORIES
C ALBUQUERQUE, NEW MEXICO 87115
C CONTROL DATA 6600/7600 VERSION 7.2 SEPTEMBER 1977
C

C * * * * *
C *
C * ISSUED BY SANDIA LABORATORIES, *
C * A PRIME CONTRACTOR TO THE *
C * UNITED STATES ENERGY RESEARCH AND DEVELOPMENT ADMINISTRATION *
C *
C * * * * * NOTICE * * * * *

C *
C * THIS REPORT WAS PREPARED AS AN ACCOUNT OF WORK SPONSORED BY THE
C * UNITED STATES GOVERNMENT. NEITHER THE UNITED STATES NOR THE
C * UNITED STATES ENERGY RESEARCH AND DEVELOPMENT ADMINISTRATION,
C * NOR ANY OF THEIR EMPLOYEES, NOR ANY OF THEIR CONTRACTORS,
C * SUBCONTRACTORS, OR THEIR EMPLOYEES, MAKES ANY WARRANTY, EXPRESS
C * OR IMPLIED, OR ASSUMES ANY LEGAL LIABILITY OR RESPONSIBILITY
C * FOR THE ACCURACY, COMPLETENESS OR USEFULNESS OF ANY INFORMATION,
C * APPARATUS, PRODUCT OR PROCESS DISCLOSED, OR REPRESENTS THAT ITS
C * USE WOULD NOT INFRINGE PRIVATELY OWNED RIGHTS.
C *
C * * * * *
C *
C * THE PRIMARY DOCUMENT FOR THE LIBRARY OF WHICH THIS ROUTINE IS *
C * A PART IS SAND75-0545. *
C *
C * * * * *

C WRITTEN BY L. F. SHAMPINE AND M. K. GORDON
C

C ABSTRACT

C SUBROUTINE STEP1 IS NORMALLY USED INDIRECTLY THROUGH SUBROUTINE
C ODE . BECAUSE ODE SUFFICES FOR MOST PROBLEMS AND IS MUCH EASIER
C TO USE, USING IT SHOULD BE CONSIDERED BEFORE USING STEP1 ALONE.
C

C SUBROUTINE STEP1 INTEGRATES A SYSTEM OF NEQN FIRST ORDER ORDINARY
C DIFFERENTIAL EQUATIONS ONE STEP, NORMALLY FROM X TO X+H, USING A
C MODIFIED DIVIDED DIFFERENCE FORM OF THE ADAMS PECE FORMULAS. LOCAL
C EXTRAPOLATION IS USED TO IMPROVE ABSOLUTE STABILITY AND ACCURACY.
C THE CODE ADJUSTS ITS ORDER AND STEP SIZE TO CONTROL THE LOCAL ERROR
C PER UNIT STEP IN A GENERALIZED SENSE. SPECIAL DEVICES ARE INCLUDED
C TO CONTROL ROUND OFF ERROR AND TO DETECT WHEN THE USER IS REQUESTING
C TOO MUCH ACCURACY.
C

C THIS CODE IS COMPLETELY EXPLAINED AND DOCUMENTED IN THE TEXT,
C COMPUTER SOLUTION OF ORDINARY DIFFERENTIAL EQUATIONS, THE INITIAL
C VALUE PROBLEM BY L. F. SHAMPINE AND M. K. GORDON.
C FURTHER DETAILS ON USE OF THIS CODE ARE AVAILABLE IN *SOLVING

C ORDINARY DIFFERENTIAL EQUATIONS WITH ODE, STEP, AND INTRP*,
C BY L. F. SHAMPINE AND M. K. GORDON, SLA-73-1060.
C
C
C THE PARAMETERS REPRESENT --
C F -- SUBROUTINE TO EVALUATE DERIVATIVES
C NEQN -- NUMBER OF EQUATIONS TO BE INTEGRATED
C Y(*) -- SOLUTION VECTOR AT X
C X -- INDEPENDENT VARIABLE
C H -- APPROPRIATE STEP SIZE FOR NEXT STEP. NORMALLY DETERMINED BY
C CODE
C EPS -- LOCAL ERROR TOLERANCE
C WT(*) -- VECTOR OF WEIGHTS FOR ERROR CRITERION
C START -- LOGICAL VARIABLE SET .TRUE. FOR FIRST STEP, .FALSE.
C OTHERWISE
C HOLD -- STEP SIZE USED FOR LAST SUCCESSFUL STEP
C K -- APPROPRIATE ORDER FOR NEXT STEP (DETERMINED BY CODE)
C KOLD -- ORDER USED FOR LAST SUCCESSFUL STEP
C CRASH -- LOGICAL VARIABLE SET .TRUE. WHEN NO STEP CAN BE TAKEN,
C .FALSE. OTHERWISE.
C YP(*) -- DERIVATIVE OF SOLUTION VECTOR AT X AFTER SUCCESSFUL
C STEP
C THE ARRAYS PHI, PSI ARE REQUIRED FOR THE INTERPOLATION SUBROUTINE
C INTRP. THE ARRAY P IS INTERNAL TO THE CODE. THE REMAINING NINE
C VARIABLES AND ARRAYS ARE INCLUDED IN THE CALL LIST ONLY TO ELIMINATE
C LOCAL RETENTION OF VARIABLES BETWEEN CALLS.
C
C INPUT TO STEP1
C
C FIRST CALL --
C
C THE USER MUST PROVIDE STORAGE IN HIS CALLING PROGRAM FOR ALL ARRAYS
C IN THE CALL LIST, NAMELY
C
C DIMENSION Y(NEQN),WT(NEQN),PHI(NEQN,16),P(NEQN),YP(NEQN),PSI(12),
C 1 ALPHA(12),BETA(12),SIG(13),V(12),W(12),G(13)
C -- -- **NOTE**
C
C THE USER MUST ALSO DECLARE START, CRASH, PHASE1 AND NORND
C LOGICAL VARIABLES AND F AN EXTERNAL SUBROUTINE, SUPPLY THE
C SUBROUTINE F(X,Y,YP) TO EVALUATE
C $DY(I)/DX = YP(I) = F(X, Y(1), Y(2), \dots, Y(NEQN))$
C AND INITIALIZE ONLY THE FOLLOWING PARAMETERS.
C NEQN -- NUMBER OF EQUATIONS TO BE INTEGRATED
C Y(*) -- VECTOR OF INITIAL VALUES OF DEPENDENT VARIABLES
C X -- INITIAL VALUE OF THE INDEPENDENT VARIABLE
C H -- NOMINAL STEP SIZE INDICATING DIRECTION OF INTEGRATION
C AND MAXIMUM SIZE OF STEP. MUST BE VARIABLE
C EPS -- LOCAL ERROR TOLERANCE PER STEP. MUST BE VARIABLE
C WT(*) -- VECTOR OF NON-ZERO WEIGHTS FOR ERROR CRITERION
C START -- .TRUE.
C
C STEP1 REQUIRES THAT THE L2 NORM OF THE VECTOR WITH COMPONENTS
C LOCAL ERROR(L)/WT(L) BE LESS THAN EPS FOR A SUCCESSFUL STEP. THE

C ARRAY WT ALLOWS THE USER TO SPECIFY AN ERROR TEST APPROPRIATE
C FOR HIS PROBLEM. FOR EXAMPLE,
C WT(L) = 1.0 SPECIFIES ABSOLUTE ERROR,
C = ABS(Y(L)) ERROR RELATIVE TO THE MOST RECENT VALUE OF THE
C L-TH COMPONENT OF THE SOLUTION,
C = ABS(YP(L)) ERROR RELATIVE TO THE MOST RECENT VALUE OF
C THE L-TH COMPONENT OF THE DERIVATIVE,
C = AMAX1(WT(L),ABS(Y(L))) ERROR RELATIVE TO THE LARGEST
C MAGNITUDE OF L-TH COMPONENT OBTAINED SO FAR,
C = ABS(Y(L))*RELERR/EPS + ABSERR/EPS SPECIFIES A MIXED
C RELATIVE-ABSOLUTE TEST WHERE RELERR IS RELATIVE
C ERROR, ABSERR IS ABSOLUTE ERROR AND EPS =
C AMAX1(RELERR,ABSERR) .

C SUBSEQUENT CALLS —

C SUBROUTINE STEP1 IS DESIGNED SO THAT ALL INFORMATION NEEDED TO
C CONTINUE THE INTEGRATION, INCLUDING THE STEP SIZE H AND THE ORDER
C K , IS RETURNED WITH EACH STEP. WITH THE EXCEPTION OF THE STEP
C SIZE, THE ERROR TOLERANCE, AND THE WEIGHTS, NONE OF THE PARAMETERS
C SHOULD BE ALTERED. THE ARRAY WT MUST BE UPDATED AFTER EACH STEP
C TO MAINTAIN RELATIVE ERROR TESTS LIKE THOSE ABOVE. NORMALLY THE
C INTEGRATION IS CONTINUED JUST BEYOND THE DESIRED ENDPOINT AND THE
C SOLUTION INTERPOLATED THERE WITH SUBROUTINE INTRP . IF IT IS
C IMPOSSIBLE TO INTEGRATE BEYOND THE ENDPOINT, THE STEP SIZE MAY BE
C REDUCED TO HIT THE ENDPOINT SINCE THE CODE WILL NOT TAKE A STEP
C LARGER THAN THE H INPUT. CHANGING THE DIRECTION OF INTEGRATION,
C I.E., THE SIGN OF H , REQUIRES THE USER SET START = .TRUE. BEFORE
C CALLING STEP1 AGAIN. THIS IS THE ONLY SITUATION IN WHICH START
C SHOULD BE ALTERED.

C OUTPUT FROM STEP1

C SUCCESSFUL STEP --

C THE SUBROUTINE RETURNS AFTER EACH SUCCESSFUL STEP WITH START AND
C CRASH SET .FALSE. . X REPRESENTS THE INDEPENDENT VARIABLE
C ADVANCED ONE STEP OF LENGTH HOLD FROM ITS VALUE ON INPUT AND Y
C THE SOLUTION VECTOR AT THE NEW VALUE OF X . ALL OTHER PARAMETERS
C REPRESENT INFORMATION CORRESPONDING TO THE NEW X NEEDED TO
C CONTINUE THE INTEGRATION.

C UNSUCCESSFUL STEP --

C WHEN THE ERROR TOLERANCE IS TOO SMALL FOR THE MACHINE PRECISION,
C THE SUBROUTINE RETURNS WITHOUT TAKING A STEP AND CRASH = .TRUE. .
C AN APPROPRIATE STEP SIZE AND ERROR TOLERANCE FOR CONTINUING ARE
C ESTIMATED AND ALL OTHER INFORMATION IS RESTORED AS UPON INPUT
C BEFORE RETURNING. TO CONTINUE WITH THE LARGER TOLERANCE, THE USER
C JUST CALLS THE CODE AGAIN. A RESTART IS NEITHER REQUIRED NOR
C DESIRABLE.

C SUBROUTINE STEP1(F,NEQN,Y,X,H,EPS,WT,START,
1 HOLD,K,KOLD,CRASH,PHI,P,YP,PSI,

```
      2 ALPHA,BETA,SIG,V,W,G,PHASE1,NS,NORND)
C
      IMPLICIT REAL*8 (A-H,O-Z)
      IMPLICIT INTEGER*2 (I-N)
CCCCC GENERIC
      LOGICAL START,CRASH,PHASE1,NORND
      DIMENSION Y(NEQN),WT(NEQN),PHI(NEQN,16),P(NEQN),YP(NEQN),PSI(12),
1     ALPHA(12),BETA(12),SIG(13),V(12),W(12),G(13)
      DIMENSION TWO(13),GSTR(13)
      EXTERNAL F
C*****
C* THE ONLY MACHINE DEPENDENT CONSTANTS ARE BASED ON THE MACHINE UNIT *
C* ROUND OFF ERROR U WHICH IS THE SMALLEST POSITIVE NUMBER SUCH THAT *
C* 1.0+U .GT. 1.0 . THE USER MUST CALCULATE U AND INSERT *
C* TWOU=2.0*U AND FOURU=4.0*U IN THE DATA STATEMENT BEFORE CALLING *
C* THE CODE. THE ROUTINE MACHIN CALCULATES U . *
      DATA TWOU,FOURU/4.4E-16,8.8E-16/
C*****
C
      DATA TWO/2.0,4.0,8.0,16.0,32.0,64.0,128.0,256.0,512.0,1024.0,
1     2048.0,4096.0,8192.0/
      DATA GSTR/0.500,0.0833,0.0417,0.0264,0.0188,0.0143,0.0114,0.00936,
1     0.00789,0.00679,0.00592,0.00524,0.00468/
C
C
C     *** BEGIN BLOCK 0 ***
C CHECK IF STEP SIZE OR ERROR TOLERANCE IS TOO SMALL FOR MACHINE
C PRECISION. IF FIRST STEP, INITIALIZE PHI ARRAY AND ESTIMATE A
C STARTING STEP SIZE.
C     ***
C
C IF STEP SIZE IS TOO SMALL, DETERMINE AN ACCEPTABLE ONE
C
      CRASH = .TRUE.
      IF(ABS(H) .GE. FOURU*ABS(X)) GO TO 5
      H = SIGN(FOURU*ABS(X),H)
      RETURN
5     P5EPS = 0.5*EPS
C
C IF ERROR TOLERANCE IS TOO SMALL, INCREASE IT TO AN ACCEPTABLE VALUE
C
      ROUND = 0.0
      DO 10 L = 1,NEQN
10     ROUND = ROUND + (Y(L)/WT(L))**2
      ROUND = TWOU*SQRT(ROUND)
      IF(P5EPS .GE. ROUND) GO TO 15
      EPS = 2.0*ROUND*(1.0 + FOURU)
      RETURN
15     CRASH = .FALSE.
      G(1) = 1.0
      G(2) = 0.5
      SIG(1) = 1.0
      IF(.NOT.START) GO TO 99
C
```

```
C INITIALIZE. COMPUTE APPROPRIATE STEP SIZE FOR FIRST STEP
C
  CALL F(X,Y,YP)
  SUM = 0.0
  DO 20 L = 1,NEQN
    PHI(L,1) = YP(L)
    PHI(L,2) = 0.0
20  SUM = SUM + (YP(L)/WT(L))**2
  SUM = SQRT(SUM)
  ABSH = ABS(H)
  IF(EPS .LT. 16.0*SUM*H*H) ABSH = 0.25*SQRT(EPS/SUM)
  H = SIGN(MAX(ABSH,FOURU*ABS(X)),H)
  HOLD = 0.0
  K = 1
  KOLD = 0
  START = .FALSE.
  PHASE1 = .TRUE.
  NORND = .TRUE.
  IF(P5EPS .GT. 100.0*ROUND) GO TO 99
  NORND = .FALSE.
  DO 25 L = 1,NEQN
25  PHI(L,15) = 0.0
99  IFAIL = 0
C    ***      END BLOCK 0      ***
C
C    ***      BEGIN BLOCK 1      ***
C COMPUTE COEFFICIENTS OF FORMULAS FOR THIS STEP. AVOID COMPUTING
C THOSE QUANTITIES NOT CHANGED WHEN STEP SIZE IS NOT CHANGED.
C          ***
C
100 KP1 = K+1
    KP2 = K+2
    KM1 = K-1
    KM2 = K-2
C
C NS IS THE NUMBER OF STEPS TAKEN WITH SIZE H, INCLUDING THE CURRENT
C ONE. WHEN K.LT.NS, NO COEFFICIENTS CHANGE
C
  IF(H .NE. HOLD) NS = 0
  IF (NS.LE.KOLD) NS = NS+1
  NSP1 = NS+1
  IF (K .LT. NS) GO TO 199
C
C COMPUTE THOSE COMPONENTS OF ALPHA(*),BETA(*),PSI(*),SIG(*) WHICH
C ARE CHANGED
C
  BETA(NS) = 1.0
  REALNS = NS
  ALPHA(NS) = 1.0/REALNS
  TEMP1 = H*REALNS
  SIG(NSP1) = 1.0
  IF(K .LT. NSP1) GO TO 110
  DO 105 I = NSP1,K
    IM1 = I-1
```

```
      TEMP2 = PSI(IM1)
      PSI(IM1) = TEMP1
      BETA(I) = BETA(IM1)*PSI(IM1)/TEMP2
      TEMP1 = TEMP2 + H
      ALPHA(I) = H/TEMP1
      REALI = I
105     SIG(I+1) = REALI*ALPHA(I)*SIG(I)
110     PSI(K) = TEMP1
C
C     COMPUTE COEFFICIENTS G(*)
C
C     INITIALIZE V(*) AND SET W(*).
C
      IF(NS .GT. 1) GO TO 120
      DO 115 IQ = 1,K
          TEMP3 = IQ*(IQ+1)
          V(IQ) = 1.0/TEMP3
115     W(IQ) = V(IQ)
      GO TO 140
C
C     IF ORDER WAS RAISED, UPDATE DIAGONAL PART OF V(*)
C
120     IF(K .LE. KOLD) GO TO 130
          TEMP4 = K*KP1
          V(K) = 1.0/TEMP4
          NSM2 = NS-2
          IF(NSM2 .LT. 1) GO TO 130
          DO 125 J = 1,NSM2
              I = K-J
125     V(I) = V(I) - ALPHA(J+1)*V(I+1)
C
C     UPDATE V(*) AND SET W(*)
C
130     LIMIT1 = KP1 - NS
          TEMP5 = ALPHA(NS)
          DO 135 IQ = 1,LIMIT1
              V(IQ) = V(IQ) - TEMP5*V(IQ+1)
135     W(IQ) = V(IQ)
          G(NSP1) = W(1)
C
C     COMPUTE THE G(*) IN THE WORK VECTOR W(*)
C
140     NSP2 = NS + 2
          IF(KP1 .LT. NSP2) GO TO 199
          DO 150 I = NSP2,KP1
              LIMIT2 = KP2 - I
              TEMP6 = ALPHA(I-1)
              DO 145 IQ = 1,LIMIT2
                  W(IQ) = W(IQ) - TEMP6*W(IQ+1)
145     G(I) = W(1)
150
199     CONTINUE
C     ***     END BLOCK 1     ***
C
C     ***     BEGIN BLOCK 2     ***
```

C PREDICT A SOLUTION P(*), EVALUATE DERIVATIVES USING PREDICTED
C SOLUTION, ESTIMATE LOCAL ERROR AT ORDER K AND ERRORS AT ORDERS K,
C K-1, K-2 AS IF CONSTANT STEP SIZE WERE USED.

C
C CHANGE PHI TO PHI STAR
C

IF(K .LT. NSP1) GO TO 215
DO 210 I = NSP1,K
TEMP1 = BETA(I)
DO 205 L = 1,NEQN
205 PHI(L,I) = TEMP1*PHI(L,I)
210 CONTINUE

C
C PREDICT SOLUTION AND DIFFERENCES
C

215 DO 220 L = 1,NEQN
PHI(L,KP2) = PHI(L,KP1)
PHI(L,KP1) = 0.0
220 P(L) = 0.0
DO 230 J = 1,K
I = KP1 - J
IP1 = I+1
TEMP2 = G(I)
DO 225 L = 1,NEQN
P(L) = P(L) + TEMP2*PHI(L,I)
225 PHI(L,I) = PHI(L,I) + PHI(L,IP1)
230 CONTINUE
IF(NORND) GO TO 240
DO 235 L = 1,NEQN
TAU = H*P(L) - PHI(L,15)
P(L) = Y(L) + TAU
235 PHI(L,16) = (P(L) - Y(L)) - TAU
GO TO 250
240 DO 245 L = 1,NEQN
245 P(L) = Y(L) + H*P(L)
250 XOLD = X
X = X + H
ABSH = ABS(H)
CALL F(X,P,YP)

C
C ESTIMATE ERRORS AT ORDERS K,K-1,K-2
C

ERKM2 = 0.0
ERKM1 = 0.0
ERK = 0.0
DO 265 L = 1,NEQN
TEMP3 = 1.0/WT(L)
TEMP4 = YP(L) - PHI(L,1)
IF(KM2)265,260,255
255 ERKM2 = ERKM2 + ((PHI(L,KM1)+TEMP4)*TEMP3)**2
260 ERKM1 = ERKM1 + ((PHI(L,K)+TEMP4)*TEMP3)**2
265 ERK = ERK + (TEMP4*TEMP3)**2
IF(KM2)280,275,270

```
270 ERKM2 = ABSH*SIG(KM1)*GSTR(KM2)*SQRT(ERKM2)
275 ERKM1 = ABSH*SIG(K)*GSTR(KM1)*SQRT(ERKM1)
280 TEMP5 = ABSH*SQRT(ERK)
    ERR = TEMP5*(G(K)-G(KP1))
    ERK = TEMP5*SIG(KP1)*GSTR(K)
    KNEW = K
C
C TEST IF ORDER SHOULD BE LOWERED
C
    IF(KM2)299,290,285
285 IF(MAX(ERKM1,ERKM2) .LE. ERK) KNEW = KM1
    GO TO 299
290 IF(ERKM1 .LE. 0.5*ERK) KNEW = KM1
C
C TEST IF STEP SUCCESSFUL
C
299 IF(ERR .LE. EPS) GO TO 400
C    ***      END BLOCK 2      ***
C
C    ***      BEGIN BLOCK 3      ***
C THE STEP IS UNSUCCESSFUL. RESTORE X, PHI(*,*), PSI(*) .
C IF THIRD CONSECUTIVE FAILURE, SET ORDER TO ONE. IF STEP FAILS MORE
C THAN THREE TIMES, CONSIDER AN OPTIMAL STEP SIZE. DOUBLE ERROR
C TOLERANCE AND RETURN IF ESTIMATED STEP SIZE IS TOO SMALL FOR MACHINE
C PRECISION.
C          ***
C
C RESTORE X, PHI(*,*) AND PSI(*)
C
    PHASE1 = .FALSE.
    X = XOLD
    DO 310 I = 1,K
        TEMP1 = 1.0/BETA(I)
        IP1 = I+1
        DO 305 L = 1,NEQN
305     PHI(L,I) = TEMP1*(PHI(L,I) - PHI(L,IP1))
310     CONTINUE
        IF(K .LT. 2) GO TO 320
        DO 315 I = 2,K
315     PSI(I-1) = PSI(I) - H
C
C ON THIRD FAILURE, SET ORDER TO ONE. THEREAFTER, USE OPTIMAL STEP
C SIZE
C
320 IFAIL = IFAIL + 1
    TEMP2 = 0.5
    IF(IFAIL - 3) 335,330,325
325 IF(P5EPS .LT. 0.25*ERK) TEMP2 = SQRT(P5EPS/ERK)
330 KNEW = 1
335 H = TEMP2*H
    K = KNEW
    IF(ABS(H) .GE. FOURU*ABS(X)) GO TO 340
    CRASH = .TRUE.
    H = SIGN(FOURU*ABS(X),H)
```

```
      EPS = EPS + EPS
      RETURN
340  GO TO 100
C    ***      END BLOCK 3      ***
C
C    ***      BEGIN BLOCK 4      ***
C    THE STEP IS SUCCESSFUL.  CORRECT THE PREDICTED SOLUTION, EVALUATE
C    THE DERIVATIVES USING THE CORRECTED SOLUTION AND UPDATE THE
C    DIFFERENCES.  DETERMINE BEST ORDER AND STEP SIZE FOR NEXT STEP.
C          ***
400  KOLD = K
      HOLD = H
C
C    CORRECT AND EVALUATE
C
      TEMP1 = H*G(KP1)
      IF(NORND) GO TO 410
      DO 405 L = 1,NEQN
          RHO = TEMP1*(YP(L) - PHI(L,1)) - PHI(L,16)
          Y(L) = P(L) + RHO
405  PHI(L,15) = (Y(L) - P(L)) - RHO
      GO TO 420
410  DO 415 L = 1,NEQN
415  Y(L) = P(L) + TEMP1*(YP(L) - PHI(L,1))
420  CALL F(X,Y,YP)
C
C    UPDATE DIFFERENCES FOR NEXT STEP
C
      DO 425 L = 1,NEQN
          PHI(L,KP1) = YP(L) - PHI(L,1)
425  PHI(L,KP2) = PHI(L,KP1) - PHI(L,KP2)
      DO 435 I = 1,K
          DO 430 L = 1,NEQN
430  PHI(L,I) = PHI(L,I) + PHI(L,KP1)
435  CONTINUE
C
C    ESTIMATE ERROR AT ORDER K+1 UNLESS:
C    IN FIRST PHASE WHEN ALWAYS RAISE ORDER,
C    ALREADY DECIDED TO LOWER ORDER,
C    STEP SIZE NOT CONSTANT SO ESTIMATE UNRELIABLE
C
      ERKP1 = 0.0
      IF(KNEW .EQ. KM1 .OR. K .EQ. 12) PHASE1 = .FALSE.
      IF(PHASE1) GO TO 450
      IF(KNEW .EQ. KM1) GO TO 455
      IF(KP1 .GT. NS) GO TO 460
      DO 440 L = 1,NEQN
440  ERKP1 = ERKP1 + (PHI(L,KP2)/WT(L))**2
      ERKP1 = ABSH*GSTR(KP1)*SQRT(ERKP1)
C
C    USING ESTIMATED ERROR AT ORDER K+1, DETERMINE APPROPRIATE ORDER
C    FOR NEXT STEP
C
      IF(K .GT. 1) GO TO 445
```

```
      IF(ERKP1 .GE. 0.5*ERK) GO TO 460
      GO TO 450
445  IF(ERKM1 .LE. MIN(ERK,ERKP1)) GO TO 455
      IF(ERKP1 .GE. ERK .OR. K .EQ. 12) GO TO 460
C
C  HERE ERKP1 .LT. ERK .LT. AMAX1(ERKM1,ERKM2) ELSE ORDER WOULD HAVE
C  BEEN LOWERED IN BLOCK 2.  THUS ORDER IS TO BE RAISED
C
C  RAISE ORDER
C
450  K = KP1
      ERK = ERKP1
      GO TO 460
C
C  LOWER ORDER
C
455  K = KM1
      ERK = ERKM1
C
C  WITH NEW ORDER DETERMINE APPROPRIATE STEP SIZE FOR NEXT STEP
C
460  HNEW = H + H
      IF(PHASE1) GO TO 465
      IF(P5EPS .GE. ERK*TWO(K+1)) GO TO 465
      HNEW = H
      IF(P5EPS .GE. ERK) GO TO 465
      TEMP2 = K+1
      R = (P5EPS/ERK)**(1.0/TEMP2)
      HNEW = ABSH*MAX(0.5D0,MIN(0.9D0,R))
      HNEW = SIGN(MAX(HNEW,FOURU*ABS(X)),H)
465  H = HNEW
      RETURN
C      ***      END BLOCK 4      ***
      END
```

C * * * * *

C

SUBROUTINE DERT1(F,NEQN,Y,T,TOUT,RELERR,ABSERR,IFLAG,G,REROOT,
1 AEROOT,YY,WT,P,YP,YPOUT,PHI,ALPHA,BETA,SIG,V,W,GG,PHASE1,PSI,
2 X,H,HOLD,START,TOLD,DELSGN,GX,TROOT,NS,NORND,K,KOLD,ISNOLD)

C ***NAME CHANGED FROM DERT TO DERT1 TO AVOID A NAMING CONFLICT.

C

ODERT MERELY ALLOCATES STORAGE FOR DERT TO RELIEVE THE USER OF
THE INCONVENIENCE OF A LONG CALL LIST. CONSEQUENTLY DERT IS USED
AS DESCRIBED IN THE COMMENTS FOR ODERT .

C

THE CODES STEP, INTRP AND ROOT AND THAT PORTION OF DERT DIRECTING
THE INTEGRATION ARE COMPLETELY EXPLAINED AND DOCUMENTED IN THE TEXT,
COMPUTER SOLUTION OF ORDINARY DIFFERENTIAL EQUATIONS, THE INITIAL
VALUE PROBLEM BY L. F. SHAMPINE AND M. K. GORDON.

C

IMPLICIT REAL*8 (A-H,O-Z)

C

CCCC GENERIC

IMPLICIT INTEGER*2 (I-N)
LOGICAL STIFF,CRASH,START,PHASE1,NORND
DIMENSION Y(NEQN),YY(NEQN),WT(NEQN),PHI(NEQN,16),P(NEQN),YP(NEQN),
1 YPOUT(NEQN),PSI(12),ALPHA(12),BETA(12),SIG(13),V(12),W(12),
2 GG(13)
COMMON/MLDRT/SPACE(10)
EXTERNAL F,G

C

C*****

C* THE ONLY MACHINE DEPENDENT CONSTANT IS BASED ON THE MACHINE UNIT *
C* ROUND OFF ERROR U WHICH IS THE SMALLEST POSITIVE NUMBER SUCH THAT *
C* 1.0+U .GT. 1.0 . U MUST BE CALCULATED AND FOURU=4.0*U INSERTED *
C* IN THE FOLLOWING STATEMENT BEFORE USING ODERT . THE SUBROUTINE *
C* MACHIN CALCULATES U . FOURU AND TWOU=2.0*U MUST ALSO BE *
C* INSERTED IN SUBROUTINE STEP BEFORE CALLING ODERT . *

C*****

DATA FOURU/8.8E-16/

C*****

C

THE CONSTANT MAXNUM IS THE MAXIMUM NUMBER OF STEPS ALLOWED IN ONE
CALL TO ODERT . THE USER MAY CHANGE THIS LIMIT BY ALTERING THE
FOLLOWING STATEMENT

DATA MAXNUM/500/

C

C

*** *** ***

C

TEST FOR IMPROPER PARAMETERS

C

IF(IABS(IFLAG) .EQ. 7) CALL ERRCHK(-31,
1 31HIN ODERT, ENTERED WITH IFLAG=7.)
IF(NEQN .LT. 1) CALL ERRCHK(32,
1 32HIN ODERT, NEQN MUST BE POSITIVE.)
IF(NEQN .LT. 1) GO TO 10
IF(T .EQ. TOUT) CALL ERRCHK(61,
1 61HIN ODERT, ENDPOINTS OF INTEGRATION INTERVAL MUST BE DISTINCT.)
IF(T .EQ. TOUT) GO TO 10

```
IF(RELERR .LT. 0.0 .OR. ABSERR .LT. 0.0) CALL ERRCHK(49,
1 49HIN ODERT, RELERR AND ABSERR MUST BE NON-NEGATIVE.)
IF(RELERR .LT. 0.0 .OR. ABSERR .LT. 0.0) GO TO 10
EPS = MAX(RELERR,ABSERR)
IF(EPS .LE. 0.0) CALL ERRCHK(51,
1 51HIN ODERT, EITHER RELERR OR ABSERR MUST BE POSITIVE.)
IF(EPS .LE. 0.0) GO TO 10
IF(REROOT .LT. 0.0 .OR. AEROOT .LT. 0.0) CALL ERRCHK(49,
1 49HIN ODERT, REROOT AND AEROOT MUST BE NON-NEGATIVE.)
IF(REROOT .LT. 0.0 .OR. AEROOT .LT. 0.0) GO TO 10
IF(REROOT+AEROOT .LE. 0.0) CALL ERRCHK(51,
1 51HIN ODERT, EITHER REROOT OR AEROOT MUST BE POSITIVE.)
IF(REROOT+AEROOT .LE. 0.0) GO TO 10
IF(IFLAG .EQ. 0) CALL ERRCHK(34,
1 34HIN ODERT, INVALID INPUT FOR IFLAG.)
IF(IFLAG .EQ. 0) GO TO 10
ISN = ISIGN(1,IFLAG)
IFLAG = IABS(IFLAG)
IF(IFLAG .EQ. 1) GO TO 20
IF(T .NE. TOLD) CALL ERRCHK(68,
1 68HIN ODERT, INPUT VALUE OF T MUST BE OUTPUT VALUE FROM PRECEDIN
2G CALL.)
IF(T .NE. TOLD) GO TO 10
IF(IFLAG .GE. 2 .AND. IFLAG .LE. 6) GO TO 15
IF(IFLAG .GE. 8 .AND. IFLAG .LE. 10) GO TO 15
CALL ERRCHK(-34,34HIN ODERT, INVALID INPUT FOR IFLAG.)
10 IFLAG = 7
RETURN

C
15 CONTINUE
IF (ISNOLD.LT.0 .OR. DELSGN*(TOUT-T).LT.0.) GO TO 20
C-- EVALUATE G AT EITHER TOUT (OUTPUT POINT THIS CALL) OR AT
C-- X (POINT TO WHICH INTERNAL INTEGRATION HAS ALREADY
C-- PROCEEDED), WHICHEVER OCCURS FIRST.
T2=X
IF((X-T.GT.0..AND.X-TOUT.GT.0.) .OR. (X-T.LT.0..AND.X-TOUT.LT.0.))
1 T2=TOUT
CALL INTRP(X,YY,T2,Y,YPOUT,NEQN,KOLD,PHI,PSI)
GOFT2=G(T2,Y,YPOUT)
C-- NOW EVALUATE AT T1=T
T1=T
CALL INTRP(X,YY,T1,Y,YPOUT,NEQN,KOLD,PHI,PSI)
GOFT1=G(T1,Y,YPOUT)
C-- NOW SEE IF A ROOT OF G OCCURS IN CLOSED INTERVAL (T1,T2).
IF( GOFT1.EQ.0. .OR. GOFT2.EQ.0.) GO TO 134
IF( SIGN(1.DO,GOFT1) * SIGN(1.DO,GOFT2) .LT. 0.DO ) GO TO 134
GO TO 21

C
C ON EACH CALL SET INTERVAL OF INTEGRATION AND COUNTER FOR NUMBER OF
C STEPS. ADJUST INPUT ERROR TOLERANCES TO DEFINE WEIGHT VECTOR FOR
C SUBROUTINE STEP
C
20 T2=T
CALL F(T2,Y,YPOUT)
```

```
      GOFT2 = G(T2,Y,YPOUT)
21  CONTINUE
      DEL = TOUT - T
      ABSDEL = ABS(DEL)
      TEND = T + 10.0*DEL
      IF(ISN .LT. 0) TEND = TOUT
      NOSTEP = 0
      KLE4 = 0
      STIFF = .FALSE.
      RELEPS = RELERR/EPS
      ABSEPS = ABSERR/EPS
      IF(IFLAG .EQ. 1) GO TO 30
      IF(ISNOLD .LT. 0) GO TO 30
      IF(DELSGN*DEL .GT. 0.0) GO TO 50
C
C  ON START AND RESTART ALSO SET WORK VARIABLES X AND YY(*), STORE THE
C  DIRECTION OF INTEGRATION, AND INITIALIZE THE STEP SIZE.
C
30  START = .TRUE.
      X = T
      TROOT = T
      DO 40 L = 1,NEQN
40   YY(L) = Y(L)
      DELSGN = SIGN(1.0D0,DEL)
      H = SIGN(MAX(ABS(TOUT-X),FOURU*ABS(X)),TOUT-X)
C
C  IF ALREADY PAST OUTPUT POINT, INTERPOLATE AND RETURN
C
50  CONTINUE
      IF(ABS(X-T) .LT. ABSDEL) GO TO 60
      CALL INTRP(X,YY,TOUT,Y,YPOUT,NEQN,KOLD,PHI,PSI)
      IFLAG = 2
      T = TOUT
      TOLD = T
      ISNOLD = ISN
      RETURN
C
C  IF CANNOT GO PAST OUTPUT POINT AND SUFFICIENTLY CLOSE,
C  EXTRAPOLATE AND RETURN
C
60  IF(ISN .GT. 0 .OR. ABS(TOUT-X) .GE. FOURU*ABS(X)) GO TO 80
      H = TOUT - X
      CALL F(X,YY,YP)
      DO 70 L = 1,NEQN
70   Y(L) = YY(L) + H*YP(L)
C *** NEXT STMT ADDED BY LIENESCH TO ENSURE YPOUT VALUES WILL ALWAYS BE
C *** AVAILABLE UNDER ANY CIRCUMSTANCES
      CALL F(X,Y,YPOUT)
      IFLAG = 2
      T = TOUT
      TOLD = T
      ISNOLD = ISN
      RETURN
C
```

```
C TEST FOR TOO MUCH WORK
C
80 IF(NOSTEP .LT. MAXNUM) GO TO 100
   IFLAG = ISN*4
   IF(STIFF) IFLAG = ISN*5
   DO 90 L = 1,NEQN
90  Y(L) = YY(L)
   T = X
   TOLD = T
   ISNOLD = 1
   RETURN

C
C LIMIT STEP SIZE, SET WEIGHT VECTOR AND TAKE A STEP
C
100 H = SIGN(MIN(ABS(H),ABS(TEND-X)),H)
   DO 110 L = 1,NEQN
   WT(L) = RELEPS*ABS(YY(L)) + ABSEPS
   IF(WT(L) .LE. 0.0) GO TO 160
110 CONTINUE
   CALL STEP1(F,NEQN,YY,X,H,EPS,WT,START,
   1 HOLD,K,KOLD,CRASH,PHI,P,YP,PSI,
   2 ALPHA,BETA,SIG,V,W,GG,PHASE1,NS,NORND)

C
C TEST FOR TOLERANCES TOO SMALL. IF SO, SET THE DERIVATIVE AT X
C BEFORE RETURNING
C
   IF(.NOT.CRASH) GO TO 130
   IFLAG = ISN*3
   RELERR = EPS*RELEPS
   ABSERR = EPS*ABSEPS
   DO 120 L = 1,NEQN
   YP(L) = PHI(L,1)
120  Y(L) = YY(L)
   T = X
   TOLD = T
   ISNOLD = 1
   RETURN

C
C AUGMENT COUNTER ON WORK AND TEST FOR STIFFNESS. ALSO TEST FOR A
C ROOT IN THE STEP JUST COMPLETED
C
130 NOSTEP = NOSTEP + 1
   KLE4 = KLE4 + 1
   IF(KOLD .GT. 4) KLE4 = 0
   IF(KLE4 .GE. 50) STIFF = .TRUE.
   T1=T2
   GOFT1=GOFT2
   T2=TOUT
C-- EVALUATE G AT INTERNAL INTEGRATION POINT X UNLESS X IS PAST TOUT
C-- IF X IS PAST TOUT EVALUATE G AT TOUT.
   IF( ABS(X-T).LT.ABSDEL) T2=X
   CALL INTRP(X,YY,T2,Y,YPOUT,NEQN,KOLD,PHI,PSI)
   GOFT2=G(T2,Y,YPOUT)
   IF(GOFT1.EQ.0. .OR. GOFT2.EQ.0.) GO TO 134
```

```
      IF( SIGN(1.DO,GOFT1)*SIGN(1.ODO,GOFT2) .LT.0.DO)GO TO 134
      GO TO 50
C
C LOCATE ROOT OF G. INTERPOLATE WITH INTRP FOR SOLUTION AND
C DERIVATIVE VALUES
C
134  JFLAG=1
C--  HERE ROOT IS BETWEEN T1 AND T2
      B=T1
      IF(GOFT1.EQ.0.)GO TO 150
      B=T2
      IF(GOFT2.EQ.0.)GO TO 150
      C=T1
140  CALL ROOT(T,GT,B,C,REROOT,AEROOT,JFLAG)
      IF(JFLAG .GT. 0) GO TO 150
      IF( T.EQ.T1)GT=GOFT1
      IF( T.EQ.T2)GT=GOFT2
      IF( T.EQ.T1 .OR.T.EQ.T2)GO TO 140
      CALL INTRP(X,YY,T,Y,YPOUT,NEQN,KOLD,PHI,PSI)
      GT = G(T,Y,YPOUT)
      GO TO 140
150  CONTINUE
      IFLAG = JFLAG+7
      IF(JFLAG .EQ. 2 .OR. JFLAG .EQ. 4) IFLAG = 8
      IF(JFLAG .EQ. 3) IFLAG = 9
      IF(JFLAG .EQ. 5) IFLAG = 10
      IFLAG = IFLAG*ISN
      CALL INTRP(X,YY,B,Y,YPOUT,NEQN,KOLD,PHI,PSI)
      T = B
      IF(ABS(T-TROOT) .LE. REROOT*ABS(T) + AEROOT) GO TO 50
      TROOT = T
      TOLD = T
      ISNOLD = 1
      RETURN
160  CALL ERRCHK(72,72HIN ODERT, PURE ABSOLUTE ERROR IMPOSSIBLE. USE N
      1ON-ZERO VALUE OF ABSERR.)
      IFLAG = 6
      RETURN
      END
```

C * * * * *

C SANDIA MATHEMATICAL PROGRAM LIBRARY
C APPLIED MATHEMATICS DIVISION 2613
C SANDIA LABORATORIES
C ALBUQUERQUE, NEW MEXICO 87115
C CONTROL DATA 6600/7600 VERSION 7.2 SEPTEMBER 1977

C * * * * *

C *
C * ISSUED BY SANDIA LABORATORIES, *
C * A PRIME CONTRACTOR TO THE *
C * UNITED STATES ENERGY RESEARCH AND DEVELOPMENT ADMINISTRATION *
C *

C * * * * * NOTICE * * * * *

C *
C * THIS REPORT WAS PREPARED AS AN ACCOUNT OF WORK SPONSORED BY THE
C * UNITED STATES GOVERNMENT. NEITHER THE UNITED STATES NOR THE
C * UNITED STATES ENERGY RESEARCH AND DEVELOPMENT ADMINISTRATION, .
C * NOR ANY OF THEIR EMPLOYEES, NOR ANY OF THEIR CONTRACTORS,
C * SUBCONTRACTORS, OR THEIR EMPLOYEES, MAKES ANY WARRANTY, EXPRESS
C * OR IMPLIED, OR ASSUMES ANY LEGAL LIABILITY OR RESPONSIBILITY
C * FOR THE ACCURACY, COMPLETENESS OR USEFULNESS OF ANY INFORMATION,
C * APPARATUS, PRODUCT OR PROCESS DISCLOSED, OR REPRESENTS THAT ITS
C * USE WOULD NOT INFRINGE PRIVATELY OWNED RIGHTS.
C *

C * * * * *

C *
C * THE PRIMARY DOCUMENT FOR THE LIBRARY OF WHICH THIS ROUTINE IS *
C * A PART IS SAND75-0545. *
C *

C * * * * *

C WRITTEN BY L. F. SHAMPINE AND M. K. GORDON

C ABSTRACT

C THE METHODS IN SUBROUTINE STEP1 APPROXIMATE THE SOLUTION NEAR X
C BY A POLYNOMIAL. SUBROUTINE INTRP APPROXIMATES THE SOLUTION AT
C XOUT BY EVALUATING THE POLYNOMIAL THERE. INFORMATION DEFINING THIS
C POLYNOMIAL IS PASSED FROM STEP1 SO INTRP CANNOT BE USED ALONE.

C THIS CODE IS COMPLETELY EXPLAINED AND DOCUMENTED IN THE TEXT,
C COMPUTER SOLUTION OF ORDINARY DIFFERENTIAL EQUATIONS, THE INITIAL
C VALUE PROBLEM BY L. F. SHAMPINE AND M. K. GORDON.
C FURTHER DETAILS ON USE OF THIS CODE ARE AVAILABLE IN *SOLVING
C ORDINARY DIFFERENTIAL EQUATIONS WITH ODE, STEP, AND INTRP*,
C BY L. F. SHAMPINE AND M. K. GORDON, SLA-73-1060.

C INPUT TO INTRP --

C THE USER PROVIDES STORAGE IN THE CALLING PROGRAM FOR THE ARRAYS IN
C THE CALL LIST

```
C      DIMENSION Y(NEQN),YOUT(NEQN),YPOUT(NEQN),PHI(NEQN,16),PSI(12)
C      AND DEFINES
C      XOUT -- POINT AT WHICH SOLUTION IS DESIRED.
C      THE REMAINING PARAMETERS ARE DEFINED IN STEP1 AND PASSED TO
C      INTRP FROM THAT SUBROUTINE
C
C      OUTPUT FROM INTRP --
C
C      YOUT(*) -- SOLUTION AT XOUT
C      YPOUT(*) -- DERIVATIVE OF SOLUTION AT XOUT
C      THE REMAINING PARAMETERS ARE RETURNED UNALTERED FROM THEIR INPUT
C      VALUES. INTEGRATION WITH STEP1 MAY BE CONTINUED.
C
      SUBROUTINE INTRP(X,Y,XOUT,YOUT,YPOUT,NEQN,KOLD,PHI,PSI)
      IMPLICIT REAL *8 (A-H,O-Z)
      IMPLICIT INTEGER*2 (I-N)
C
C
CCCCC GENERIC
      DIMENSION Y(NEQN),YOUT(NEQN),YPOUT(NEQN),PHI(NEQN,16),PSI(12)
      DIMENSION G(13),W(13),RHO(13)
      DATA G(1)/1.0/,RHO(1)/1.0/
C
      HI = XOUT - X
      KI = KOLD + 1
      KIP1 = KI + 1
C
C      INITIALIZE W(*) FOR COMPUTING G(*)
C
      DO 5 I = 1,KI
          TEMP1 = I
      5      W(I) = 1.0/TEMP1
          TERM = 0.0
C
C      COMPUTE G(*)
C
      DO 15 J = 2,KI
          JM1 = J - 1
          PSIJM1 = PSI(JM1)
          GAMMA = (HI + TERM)/PSIJM1
          ETA = HI/PSIJM1
          LIMIT1 = KIP1 - J
          DO 10 I = 1,LIMIT1
      10      W(I) = GAMMA*W(I) - ETA*W(I+1)
          G(J) = W(1)
          RHO(J) = GAMMA*RHO(JM1)
      15      TERM = PSIJM1
C
C      INTERPOLATE
C
      DO 20 L = 1,NEQN
          YPOUT(L) = 0.0
      20      YOUT(L) = 0.0
          DO 30 J = 1,KI
```

```
I = KIP1 - J
TEMP2 = G(I)
TEMP3 = RHO(I)
DO 25 L = 1,NEQN
  YOUT(L) = YOUT(L) + TEMP2*PHI(L,I)
25  YPOUT(L) = YPOUT(L) + TEMP3*PHI(L,I)
30  CONTINUE
DO 35 L = 1,NEQN
35  YOUT(L) = Y(L) + HI*YOUT(L)
RETURN
END
```

C * * * * *

C
C ROOT COMPUTES A ROOT OF THE NONLINEAR EQUATION $F(X)=0$
C WHERE $F(X)$ IS A CONTINUOUS REAL FUNCTION OF A SINGLE REAL
C VARIABLE X . THE METHOD USED IS A COMBINATION OF BISECTION
C AND THE SECANT RULE.

C
C NORMAL INPUT CONSISTS OF A CONTINUOUS FUNCTION F AND AN
C INTERVAL (B,C) SUCH THAT $F(B)*F(C).LE.0.0$. EACH ITERATION
C FINDS NEW VALUES OF B AND C SUCH THAT THE INTERVAL (B,C) IS
C SHRUNK AND $F(B)*F(C).LE.0.0$. THE STOPPING CRITERION IS

$$ABS(B-C).LE.2.0*(RELERR*ABS(B)+ABSERR)$$

C
C WHERE RELERR=RELATIVE ERROR AND ABSERR=ABSOLUTE ERROR ARE
C INPUT QUANTITIES. SET THE FLAG, IFLAG, POSITIVE TO INITIALIZE
C THE COMPUTATION. AS B,C AND IFLAG ARE USED FOR BOTH INPUT AND
C OUTPUT, THEY MUST BE VARIABLES IN THE CALLING PROGRAM.

C IF 0 IS A POSSIBLE ROOT, ONE SHOULD NOT CHOOSE ABSERR=0.0.

C THE OUTPUT VALUE OF B IS THE BETTER APPROXIMATION TO A ROOT
C AS B AND C ARE ALWAYS REDEFINED SO THAT $ABS(F(B)).LE.ABS(F(C))$.

C TO SOLVE THE EQUATION, ROOT MUST EVALUATE $F(X)$ REPEATEDLY. THIS
C IS DONE IN THE CALLING PROGRAM. WHEN AN EVALUATION OF F IS
C NEEDED AT T , ROOT RETURNS WITH IFLAG NEGATIVE. EVALUATE $FT=F(T)$
C AND CALL ROOT AGAIN. DO NOT ALTER IFLAG.

C WHEN THE COMPUTATION IS COMPLETE, ROOT RETURNS TO THE CALLING
C PROGRAM WITH IFLAG POSITIVE.

C IFLAG=1 IF $F(B)*F(C).LT.0$ AND THE STOPPING CRITERION IS MET.

C =2 IF A VALUE B IS FOUND SUCH THAT THE COMPUTED VALUE
C $F(B)$ IS EXACTLY ZERO. THE INTERVAL (B,C) MAY NOT
C SATISFY THE STOPPING CRITERION.

C =3 IF $ABS(F(B))$ EXCEEDS THE INPUT VALUES $ABS(F(B))$,
C $ABS(F(C))$. IN THIS CASE IT IS LIKELY THAT B IS CLOSE
C TO A POLE OF F .

C =4 IF NO ODD ORDER ROOT WAS FOUND IN THE INTERVAL. A
C LOCAL MINIMUM MAY HAVE BEEN OBTAINED.

C =5 IF TOO MANY FUNCTION EVALUATIONS WERE MADE.
C (AS PROGRAMMED, 500 ARE ALLOWED.)

C THIS CODE IS A MODIFICATION OF THE CODE ZEROIN WHICH IS COMPLETELY
C EXPLAINED AND DOCUMENTED IN THE TEXT, NUMERICAL COMPUTING, AN
C INTRODUCTION BY L. F. SHAMPINE AND R. C. ALLEN.

C SUBROUTINE ROOT(T,FT,B,C,RELERR,ABSERR,IFLAG)

C

```
      IMPLICIT REAL*8 (A-H,O-Z)
CCCC  GENERIC
      COMMON/MLDRT/A,ACBS,AE,FA,FB,FC,FX,IC,KOUNT,RE
C*****
C* THE ONLY MACHINE DEPENDENT CONSTANT IS BASED ON THE MACHINE UNIT *
C* ROUND OFF ERROR U WHICH IS THE SMALLEST POSITIVE NUMBER SUCH THAT *
C* 1.0+U .GT. 1.0 . U MUST BE CALCULATED AND INSERTED IN THE *
C* FOLLOWING DATA STATEMENT BEFORE USING ROOT . THE ROUTINE MACHIN *
C* CALCULATES U . *
C*****
      DATA U /2.2E-16/
C*****
C
      IF(IFLAG.LT.0.0) GO TO 100
      RE=MAX(RELERR,U)
      AE=MAX(ABSERR,0.0D0)
      IC=0
      ACBS=ABS(B-C)
      A=C
      T=A
      IFLAG=-1
      RETURN
100 IFLAG=IABS(IFLAG)
      GO TO (200,300,400),IFLAG
200 FA=FT
      T=B
      IFLAG=-2
      RETURN
300 FB=FT
      FC=FA
      KOUNT=2
      FX=MAX(ABS(FB),ABS(FC))
      GO TO 1
400 FB=FT
      IF(FB.EQ.0.0) GO TO 9
      KOUNT=KOUNT+1
      IF(SIGN(1.0D0,FB).NE.SIGN(1.0D0,FC))GO TO 1
      C=A
      FC=FA
      1 IF(ABS(FC).GE.ABS(FB))GO TO 2
C
C INTERCHANGE B AND C SO THAT ABS(F(B)).LE.ABS(F(C)).
C
      A=B
      FA=FB
      B=C
      FB=FC
      C=A
      FC=FA
      2 CMB=0.5*(C-B)
      ACMB=ABS(CMB)
      TOL=RE*ABS(B)+AE
C
C TEST STOPPING CRITERION AND FUNCTION COUNT.
```

```
C
  IF(ACMB.LE.TOL)GO TO 8
  IF(KOUNT.GE.500)GO TO 12
C
C CALCULATE NEW ITERATE IMPLICITLY AS B+P/Q
C WHERE WE ARRANGE P.GE.0. THE IMPLICIT
C FORM IS USED TO PREVENT OVERFLOW.
C
  P=(B-A)*FB
  Q=FA-FB
  IF(P.GE.0.0)GO TO 3
  P=-P
  Q=-Q
C
C UPDATE A, CHECK IF REDUCTION IN THE SIZE OF BRACKETING
C INTERVAL IS SATISFACTORY. IF NOT, BISECT UNTIL IT IS.
C
  3 A=B
  FA=FB
  IC=IC+1
  IF(IC.LT.4)GO TO 4
  IF(8.0*ACMB.GE.ACBS)GO TO 6
  IC=0
  ACBS=ACMB
C
C TEST FOR TOO SMALL A CHANGE.
C
  4 IF(P.GT.ABS(Q)*TOL)GO TO 5
C
C INCREMENT BY TOLERANCE.
C
  B=B+SIGN(TOL,CMB)
  GO TO 7
C
C ROOT OUGHT TO BE BETWEEN B AND (C+B)/2.
C
  5 IF(P.GE.CMB*Q)GO TO 6
C
C USE SECANT RULE.
C
  B=B+P/Q
  GO TO 7
C
C USE BISECTION.
C
  6 B=0.5*(C+B)
C
C HAVE COMPLETED COMPUTATION FOR NEW ITERATE B.
C
  7 T=B
  IFLAG=-3
  RETURN
C
C FINISHED. SET IFLAG.
```

C

```
8 IF(SIGN(1.0D0,FB).EQ.SIGN(1.0D0,FC))GO TO 11
  IF(ABS(FB).GT.FX)GO TO 10
  IFLAG=1
  RETURN
9 IFLAG=2
  RETURN
10 IFLAG=3
  RETURN
11 IFLAG=4
  RETURN
12 IFLAG=5
  RETURN
  END
```

```
C * * * * *
C
C SANDIA MATHEMATICAL PROGRAM LIBRARY
C APPLIED MATHEMATICS DIVISION 2613
C SANDIA LABORATORIES
C ALBUQUERQUE, NEW MEXICO 87115
C CONTROL DATA 6600/7600 VERSION 7.2 SEPTEMBER 1977
C
C * * * * *
C *
C * ISSUED BY SANDIA LABORATORIES,
C * A PRIME CONTRACTOR TO THE
C * UNITED STATES ENERGY RESEARCH AND DEVELOPMENT ADMINISTRATION *
C *
C * * * * * NOTICE * * * * *
C *
C * THIS REPORT WAS PREPARED AS AN ACCOUNT OF WORK SPONSORED BY THE
C * UNITED STATES GOVERNMENT. NEITHER THE UNITED STATES NOR THE
C * UNITED STATES ENERGY RESEARCH AND DEVELOPMENT ADMINISTRATION,
C * NOR ANY OF THEIR EMPLOYEES, NOR ANY OF THEIR CONTRACTORS,
C * SUBCONTRACTORS, OR THEIR EMPLOYEES, MAKES ANY WARRANTY, EXPRESS
C * OR IMPLIED, OR ASSUMES ANY LEGAL LIABILITY OR RESPONSIBILITY
C * FOR THE ACCURACY, COMPLETENESS OR USEFULNESS OF ANY INFORMATION,
C * APPARATUS, PRODUCT OR PROCESS DISCLOSED, OR REPRESENTS THAT ITS
C * USE WOULD NOT INFRINGE PRIVATELY OWNED RIGHTS.
C *
C * * * * *
C *
C * THE PRIMARY DOCUMENT FOR THE LIBRARY OF WHICH THIS ROUTINE IS *
C * A PART IS SAND75-0545.
C *
C * * * * *
C
C SUBROUTINE ERRCHK(N,M)
C INTEGER*2 M
C DIMENSION M(100)
C NWDS = (IABS(N)+1)/2
C PRINT 10, (M(I), I=1,NWDS)
10 FORMAT(1H0, 60A2)
C IF (N .GT. 0) RETURN
C STOP
C END
```

APPENDIX G
DEFINITIONS OF INPUT VARIABLES
FOR COMPUTER CODE

FILE : "INPUT.DAT"

POWER = Logical variable
(.TRUE.= Turbocharged Turbocompounded Case,
.FALSE.= Turbocharged Only Case)

SPDEL = Logical variable
(.TRUE.= Specified ignition delay option)
.FALSE.= Predicted ignition delay option)

SPTemp = Logical variable
(.TRUE.= Specified inside wall surface temperatures,
.FALSE.= Predicted steady-state wall surface temperatures)

TRANS = Logical variable
(.TRUE.= Calculation of time-dependent wall temperature profile
for piston and head, following steady-state calculation;
used only when SPTemp=.TRUE.,
.FALSE.= Calculation ends after prediction of steady-state
wall temperatures)

ANNAND = Logical variable
(.TRUE.= Annand radiation model option,
.FALSE.= Flame radiation model option)

TIVO = Timing for intake valve opening (CA)

TIVC = Timing for intake valve closing (CA)

TEVO = Timing for exhaust valve opening (CA)

TEVC = Timing for exhaust valve closing (CA)

TINJ = Injection timing (CA)

TIGN = Timing for start of combustion (with specified delay only)

ERPM = Reciprocator speed (RPM)

FUELTP = Type of fuel (1 = #2 diesel fuel)

FMIN = Mass of fuel injected (grams per cylinder per cycle)

DTBRN = Nominal burning duration /CMBSTN only

PATM = Atmospheric pressure (atm)

TATM = Atmospheric temperature (Kelvins)

PINLET = Compressor inlet pressure (atm)

RTEMP(1) = Compressor inlet temperature (Kelvins)

ICYL = Number of reciprocator cylinders

BORE = Cylinder bore (cm)

CLVTDC = Clearance volume at top dead center (cm**3)

CFR2 = Constant for friction model

CFR3 = Constant for friction model

ELNG(1) = Equivalent length of intake manifold (m)

ELNG(2) = Equivalent length of exhaust manifold (m)

ELNG(3) = Length of connecting pipe between the two turbines (m)

EDIAM(1) = Equivalent diameter of intake manifold (m)

EDIAM(2) = Equivalent diameter of exhaust manifold (m)

EDIAM(3) = Diameter of connecting pipe between the two turbines (m)

HI(1) = Intercooler effectiveness, I/G

HI(2) = Intercooler coolant inlet temperature (Kelvins)

HI(3) = Intercooler outlet temperature, I/G (Kelvins)

HI(5) = Intercooler "A*U" (W/K)

B(1) = Turbocharger rotational inertia

B(2) = Turbocharger rotational damping

RCORR(1) = Power turbine gear ratio

PTTEF = Power turbine transmission efficiency

CBETA = Turbulent dissipation constant

CFACTR = Diffusion burning constant for combustion correlation /CMBSTN

CRAD = Radiation Model Constant/with Annand radiation model only

EXPHT = Exponent for convective heat transfer correlation

CONHT = Constant convective heat transfer correlation (cylinder)

TPSTON = Temperature of piston top (Kelvins)

THEAD = Inside wall temperature of cylinder head (Kelvins)

TCW = Temperature of cylinder walls (Kelvins)

ECONHT = Convective heat transfer correlation constant (manifolds)

ETWALL(1) = Inside wall temperature of intake manifold (Kelvins)

ETWALL(2) = Inside wall temperature of exhaust manifold (Kelvins)

ETWALL(3) = Inside wall temperature of turbine connecting pipe (Kelvins)

DP(1) = Pressure drop between compressor discharge and intercooler inlet (PA)

DP(2) = " " across intercooler (Pa)

DP(3) = " " between exhaust manifold and turbine inlet (Pa)

DP(4) = " " between turbine outlet and power turbine inlet (PA)

DP(5) = " " between power turbine outlet and atmosphere (Pa)

PRSS(1) = Pressure at compressor outlet, I/G (atm)

PRSS(2) = Pressure at turbine inlet, I/G (atm)

PRSS(3) = Pressure at turbine outlet, I/G (atm)

PRSS(4) = Pressure at power turbine inlet, I/G (atm)

PRSS(5) = Pressure at power turbine outlet, I/G (atm)

PSTART = Master cylinder pressure, I/G (atm)

TSTART = Master cylinder temperature, I/G (Kelvins)

PHISTA = Master cylinder average fuel fraction, I/G

MKESTA = Master cylinder mean kinetic energy, I/G

TKESTA = Master cylinder turbulent kinetic energy, I/G

YO(2) = Intake manifold temperature, I/G (Kelvins)
YO(3) = Intake manifold pressure, I/G (atm)
YO(4) = Intake manifold average fuel fraction, I/G
YO(6) = Exhaust manifold temperature, I/G (Kelvins)
YO(7) = Exhaust manifold pressure, I/G (atm)
YO(8) = Exhaust manifold average fuel fraction, I/G
YO(9) = Turbocharger speed, I/G (thousands of RPM)
EMKT(1) = Intake manifold friction coefficient
EMKT(2) = Exhaust manifold friction coefficient
EMKT(3) = Turbine connecting pipe friction coefficient
TCALL = Crank angle interval at which ODERT is to be called
TPRINT = Printing interval for hardcopy output files
TSCREN = Printing interval for screen output
REL = Relative error tolerance in ODERT
AREROT = Error tolerance for calculating the root of G /see ODERT
CIINTG = " " for integration during intake
CCINTG = " " " " " compression
CBINTG = " " " " " combustion
CEINTG = " " " " " exhaust
MAXERR = See subroutine ITRATE
MAXTRY = See subroutine ITRATE
MAXITS = Maximum allowed number of iterations of cycle simulation
FSEC1 = Criterion for convergence of average gas-to-wall heat transfer
used with quasi-steady wall conduction models
FSEC2 = Criterion for convergence of average gas-to-wall heat transfer
used with transient wall conduction models
* I/G = Initial Guess

FILE : "CHEAT.DAT"

- NCC = Total number of components with cylindrical composite wall structures (eg. cylinder liner, manifold sections, connecting pipe).
- CDIAM(I) = Inside diameter of Ith component, (m)
- NCLA(I) = Number of material layers of Ith component.
- CHCOOL(I) = Heat transfer coefficient from the outside wall surface of Ith component to the coolant or ambient (W/m²/K). A value of zero means that the wall temperature on outside surface of Ith component is specified.
- CTCOOL(I) = Ambient temperature, coolant temperature, or specified wall temperature on the outside surface (for CHCOOL=0) of Ith component (Kelvins).
- CTHIK(I,J) = Thickness of Jth layer of Ith component (m).
- CCOND(I,J) = Thermal conductivity of Jth layer of Ith component (W/m/K)

NOTE:

First array dimension : component description

Second array dimension : layer description

FILE : "PHEAT.DAT"

- NPC = Total number of components with parallel composite wall structures (cylinder head, piston).
- NPLA(I) = Number of material layers of Ith component.
- PHCOOL(I) = Heat transfer coefficient from the outside wall surface of Ith component to the coolant or ambient (W/m²/K). A value of zero means that the wall temperature on outside surface of Ith component is specified.
- PTCOOL(I) = Ambient temperature, coolant temperature, or specified wall temperature on the outside surface (for CHCOOL=0) of Ith component (Kelvins).
- PTHIK(I,J) = Thickness of Jth layer of Ith component (m).
- PCOND(I,J) = Thermal conductivity of Jth layer of Ith component (W/m/K).
- PDIFU(I,J) = Thermal diffusivity of Jth layer of Ith component (m²/sec).
- INNODE(I,J) = Number of nodes placed in Jth layer of Ith component.
- FACT = Fraction of nodes of first layer placed within the penetration depth.

Note:

First array dimension : Component description

Second array dimension : Layer description

APPENDIX H
SAMPLE INPUT FILES
FOR COMPUTER CODE

\$INPUT

ANNAND = .FALSE.
SPTMP = .FALSE.
POWER = .TRUE.
SPDEL = .TRUE.
TRANS = .TRUE.
TINJ = 338.
TIGN = 342.
ERPM = 1901.9
FUELTP = 1
FMIN = 0.1879
PATM = 0.9378
TATM = 302.6
PINLET = 0.9378
RTEMP(1) = 302.6
ICYL = 6
BORE = 13.97
CFR2 = 7.0
CFR3 = 1.5
ELNG = 0.7, 1.0, 0.5
EDIAM = 0.1, 0.1, 0.13
HI = .9, 305., 305., 0., 1200.
B = 4.E-5, 5.E-7
RCORR(1) = 0.017
PTTEF = .90
CSC = 1.0
TSC = 1.0
PTSC = 1.0
CBETA = 1.5
CFACTR = 1.05
DTBRN = 125.
CRAD = 2.0
CONHT = 0.055
TPSTON = 800.
THEAD = 800.
TCW = 450.
ECONHT(1) = 0.035
ECONHT(2) = 0.035
ECONHT(3) = 0.035
ETWALL = 305., 750., 600.
DP = 2000., 1000., 1000., 1000., 5000.
EMKT(1) = 1.0
EMKT(2) = 2.0
EMKT(3) = 1.0
PRSS = 0., 0., 0., 1.3E5, 1.05E5
PSTART = 3.67
TSTART = 807.
PHISTA = 0.47
MKESTA = 2.5E-3
TKESTA = 1.1E-3
Y0(2) = 321.
Y0(3) = 240.E3
Y0(4) = 0.0
Y0(6) = 864.
Y0(7) = 330.E3
Y0(8) = 0.0338
Y0(9) = 65.
TCALL = 1.
TPRINT = 6.
TSCREEN = 100.
REL = .1E-4
AREROT = .1E-4
CIINTG = 1.E-4
CCINTG = 1.E-4
CBINTG = 1.E-5
CEINTG = 1.E-4
MAXERR = 1.E-4
MAXTRY = 100
MAXITS = 20
MINITS = 1
FSEC1 = 0.20
FSEC2 = 0.20

\$END

```
$CHEAT
NCC          = 1
CDIAM(1)    = 0.11
NCLA(1)      = 1
CHCOOL(1)   = 0.
CTCOOL(1)   = 380.
CTHIK(1,1)  = 7.E-3
CCOND(1,1)  = 54.4
$END
```

```
$PHEAT
NPC          = 2
FACT        = 0.6
NPLA(1)     = 3
PTCOOL(1)   = 380.
PHCOOL(1)   = 0.
INNODE(1,1) = 15
INNODE(1,2) = 5
INNODE(1,3) = 5
PTHIK(1,1)  = 1.5E-3
PTHIK(1,2)  = 7.E-3
PTHIK(1,3)  = 3.E-3
PCOND(1,1)  = 0.6
PCOND(1,2)  = 54.4
PCOND(1,3)  = 54.4
PDIFU(1,1)  = 0.55E-6
PDIFU(1,2)  = 1.57E-5
PDIFU(1,3)  = 1.57E-5
NPLA(2)     = 3
PTCOOL(2)   = 380.
PHCOOL(2)   = 0.
INNODE(2,1) = 15
INNODE(2,2) = 5
INNODE(2,3) = 5
PTHIK(2,1)  = 1.5E-3
PTHIK(2,2)  = 7.E-3
PTHIK(2,3)  = 3.E-3
PCOND(2,1)  = 0.6
PCOND(2,2)  = 54.4
PCOND(2,3)  = 54.4
PDIFU(2,1)  = 0.55E-6
PDIFU(2,2)  = 1.57E-5
PDIFU(2,3)  = 1.57E-5
$END
```

"COMAP.DAT"

9.94E4,303.
33.
34.3,.549,1.219
32.7,.648,1.263
31.5,.705,1.290
28.0,.789,1.337
24.6,.802,1.363
20.2,.791,1.383
15.2,.727,1.388
45.
50.5,.582,1.444
48.6,.691,1.547
46.8,.739,1.601
42.9,.802,1.680
38.3,.831,1.753
33.4,.822,1.779
27.7,.774,1.780
51.
59.3,.595,1.617
57.5,.704,1.759
55.6,.752,1.834
51.7,.812,1.940
47.7,.825,2.006
43.1,.833,2.057
38.0,.809,2.080
57.
69.2,.610,1.827
66.5,.729,2.048
64.4,.774,2.150
60.4,.807,2.264
55.8,.831,2.354
51.1,.829,2.417
45.7,.810,2.444
63.
76.9,.598,2.049
74.9,.736,2.398
73.1,.763,2.494
69.1,.803,2.661
64.9,.812,2.759
60.2,.811,2.825
55.3,.793,2.831
69.
82.4,.604,2.335
80.7,.728,2.765
79.2,.755,2.895
75.8,.789,3.114
72.3,.794,3.211
68.4,.798,3.327
64.6,.785,3.338

"TMAP.DAT"

9.955E4,922.
30.
0., 0., 1.0
16.85, 0.664, 1.378
19.11, 0.643, 1.422
21.41, 0.6, 1.5
24.67, 0.525, 1.8
26.75, 0.473, 2.2
28.48, 0.429, 2.8
29.26, 0.41, 3.4
40.
0., 0., 1.0
0., 0., 1.0
18.66, 0.71, 1.453
20.37, 0.7, 1.5
24.0, 0.638, 1.8
26.34, 0.588, 2.2
28.0, 0.541, 2.8
28.88, 0.519, 3.4
50.
0., 0., 1.0
0., 0., 1.0
19.2, 0.709, 1.5
20.47, 0.759, 1.6
22.96, 0.728, 1.8
25.6, 0.68, 2.2
27.52, 0.631, 2.8
28.33, 0.61, 3.4
60.
0., 0., 1.0
0., 0., 1.0
0., 0., 1.0
18.0, 0.645, 1.5
21.68, 0.781, 1.8
24.7, 0.75, 2.2
26.8, 0.712, 2.8
27.69, 0.693, 3.4
70.
0., 0., 1.0
0., 0., 1.0
16.3, 0.566, 1.5
20.32, 0.704, 1.8
22.87, 0.79, 2.12
23.44, 0.789, 2.2
26.0, 0.766, 2.8
26.85, 0.748, 3.4
80.
0., 0., 1.0
14.63, 0.488, 1.5
18.8, 0.627, 1.8
22., 0.73, 2.2
24., 0.8, 2.65
24.79, 0.795, 2.8
25., 0.792, 2.92
25.61, 0.785, 3.4

"PTMAP.DAT"

9.955E4, 922.

20.
0., 0., 1.
20., 0.685, 1.035
25., 0.762, 1.09
30., 0.757, 1.14
35., 0.722, 1.221
37.5, 0.700, 1.256
40., 0.677, 1.301
45., 0.630, 1.413
47.5, 0.600, 1.474
50., 0.561, 1.57
52.5, 0.530, 1.689
25.
0., 0., 1.
20., 0.62, 1.076
25., 0.75, 1.13
30., 0.797, 1.194
35., 0.77, 1.262
37.5, 0.752, 1.306
40., 0.73, 1.35
45., 0.68, 1.472
47.5, 0.647, 1.542
50., 0.62, 1.644
52.5, 0.582, 1.756
30.
0., 0., 1.
20., 0.52, 1.108
25., 0.642, 1.162
30., 0.761, 1.23
35., 0.81, 1.312
37.5, 0.795, 1.36
40., 0.773, 1.404
45., 0.725, 1.54
47.5, 0.7, 1.62
50., 0.66, 1.748
52.5, 0.63, 1.832
35.
0., 0., 1.
20., 0.46, 1.143
25., 0.575, 1.205
30., 0.698, 1.28
35., 0.795, 1.36
37.5, 0.812, 1.405
40., 0.807, 1.47
45., 0.77, 1.62
47.5, 0.741, 1.715
50., 0.703, 1.83
52.5, 0.667, 1.92
40.
0., 0., 1.
20., 0.40, 1.19
25., 0.52, 1.256
30., 0.641, 1.325
35., 0.75, 1.41
37.5, 0.778, 1.47
40., 0.793, 1.54
45., 0.801, 1.72
47.5, 0.789, 1.804
50., 0.753, 1.91
52.5, 0.72, 1.995
45.
0., 0., 1.
20., 0.35, 1.23
25., 0.471, 1.301
30., 0.595, 1.373
35., 0.7, 1.471
37.5, 0.733, 1.54
40., 0.755, 1.62
45., 0.79, 1.813
47.5, 0.795, 1.9
50., 0.79, 2.005
52.5, 0.762, 2.095

"TABLIN.DAT"

-11. .0000000
-6. .0007920
-1. .0022120
4. .0028850
9. .0059450
14. .0077140
19. .0091950
24. .0108060
29. .0124590
34. .0140720
39. .0152660
44. .0163960
49. .0170110
54. .0173840
59. .0177170
64. .0178840
69. .0179970
74. .0180890
79. .0181600
84. .0182110
89. .0182410
94. .0182500
99. .0182380
104. .0182040
109. .0181480
114. .0180720
119. .0179760
124. .0178600
129. .0176620
134. .0173290
139. .0169580
144. .0162660
149. .0151510
154. .0139780
159. .0124360
164. .0109120
169. .0094500
174. .0080980
179. .0068600
184. .0048780
189. .0033000
194. .0021190
199. .0012830
204. .0006920
209. .0002230
212. .0000000

"TABLEX.DAT"

505., .0000000
510., .0006440
515., .0017120
520., .0029590
525., .0045410
530., .0057490
535., .0066270
540., .0077170
545., .0091650
550., .0105680
555., .0118100
560., .0129640
565., .0135850
570., .0141540
575., .0145110
580., .0147210
585., .0149000
590., .0150510
595., .0151210
600., .0151660
605., .0151970
610., .0152130
615., .0152130
620., .0151970
625., .0151670
630., .0151220
635., .0150550
640., .0149050
645., .0147250
650., .0145180
655., .0141810
660., .0136350
665., .0130430
670., .0120080
675., .0108220
680., .0095270
685., .0081720
690., .0070040
695., .0062000
700., .0054560
705., .0041210
710., .0028200
715., .0018450
720., .0011610
725., .0006900
730., .0003370
735., .0000380
736., .0000000

APPENDIX I
SAMPLE OUTPUT FILES
FROM COMPUTER CODE

M.I.T. TURBOCOMPOUND DIESEL ENGINE CYCLE SIMULATION

>>>> INPUT DATA

>>>> OPERATING MODE

SPECIFIED IGNITION DELAY OPTION

PREDICTED QUASI-STEADY WALL TEMPERATURES

FLAME RADIATION MODEL

>>>> OPERATING CONDITIONS

FUEL USED IS DIESEL #2

ENGINE SPEED	=	1901.9 RPM
INJECTION TIMING	=	338.0 DEG CA
FUEL INJECTED /CYL /CYCLE	=	0.1879 G
TOTAL FUELING RATE	=	2.3614 LB/MIN
COMPRESSOR INLET PRESSURE	=	0.9378 ATM
COMPRESSOR INLET TEMPERATURE	=	302.60 K
ATMOSPHERIC PRESSURE	=	0.9378 ATM
ATMOSPHERIC TEMPERATURE	=	302.60 K

>>>> ENGINE DESIGN PARAMETERS

NUMBER OF CYLINDERS = 6
 CYLINDER BORE = 13.970 CM
 CRANKSHAFT STROKE = 15.240 CM
 CONNECTING ROD LENGTH = 30.480 CM
 COMPRESSION RATIO = 14.500
 DISPLACED VOLUME = 2335.974 CC
 CLEARANCE VOLUME = 173.035 CC
 ENGINE DISPLACEMENT = 14.016 LT
 FRICTION CONSTANT 2 = 7.000
 FRICTION CONSTANT 3 = 1.500
 INTAKE VALVE OPENS = -11.0 DEG CA
 INTAKE VALVE CLOSES = 212.0 DEG CA
 EXHAUST VALVE OPENS = 505.0 DEG CA
 EXHAUST VALVE CLOSES = 736.0 DEG CA

>>>> MANIFOLD DIMENSIONS

		INTAKE	EXHAUST
LENGTH	(M)	0.7000000	1.0000000
DIAMETER	(M)	0.1000000	0.1000000
CROSS-SECTIONAL AREA	(M**2)	7.8539820E-03	7.8539820E-03
INTERNAL SURFACE AREA	(M**2)	0.2199115	0.3141593
VOLUME	(LT)	5.497787	7.853982

>>>> TURBINE CONNECTING PIPE DIMENSIONS

LENGTH	(M)	0.5000000
DIAMETER	(M)	0.1300000
CROSS-SECTIONAL AREA	(M**2)	1.3273228E-02
INTERNAL SURFACE AREA	(M**2)	0.2042035
VOLUME	(LT)	6.636614

>>>> TURBOMACHINERY DATA

T/C INERTIA (KG-M**2) 3.9999999E-05
T/C DAMPING (KG-M**2/S) 5.0000000E-07
P.TURBINE TRANSMISSION EFFIC. 0.9000000
P.TURBINE GEAR RATIO 1.7000001E-02

>>>> SYSTEM PRESSURE DROPS IN PA

COMPRESSOR EXIT - INTERCOOLER INLET 2000.000
INTERCOOLER INLET - INTAKE MANIFOLD 742.5497
EXHAUST MANIFOLD - TURBINE INLET 1614.407
TURBINE EXIT - POWER TURBINE INLET 1307.745
POWER TURBINE EXIT - ATMOSPHERIC 5000.000

>>>>> HEAT TRANSFER AND TURBULENCE PARAMETERS

HEAT TRANSFER CONSTANT(CHAMBER)= 0.0550
HEAT TRANSFER CONSTANT(INT MAN)= 0.0350
HEAT TRANSFER CONSTANT(EXH MAN)= 0.0350
HEAT TRANSFER CONSTANT(C. PIPE)= 0.0350
HEAT TRANSFER EXPONENT = 0.8000
PISTON TEMPERATURE = 799.57 K
CYLINDER HEAD TEMPERATURE = 799.57 K
CYLINDER WALL TEMPERATURE = 435.35 K
INT. MANIFOLD WALL TEMPERATURE = 305.00 K
EXH. MANIFOLD WALL TEMPERATURE = 750.00 K
CONN. PIPE WALL TEMPERATURE = 600.00 K
TURBULENT DISSIPATION CONSTANT = 1.5000

>>>> WALL CONDUCTION MODELS

>>>> PISTON WALL STRUCTURE

LAYER	1	2	3
THICKNESS (M)	0.00150	0.00700	0.00300
THERMAL CONDUCTIVITY (W/M/K)	0.600	54.400	54.400
THERMAL DIFFUSIVITY (M2/SEC)	0.550E-06	0.157E-04	0.157E-04
NUMBER OF NODES	15	5	5
NODES WITHIN SKIN DEPTH	9		
COURANT NUMBER	238.179	2225.950	408.848
OUTSIDE WALL TEMPERATURE (K)	380.0		
OVERALL CONDUCTIVITY (W/M/K)	372.6		

>>>> CYL. HEAD WALL STRUCTURE

LAYER	1	2	3
THICKNESS (M)	0.00150	0.00700	0.00300
THERMAL CONDUCTIVITY (W/M/K)	0.600	54.400	54.400
THERMAL DIFFUSIVITY (M2/SEC)	0.550E-06	0.157E-04	0.157E-04
NUMBER OF NODES	15	5	5
NODES WITHIN SKIN DEPTH	9		
COURANT NUMBER	238.179	2225.950	408.848
OUTSIDE WALL TEMPERATURE (K)	380.0		
OVERALL CONDUCTIVITY (W/M/K)	372.6		

>>>> CYL. LINER WALL STRUCTURE

LAYER	1
INSIDE DIAMETER (M)	0.11000
THICKNESS (M)	0.00700
THERMAL CONDUCTIVITY (W/M/K)	54.400
OUTSIDE WALL TEMPERATURE (K)	380.0
OVERALL CONDUCTIVITY (W/M/K)	8258.1

>>>> COMPUTATIONAL PARAMETERS

MAXIMUM # OF ITERATIONS	-	20
OUTPUT AT ITERATION #	-	6
TCALL	-	1.00
TPRINT	-	6.00
TSCREEN	-	100.00
CIINTG	-	0.000100
CCINTG	-	0.000100
CBINTG	-	0.000010
CEINTG	-	0.000100
AREROT	-	0.000010
REL	-	0.000010
MAXERR	-	0.000100
MAXTRY	-	100

>>>> OUTPUT DATA

>>>> ENGINE CRANK-ANGLE BY CRANK-ANGLE RESULTS

>>>> START OF INTAKE PROCESS

CA (DEG)	P (ATM)	TEMP (K)	MIN (G)	MEX (G)	PHI (-)	PIM (ATM)	TIM (K)	PEM (ATM)	TEM (K)	IFG (-)
-11.0	3.5908	855.31	0.00000	0.00000	0.49290	2.5293	321.74	3.2437	885.50	2
-6.0	3.4289	845.51	-0.00715	0.02977	0.49290	2.5359	322.12	3.1971	881.67	2
0.0	2.9973	817.93	-0.03618	0.03602	0.49289	2.5575	323.76	3.1351	876.74	2
6.0	2.5767	787.81	-0.06214	0.02487	0.49266	2.5799	325.41	3.0719	871.73	2
12.0	2.5242	723.19	-0.02527	0.01848	0.41950	2.5807	325.30	3.0165	867.19	2
18.0	2.4690	630.99	0.05817	0.01745	0.31506	2.5771	325.01	2.9678	863.07	2
24.0	2.4370	556.17	0.18167	0.01745	0.23083	2.5713	324.65	2.9235	859.22	2
30.0	2.4178	504.01	0.33976	0.01745	0.17268	2.5655	324.29	2.8869	856.07	2
36.0	2.4061	468.61	0.52873	0.01745	0.13330	2.5591	323.91	2.8710	855.16	2
42.0	2.3921	444.02	0.74278	0.01745	0.10640	2.5530	323.55	2.8820	857.19	2
48.0	2.3785	426.36	0.97893	0.01745	0.08739	2.5474	323.21	2.9204	862.07	2
54.0	2.3625	413.30	1.23139	0.01745	0.07365	2.5433	322.93	2.9753	868.31	2
60.0	2.3493	403.50	1.49843	0.01745	0.06338	2.5426	322.79	3.0373	874.70	2
66.0	2.3397	396.05	1.77682	0.01745	0.05551	2.5424	322.70	3.1067	881.10	2
72.0	2.3327	390.35	2.06247	0.01745	0.04937	2.5415	322.61	3.1821	887.17	2
78.0	2.3292	386.02	2.35223	0.01745	0.04451	2.5397	322.48	3.2514	891.88	2
84.0	2.3288	382.74	2.64291	0.01745	0.04059	2.5369	322.31	3.3014	894.42	2
90.0	2.3313	380.27	2.93167	0.01745	0.03740	2.5336	322.11	3.3248	894.77	2
96.0	2.3365	378.44	3.21590	0.01745	0.03476	2.5303	321.90	3.3196	893.14	2
102.0	2.3449	377.13	3.49380	0.01745	0.03256	2.5289	321.75	3.2899	890.02	2
108.0	2.3566	376.28	3.76392	0.01745	0.03071	2.5295	321.69	3.2459	886.09	2
114.0	2.3718	375.82	4.02489	0.01745	0.02914	2.5337	321.84	3.1936	881.72	2
120.0	2.3934	375.82	4.27945	0.01745	0.02779	2.5523	323.22	3.1344	876.95	2
126.0	2.4239	376.37	4.53075	0.01745	0.02664	2.5771	325.12	3.0706	871.93	2
132.0	2.4565	377.17	4.76754	0.01745	0.02569	2.5830	325.39	3.0140	867.33	2
138.0	2.4821	377.92	4.97398	0.01745	0.02493	2.5790	325.10	2.9651	863.19	2
144.0	2.5010	378.61	5.14775	0.01745	0.02433	2.5722	324.70	2.9208	859.35	2
150.0	2.5134	379.28	5.28733	0.01745	0.02388	2.5654	324.30	2.8821	855.97	2
156.0	2.5215	379.98	5.39544	0.01745	0.02354	2.5579	323.88	2.8637	854.78	2
162.0	2.5269	380.77	5.47409	0.01745	0.02330	2.5511	323.50	2.8710	856.41	2
168.0	2.5318	381.71	5.52699	0.01745	0.02314	2.5450	323.14	2.9053	860.91	2
174.0	2.5372	382.83	5.55574	0.01745	0.02305	2.5402	322.83	2.9587	867.07	2
180.0	2.5401	384.05	5.55517	0.01745	0.02304	2.5382	322.64	3.0202	873.52	2
186.0	2.5492	385.51	5.54272	0.01745	0.02304	2.5380	322.55	3.0903	880.06	2
192.0	2.5697	387.41	5.52707	0.01745	0.02304	2.5371	322.46	3.1660	886.28	2
198.0	2.6048	389.88	5.51277	0.01745	0.02304	2.5355	322.35	3.2371	891.29	2
204.0	2.6571	393.01	5.50223	0.01745	0.02304	2.5330	322.20	3.2936	894.46	2
210.0	2.7291	396.88	5.49694	0.01745	0.02304	2.5298	322.01	3.3189	894.94	2

>>>> START OF COMPRESSION PROCESS

CA (DEG)	P (ATM)	TEMP (K)	PHI (-)	PIM (ATM)	TIM (K)	PEM (ATM)	TEM (K)	IFG (-)
216.0	2.8118	399.94	0.02304	2.5266	321.79	3.3120	893.20	2
222.0	2.9102	402.99	0.02304	2.5251	321.65	3.2832	890.13	2
228.0	3.0328	406.87	0.02304	2.5260	321.59	3.2374	886.08	2
234.0	3.1838	411.66	0.02304	2.5315	321.85	3.1837	881.61	2
240.0	3.3686	417.46	0.02304	2.5515	323.36	3.1238	876.79	2
246.0	3.5943	424.36	0.02304	2.5749	325.11	3.0609	871.80	2
252.0	3.8700	432.50	0.02304	2.5777	325.14	3.0055	867.25	2
258.0	4.2079	442.03	0.02304	2.5735	324.84	2.9572	863.14	2
264.0	4.6240	453.12	0.02304	2.5670	324.45	2.9133	859.31	2
270.0	5.1400	466.00	0.02304	2.5606	324.07	2.8765	856.11	2
276.0	5.7851	480.92	0.02304	2.5534	323.67	2.8600	855.10	2
282.0	6.5998	498.17	0.02304	2.5468	323.29	2.8695	856.97	2
288.0	7.6445	518.42	0.02304	2.5410	322.95	2.9072	861.78	2
294.0	8.9948	541.75	0.02304	2.5367	322.66	2.9626	868.10	2
300.0	10.7624	568.55	0.02304	2.5352	322.50	3.0251	874.55	2
306.0	13.1103	599.38	0.02304	2.5348	322.40	3.0955	881.05	2
312.0	16.2744	634.84	0.02304	2.5339	322.31	3.1716	887.19	2
318.0	20.5951	675.57	0.02304	2.5318	322.18	3.2407	891.87	2
324.0	26.5493	722.10	0.02304	2.5289	322.01	3.2910	894.42	2
330.0	34.7536	774.62	0.02304	2.5256	321.81	3.3136	894.70	2
336.0	45.8477	832.31	0.02304	2.5223	321.60	3.3079	893.05	2
342.0	60.0423	892.30	0.02304	2.5210	321.47	3.2779	889.91	2

>>>> START OF COMBUSTION AND EXPANSION PROCESSES

CA (DEG)	P (ATM)	TEMP (K)	PHI (-)	PIM (ATM)	TIM (K)	PEM (ATM)	TEM (K)	IFG (-)
348.0	88.4896	1100.30	0.07019	2.5222	321.43	3.2304	885.76	2
354.0	113.3955	1243.25	0.10400	2.5290	321.79	3.1762	881.26	2
360.0	136.4043	1424.32	0.16194	2.5506	323.44	3.1152	876.37	2
366.0	147.1637	1600.37	0.23503	2.5726	325.07	3.0530	871.41	2
372.0	141.5676	1734.20	0.31036	2.5729	324.94	2.9987	866.92	2
378.0	124.3830	1808.53	0.37619	2.5683	324.62	2.9510	862.85	2
384.0	103.0607	1824.76	0.42574	2.5618	324.23	2.9076	859.04	2
390.0	82.7548	1795.42	0.45810	2.5553	323.86	2.8725	856.02	2
396.0	65.6851	1737.05	0.47648	2.5483	323.46	2.8593	855.38	2
402.0	52.2328	1664.96	0.48558	2.5419	323.09	2.8723	857.61	2
408.0	41.9627	1590.28	0.48949	2.5361	322.75	2.9127	862.68	2
414.0	34.2120	1519.43	0.49095	2.5319	322.48	2.9687	869.00	2
420.0	28.3563	1455.16	0.49143	2.5309	322.33	3.0314	875.41	2
426.0	23.8953	1398.03	0.49156	2.5306	322.25	3.1031	881.93	2
432.0	20.4572	1347.65	0.49160	2.5296	322.16	3.1789	887.94	2
438.0	17.7742	1303.27	0.49160	2.5275	322.03	3.2472	892.50	2
444.0	15.6553	1264.19	0.49160	2.5246	321.86	3.2944	894.77	2
450.0	13.9637	1229.70	0.49160	2.5213	321.67	3.3158	894.97	2
456.0	12.6005	1199.44	0.49160	2.5183	321.47	3.3072	893.10	2
462.0	11.4929	1172.77	0.49160	2.5171	321.34	3.2772	889.96	2
468.0	10.5871	1149.34	0.49160	2.5183	321.30	3.2303	885.85	2
474.0	9.8426	1128.83	0.49160	2.5249	321.65	3.1763	881.36	2
480.0	9.2287	1110.95	0.49160	2.5464	323.29	3.1157	876.49	2
486.0	8.7217	1095.45	0.49160	2.5690	324.97	3.0533	871.52	2
492.0	8.3035	1082.10	0.49160	2.5696	324.86	2.9988	867.02	2
498.0	7.9601	1070.73	0.49160	2.5650	324.54	2.9511	862.94	2
504.0	7.6804	1061.20	0.49160	2.5584	324.15	2.9076	859.13	2

>>>> START OF EXHAUST PROCESS

CA (DEG)	P (ATM)	TEMP (K)	MEX (G)	PHI (-)	PIM (ATM)	TIM (K)	PEM (ATM)	TEM (K)	IFG (-)
510.0	7.4362	1052.68	0.02955	0.49160	2.5516	323.77	2.8700	855.84	2
516.0	7.1695	1043.14	0.08611	0.49160	2.5447	323.38	2.8552	855.01	2
522.0	6.8554	1031.49	0.20208	0.49160	2.5383	323.01	2.8673	857.13	2
528.0	6.4830	1017.04	0.38436	0.49160	2.5328	322.68	2.9048	861.89	2
534.0	6.0842	1000.74	0.61222	0.49160	2.5285	322.40	2.9593	868.09	2
540.0	5.6802	983.29	0.86996	0.49160	2.5273	322.25	3.0205	874.43	2
546.0	5.2590	964.03	1.16352	0.49160	2.5270	322.16	3.0901	880.86	2
552.0	4.8271	942.98	1.48645	0.49160	2.5262	322.08	3.1659	886.99	2
558.0	4.4137	921.41	1.81565	0.49160	2.5243	321.96	3.2367	891.85	2
564.0	4.0513	901.13	2.12479	0.49160	2.5214	321.80	3.2915	894.78	2
570.0	3.7706	884.34	2.38854	0.49160	2.5182	321.60	3.3193	895.40	2
576.0	3.5771	872.03	2.60064	0.49160	2.5150	321.40	3.3190	894.02	2
582.0	3.4594	864.03	2.76896	0.49160	2.5136	321.26	3.2933	891.07	2
588.0	3.3882	858.83	2.91466	0.49160	2.5145	321.22	3.2494	887.09	2
594.0	3.3374	854.85	3.05634	0.49160	2.5197	321.45	3.1958	882.57	2
600.0	3.2941	851.27	3.20264	0.49160	2.5370	322.71	3.1375	877.80	2
606.0	3.2517	847.70	3.35700	0.49160	2.5618	324.62	3.0740	872.74	2
612.0	3.2096	844.09	3.51883	0.49160	2.5709	325.14	3.0165	868.03	2
618.0	3.1713	840.68	3.68499	0.49160	2.5671	324.84	2.9670	863.80	2
624.0	3.1369	837.50	3.85430	0.49160	2.5611	324.47	2.9220	859.86	2
630.0	3.1053	834.49	4.02613	0.49160	2.5547	324.10	2.8821	856.32	2
636.0	3.0799	831.87	4.19756	0.49160	2.5472	323.68	2.8611	854.79	2
642.0	3.0709	830.37	4.36332	0.49160	2.5405	323.30	2.8666	856.17	2
648.0	3.0849	830.42	4.52101	0.49160	2.5349	322.96	2.8987	860.36	2
654.0	3.1262	832.28	4.66985	0.49160	2.5303	322.67	2.9533	866.59	2
660.0	3.1885	835.47	4.81247	0.49160	2.5287	322.49	3.0148	872.98	2
666.0	3.2637	839.41	4.95064	0.49160	2.5286	322.41	3.0854	879.51	2
672.0	3.3557	844.29	5.08222	0.49160	2.5279	322.33	3.1614	885.69	2
678.0	3.4590	849.73	5.20683	0.49160	2.5262	322.21	3.2334	890.76	2
684.0	3.5642	855.14	5.32362	0.49160	2.5238	322.07	3.2924	894.08	2
690.0	3.6554	859.60	5.43125	0.49160	2.5208	321.89	3.3260	895.15	2
696.0	3.6898	860.78	5.52951	0.49160	2.5176	321.68	3.3290	893.99	2
702.0	3.6492	857.76	5.61399	0.49160	2.5160	321.53	3.3038	891.07	2
708.0	3.6055	854.68	5.67551	0.49160	2.5170	321.48	3.2586	887.00	2

>>>>PRESSURE DATA	(ATM)	(IN-HG)
COMPRESSOR INLET	0.9378000	28.06017
COMPRESSOR DISCHARGE	2.569204	76.87384
INTAKE MANIFOLD	2.542093	76.06265
EXHAUST MANIFOLD	3.086776	92.36026
TURBINE INLET	3.070631	91.87719
TURBINE DISCHARGE	1.539789	46.07243
POWER TURBINE INLET	1.526774	45.68301
P. TURBINE DISCHARGE	0.9871462	29.53667
DELTA P ENGINE	-0.5446831	-16.29761

>>>>TEMPERATURE DATA	(K)	(F)
COMPRESSOR INLET	302.6000	84.99200
COMPRESSOR DISCHARGE	428.8837	312.3027
INTERCOOLER OUTLET	317.8910	112.5158
INTAKE MANIFOLD	322.9528	121.6270
ENGINE EXHAUST	894.9536	1151.229
EXHAUST MANIFOLD	875.5369	1116.278
TURBINE INLET	875.5369	1116.278
TURBINE EXHAUST	769.8907	926.1153
POWER TURBINE INLET	758.5132	905.6357
P. TURBINE EXHAUST	697.6116	796.0129

>>>TURBOCHARGER DATA	COMPRESSOR	TURBINE	P.TURBINE
MAP FLOW (LB/MIN)	71.78577	22.32654	41.77164
MAP SPEED (KRPM)	64.61178	66.26661	35.64872
PRESSURE RATIOS:	2.739607	1.994190	1.546654
EFFICIENCIES:	0.7903797	0.7759525	0.7933508

>>>> INTERCOOLER DATA

INTERCOOLER EFFECTIVENESS:	0.8959758
COOLANT INLET TEMPERATURE:	305.0000
INTERCOOLER "A+U" (W/K)	1200.000

>>>> DIESEL ENGINE PERFORMANCE RESULTS

VOLUMETRIC EFFICIENCY; (%) BASED ON: INTAKE / ATM	85.2	216.0
PUMPING MEAN EFF. PRESSURE (ATM, PSI) : PMEP	-0.95	-14.00
GROSS IND. MEAN EFF. PRESSURE (ATM, PSI) : IMEP	16.64	244.50
FRICITION MEAN EFF. PRESSURE (ATM, PSI) : FMEP	1.65	24.32
BRAKE MEAN EFF. PRESSURE (ATM, PSI) : BMEP	14.03	206.18
GROSS INDICATED S.F.C. (G/KW/HR, LB/HP/HR) : ISFC	171.774	0.282
BRAKE S.F.C. (G/KW/HR, LB/HP/HR) : BSFC	203.701	0.335
GROSS INDICATED THERMAL EFFICIENCY; (%)	48.8	
NET INDICATED THERMAL EFFICIENCY; (%)	46.0	
CYLINDER BRAKE THERMAL EFFICIENCY; (%)	41.2	
(CYL. HEAT TRANSFER PER CYCLE)/ (MASS OF FUEL TIMES LHV) : (%)	7.6	
MEAN EXHAUST TEMPERATURE; (K)	895.0	

>>>> TOTAL SYSTEM PERFORMANCE RESULTS

DIESEL WORK PER CYCLE; (KJ)	19.924524	
POWER TURBINE WORK PER CYCLE (KJ)	2.145280	
TOTAL HEAT INPUT PER CYCLE (KJ)	48.376740	
DIESEL BRAKE POWER (KW, HP) : ENBHP	315.8	423.5
POWER TRB. BRAKE POWER (KW, HP) : PTBHP	34.0	45.6
OVERALL BRAKE S.F.C. (G/KW/HR, LB/HP/HR) : BSFC	183.900	0.302
OVERALL BRAKE THERMAL EFFICIENCY; (%)	45.6	

>>>> CYLINDER MASS SUMMARY

MASS IN CYLINDER AT TIVO = 0.29577 G
MASS IN CYLINDER AT TIVC = 5.77489 G
MASS OF AIR INDUCTED = 5.49657 G
MASS OF FUEL INJECTED = 0.18790 G

>>>> CYLINDER HEAT & WORK TRANSFERS

HEATI = -0.214500 KJ (TIVO - 180)
WORKI = 0.555942 KJ

HEATC = -0.092183 KJ (180 - TIGN)
WORKC = -2.352692 KJ

HEATCE = 0.746053 KJ (180 - 540)
WORKCE = 3.937970 KJ

HEATE = 0.081218 KJ (540 - TIVO)
WORKE = -0.781500 KJ

>>>> CYLINDER ENERGY BALANCE

INITIAL ENTHALPY /CYL / CYCLE = -0.15833 KJ
TOTAL ENTHALPY IN /CYL/ CYCLE = 1.69891 KJ
TOTAL ENTHALPY OUT/CYL/ CYCLE = -2.74756 KJ
TOTAL HEAT LOSS / CYL / CYCLE = 0.61277 KJ
IND. WORK OUTPUT / CYL /CYCLE = 3.71241 KJ
BRAKE WORK OUTPUT /CYL /CYCLE = 3.32075 KJ
RESIDUAL ENTHALPY /CYL/ CYCLE = -0.15818 KJ
NET ENERGY GAIN / CYL/CYCLE = -0.12115 KJ
(ENERGY GAIN)/(H @ IVC) = -7.86360 %
(ENERGY GAIN)/(MFUEL*LHV) = -1.50252 %

>>>> COMBUSTION SUMMARY

IGNITION DELAY PERIOD = 4.000 DEG CA
IGNITION TIMING = 342.000 DEG CA
BURN DURATION = 125.000 DEG CA
WEIGHTING FACTOR = 0.081
PREMIXED CONSTANT 1 = 2.075
PREMIXED CONSTANT 2 = 5000.000
DIFFUSION CONSTANT 1 = 23.137
DIFFUSION CONSTANT 2 = 2.303
CFACTR = 1.050

M.I.T. TURBOCOMPOUND DIESEL ENGINE CYCLE SIMULATION

>>>> INPUT DATA

>>>> OPERATING MODE

SPECIFIED IGNITION DELAY OPTION

PREDICTED TRANSIENT WALL TEMPERATURES

FLAME RADIATION MODEL

>>>> OPERATING CONDITIONS

FUEL USED IS DIESEL #2

ENGINE SPEED	=	1901.9 RPM
INJECTION TIMING	=	338.0 DEG CA
FUEL INJECTED /CYL /CYCLE	=	0.1879 G
TOTAL FUELING RATE	=	2.3614 LB/MIN
COMPRESSOR INLET PRESSURE	=	0.9378 ATM
COMPRESSOR INLET TEMPERATURE	=	302.60 K
ATMOSPHERIC PRESSURE	=	0.9378 ATM
ATMOSPHERIC TEMPERATURE	=	302.60 K

>>>> ENGINE DESIGN PARAMETERS

NUMBER OF CYLINDERS = 6
 CYLINDER BORE = 13.970 CM
 CRANKSHAFT STROKE = 15.240 CM
 CONNECTING ROD LENGTH = 30.480 CM
 COMPRESSION RATIO = 14.500
 DISPLACED VOLUME = 2335.974 CC
 CLEARANCE VOLUME = 173.035 CC
 ENGINE DISPLACEMENT = 14.016 LT
 FRICTION CONSTANT 2 = 7.000
 FRICTION CONSTANT 3 = 1.500
 INTAKE VALVE OPENS = -11.0 DEG CA
 INTAKE VALVE CLOSES = 212.0 DEG CA
 EXHAUST VALVE OPENS = 505.0 DEG CA
 EXHAUST VALVE CLOSES = 736.0 DEG CA

>>>> MANIFOLD DIMENSIONS		INTAKE	EXHAUST
LENGTH	(M)	0.7000000	1.000000
DIAMETER	(M)	0.1000000	0.1000000
CROSS-SECTIONAL AREA	(M**2)	7.8539820E-03	7.8539820E-03
INTERNAL SURFACE AREA	(M**2)	0.2199115	0.3141593
VOLUME	(LT)	5.497787	7.853982

>>>> TURBINE CONNECTING PIPE DIMENSIONS

LENGTH (M) 0.5000000
 DIAMETER (M) 0.1300000
 CROSS-SECTIONAL AREA (M**2) 1.3273228E-02
 INTERNAL SURFACE AREA (M**2) 0.2042035
 VOLUME (LT) 6.636614

>>>> TURBOMACHINERY DATA

T/C INERTIA (KG-M**2) 3.9999999E-05
T/C DAMPING (KG-M**2/S) 5.0000000E-07
P.TURBINE TRANSMISSION EFFIC. 0.9000000
P.TURBINE GEAR RATIO 1.7000001E-02

>>>> SYSTEM PRESSURE DROPS IN PA

COMPRESSOR EXIT - INTERCOOLER INLET 2000.000
INTERCOOLER INLET - INTAKE MANIFOLD 746.9940
EXHAUST MANIFOLD - TURBINE INLET 1635.860
TURBINE EXIT - POWER TURBINE INLET 1318.737
POWER TURBINE EXIT - ATMOSPHERIC 5000.000

>>>>> HEAT TRANSFER AND TURBULENCE PARAMETERS

HEAT TRANSFER CONSTANT(CHAMBER)= 0.0550
HEAT TRANSFER CONSTANT(INT MAN)= 0.0350
HEAT TRANSFER CONSTANT(EXH MAN)= 0.0350
HEAT TRANSFER CONSTANT(C. PIPE)= 0.0350
HEAT TRANSFER EXPONENT = 0.8000
PISTON TEMPERATURE = 799.34 K
CYLINDER HEAD TEMPERATURE = 799.34 K
CYLINDER WALL TEMPERATURE = 435.39 K
INT. MANIFOLD WALL TEMPERATURE = 305.00 K
EXH. MANIFOLD WALL TEMPERATURE = 750.00 K
CONN. PIPE WALL TEMPERATURE = 600.00 K
TURBULENT DISSIPATION CONSTANT = 1.5000

>>>> WALL CONDUCTION MODELS

>>>> PISTON WALL STRUCTURE

LAYER	1	2	3
THICKNESS (M)	0.00150	0.00700	0.00300
THERMAL CONDUCTIVITY (W/M/K)	0.600	54.400	54.400
THERMAL DIFFUSIVITY (M2/SEC)	0.550E-06	0.157E-04	0.157E-04
NUMBER OF NODES	15	5	5
NODES WITHIN SKIN DEPTH	9		
COURANT NUMBER	238.179	2225.950	408.848
OUTSIDE WALL TEMPERATURE (K)	380.0		
OVERALL CONDUCTIVITY (W/M/K)	372.6		

>>>> CYL. HEAD WALL STRUCTURE

LAYER	1	2	3
THICKNESS (M)	0.00150	0.00700	0.00300
THERMAL CONDUCTIVITY (W/M/K)	0.600	54.400	54.400
THERMAL DIFFUSIVITY (M2/SEC)	0.550E-06	0.157E-04	0.157E-04
NUMBER OF NODES	15	5	5
NODES WITHIN SKIN DEPTH	9		
COURANT NUMBER	238.179	2225.950	408.848
OUTSIDE WALL TEMPERATURE (K)	380.0		
OVERALL CONDUCTIVITY (W/M/K)	372.6		

>>>> CYL. LINER WALL STRUCTURE

LAYER	1		
INSIDE DIAMETER (M)	0.11000		
THICKNESS (M)	0.00700		
THERMAL CONDUCTIVITY (W/M/K)	54.400	0.000	0.000
OUTSIDE WALL TEMPERATURE (K)	380.0		
OVERALL CONDUCTIVITY (W/M/K)	8256.1		

>>>> COMPUTATIONAL PARAMETERS

MAXIMUM # OF ITERATIONS	=	20
OUTPUT AT ITERATION #	=	7
TCALL	=	1.00
TPRINT	=	6.00
TSCREN	=	100.00
CIINTG	=	0.000100
CCINTG	=	0.000100
CBINTG	=	0.000010
CEINTG	=	0.000100
AREROT	=	0.000010
REL	=	0.000010
MAXERR	=	0.000100
MAXTRY	=	100

>>>> OUTPUT DATA

>>>> ENGINE CRANK-ANGLE BY CRANK-ANGLE RESULTS

>>>> START OF INTAKE PROCESS

CA (DEG)	P (ATM)	TEMP (K)	MIN (G)	MEX (G)	PHI (-)	PIM (ATM)	TIM (K)	PEM (ATM)	TEM (K)	IFG (-)
-11.0	3.5978	854.16	0.00000	0.00000	0.49160	2.5174	321.49	3.2500	886.27	2
-6.0	3.4354	844.35	-0.00720	0.02984	0.49160	2.5242	321.87	3.2034	882.39	2
0.0	3.0003	816.61	-0.03656	0.03603	0.49161	2.5459	323.53	3.1413	877.39	2
6.0	2.5698	785.53	-0.06317	0.02477	0.49123	2.5689	325.23	3.0772	872.28	2
12.0	2.5135	721.29	-0.02683	0.01831	0.41909	2.5703	325.17	3.0210	867.64	2
18.0	2.4577	629.02	0.05651	0.01726	0.31476	2.5660	324.86	2.9717	863.43	2
24.0	2.4249	554.09	0.17994	0.01726	0.23060	2.5599	324.48	2.9268	859.49	2
30.0	2.4053	501.80	0.33809	0.01726	0.17246	2.5536	324.11	2.8900	856.29	2
36.0	2.3928	466.32	0.52706	0.01726	0.13314	2.5469	323.72	2.8741	855.34	2
42.0	2.3786	441.63	0.74132	0.01726	0.10626	2.5406	323.36	2.8852	857.34	2
48.0	2.3647	423.89	0.97774	0.01726	0.08727	2.5350	323.02	2.9241	862.19	2
54.0	2.3487	410.76	1.23065	0.01726	0.07356	2.5310	322.74	2.9794	868.38	2
60.0	2.3347	400.88	1.49775	0.01726	0.06331	2.5292	322.56	3.0400	874.59	2
66.0	2.3247	393.37	1.77642	0.01726	0.05546	2.5293	322.49	3.1095	880.92	2
72.0	2.3176	387.61	2.06260	0.01726	0.04933	2.5286	322.41	3.1845	886.91	2
78.0	2.3140	383.21	2.35301	0.01726	0.04447	2.5268	322.29	3.2545	891.67	2
84.0	2.3135	379.87	2.64453	0.01726	0.04056	2.5243	322.14	3.3109	894.75	2
90.0	2.3160	377.33	2.93438	0.01726	0.03737	2.5213	321.96	3.3417	895.59	2
96.0	2.3213	375.43	3.21988	0.01726	0.03474	2.5181	321.75	3.3418	894.23	2
102.0	2.3296	374.04	3.49904	0.01726	0.03254	2.5165	321.60	3.3166	891.31	2
108.0	2.3412	373.10	3.77050	0.01726	0.03069	2.5170	321.54	3.2729	887.34	2
114.0	2.3561	372.55	4.03260	0.01726	0.02912	2.5198	321.58	3.2208	882.94	2
120.0	2.3764	372.43	4.28717	0.01726	0.02777	2.5370	322.83	3.1616	878.14	2
126.0	2.4063	372.88	4.53935	0.01726	0.02662	2.5620	324.73	3.0962	872.97	2
132.0	2.4380	373.57	4.77672	0.01726	0.02567	2.5666	324.92	3.0385	868.25	2
138.0	2.4633	374.21	4.98471	0.01726	0.02490	2.5627	324.63	2.9882	863.98	2
144.0	2.4823	374.80	5.16076	0.01726	0.02429	2.5564	324.26	2.9425	859.99	2
150.0	2.4950	375.36	5.30317	0.01726	0.02382	2.5497	323.87	2.9013	856.36	2
156.0	2.5034	375.94	5.41399	0.01726	0.02348	2.5422	323.47	2.8803	854.87	2
162.0	2.5090	376.60	5.49538	0.01726	0.02323	2.5354	323.09	2.8846	856.17	2
168.0	2.5140	377.40	5.55085	0.01726	0.02306	2.5292	322.74	2.9203	860.75	2
174.0	2.5198	378.39	5.58273	0.01726	0.02296	2.5243	322.44	2.9753	866.98	2
180.0	2.5235	379.48	5.58584	0.01726	0.02295	2.5218	322.23	3.0362	873.26	2
186.0	2.5319	380.77	5.57411	0.01726	0.02295	2.5220	322.17	3.1059	879.68	2
192.0	2.5516	382.50	5.55916	0.01726	0.02295	2.5214	322.09	3.1812	885.76	2
198.0	2.5857	384.79	5.54532	0.01726	0.02295	2.5202	321.99	3.2524	890.74	2
204.0	2.6368	387.73	5.53500	0.01726	0.02295	2.5181	321.87	3.3105	894.06	2
210.0	2.7073	391.40	5.52981	0.01726	0.02295	2.5154	321.70	3.3383	894.71	2

>>>> START OF COMPRESSION PROCESS

CA (DEG)	P (ATM)	TEMP (K)	PHI (-)	PIM (ATM)	TIM (K)	PEM (ATM)	TEM (K)	IFG (-)
216.0	2.7897	394.48	0.02295	2.5125	321.51	3.3347	893.14	2
222.0	2.8885	397.64	0.02295	2.5114	321.38	3.3091	890.22	2
228.0	3.0114	401.63	0.02295	2.5123	321.34	3.2649	886.25	2
234.0	3.1626	406.53	0.02295	2.5177	321.56	3.2114	881.78	2
240.0	3.3476	412.42	0.02295	2.5374	323.02	3.1514	876.93	2
246.0	3.5734	419.42	0.02295	2.5624	324.91	3.0867	871.82	2
252.0	3.8492	427.65	0.02295	2.5665	325.05	3.0296	867.15	2
258.0	4.1872	437.27	0.02295	2.5625	324.76	2.9799	862.94	2
264.0	4.6034	448.46	0.02295	2.5561	324.38	2.9346	859.00	2
270.0	5.1197	461.44	0.02295	2.5500	324.01	2.8971	855.76	2
276.0	5.7652	476.45	0.02295	2.5432	323.63	2.8800	854.69	2
282.0	6.5807	493.82	0.02295	2.5368	323.26	2.8889	856.49	2
288.0	7.6265	514.17	0.02295	2.5311	322.92	2.9270	861.29	2
294.0	8.9797	537.67	0.02295	2.5263	322.63	2.9823	867.51	2
300.0	10.7522	564.68	0.02295	2.5248	322.46	3.0438	873.81	2
306.0	13.1077	595.75	0.02295	2.5249	322.39	3.1146	880.24	2
312.0	16.2844	631.50	0.02295	2.5242	322.30	3.1898	886.21	2
318.0	20.6255	672.60	0.02295	2.5224	322.18	3.2587	890.90	2
324.0	26.6125	719.58	0.02295	2.5198	322.02	3.3100	893.55	2
330.0	34.8691	772.64	0.02295	2.5167	321.83	3.3355	894.05	2
336.0	46.0437	830.97	0.02295	2.5139	321.64	3.3312	892.46	2
342.0	60.3532	891.75	0.02295	2.5130	321.52	3.3021	889.34	2

>>>> START OF COMBUSTION AND EXPANSION PROCESSES

CA (DEG)	P (ATM)	TEMP (K)	PHI (-)	PIM (ATM)	TIM (K)	PEM (ATM)	TEM (K)	IFG (-)
348.0	89.0783	1101.09	0.07070	2.5143	321.49	3.2547	885.20	2
354.0	114.0434	1243.00	0.10421	2.5217	321.88	3.2001	880.67	2
360.0	137.0992	1423.20	0.16170	2.5443	323.59	3.1382	875.72	2
366.0	147.8772	1598.77	0.23427	2.5665	325.22	3.0747	870.68	2
372.0	142.2493	1732.46	0.30908	2.5666	325.09	3.0193	866.12	2
378.0	124.9871	1806.85	0.37444	2.5622	324.78	2.9705	861.97	2
384.0	103.5674	1823.22	0.42360	2.5558	324.40	2.9260	858.08	2
390.0	83.1680	1794.07	0.45567	2.5497	324.03	2.8901	855.01	2
396.0	66.0199	1735.95	0.47386	2.5427	323.64	2.8759	854.27	2
402.0	52.5062	1664.14	0.48284	2.5363	323.27	2.8883	856.45	2
408.0	42.1890	1589.76	0.48669	2.5305	322.93	2.9287	861.49	2
414.0	34.4025	1519.19	0.48813	2.5258	322.63	2.9845	867.74	2
420.0	28.5189	1455.17	0.48859	2.5245	322.47	3.0464	874.05	2
426.0	24.0360	1398.26	0.48872	2.5243	322.39	3.1180	880.50	2
432.0	20.5805	1348.05	0.48875	2.5235	322.30	3.1933	886.44	2
438.0	17.8835	1303.83	0.48876	2.5215	322.17	3.2612	890.98	2
444.0	15.7533	1264.86	0.48876	2.5187	322.00	3.3109	893.49	2
450.0	14.0525	1230.54	0.48876	2.5156	321.81	3.3334	893.76	2
456.0	12.6817	1200.30	0.48876	2.5128	321.61	3.3276	892.08	2
462.0	11.5679	1173.69	0.48876	2.5119	321.50	3.2988	889.00	2
468.0	10.6569	1150.33	0.48876	2.5130	321.46	3.2528	884.94	2
474.0	9.9080	1129.86	0.48876	2.5204	321.85	3.1983	880.42	2
480.0	9.2904	1112.02	0.48876	2.5427	323.54	3.1367	875.50	2
486.0	8.7805	1096.55	0.48876	2.5653	325.21	3.0733	870.47	2
492.0	8.3598	1083.23	0.48876	2.5658	325.09	3.0177	865.90	2
498.0	8.0142	1071.88	0.48876	2.5615	324.78	2.9689	861.76	2
504.0	7.7329	1062.36	0.48876	2.5550	324.40	2.9242	857.88	2

>>>> START OF EXHAUST PROCESS

CA (DEG)	P (ATM)	TEMP (K)	MEX (G)	PHI (-)	PIM (ATM)	TIM (K)	PEM (ATM)	TEM (K)	IFG (-)
510.0	7.4871	1053.85	0.02944	0.48876	2.5487	324.03	2.8858	854.53	2
516.0	7.2187	1044.33	0.08635	0.48876	2.5416	323.63	2.8705	853.68	2
522.0	6.9025	1032.69	0.20304	0.48876	2.5351	323.25	2.8818	855.76	2
528.0	6.5276	1018.25	0.38649	0.48876	2.5291	322.91	2.9207	860.69	2
534.0	6.1260	1001.95	0.61581	0.48876	2.5244	322.61	2.9759	866.98	2
540.0	5.7192	984.51	0.87517	0.48876	2.5224	322.42	3.0375	873.37	2
546.0	5.2951	965.25	1.17060	0.48876	2.5223	322.34	3.1076	879.85	2
552.0	4.8599	944.20	1.49566	0.48876	2.5216	322.25	3.1826	886.03	2
558.0	4.4433	922.61	1.82714	0.48876	2.5200	322.14	3.2547	891.12	2
564.0	4.0778	902.31	2.13849	0.48876	2.5174	321.98	3.3129	894.41	2
570.0	3.7958	885.55	2.40336	0.48876	2.5144	321.79	3.3448	895.37	2
576.0	3.6027	873.34	2.61555	0.48876	2.5113	321.60	3.3476	894.22	2
582.0	3.4868	865.53	2.78301	0.48876	2.5097	321.45	3.3246	891.46	2
588.0	3.4181	860.53	2.92758	0.48876	2.5102	321.39	3.2819	887.58	2
594.0	3.3689	856.68	3.06900	0.48876	2.5146	321.54	3.2283	883.11	2
600.0	3.3262	853.19	3.21570	0.48876	2.5326	322.85	3.1686	878.31	2
606.0	3.2831	849.60	3.37150	0.48876	2.5583	324.82	3.1035	873.20	2
612.0	3.2404	845.98	3.53469	0.48876	2.5663	325.24	3.0453	868.49	2
618.0	3.2012	842.55	3.70232	0.48876	2.5635	324.99	2.9948	864.25	2
624.0	3.1661	839.35	3.87307	0.48876	2.5573	324.62	2.9493	860.33	2
630.0	3.1341	836.33	4.04619	0.48876	2.5512	324.25	2.9103	856.97	2
636.0	3.1097	833.80	4.21834	0.48876	2.5445	323.87	2.8912	855.70	2
642.0	3.1026	832.43	4.38455	0.48876	2.5385	323.51	2.9000	857.49	2
648.0	3.1200	832.70	4.54234	0.48876	2.5326	323.16	2.9351	861.99	2
654.0	3.1636	834.69	4.69187	0.48876	2.5276	322.85	2.9891	868.12	2
660.0	3.2258	837.83	4.83600	0.48876	2.5254	322.65	3.0501	874.42	2
666.0	3.3005	841.69	4.97572	0.48876	2.5258	322.58	3.1187	880.77	2
672.0	3.3916	846.46	5.10880	0.48876	2.5255	322.51	3.1951	886.87	2
678.0	3.4947	851.83	5.23462	0.48876	2.5240	322.39	3.2660	891.68	2
684.0	3.5977	857.04	5.35277	0.48876	2.5217	322.25	3.3207	894.56	2
690.0	3.6855	861.25	5.46164	0.48876	2.5189	322.06	3.3502	895.32	2
696.0	3.7152	862.12	5.56096	0.48876	2.5160	321.87	3.3494	893.93	2
702.0	3.6694	858.78	5.64626	0.48876	2.5149	321.74	3.3221	890.93	2
708.0	3.6252	855.64	5.70804	0.48876	2.5160	321.70	3.2766	886.90	2

>>>>PRESSURE DATA	(ATM)	(IN-HG)
COMPRESSOR INLET	0.9378000	28.06017
COMPRESSOR DISCHARGE	2.560815	76.62284
INTAKE MANIFOLD	2.533640	75.80974
EXHAUST MANIFOLD	3.106366	92.94643
TURBINE INLET	3.090644	92.47601
TURBINE DISCHARGE	1.545379	46.23971
POWER TURBINE INLET	1.532325	45.84912
P. TURBINE DISCHARGE	0.9871462	29.53667
DELTA P ENGINE	-0.5727262	-17.13670

>>>>TEMPERATURE DATA	(K)	(F)
COMPRESSOR INLET	302.6000	84.99200
COMPRESSOR DISCHARGE	429.0883	312.6708
INTERCOOLER OUTLET	318.1324	112.9503
INTAKE MANIFOLD	322.9378	121.6000
ENGINE EXHAUST	839.3190	1141.086
EXHAUST MANIFOLD	875.3640	1115.967
TURBINE INLET	875.3640	1115.967
TURBINE EXHAUST	769.2676	924.9937
POWER TURBINE INLET	757.9517	904.6249
P. TURBINE EXHAUST	696.6994	794.3709

>>>TURBOCHARGER DATA	COMPRESSOR	TURBINE	P.TURBINE
MAP FLOW (LB/MIN)	72.32477	22.35425	41.93477
MAP SPEED (KRPM)	64.74531	66.41006	35.66196
PRESSURE RATIOS:	2.730662	1.999926	1.552278
EFFICIENCIES:	0.7861692	0.7763249	0.7924770

>>>> INTERCOOLER DATA

INTERCOOLER EFFECTIVENESS	0.8942004
COOLANT INLET TEMPERATURE	305.0000
INTERCOOLER "A*U" (W/K)	1200.000

>>>> DIESEL ENGINE PERFORMANCE RESULTS

VOLUMETRIC EFFICIENCY; (%) BASED ON: INTAKE / ATM	86.2	217.3
PUMPING MEAN EFF. PRESSURE (ATM, PSI) : PMEP	-1.00	-14.69
GROSS IND. MEAN EFF. PRESSURE (ATM, PSI) : IMEP	16.78	246.59
FRICITION MEAN EFF. PRESSURE (ATM, PSI) : FMEP	1.65	24.32
BRAKE MEAN EFF. PRESSURE (ATM, PSI) : BMEP	14.13	207.59
GROSS INDICATED S.F.C. (G/KW/HR, LB/HP/HR) : ISFC	170.319	0.280
BRAKE S.F.C. (G/KW/HR, LB/HP/HR) : BSFC	202.321	0.333
GROSS INDICATED THERMAL EFFICIENCY; (%)	49.3	
NET INDICATED THERMAL EFFICIENCY; (%)	46.3	
CYLINDER BRAKE THERMAL EFFICIENCY; (%)	41.5	
(CYL. HEAT TRANSFER PER CYCLE)/ (MASS OF FUEL TIMES LHV) : (%)	7.7	
MEAN EXHAUST TEMPERATURE; (K)	889.3	

>>>> TOTAL SYSTEM PERFORMANCE RESULTS

DIESEL WORK PER CYCLE; (KJ)	20.060429	
POWER TURBINE WORK PER CYCLE (KJ)	2.173448	
TOTAL HEAT INPUT PER CYCLE (KJ)	48.376740	
DIESEL BRAKE POWER (KW, HP) : ENBHP	317.9	426.4
POWER TRB. BRAKE POWER (KW, HP) : PTBHP	34.4	46.2
OVERALL BRAKE S.F.C. (G/KW/HR, LB/HP/HR) : BSFC	182.543	0.300
OVERALL BRAKE THERMAL EFFICIENCY; (%)	46.0	

>>>> CYLINDER MASS SUMMARY

MASS IN CYLINDER AT TIVO = 0.29675 G
MASS IN CYLINDER AT TIVC = 5.80892 G
MASS OF AIR INDUCTED = 5.52944 G
MASS OF FUEL INJECTED = 0.18790 G

>>>> CYLINDER HEAT & WORK TRANSFERS

HEATI = -0.191397 KJ (TIVO - 180)
WORKI = 0.552331 KJ

HEATC = -0.055231 KJ (180 - TIGN)
WORKC = -2.353111 KJ

HEATCE = 0.734155 KJ (180 - 540)
WORKCE = 3.971812 KJ

HEATE = 0.080419 KJ (540 - TIVO)
WORKE = -0.788881 KJ

>>>> CYLINDER ENERGY BALANCE

INITIAL ENTHALPY /CYL / CYCLE = -0.15818 KJ
TOTAL ENTHALPY IN /CYL/ CYCLE = 1.71209 KJ
TOTAL ENTHALPY OUT/CYL/ CYCLE = -2.70709 KJ
TOTAL HEAT LOSS / CYL / CYCLE = 0.62318 KJ
IND. WORK OUTPUT / CYL /CYCLE = 3.73506 KJ
BRAKE WORK OUTPUT /CYL /CYCLE = 3.34340 KJ
RESIDUAL ENTHALPY /CYL/ CYCLE = -0.15615 KJ
NET ENERGY GAIN / CYL/CYCLE = -0.05891 KJ
(ENERGY GAIN)/(H * IVC) = -3.79137 %
(ENERGY GAIN)/(MFUEL*LHV) = -0.73070 %

>>>> COMBUSTION SUMMARY

IGNITION DELAY PERIOD = 4.000 DEG CA
IGNITION TIMING = 342.000 DEG CA
BURN DURATION = 125.000 DEG CA
WEIGHTING FACTOR = 0.083
PREMIXED CONSTANT 1 = 2.075
PREMIXED CONSTANT 2 = 5000.000
DIFFUSION CONSTANT 1 = 23.225
DIFFUSION CONSTANT 2 = 2.305
CFACTR = 1.050

>>>> TURBULENT FLOW MODEL

>>>> START OF INTAKE PROCESS

CA (DEG)	MEANKE (J)	TURBKE (J)	VIV (M/SEC)	VEV (M/SEC)	VMKE (M/SEC)	UPRIME (M/SEC)	CVHTRN (M/SEC)
-6.0	0.00045	0.00147	-299.704	170.840	1.867	1.939	2.857
0.0	0.01884	0.00131	-242.490	-147.273	13.103	1.979	13.252
6.0	0.25493	0.01527	26.959	-260.518	51.284	7.792	51.883
12.0	0.41080	0.10612	65.497	-260.686	56.983	17.231	59.566
18.0	0.50819	0.22015	88.143	0.000	55.147	21.074	59.112
24.0	0.78899	0.34799	96.649	0.000	58.744	22.513	63.026
30.0	1.22489	0.52604	101.103	0.000	63.273	23.928	67.808
36.0	1.76677	0.75850	102.803	0.000	66.232	25.057	71.018
42.0	2.39979	1.03619	105.394	0.000	68.705	26.067	73.734
48.0	3.13252	1.35436	107.763	0.000	70.598	26.801	75.802
54.0	3.97121	1.71037	111.707	0.000	72.820	27.577	78.191
60.0	4.92640	2.10521	115.158	0.000	74.839	28.221	80.331
66.0	5.98469	2.53994	117.273	0.000	76.362	28.720	81.943
72.0	7.09244	3.01482	118.909	0.000	77.915	29.348	83.623
78.0	8.12077	3.55972	119.312	0.000	78.578	30.123	84.516
84.0	8.99669	4.16356	118.408	0.000	78.216	31.101	84.524
90.0	9.68702	4.79733	117.275	0.000	77.532	31.611	84.070
96.0	10.17182	5.42898	115.218	0.000	76.229	32.166	83.062
102.0	10.45377	6.02740	111.900	0.000	73.906	32.689	81.110
108.0	10.55255	6.56692	108.965	0.000	71.848	32.902	79.297
114.0	10.48410	7.02875	104.953	0.000	68.957	32.956	76.668
120.0	10.31825	7.40193	104.802	0.000	67.186	32.869	75.014
126.0	10.15778	7.69436	101.997	0.000	64.459	32.565	72.399
132.0	9.84115	7.91027	93.117	0.000	62.092	32.257	70.123
138.0	9.26126	8.02989	81.478	0.000	58.750	31.810	66.930
144.0	8.51082	8.04008	70.051	0.000	55.102	31.255	63.440
150.0	7.68465	7.94384	62.439	0.000	52.435	30.794	60.881
156.0	6.85794	7.75565	52.151	0.000	48.798	30.075	57.369
162.0	6.07445	7.49545	43.593	0.000	45.806	29.401	54.459
168.0	5.35836	7.18385	32.524	0.000	42.695	28.613	51.409
174.0	4.71961	6.83951	14.068	0.000	39.655	27.749	48.402
180.0	4.16019	6.47489	-12.659	0.000	37.611	27.111	46.364
186.0	3.67386	6.09700	-31.032	0.000	35.245	26.283	43.971
192.0	3.25431	5.72283	-58.654	0.000	32.721	25.289	41.378
198.0	2.89360	5.36309	-80.006	0.000	31.071	24.577	39.663
204.0	2.58366	5.02356	-101.687	0.000	29.548	23.875	38.069
210.0	2.31706	4.70707	-123.166	0.000	28.140	23.190	36.588

>>>> START OF COMPRESSION PROCESS

CA (DEG)	MEANKE (J)	TURBKE (J)	VIV (M/SEC)	VEV (M/SEC)	VMKE (M/SEC)	UPRIME (M/SEC)	CVHTRN (M/SEC)
216.0	2.08646	4.45699	0.000	0.000	26.577	22.527	35.029
222.0	1.88377	4.24840	0.000	0.000	25.258	21.997	33.758
228.0	1.70480	4.05904	0.000	0.000	24.033	21.506	32.601
234.0	1.54620	3.88844	0.000	0.000	22.892	21.054	31.551
240.0	1.40518	3.73596	0.000	0.000	21.827	20.643	30.599
246.0	1.27934	3.60112	0.000	0.000	20.829	20.273	29.737
252.0	1.16666	3.48364	0.000	0.000	19.939	19.961	28.995
258.0	1.06544	3.38319	0.000	0.000	19.142	19.701	28.354
264.0	0.97419	3.29916	0.000	0.000	18.264	19.445	27.674
270.0	0.89167	3.23166	0.000	0.000	17.435	19.240	27.057
276.0	0.81679	3.18104	0.000	0.000	16.761	19.106	26.571
282.0	0.74863	3.14717	0.000	0.000	16.012	19.001	26.050
288.0	0.68640	3.13143	0.000	0.000	15.339	18.957	25.598
294.0	0.62799	3.12817	0.000	0.000	14.613	18.946	25.114
300.0	0.56823	3.11467	0.000	0.000	13.930	18.902	24.616
306.0	0.50682	3.08251	0.000	0.000	13.193	18.806	24.030
312.0	0.44410	3.02008	0.000	0.000	12.277	18.594	23.223
318.0	0.38075	2.91981	0.000	0.000	11.406	18.289	22.375
324.0	0.31790	2.76842	0.000	0.000	10.334	17.753	21.210
330.0	0.25719	2.55799	0.000	0.000	9.335	17.078	19.991
336.0	0.20083	2.28376	0.000	0.000	8.299	16.174	18.568
342.0	0.15124	1.95499	0.000	0.000	7.169	14.920	16.799

>>>> START OF COMBUSTION AND EXPANSION PROCESSES

CA (DEG)	MEANKE (J)	TURBKE (J)	VIV (M/SEC)	VEV (M/SEC)	VMKE (M/SEC)	UPRIME (M/SEC)	CVHTRN (M/SEC)
348.0	0.11058	1.59734	0.000	0.000	6.114	13.448	14.895
354.0	0.07990	1.24283	0.000	0.000	5.216	11.883	13.014
360.0	0.05865	0.93301	0.000	0.000	4.463	10.278	11.203
366.0	0.04494	0.68985	0.000	0.000	3.894	8.803	9.679
372.0	0.03643	0.51347	0.000	0.000	3.500	7.580	8.581
378.0	0.03116	0.39049	0.000	0.000	3.231	6.598	7.905
384.0	0.02782	0.30525	0.000	0.000	3.047	5.811	7.597
390.0	0.02563	0.24542	0.000	0.000	2.925	5.217	7.570
396.0	0.02413	0.20251	0.000	0.000	2.837	4.740	7.714
402.0	0.02306	0.17095	0.000	0.000	2.772	4.353	7.950
408.0	0.02226	0.14721	0.000	0.000	2.723	4.032	8.219
414.0	0.02166	0.12895	0.000	0.000	2.687	3.782	8.454
420.0	0.02118	0.11464	0.000	0.000	2.657	3.567	8.649
426.0	0.02079	0.10324	0.000	0.000	2.633	3.383	8.779
432.0	0.02047	0.09402	0.000	0.000	2.613	3.231	8.831
438.0	0.02018	0.08639	0.000	0.000	2.594	3.099	8.803
444.0	0.01990	0.08002	0.000	0.000	2.575	2.975	8.685
450.0	0.01964	0.07466	0.000	0.000	2.558	2.877	8.502
456.0	0.01938	0.07012	0.000	0.000	2.541	2.784	8.230
462.0	0.01914	0.06625	0.000	0.000	2.525	2.707	7.912
468.0	0.01891	0.06293	0.000	0.000	2.511	2.644	7.571
474.0	0.01868	0.06009	0.000	0.000	2.496	2.584	7.168
480.0	0.01846	0.05764	0.000	0.000	2.481	2.531	6.735
486.0	0.01825	0.05553	0.000	0.000	2.467	2.484	6.273
492.0	0.01805	0.05371	0.000	0.000	2.453	2.441	5.794
498.0	0.01785	0.05214	0.000	0.000	2.439	2.406	5.335
504.0	0.01766	0.05079	0.000	0.000	2.426	2.374	4.875

>>>> START OF EXHAUST PROCESS

CA (DEG)	MEANKE (J)	TURBKE (J)	VIV (M/SEC)	VEV (M/SEC)	VMKE (M/SEC)	UPRIME (M/SEC)	CVHTRN (M/SEC)
510.0	0.01743	0.05014	0.000	367.723	2.413	2.363	4.723
516.0	0.01708	0.04926	0.000	366.149	2.400	2.354	6.029
522.0	0.01656	0.04791	0.000	364.110	2.387	2.344	9.048
528.0	0.01587	0.04602	0.000	361.850	2.375	2.335	12.102
534.0	0.01506	0.04379	0.000	358.559	2.360	2.324	14.885
540.0	0.01419	0.04136	0.000	355.974	2.349	2.316	17.142
546.0	0.01323	0.03867	0.000	348.335	2.334	2.304	21.315
552.0	0.01221	0.03579	0.000	335.931	2.323	2.296	23.263
558.0	0.01120	0.03290	0.000	300.665	2.308	2.285	24.048
564.0	0.01026	0.03021	0.000	264.989	2.298	2.277	22.305
570.0	0.00946	0.02793	0.000	227.727	2.289	2.271	20.035
576.0	0.00881	0.02608	0.000	174.190	2.275	2.260	16.153
582.0	0.00829	0.02460	0.000	142.784	2.262	2.250	13.924
588.0	0.00784	0.02332	0.000	137.140	2.253	2.244	13.703
594.0	0.00740	0.02208	0.000	141.193	2.240	2.234	14.346
600.0	0.00696	0.02081	0.000	151.372	2.228	2.224	15.438
606.0	0.00651	0.01950	0.000	160.793	2.216	2.215	16.425
612.0	0.00605	0.01816	0.000	165.197	2.208	2.210	16.909
618.0	0.00558	0.01680	0.000	170.777	2.196	2.200	17.529
624.0	0.00512	0.01544	0.000	176.834	2.181	2.188	18.141
630.0	0.00466	0.01408	0.000	177.684	2.175	2.184	18.229
636.0	0.00421	0.01275	0.000	175.685	2.164	2.175	18.029
642.0	0.00378	0.01149	0.000	169.177	2.152	2.166	17.343
648.0	0.00338	0.01029	0.000	162.579	2.143	2.159	16.638
654.0	0.00301	0.00918	0.000	157.453	2.132	2.151	15.878
660.0	0.00265	0.00811	0.000	156.966	2.119	2.141	15.183
666.0	0.00230	0.00707	0.000	158.301	2.105	2.130	14.362
672.0	0.00198	0.00610	0.000	162.710	2.090	2.118	13.403
678.0	0.00167	0.00518	0.000	176.084	2.066	2.100	12.135
684.0	0.00139	0.00432	0.000	189.848	2.045	2.083	11.038
690.0	0.00113	0.00354	0.000	202.436	2.022	2.065	10.036
696.0	0.00090	0.00284	0.000	208.381	1.989	2.038	8.789
702.0	0.00071	0.00224	0.000	204.054	1.953	2.009	7.044
708.0	0.00056	0.00180	0.000	205.582	1.910	1.975	5.129

>>>> HEAT TRANSFER DATA

>>>> START OF INTAKE PROCESS

CA (DEG)	HTRCOE (W/M**2/K)	HTPAPI (KW/M**2)	HTPAHD (KW/M**2)	HTPACW (KW/M**2)	THTRAN (KW)
-6.0	89.0	4.324	4.324	38.321	0.157
0.0	280.0	6.652	6.652	106.706	0.230
6.0	742.7	-5.317	-5.317	258.806	-0.115
12.0	829.7	-60.759	-60.759	232.316	-1.871
18.0	836.4	-136.840	-136.840	155.539	-4.387
24.0	893.2	-203.849	-203.849	104.369	-6.656
30.0	959.5	-265.820	-265.820	60.660	-8.829
36.0	996.5	-303.924	-303.924	30.349	-10.250
42.0	1018.2	-331.903	-331.903	5.065	-11.401
48.0	1028.0	-347.778	-347.778	-11.865	-12.162
54.0	1033.3	-360.876	-360.876	-27.198	-12.918
60.0	1036.3	-368.411	-368.411	-37.473	-13.486
66.0	1037.7	-372.335	-372.335	-43.835	-13.880
72.0	1046.8	-377.989	-377.989	-50.432	-14.419
78.0	1062.5	-385.649	-385.649	-55.932	-15.044
84.0	1069.8	-388.843	-388.843	-60.516	-15.569
90.0	1069.2	-387.991	-387.991	-62.293	-15.759
96.0	1063.9	-385.197	-385.197	-63.811	-15.922
102.0	1050.6	-379.247	-379.247	-64.717	-16.014
108.0	1037.2	-373.016	-373.016	-64.702	-15.983
114.0	1016.8	-364.621	-364.621	-63.979	-15.875
120.0	1004.5	-358.448	-358.448	-63.233	-15.746
126.0	987.3	-349.832	-349.832	-61.579	-15.543
132.0	970.2	-341.705	-341.705	-59.909	-15.290
138.0	941.6	-329.741	-329.741	-57.502	-14.859
144.0	906.6	-316.061	-316.061	-54.802	-14.324
150.0	879.2	-305.411	-305.411	-52.767	-13.890
156.0	839.8	-290.382	-290.382	-49.874	-13.253
162.0	806.0	-277.638	-277.638	-47.366	-12.692
168.0	769.9	-264.031	-264.031	-44.594	-12.072
174.0	733.7	-250.448	-250.448	-41.671	-11.427
180.0	708.4	-240.917	-240.917	-39.586	-10.962
186.0	679.4	-229.815	-229.815	-37.015	-10.401
192.0	650.4	-218.280	-218.280	-33.923	-9.777
198.0	633.2	-210.960	-210.960	-31.606	-9.349
204.0	619.2	-204.389	-204.389	-29.173	-8.936
210.0	608.4	-198.528	-198.528	-26.586	-8.536

>>>> START OF COMPRESSION PROCESS

CA (DEG)	HTRCOE (W/M**2/K)	HTPAPI (KW/M**2)	HTPAHD (KW/M**2)	HTPACW (KW/M**2)	THTRAN (KW)
216.0	600.1	-193.694	-193.694	-24.270	-8.182
222.0	596.3	-190.319	-190.319	-22.155	-7.895
228.0	596.1	-187.570	-187.570	-19.683	-7.611
234.0	599.6	-185.411	-185.411	-16.769	-7.329
240.0	607.1	-183.794	-183.794	-13.297	-7.047
246.0	619.0	-182.657	-182.657	-9.106	-6.760
252.0	634.7	-181.928	-181.928	-4.266	-6.480
258.0	654.1	-181.453	-181.453	1.319	-6.204
264.0	683.0	-181.073	-181.073	9.446	-5.863
270.0	719.9	-180.555	-180.555	19.889	-5.490
276.0	759.1	-179.638	-179.638	31.319	-5.132
282.0	815.4	-177.622	-177.622	48.590	-4.657
288.0	879.2	-173.258	-173.258	70.258	-4.099
294.0	988.0	-168.946	-168.946	104.354	-3.440
300.0	1112.7	-161.134	-161.134	146.321	-2.688
306.0	1265.7	-145.836	-145.836	203.851	-1.673
312.0	1484.1	-113.843	-113.843	296.814	-0.044
318.0	1722.2	-66.542	-66.542	411.958	1.967
324.0	2057.7	21.381	21.381	597.765	5.240
330.0	2409.7	136.976	136.976	822.108	9.152
336.0	2804.6	296.729	296.729	1111.915	14.198
342.0	3236.8	515.713	515.713	1485.684	20.738

>>>> START OF COMBUSTION AND EXPANSION PROCESSES

CA (DEG)	HTRCOE (W/M**2/K)	HTPAPI (KW/M**2)	HTPAHD (KW/M**2)	HTPACW (KW/M**2)	THTRAN (KW)
348.0	3775.8	1861.270	1861.270	3149.334	66.978
354.0	3961.6	2432.646	2432.646	3932.193	84.828
360.0	3842.8	3047.421	3047.421	4665.354	105.175
366.0	3404.3	3377.767	3377.767	4957.461	117.762
372.0	2822.9	3311.978	3311.978	4721.730	118.694
378.0	2267.6	2975.784	2975.784	4161.490	111.297
384.0	1812.6	2521.268	2521.268	3491.959	99.777
390.0	1480.1	2080.107	2080.107	2878.906	87.845
396.0	1226.4	1682.792	1682.792	2342.886	76.543
402.0	1031.2	1349.942	1349.942	1899.830	66.609
408.0	876.5	1079.656	1079.656	1541.352	58.138
414.0	760.2	880.725	880.725	1275.413	51.576
420.0	662.5	721.918	721.918	1060.858	46.074
426.0	580.4	594.310	594.310	886.954	41.338
432.0	517.7	497.704	497.704	754.930	37.563
438.0	470.0	421.536	421.536	651.579	34.462
444.0	424.3	353.376	353.376	558.040	31.383
450.0	386.9	301.263	301.263	485.199	28.750
456.0	350.4	252.925	252.925	417.085	26.021
462.0	319.1	213.875	213.875	361.257	23.548
468.0	292.6	182.141	182.141	315.337	21.318
474.0	266.6	151.869	151.869	271.425	18.980
480.0	242.9	124.916	124.916	232.142	16.697
486.0	220.5	99.985	99.985	195.749	14.397
492.0	199.6	76.876	76.876	161.998	12.093
498.0	181.3	56.441	56.441	132.308	9.924
504.0	164.3	36.850	36.850	104.168	7.739

>>>> START OF EXHAUST PROCESS

CA (DEG)	HTRCOE (W/M**2/K)	HTPAPI (KW/M**2)	HTPAHD (KW/M**2)	HTPACW (KW/M**2)	THTRAN (KW)
510.0	156.8	33.332	33.332	96.978	7.305
516.0	185.7	38.201	38.201	113.034	8.632
522.0	248.3	48.601	48.601	148.107	11.409
528.0	301.9	55.563	55.563	175.932	13.589
534.0	337.6	56.164	56.164	190.144	14.640
540.0	363.4	55.724	55.724	199.270	15.251
546.0	404.7	52.713	52.713	211.832	15.938
552.0	413.1	46.998	46.998	208.814	15.455
558.0	393.3	34.961	34.961	188.166	13.490
564.0	353.6	26.355	26.355	163.417	11.432
570.0	313.3	19.911	19.911	140.947	9.627
576.0	253.9	13.285	13.285	110.793	7.293
582.0	220.5	10.233	10.233	94.494	5.985
588.0	215.8	9.543	9.543	91.687	5.650
594.0	221.5	9.184	9.184	93.177	5.478
600.0	232.8	9.148	9.148	97.039	5.415
606.0	242.6	8.958	8.958	100.200	5.284
612.0	246.9	8.725	8.725	101.370	5.127
618.0	251.9	8.348	8.348	102.455	4.796
624.0	256.5	7.696	7.696	103.223	4.327
630.0	256.8	7.573	7.573	102.932	4.133
636.0	253.3	7.132	7.132	100.859	3.657
642.0	245.4	6.869	6.869	97.428	3.157
648.0	238.4	6.966	6.966	94.721	2.787
654.0	236.0	7.585	7.585	94.244	2.451
660.0	237.4	8.684	8.684	95.597	2.175
666.0	238.0	9.892	9.892	96.828	1.906
672.0	236.3	11.097	11.097	97.186	1.668
678.0	233.9	12.776	12.776	97.802	1.384
684.0	228.9	13.768	13.768	96.796	1.178
690.0	222.7	14.280	14.280	94.888	0.997
696.0	210.0	13.712	13.712	89.538	0.770
702.0	181.2	11.349	11.349	76.657	0.535
708.0	144.3	8.707	8.707	60.595	0.349

>>>> RADIATIVE HEAT TRANSFER DATA

CA (DEG)	PRES (ATM)	TAIR (K)	TGAS (K)	TFLAME (K)	TRAD (K)	EMIS (-)	QRAD (KW)	QTOT (KW)
348.0	89.1	759.6	1101.1	2661.1	1883.7	0.865	21.254	66.978
354.0	114.0	826.7	1243.0	2710.8	1978.3	0.833	24.432	84.828
360.0	137.1	880.3	1423.2	2748.0	2087.0	0.800	28.883	105.175
366.0	147.9	902.7	1598.8	2762.6	2182.5	0.767	33.328	117.762
372.0	142.2	890.3	1732.5	2754.6	2244.6	0.734	36.374	118.694
378.0	125.0	851.3	1806.9	2728.2	2268.0	0.701	37.344	111.297
384.0	103.6	795.9	1823.2	2688.2	2255.5	0.667	36.259	99.777
390.0	83.2	736.3	1794.1	2643.5	2218.3	0.634	33.865	87.845
396.0	66.0	675.8	1735.0	2597.3	2166.0	0.601	30.840	76.543
402.0	52.5	617.7	1664.1	2553.1	2107.8	0.568	27.738	66.609
408.0	42.2	563.2	1589.8	2512.2	2049.2	0.534	24.835	58.138
414.0	34.4	516.5	1519.2	2477.7	1997.9	0.502	22.431	51.576
420.0	28.5	482.0	1455.2	2451.9	1953.1	0.469	20.389	46.074
426.0	24.0	448.8	1398.3	2427.7	1912.2	0.435	18.524	41.338
432.0	20.6	421.2	1348.1	2407.8	1877.6	0.403	16.899	37.563
438.0	17.9	397.7	1303.8	2391.0	1847.3	0.370	15.400	34.462
444.0	15.8	376.0	1264.9	2375.6	1819.1	0.335	13.877	31.383
450.0	14.1	359.1	1230.5	2363.7	1796.5	0.302	12.534	28.750
456.0	12.7	343.3	1200.3	2352.7	1775.2	0.267	11.103	26.021
462.0	11.6	330.6	1173.7	2343.8	1757.6	0.234	9.764	23.548
468.0	10.7	320.3	1150.3	2336.7	1743.3	0.204	8.519	21.318
474.0	9.9	310.8	1129.9	2330.1	1729.9	0.171	7.175	18.980
480.0	9.3	302.7	1112.0	2324.5	1718.2	0.138	5.822	16.697
486.0	8.8	295.6	1096.6	2319.6	1707.9	0.104	4.422	14.397
492.0	8.4	289.4	1083.2	2315.4	1699.0	0.070	2.982	12.093
498.0	8.0	284.4	1071.9	2312.0	1691.7	0.037	1.580	9.924
504.0	7.7	280.2	1062.4	2309.1	1685.4	0.003	0.119	7.739

>>>> TRANSIENT TEMPERATURE PROFILES WITHIN PISTON

-6.00	-4.2	-2.0	-0.7	-0.1	0.0	0.0	0.0	0.0	0.0
0.00	-6.3	-4.0	-2.1	-0.9	-0.3	0.0	0.0	0.0	0.0
6.00	-8.0	-5.5	-3.4	-1.8	-0.8	-0.2	0.0	0.0	0.0
12.00	-10.7	-7.4	-4.7	-2.8	-1.3	-0.5	-0.1	0.0	0.0
18.00	-14.5	-10.1	-6.6	-3.9	-2.1	-0.9	-0.3	-0.1	0.0
24.00	-19.1	-13.5	-8.9	-5.5	-3.0	-1.4	-0.5	-0.1	0.0
30.00	-23.9	-17.4	-11.8	-7.4	-4.1	-2.0	-0.8	-0.2	0.0
36.00	-28.7	-21.4	-14.9	-9.6	-5.6	-2.8	-1.2	-0.4	-0.1
42.00	-33.2	-25.3	-18.2	-12.1	-7.3	-3.8	-1.6	-0.5	-0.1
48.00	-37.3	-29.1	-21.4	-14.7	-9.1	-5.0	-2.2	-0.8	-0.2
54.00	-41.1	-32.6	-24.5	-17.3	-11.1	-6.3	-3.0	-1.1	-0.3
60.00	-44.6	-35.9	-27.6	-19.8	-13.1	-7.7	-3.8	-1.5	-0.4
66.00	-47.9	-39.1	-30.5	-22.4	-15.1	-9.1	-4.7	-1.9	-0.6
72.00	-51.0	-42.0	-33.2	-24.8	-17.2	-10.7	-5.7	-2.4	-0.7
78.00	-54.1	-45.0	-35.9	-27.2	-19.2	-12.2	-6.7	-3.0	-1.0
84.00	-57.0	-47.8	-38.6	-29.6	-21.2	-13.8	-7.8	-3.6	-1.2
90.00	-59.6	-50.4	-41.1	-31.9	-23.2	-15.4	-9.0	-4.3	-1.5
96.00	-62.1	-52.9	-43.5	-34.2	-25.2	-17.0	-10.2	-5.0	-1.9
102.00	-64.4	-55.2	-45.8	-36.3	-27.1	-18.6	-11.4	-5.8	-2.3
108.00	-66.4	-57.4	-47.9	-38.4	-29.0	-20.2	-12.6	-6.6	-2.7
114.00	-68.3	-59.3	-49.9	-40.4	-30.8	-21.8	-13.8	-7.4	-3.1
120.00	-70.0	-61.2	-51.8	-42.2	-32.6	-23.4	-15.1	-8.3	-3.6
126.00	-71.7	-62.9	-53.6	-44.0	-34.3	-24.9	-16.3	-9.2	-4.1
132.00	-73.1	-64.5	-55.3	-45.7	-35.9	-26.4	-17.5	-10.0	-4.6
138.00	-74.4	-65.9	-56.9	-47.3	-37.5	-27.8	-18.7	-11.0	-5.1
144.00	-75.5	-67.2	-58.3	-48.8	-39.0	-29.2	-20.0	-11.9	-5.7
150.00	-76.5	-68.3	-59.6	-50.2	-40.5	-30.6	-21.1	-12.8	-6.3
156.00	-77.2	-69.3	-60.8	-51.5	-41.8	-31.9	-22.3	-13.7	-6.9
162.00	-77.9	-70.2	-61.8	-52.7	-43.1	-33.2	-23.4	-14.6	-7.5
168.00	-78.4	-71.0	-62.7	-53.8	-44.3	-34.4	-24.6	-15.5	-8.1
174.00	-78.9	-71.6	-63.6	-54.8	-45.4	-35.5	-25.6	-16.4	-8.7
180.00	-79.3	-72.2	-64.4	-55.7	-46.4	-36.6	-26.7	-17.3	-9.4
186.00	-79.6	-72.7	-65.1	-56.6	-47.4	-37.6	-27.7	-18.2	-10.0
192.00	-79.9	-73.2	-65.7	-57.4	-48.3	-38.6	-28.7	-19.0	-10.6
198.00	-80.2	-73.6	-66.3	-58.1	-49.1	-39.5	-29.6	-19.9	-11.3
204.00	-80.5	-74.0	-66.8	-58.8	-50.0	-40.4	-30.5	-20.7	-11.9
210.00	-80.8	-74.4	-67.3	-59.4	-50.7	-41.3	-31.4	-21.5	-12.6

216.00	-81.1	-74.8	-67.8	-60.0	-51.4	-42.1	-32.2	-22.3	-13.2
222.00	-81.4	-75.2	-68.3	-60.6	-52.1	-42.8	-33.0	-23.1	-13.8
228.00	-81.8	-75.7	-68.8	-61.2	-52.8	-43.6	-33.8	-23.8	-14.5
234.00	-82.2	-76.1	-69.3	-61.8	-53.4	-44.3	-34.5	-24.5	-15.1
240.00	-82.6	-76.5	-69.8	-62.3	-54.0	-45.0	-35.2	-25.2	-15.7
246.00	-83.1	-77.0	-70.3	-62.9	-54.6	-45.6	-35.9	-25.9	-16.3
252.00	-83.5	-77.5	-70.8	-63.4	-55.3	-46.3	-36.6	-26.6	-16.9
258.00	-84.0	-78.0	-71.4	-64.0	-55.8	-46.9	-37.3	-27.3	-17.4
264.00	-84.5	-78.5	-71.9	-64.5	-56.4	-47.6	-37.9	-27.9	-18.0
270.00	-85.0	-79.0	-72.4	-65.1	-57.0	-48.2	-38.6	-28.5	-18.6
276.00	-85.6	-79.6	-73.0	-65.7	-57.6	-48.8	-39.2	-29.2	-19.1
282.00	-86.0	-80.1	-73.5	-66.2	-58.2	-49.4	-39.8	-29.8	-19.7
288.00	-86.5	-80.6	-74.0	-66.8	-58.8	-50.0	-40.4	-30.4	-20.2
294.00	-86.8	-81.0	-74.5	-67.3	-59.4	-50.6	-41.0	-31.0	-20.8
300.00	-87.1	-81.4	-75.0	-67.8	-59.9	-51.2	-41.6	-31.5	-21.3
306.00	-87.1	-81.6	-75.4	-68.3	-60.4	-51.7	-42.2	-32.1	-21.8
312.00	-86.5	-81.5	-75.6	-68.7	-60.9	-52.3	-42.8	-32.7	-22.4
318.00	-85.3	-80.9	-75.5	-68.9	-61.4	-52.8	-43.4	-33.2	-22.9
324.00	-82.6	-79.6	-74.9	-68.9	-61.7	-53.3	-43.9	-33.8	-23.4
330.00	-78.2	-76.9	-73.6	-68.5	-61.8	-53.6	-44.4	-34.3	-23.9
336.00	-71.5	-72.5	-71.1	-67.4	-61.5	-53.9	-44.8	-34.8	-24.4
342.00	-61.8	-66.2	-67.3	-65.4	-60.8	-53.9	-45.2	-35.3	-24.8
348.00	-20.3	-43.6	-56.9	-61.3	-59.3	-53.5	-45.4	-35.8	-25.3
354.00	17.0	-15.9	-38.7	-51.4	-55.3	-52.5	-45.4	-36.1	-25.8
360.00	59.0	16.0	-16.4	-37.7	-48.3	-49.9	-45.0	-36.4	-26.2
366.00	99.3	49.8	9.1	-20.6	-38.6	-45.5	-43.7	-36.4	-26.6
372.00	130.1	79.7	34.7	-1.5	-26.5	-39.3	-41.5	-36.1	-26.9
378.00	148.5	101.8	56.8	17.3	-13.0	-31.5	-38.2	-35.4	-27.1
384.00	156.2	115.6	73.6	33.8	0.4	-22.8	-33.9	-34.1	-27.1
390.00	156.6	122.4	84.9	47.0	12.7	-13.7	-28.8	-32.2	-26.9
396.00	152.1	124.0	91.5	56.8	23.2	-4.9	-23.2	-29.9	-26.5
402.00	144.8	122.2	94.6	63.5	31.6	3.1	-17.5	-27.1	-25.9
408.00	136.5	118.4	95.1	67.7	38.2	10.1	-12.0	-24.0	-24.9
414.00	128.0	113.3	93.8	69.9	43.0	16.0	-6.7	-20.7	-23.8
420.00	119.6	107.8	91.5	70.7	46.4	20.9	-1.9	-17.4	-22.4
426.00	111.7	102.2	88.5	70.5	48.6	24.8	2.4	-14.2	-20.9
432.00	104.4	96.7	85.2	69.5	50.0	27.9	6.1	-11.1	-19.3
438.00	97.6	91.4	81.7	68.1	50.6	30.3	9.4	-8.1	-17.6
444.00	91.3	86.3	78.2	66.4	50.8	32.0	12.1	-5.4	-15.9

450.00	85.4	81.5	74.7	64.4	50.5	33.3	14.5	-2.9	-14.1
456.00	79.9	76.9	71.2	62.3	49.9	34.2	16.4	-0.6	-12.4
462.00	74.7	72.5	67.8	60.1	49.1	34.7	18.1	1.5	-10.8
468.00	69.9	68.3	64.5	57.9	48.1	35.0	19.4	3.4	-9.2
474.00	65.3	64.3	61.3	55.6	46.9	35.0	20.4	5.0	-7.7
480.00	60.9	60.5	58.2	53.4	45.7	34.9	21.3	6.5	-6.3
486.00	56.8	56.8	55.1	51.1	44.4	34.5	21.9	7.7	-4.9
492.00	52.8	53.3	52.1	48.9	43.0	34.1	22.4	8.9	-3.6
498.00	49.0	49.9	49.2	46.6	41.5	33.5	22.6	9.8	-2.5
504.00	45.2	46.5	46.4	44.4	40.0	32.8	22.8	10.7	-1.4
510.00	42.0	43.4	43.7	42.2	38.5	32.1	22.8	11.4	-0.4
516.00	39.2	40.7	41.1	40.1	36.9	31.3	22.8	11.9	0.5
522.00	37.0	38.3	38.9	38.1	35.4	30.4	22.6	12.4	1.4
528.00	35.0	36.3	36.9	36.3	34.0	29.5	22.4	12.8	2.1
534.00	33.1	34.4	35.1	34.6	32.6	28.6	22.1	13.1	2.8
540.00	31.3	32.7	33.4	33.1	31.4	27.7	21.7	13.3	3.5
546.00	29.5	31.0	31.7	31.6	30.1	26.9	21.4	13.5	4.0
552.00	27.7	29.3	30.2	30.2	29.0	26.0	21.0	13.6	4.5
558.00	25.8	27.5	28.6	28.8	27.8	25.2	20.8	13.6	4.9
564.00	23.9	25.8	27.0	27.5	26.7	24.4	20.1	13.6	5.3
570.00	22.0	24.0	25.5	26.1	25.6	23.6	19.7	13.6	5.7
576.00	20.1	22.3	23.9	24.8	24.5	22.8	19.3	13.5	6.0
582.00	18.4	20.6	22.4	23.4	23.4	22.0	18.8	13.5	6.2
588.00	18.8	19.1	20.9	22.1	22.3	21.2	18.3	13.3	6.5
594.00	15.3	17.6	19.5	20.8	21.2	20.4	17.8	13.2	6.7
600.00	13.9	16.2	18.2	19.6	20.2	19.6	17.3	13.0	6.8
606.00	12.5	14.9	16.9	18.4	19.2	18.8	16.8	12.8	6.9
612.00	11.2	13.6	15.7	17.3	18.2	18.0	16.2	12.6	7.0
618.00	10.0	12.4	14.5	16.2	17.2	17.2	15.7	12.4	7.1
624.00	8.8	11.2	13.3	15.1	16.3	16.4	15.2	12.1	7.2
630.00	7.6	10.0	12.2	14.1	15.3	15.7	14.6	11.9	7.2
636.00	6.5	8.9	11.2	13.1	14.4	14.9	14.1	11.6	7.2
642.00	5.4	7.9	10.2	12.1	13.6	14.2	13.6	11.3	7.2
648.00	4.4	6.8	9.2	11.2	12.7	13.5	13.0	11.0	7.2
654.00	3.4	5.9	8.2	10.3	11.9	12.8	12.5	10.7	7.1
660.00	2.5	4.9	7.3	9.4	11.1	12.1	12.0	10.4	7.0
666.00	1.6	4.0	6.4	8.5	10.3	11.4	11.5	10.1	7.0
672.00	0.7	3.2	5.5	7.7	9.5	10.7	11.0	9.8	6.9
678.00	-0.1	2.3	4.7	6.9	8.8	10.1	10.4	9.5	6.8
684.00	-0.8	1.6	3.9	6.1	8.1	9.4	9.9	9.1	6.7
690.00	-1.6	0.8	3.2	5.4	7.4	8.8	9.4	8.8	6.5
696.00	-2.4	0.0	2.4	4.7	6.7	8.2	8.9	8.5	6.4
702.00	-3.2	-0.7	1.7	4.0	6.0	7.6	8.5	8.2	6.3
708.00	-4.0	-1.5	0.9	3.3	5.4	7.0	8.0	7.8	6.1

>>>> TRANSIENT TEMPERATURE PROFILES WITHIN HEAD

-6.00	-4.2	-2.0	-0.7	-0.1	0.0	0.0	0.0	0.0	0.0
0.00	-6.3	-4.0	-2.1	-0.9	-0.3	0.0	0.0	0.0	0.0
6.00	-8.0	-5.5	-3.4	-1.8	-0.8	-0.2	0.0	0.0	0.0
12.00	-10.7	-7.4	-4.7	-2.8	-1.3	-0.5	-0.1	0.0	0.0
18.00	-14.5	-10.1	-6.6	-3.9	-2.1	-0.9	-0.3	-0.1	0.0
24.00	-19.1	-13.5	-8.9	-5.5	-3.0	-1.4	-0.5	-0.1	0.0
30.00	-23.9	-17.4	-11.8	-7.4	-4.1	-2.0	-0.8	-0.2	0.0
36.00	-28.7	-21.4	-14.9	-9.6	-5.6	-2.8	-1.2	-0.4	-0.1
42.00	-33.2	-25.3	-18.2	-12.1	-7.3	-3.8	-1.6	-0.5	-0.1
48.00	-37.3	-29.1	-21.4	-14.7	-9.1	-5.0	-2.2	-0.8	-0.2
54.00	-41.1	-32.6	-24.5	-17.3	-11.1	-6.3	-3.0	-1.1	-0.3
60.00	-44.6	-35.9	-27.6	-19.8	-13.1	-7.7	-3.8	-1.5	-0.4
66.00	-47.9	-39.1	-30.5	-22.4	-15.1	-9.1	-4.7	-1.9	-0.6
72.00	-51.0	-42.0	-33.2	-24.8	-17.2	-10.7	-5.7	-2.4	-0.7
78.00	-54.1	-45.0	-35.9	-27.2	-19.2	-12.2	-6.7	-3.0	-1.0
84.00	-57.0	-47.8	-38.6	-29.6	-21.2	-13.8	-7.8	-3.6	-1.2
90.00	-59.6	-50.4	-41.1	-31.9	-23.2	-15.4	-9.0	-4.3	-1.5
96.00	-62.1	-52.9	-43.5	-34.2	-25.2	-17.0	-10.2	-5.0	-1.9
102.00	-64.4	-55.2	-45.8	-36.3	-27.1	-18.6	-11.4	-5.8	-2.3
108.00	-66.4	-57.4	-47.9	-38.4	-29.0	-20.2	-12.6	-6.6	-2.7
114.00	-68.3	-59.3	-49.9	-40.4	-30.8	-21.8	-13.8	-7.4	-3.1
120.00	-70.0	-61.2	-51.8	-42.2	-32.6	-23.4	-15.1	-8.3	-3.6
126.00	-71.7	-62.9	-53.6	-44.0	-34.3	-24.9	-16.3	-9.2	-4.1
132.00	-73.1	-64.5	-55.3	-45.7	-35.9	-26.4	-17.5	-10.0	-4.6
138.00	-74.4	-65.9	-56.9	-47.3	-37.5	-27.8	-18.7	-11.0	-5.1
144.00	-75.5	-67.2	-58.3	-48.8	-39.0	-29.2	-20.0	-11.9	-5.7
150.00	-76.5	-68.3	-59.6	-50.2	-40.5	-30.6	-21.1	-12.8	-6.3
156.00	-77.2	-69.3	-60.8	-51.5	-41.8	-31.9	-22.3	-13.7	-6.9
162.00	-77.9	-70.2	-61.8	-52.7	-43.1	-33.2	-23.4	-14.6	-7.5
168.00	-78.4	-71.0	-62.7	-53.8	-44.3	-34.4	-24.6	-15.5	-8.1
174.00	-78.9	-71.6	-63.6	-54.8	-45.4	-35.5	-25.6	-16.4	-8.7
180.00	-79.3	-72.2	-64.4	-55.7	-46.4	-36.6	-26.7	-17.3	-9.4
186.00	-79.6	-72.7	-65.1	-56.6	-47.4	-37.6	-27.7	-18.2	-10.0
192.00	-79.9	-73.2	-65.7	-57.4	-48.3	-38.6	-28.7	-19.0	-10.6
198.00	-80.2	-73.6	-66.3	-58.1	-49.1	-39.5	-29.6	-19.9	-11.3
204.00	-80.5	-74.0	-66.8	-58.8	-50.0	-40.4	-30.5	-20.7	-11.9
210.00	-80.8	-74.4	-67.3	-59.4	-50.7	-41.3	-31.4	-21.5	-12.6

216.00	-81.1	-74.8	-67.8	-60.0	-51.4	-42.1	-32.2	-22.3	-13.2
222.00	-81.4	-75.2	-68.3	-60.6	-52.1	-42.8	-33.0	-23.1	-13.8
228.00	-81.8	-75.7	-68.8	-61.2	-52.8	-43.6	-33.8	-23.8	-14.5
234.00	-82.2	-76.1	-69.3	-61.8	-53.4	-44.3	-34.5	-24.5	-15.1
240.00	-82.6	-76.5	-69.8	-62.3	-54.0	-45.0	-35.2	-25.2	-15.7
246.00	-83.1	-77.0	-70.3	-62.9	-54.6	-45.6	-35.9	-25.9	-16.3
252.00	-83.5	-77.5	-70.8	-63.4	-55.3	-46.3	-36.6	-26.6	-16.9
258.00	-84.0	-78.0	-71.4	-64.0	-55.8	-46.9	-37.3	-27.3	-17.4
264.00	-84.5	-78.5	-71.9	-64.5	-56.4	-47.6	-37.9	-27.9	-18.0
270.00	-85.0	-79.0	-72.4	-65.1	-57.0	-48.2	-38.6	-28.5	-18.6
276.00	-85.6	-79.6	-73.0	-65.7	-57.6	-48.8	-39.2	-29.2	-19.1
282.00	-86.0	-80.1	-73.5	-66.2	-58.2	-49.4	-39.8	-29.8	-19.7
288.00	-86.5	-80.6	-74.0	-66.8	-58.8	-50.0	-40.4	-30.4	-20.2
294.00	-86.8	-81.0	-74.5	-67.3	-59.4	-50.6	-41.0	-31.0	-20.8
300.00	-87.1	-81.4	-75.0	-67.8	-59.9	-51.2	-41.6	-31.5	-21.3
306.00	-87.1	-81.6	-75.4	-68.3	-60.4	-51.7	-42.2	-32.1	-21.8
312.00	-86.5	-81.5	-75.6	-68.7	-60.9	-52.3	-42.8	-32.7	-22.4
318.00	-85.3	-80.9	-75.5	-68.9	-61.4	-52.8	-43.4	-33.2	-22.9
324.00	-82.6	-79.6	-74.9	-68.9	-61.7	-53.3	-43.9	-33.8	-23.4
330.00	-78.2	-76.9	-73.6	-68.5	-61.8	-53.6	-44.4	-34.3	-23.9
336.00	-71.5	-72.5	-71.1	-67.4	-61.5	-53.9	-44.8	-34.8	-24.4
342.00	-61.8	-66.2	-67.3	-65.4	-60.8	-53.9	-45.2	-35.3	-24.8
348.00	-20.3	-43.6	-56.9	-61.3	-59.3	-53.5	-45.4	-35.8	-25.3
354.00	17.0	-15.9	-38.7	-51.4	-55.3	-52.5	-45.4	-36.1	-25.8
360.00	59.0	16.0	-16.4	-37.7	-48.3	-49.9	-45.0	-36.4	-26.2
366.00	99.3	49.8	9.1	-20.6	-38.6	-45.5	-43.7	-36.4	-26.6
372.00	130.1	79.7	34.7	-1.5	-26.5	-39.3	-41.5	-36.1	-26.9
378.00	148.5	101.8	56.8	17.3	-13.0	-31.5	-38.2	-35.4	-27.1
384.00	156.2	115.6	73.6	33.8	0.4	-22.8	-33.9	-34.1	-27.1
390.00	156.6	122.4	84.9	47.0	12.7	-13.7	-28.8	-32.2	-26.9
396.00	152.1	124.0	91.5	56.8	23.2	-4.9	-23.2	-29.9	-26.5
402.00	144.8	122.2	94.6	63.5	31.6	3.1	-17.5	-27.1	-25.9
408.00	136.5	118.4	95.1	67.7	38.2	10.1	-12.0	-24.0	-24.9
414.00	128.0	113.3	93.8	69.9	43.0	16.0	-6.7	-20.7	-23.8
420.00	119.6	107.8	91.5	70.7	46.4	20.9	-1.9	-17.4	-22.4
426.00	111.7	102.2	88.5	70.5	48.6	24.8	2.4	-14.2	-20.9
432.00	104.4	96.7	85.2	69.5	50.0	27.9	6.1	-11.1	-19.3
438.00	97.6	91.4	81.7	68.1	50.6	30.3	9.4	-8.1	-17.6
444.00	91.3	86.3	78.2	66.4	50.8	32.0	12.1	-5.4	-15.9

450.00	85.4	81.5	74.7	64.4	50.5	33.3	14.5	-2.9	-14.1
456.00	79.9	76.9	71.2	62.3	49.9	34.2	16.4	-0.6	-12.4
462.00	74.7	72.5	67.8	60.1	49.1	34.7	18.1	1.5	-10.8
468.00	69.9	68.3	64.5	57.9	48.1	35.0	19.4	3.4	-9.2
474.00	65.3	64.3	61.3	55.6	46.9	35.0	20.4	5.0	-7.7
480.00	60.9	60.5	58.2	53.4	45.7	34.9	21.3	6.5	-6.3
486.00	56.8	56.8	55.1	51.1	44.4	34.5	21.9	7.7	-4.9
492.00	52.8	53.3	52.1	48.9	43.0	34.1	22.4	8.9	-3.6
498.00	49.0	49.9	49.2	46.6	41.5	33.5	22.6	9.8	-2.5
504.00	45.2	46.5	46.4	44.4	40.0	32.8	22.8	10.7	-1.4
510.00	42.0	43.4	43.7	42.2	38.5	32.1	22.8	11.4	-0.4
516.00	39.2	40.7	41.1	40.1	36.9	31.3	22.8	11.9	0.5
522.00	37.0	38.3	38.9	38.1	35.4	30.4	22.6	12.4	1.4
528.00	35.0	36.3	36.9	36.3	34.0	29.5	22.4	12.8	2.1
534.00	33.1	34.4	35.1	34.6	32.6	28.6	22.1	13.1	2.8
540.00	31.3	32.7	33.4	33.1	31.4	27.7	21.7	13.3	3.5
546.00	29.5	31.0	31.7	31.6	30.1	26.9	21.4	13.5	4.0
552.00	27.7	29.3	30.2	30.2	29.0	26.0	21.0	13.6	4.5
558.00	25.8	27.5	28.6	28.8	27.8	25.2	20.6	13.6	4.9
564.00	23.9	25.6	27.0	27.5	26.7	24.4	20.1	13.6	5.3
570.00	22.0	24.0	25.5	26.1	25.6	23.6	19.7	13.6	5.7
576.00	20.1	22.3	23.9	24.8	24.5	22.8	19.3	13.5	6.0
582.00	18.4	20.6	22.4	23.4	23.4	22.0	18.8	13.5	6.2
588.00	16.8	19.1	20.9	22.1	22.3	21.2	18.3	13.3	6.5
594.00	15.3	17.6	19.5	20.8	21.2	20.4	17.8	13.2	6.7
600.00	13.9	16.2	18.2	19.6	20.2	19.6	17.3	13.0	6.8
606.00	12.5	14.9	16.9	18.4	19.2	18.8	16.8	12.8	6.9
612.00	11.2	13.6	15.7	17.3	18.2	18.0	16.2	12.6	7.0
618.00	10.0	12.4	14.5	16.2	17.2	17.2	15.7	12.4	7.1
624.00	8.8	11.2	13.3	15.1	16.3	16.4	15.2	12.1	7.2
630.00	7.6	10.0	12.2	14.1	15.3	15.7	14.6	11.9	7.2
636.00	6.5	8.9	11.2	13.1	14.4	14.9	14.1	11.6	7.2
642.00	5.4	7.9	10.2	12.1	13.6	14.2	13.6	11.3	7.2
648.00	4.4	6.8	9.2	11.2	12.7	13.5	13.0	11.0	7.2
654.00	3.4	5.9	8.2	10.3	11.9	12.8	12.5	10.7	7.1
660.00	2.5	4.9	7.3	9.4	11.1	12.1	12.0	10.4	7.0
666.00	1.6	4.0	6.4	8.5	10.3	11.4	11.5	10.1	7.0
672.00	0.7	3.2	5.5	7.7	9.5	10.7	11.0	9.8	6.9
678.00	-0.1	2.3	4.7	6.9	8.8	10.1	10.4	9.5	6.8
684.00	-0.8	1.6	3.9	6.1	8.1	9.4	9.9	9.1	6.7
690.00	-1.6	0.8	3.2	5.4	7.4	8.8	9.4	8.8	6.5
696.00	-2.4	0.0	2.4	4.7	6.7	8.2	8.9	8.5	6.4
702.00	-3.2	-0.7	1.7	4.0	6.0	7.6	8.5	8.2	6.3
708.00	-4.0	-1.5	0.9	3.3	5.4	7.0	8.0	7.8	6.1